



# **3<sup>rd</sup> EFRC-Conference**

***Reliability and  
economics of compression systems  
– recent trends in the market of  
reciprocating compressors***

**BASF**



Burckhardt Compression

**HGC** HAMBURG  
GAS  
CONSULT

**HOERBIGER**



KOMPRESSOREN



TECHNISCHE  
UNIVERSITÄT  
DRESDEN

THOMASSEN  
COMPRESSION  
SYSTEMS



**ZM**

**March 27–28, 2003 Vienna, Austria**



## Content

---

- **General**
- **Fundamentals**
- **Selection and Sizing**
- **Innovation and Technology**
- **Operation and Maintenance**





## General

---

H. Hefe / BASF AG

- **Keynote speech**

S. Cierniak / HGC Hamburg Gas Consult GmbH

- **Educating reciprocating compressor engineers at the EFRC**

P. Steinrück / HOERBIGER Kompressortechnik Services

- **Joint research at the EFRC**



# **Keynote speech**

by:

**Dipl.-Ing. Heinz Hefele  
BASF AG, Ludwigshafen**

**Reliability and economics of compression  
systems - recent trends in the market of  
reciprocating compressors  
March 27th / 28<sup>th</sup>, 2003   Vienna**


## Der Kolbenkompressor, fit für die Zukunft?

Einen guten Tag und einen erfolgreichen Kongress in der Hauptstadt des wunderschönen europäischen Landes Österreich wünsche ich Ihnen, meine sehr verehrten Damen und Herren.

Entsprechend dem Motto unserer dritten EFRC-Konferenz "Zuverlässigkeit und Wirtschaftlichkeit von Kompressorenanlagen" wollen wir den steigenden Anforderungen des Marktes, hin zu preiswerteren und höherwertigen Produkten Rechnung tragen. Wir alle hier - sei es Maschinenhersteller, Anlagenbetreiber oder Instandhalter - sind nur ein Teil, aber ein wesentlicher Bestandteil, in der Prozesskette um diesen Marktmechanismus positiv beeinflussen zu können.

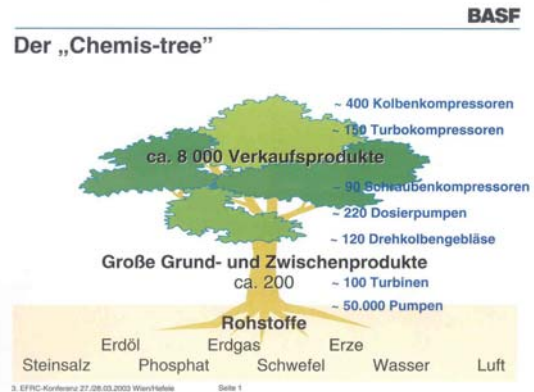
Die Lebenszykluskosten der im Prozess eingesetzten Arbeitsmaschinen spielen hierbei eine beachtliche Rolle. Denn wie wir wissen sind die Einmalaufwendungen wie Planung, Konstruktion und Beschaffung als Kosten kalkulierbar und fix, die geplanten Betriebskosten wie geplante Instandhaltung, Energie und Ersatzteile variabel und beeinflussbar, aber ungeplante Stillstände mit Produktionsausfall und Störinstandhaltung teuer und nicht überschaubar. Diese ungeplanten Folgekosten gilt es daher zu minimieren.

Doch zunächst möchte ich Ihnen gerne unser Unternehmen vorstellen und verdeutlichen was uns mit Kompressoren verbindet.

	<p>Autor</p> <p>Dipl.-Ing. Heinz Hefele</p> <p>Leiter Kompressoren- und Turbinentechnik</p> <p>BASF AG, Ludwigshafen</p>
---	--

Die Produktpalette unseres Unternehmens ist vergleichbar mit einem Baum, wir nennen ihn "Chemis-tree". An diesem möchte ich zum Ausdruck bringen, wie viele Strömungs- und Kolbenmaschinen für die Erzeugung von 8000 Verkaufsprodukten benötigt werden.

Bild 1, der "Chemis-tree"



Wenige Rohstoffe, wie Erdgas, Erdöl, Erze und Mineralien werden in der BASF zu etwa 200 wichtigen Grund- und Zwischenprodukten höherveredelt und bilden die Basis der rund 8000 Verkaufsprodukte.

Hierzu haben wir folgende Anzahl von Maschinen, differenziert nach Maschinenarten am Produktionsstandort in Ludwigshafen im Einsatz:

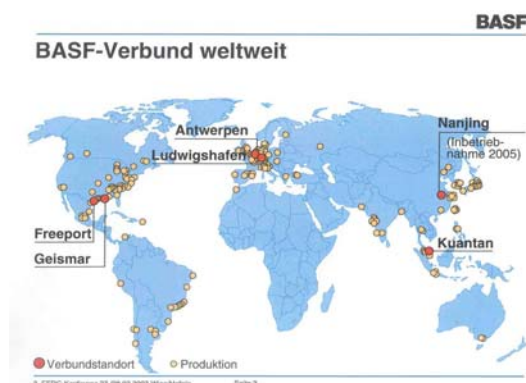
- ~ 400 Kolbenkompressoren
- ~ 150 Turbokompressoren
- ~ 90 Schraubenkompressoren
- ~ 220 Dosierpumpen
- ~ 120 Drehkolbengebläse
- ~ 100 Turbinen
- ~ 50.000 Pumpen

Bild 2



Ludwigshafen ist das Stammwerk der BASF-Gruppe. Das Werk am Rhein ist der größte Produktionsstandort der BASF, auch Sitz der Unternehmensleitung und das Zentrum der Forschung.

Bild 3



Als weltweit tätiges Unternehmen begreifen und nutzen wir die Globalisierung als Chance. Daher errichten und betreiben wir rund um den Globus Produktions- und Vertriebsstandorte um die Anforderungen der Kunden weltweit erfüllen zu können. Viele hier im Auditorium unterstützen uns dabei als Hersteller und Lieferanten von Kompressoren oder deren Komponenten. Die Zuverlässigkeit und Wirtschaftlichkeit von Kompressorenanlagen wird daher entscheidend dazu beitragen, die Herstellkosten der End- oder Verkaufsprodukte zu beeinflussen. Die anerkannten Vorteile von Kolbenkompressoren, (Bild 4) wie hoher Wirkungsgrad auch bei unterschiedlichen Betriebsbedingungen, vergleichsweise gute Regelbarkeit auch mit leichten Gasen und hohen

Verdichtungsverhältnissen und Erzeugung von sehr hohen Drücken haben diese Kompressorbauart über Jahrzehnte hinweg bestätigt.



Trotzdem bestehen gegenüber anderen Bauarten immer noch Vorbehalte wegen des relativ komplexen mechanischen Aufbaues und der damit verbundenen Annahme, Kolbenmaschinen verursachen hohe Instandhaltungskosten oder seien unzuverlässiger. Dem ist entgegenzuwirken und kann meines Erachtens auch erfolgreich versprechend angegangen werden. Lassen Sie mich dieses erläutern.

Fakt ist, und so sehen wir es in unserem Unternehmen an der respektablen Anzahl betriebener Kompressoren, dass sich hinsichtlich der Ausstattung beim Maschinenschutz und der Maschinenüberwachung Turbokompressoren und Kolbenkompressoren unterschiedlich entwickelt haben.

Während bei Turbokompressoren schon parallel mit der Entwicklung von Maschinenüberwachungssystemen diese auch eingesetzt wurden, wird bei Kolbenkompressoren der Einsatz von solchen Systemen noch zögerlich angegangen.

Großanlagen in der chemischen Industrie, sogenannte Einstranganlagen, sind aus Kostengründen im Turbobereich singulär ausgelegt und deswegen umfangreicher überwacht. Bei Kolbenmaschinen ist jedoch noch eher Redundanz bevorzugt vorzufinden, was nicht zuletzt auch mit kürzeren Revisionszyklen der Kolbenmaschinen zusammenhängt.

Wo sehen wir als Betreiber und Instandhalter von Kolbenkompressoren nun Ansätze um Laufzeiten zu verlängern um dadurch die Lebenszykluskosten zu senken?

Zum einen wären das konstruktiv und fertigungsbedingte Maßnahmen auf die ich gleich eingehen werde und zum anderen eine erforderliche Funktionalität zur Überwachung von Kolbenkompressoren.

So könnte man reproduzierbare Werkstoffkombinationen sowohl bei Kolbenstangen/Stopfbuchsen als auch Kolbenringe/Laufbuchsen in Abhängigkeit der zu komprimierenden Gase in einem Schaubild vereinen, dessen Daten aus gesicherten Betriebserfahrungen stammen.

Voraussetzung dazu wäre das Wissen über die exakten Analysedaten der eingesetzten Werkstoffe. Hierbei denke ich insbesondere an die Technischen Kunststoffe.

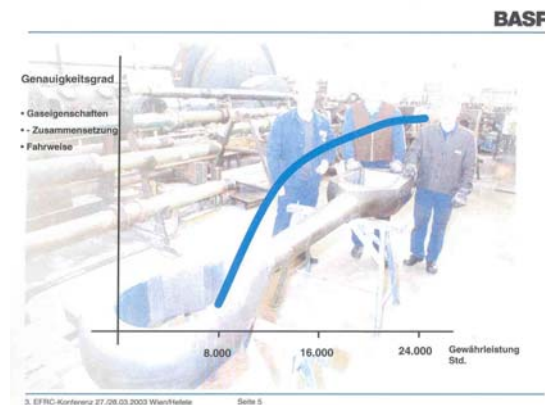
Dieses Wissen unterliegt jedoch dem Know-how-Schutz der Packungs- und Kolbenringlieferanten im Dialog mit den Halbzeugherstellern, sofern nicht der Betreiber selbst Eigenerfahrungen eingebracht hat. Ziel und Wunsch der Betreiber ist aber weiterhin die Gewährleistung auf Verschleißteile zu verlängern was meines Erachtens auch machbar sein wird, wenn der Anforderer als Kunde und Betreiber der Anlage die Gaseigenschaften, die Gaszusammensetzung und auch die Fahrweise genauer spezifiziert.

Des weiteren könnten Herstellkosten und Herstellzeiten verringert werden, wenn auf die Gussfertigung ein größeres Augenmerk gerichtet werden würde. Dies gilt insbesondere für die Problematiken der Modellgestaltung wie Ausformradien oder Modellwerkstoffe. Selbst als Hersteller von Styropor würde ich bei solch hochwertigen Teilen wie z. B. Zylinder oder andere hochbeanspruchte Bauteile dabei eher zu Holzmodellen raten um poröse Gussstrukturen sowie Seigerungen zu verhindern, um damit teure und zeitaufwendige Fertigungsschweißungen zu vermeiden.

Auch wäre die dauerhaft auszulegende, gewindelose Kolbenstangenverbindung aufzuführen, die noch nicht von jedem Hersteller angeboten wird.

Die Überwachung von vielen installierten Kolbenkompressoren erfolgt gegenüber früheren Zeiten heute schon etwas fortschrittlicher.

Bild 5



Mit dem Ansteigen des Genauigkeitsgrades müsste dann auch der Leistungsanspruch steigen dürfen, d. h. mehr als 8.000 Betriebsstunden hin zu 16.000 Std. und mehr.



Bild 6



Prozessgrößen werden bereits heute schon im Betriebsdateninformationssystem die sich aus Daten des Prozessleitsystems generieren erfasst und ausgewertet. Bei der elektronischen Überwachung von mechanischen Bauteilen jedoch gibt es noch Nachholbedarf. Gerade diese mechanischen Bauteile sind es, die den Betreiber von Anlagen - wenn diese nicht ausreichend überwacht, sei es instrumentell oder durch Personal - vor vollendete Tatsachen wie Ausfall oder Havarie stellen. Der Markt bietet dazu komfortable aber auch teure, selbstlernende Systeme an.

Wichtig erscheinen für uns jedoch folgend aufgeführte Mindestanforderungen, die recht preiswert sein können, wenn sie bereits bei der Projektierungsphase Berücksichtigung finden. Eine Schwingungsüberwachung durch getriggerte Erfassung des Zeitsignals je Umdrehung mit Beschleunigungsmessung und eine Kolben- und Führungsringlagenüberwachung im Vergleich des gemessenen Zeitsignals mit Referenzsignalen. Des weiteren eine bereits bei Sauerstoffkompressoren bewährte Praxis der Ventilstemperaturüberwachung auf modellbasierten Algorithmen um anbahnende Ventilschäden zu detektieren und eine Spritzöltemperaturüberwachung im Kurbelbereich die Auskunft über Veränderungen im Pleuellager signalisieren kann.

Weitere Innovationsmöglichkeiten sehe ich noch bei der Automation von Ölabbstreifvorgängen insbesondere bei hohen Drücken und Automatisierung der Anfahrprozesse von Kolbenkompressoren auch nach längeren betriebsbedingten Stillständen bei eventuellem Kondensatanfall.

Weitere Innovationskeime sind durch das Einbinden junger Leute in diese Problematik

zu erwarten, wenn wir in Verbindung mit Technischen Hochschulen oder Fachhochschulen Themen für Studien- oder Diplomarbeiten vergeben oder Praxissemester anbieten.

Außerdem gilt es nachzudenken und zu reagieren auf die europäische Rahmengesetzgebung hinsichtlich der Forderungen des Explosionsschutzes an nichtelektrischen Anlagen wozu auch die Kompressoren zählen. Diesen Themenkomplex müsste auch in einem solchen Kreis bearbeitet werden da sowohl Hersteller, Betreiber und auch Instandhalter davon betroffen sind. Es macht daher Sinn, eine einheitliche Umsetzung anzustreben.

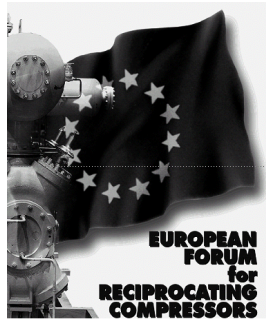
Ein großes Potential sich gegenseitig zu befruchten und Wissen auszutauschen bietet auch diese Veranstaltung des EFRC bei der erfahrene und kompetente Fachspezialisten Performance-Indikatoren weiterentwickeln oder sogar neu entdecken können.

Mit diesem Ausblick brauchen wir die Zukunft nicht zu scheuen und wenn wir dabei noch stetig das Interesse unserer Kunden im Blick haben und den Kolbenkompressor diesen Bedürfnissen anpassen können, bleibt er auch weiterhin eine zeitgemäße Arbeitsmaschine.

Bild 7



Und so wird das Glück dann strahlen bei zufriedenen Kunden mit preiswerten Endprodukten, hervorgebracht aus einer Produktkette mit sehr guten Kunden-Lieferantenbeziehungen, an der wir dann alle mitgewirkt haben.



# **Educating reciprocating compressor engineers at the EFRC**

by:

**Dr.-Ing. Siegmund V. Cierniak**  
**HGC Hamburg Gas Consult GmbH**  
**Hamburg, Germany**

**Chairman of the EFRC Educating Committee**

**Reliability and economics of compression systems -  
recent trends in the market of  
reciprocating compressors  
March 27th / 28th, 2003 Vienna**

## Why educate reciprocating compressor engineers?

The design, selection, operation and maintenance of reciprocating compressors makes the education and training of different types of engineers a must. Due to these facts all compressor manufacturers, packagers and end users have a need for highly qualified, educated and skilled engineers. Our branch need snow and in the future, well educated and highly motivated graduates from the best universities and colleges.

The EUROPEAN FORUM for RECIPROCATING COMPRESSORS - EFRC is creating co-operation between the members of EFRC, other compressor makers, packagers, subsuppliers users and the well known universities, colleges, institutes and their students.

### 1 Some examples of these co-operative efforts:

- common supported theses
- presentations – made by people from companies at the universities
- excursions to workshops and facilities in our branch
- practical work of students in firms
- information about jobs for graduates
- sponsoring of first class results of student's (thesis', etc.)
- realisation of workshops as platform for recent students and graduates
- publication of studies, theses, research work

### 2 What EFRC members are already doing:

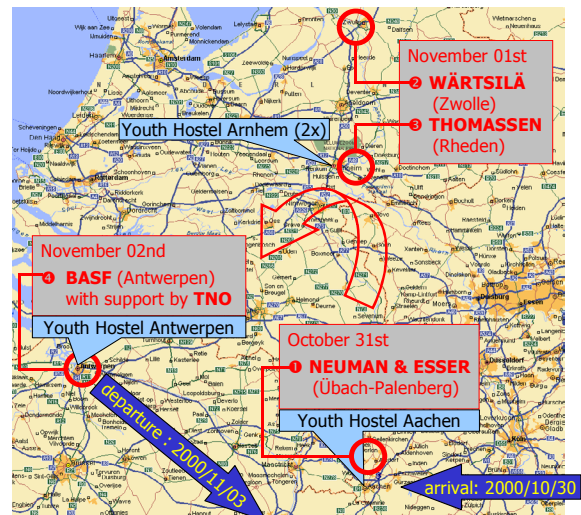
- participating in EFRC promotion committee
- hosting of excursions
- organizing of internships
- sponsoring of events
- subsidizing highly qualified students and graduates

### 4 Advantages for EFRC members:

- access to qualified engineers
- influence on the education of students
- part time jobs of students

## 5 Important results of the EFRC activity „Educating reciprocating compressor engineers”

### 5.1 Autumn 2000: Student's excursion to Germany, the Netherland and Belgium



Picture 1: Student's excursion  
Tour the facilities of

NEUMAN & ESSER GmbH,  
Übach-Palenberg / Germany

WÄRTSILÄ Nederland BV,  
Zwolle / The Netherlands

THOMASSEN Intern. BV,  
Rheden / The Netherlands

BASF AG,  
Antwerpen / Belgium

TNO Inst. of Applied Physics,  
Delft / The Netherlands

### 5.2 Spring 2001: Workshop “Reciprocating compressors in Natural Gas Underground storages”

#### 5.2.1 Location and participants

- Natural Gas Underground Storage Kraak (near Schwerin / Germany)  
“HEINGAS Hamburger Gaswerke GmbH” / compressors “ARIEL / HGC”
- Natural Gas Underground Storage Hamburg-Reitbrook  
“HEINGAS Hamburger Gaswerke GmbH” / compressors “ARIEL / HGC”

The participants were students and post graduate students from different European Universities (i.e. Dresden / D, Erlangen /D, Freiberg / D, Delft /NL, Enschede / NL), with a particular interest in this discipline. Of course there was a tour on the on-ground facilities and many technical details were discussed with a focus on the on site running ARIEL-compressors. The participants had a chance to see both e-motor-driven and gas-engine-driven reciprocating compressors, and there was also a compressor in the erection phase to see.



*Picture 2: Workshop participants at the Natural Gas underground storage Kraak*

The seminar program included presentations made by Dr. Ralf Luy, Heingas „Underground Storage technology“, Dr. Andy Laschet, ARLA „Torsional analysis“, Bernd Schmidt, Prognost „Condition Monitoring“, Andre Eijk, TNO Delft „Pulsations“ and also some compressor technologies presented by Dr. Klaus Hoff, Neuman & Esser and Dr. Siegmund Cierniak, HGC-Hamburg.

As a real highlight Prof. Dr. Gotthard Will (University of Dresden) advised the participants to work within the next 4 months on a study, which has to have as a result a computerized simulations-program „Reciprocating Compressors in Natural Gas Underground Storages“.

The committee of the EFRC decided to award a prize to the best results (working groups of app. 3 students) with a cost free participation (incl. travelling costs and accomodation) on the next EFRC-Conference on March 27 and 28 in 2003 in Vienna/Austria and in addition to that 1.000,-- EUR extra for the best and 500 EUR for the second best group and will also present the computer programs and its results to the conference's participants .

## 5.2.2 Results of the EFRC Workshop 2002

All participants worked very diligently on their tasks and the results are excellent. Because of this it was very difficult for the committee to evaluate the student's reports (incl. the programmed computer programs).

The outline of the reports and the different softwares (Excel, Matlab, html) are all basically marked with a variety of solutions in which the most important criterias are simulated for different pressures and gas flows. All participants acted with combinations of all existing parameters. In all reports the effects at the indicator diagram and the pressure pulsations on the discharge side are clearly estimated and nicely illustrated.

The committee thanks all participants for their excellent work. They did a very good job. The prize winners have shown their interest in reciprocating compressor technology and have given our branch a push in order to see a great future.

## 5.2.3 Prize winners of the EFRC Workshop 2002

### 1<sup>st</sup> Grade: 1,000.-- EUR - Karsten Starke

Bergakademie Freiberg / TU  
Institut für Fluidmechanik und  
Fluidenergiemaschinen  
Lampadiusstraße 4  
09596 Freiberg / Germany  
Tel. +49 3731 39-3277  
Fax +49 3731 39-3455  
E-Mail: [Gottfried.Gneipel@imfd.tu-freiberg.de](mailto:Gottfried.Gneipel@imfd.tu-freiberg.de)

### 2<sup>nd</sup> Grade: 500.-- EUR - Uwe Seiffert - David Bolz - Ulrich Klapp - Jan Leilich - Ronald Schmidt

Friedrich-Alexander-Universität Erlangen-Nürnberg  
Lehrstuhl für Prozessmaschinen und  
Anlagentechnik  
Cauerstraße 4  
91058 Erlangen / Germany  
Tel. +49 9131 85-2 9458  
Fax +49 9131 85-2 9449  
E-Mail: [sei@ipat.uni-erlangen.de](mailto:sei@ipat.uni-erlangen.de)

**3<sup>rd</sup> Grade**

- **Georg Flade**
- **Matthias Huschenbett**

TU Dresden  
Institut für Energiemaschinen und  
Maschinenlabor  
Professur Pumpen, Verdichter und  
Apparate  
01062 Dresden / Germany  
Tel. +49 351 463-3 2603  
Fax +49 351 463-3 7182  
E-Mail: [g.flade@memkn1.mw.tu-dresden.de](mailto:g.flade@memkn1.mw.tu-dresden.de)

**6 Next EFRC Workshop / Excursion  
2004**

- Spring 2004
- Central Europe (Czech Republic or Slovakian Republic or Hungary or Poland)
- For students: free of charge
- Details will be published in Fall 2003





# **Joint research at the EFRC**

**by:**

**Dr. Peter Steinrück**

**Hoerbiger Kompressortechnik Services**

**Vienna, Austria**

**Chairman of the EFRC Research Committee**

## **Reliability and economics of compression systems - recent trends in the market of reciprocating compressors**

**March 27th / 28th, 2003 Vienna**

### **Abstract:**

Under EFRC statutes, one of the purposes of EFRC is to promote research on reciprocating compressors. To pursue this goal in an effective R&D Working Group has been set up. Currently the EFRC promotes four research projects. For these projects a synopsis will be presented. Terms and conditions how to participate and how to benefit from EFRC's joint research will be given.

## Why joint research

Over more than 100 years reciprocating compressors have been the working horses boosting the pressure of gases in various consumer and industrial applications. Especially for the latter services most of the recips have been custom built, thus being individually engineered. Design work has been conducted by a number of competitive companies, thus duplicating engineering efforts. For obvious economic reasons comparably little amount of research has been attributed to these machines. Much of the design knowledge has been acquired by experience. Although in regard to plant availability recips have left behind an image of bad actors, it can be expected that better understanding of the basics will help to boost reliability and performance of these well proven machines. A solution to overcome the financial problems associated with economics of scale of the rather fragmented compressor industry is joint research funded by the manufactures and users of compressors.

Such research has been already conducted by the US pipeline industry improving the impressive fleet of more than 8000 natural gas compressors. However, no joint research addresses the problems of other type of recips, such as process gas, refrigeration, air compressors. Consequently there is only a very small scientific community dealing with recip subjects and well educated compressor engineers are scarce.

## EFRC Joint Research

Organizing joint research on topics fundamental for the design and operation of reciprocating compressors is one of the most prominent objectives of the European Forum for Reciprocating Compressors - EFRC.

The combined knowledge and resources of

- Universities,
- Research institutes
- Manufactures
- Component manufactures and
- Users

are used to address research topics, which are basic to the industry but are beyond the

commercial interest of a single party. It is intended to address national and international funds to support this work.

## Results of EFRC joint research program

The first research project carried out under the EFRC was aiming at evaluating the effectiveness of various low frequency pulsation damping devices used in reciprocating compressor applications such as orifice plates and perforated plates with multiple holes. Also special designs such as developed by Kotter and NEA have been analysed. The project was funded by Wartsila compression systems, NEA, Thomassen Compression Systems and LMF and carried out by TNO TPD in Delft.

The results of this EFRC joint research have been published at occasion of the 2<sup>nd</sup> EFRC Conference<sup>1</sup>.

It appeared that for low frequency pulsations, the static pressure drop over de pulsation damper and its location are critical for its performance, while details of the perforations, such as number of holes and its form have no influence. For higher frequency pulsations, such as encountered for example in screw compressor applications or at roots blowers, the behaviour of multi-perforated plates is more effective compared to single hole orifices. Critical parameters determining the effectiveness have been determined in this project.

## Working program

Since June 2002 EFRC joint research is handled by the EFRC R&D working group which is funded by a number of EFRC members. These members decide on the working program and have access to the results generated by the sponsored work. The current working program consists of projects covering design and operational problems of reciprocating compressors. It has been started in August 2002 and has already delivered interesting results.

### 3D CFD Simulation of Cylinder Flow

The pressure distribution driving the flow into and out of a compressor cylinder defines the loading on compressor components such as valves, pistons, piston rods, liners etc. It commands compressor efficiency and compressor performance. With increasing compressor speed flow induced pressure effects become more pronounced. In general the pressure drop across valve passages and pressure pulsations have been modelled using one dimensional flow models. To optimise cylinder geometry flow patterns have been studied solving the governing equations (Navier Stokes Equations) applying numerical methods (Computational Fluid Dynamics – CFD methods). Most of these studies have assumed steady state flow, thus neglecting the strongly time dependent (instationary) character of the cylinder flow. However, former work conducted by E. Machu<sup>2</sup> and L. Böswirth<sup>3</sup> has yield general estimates for the magnitudes of the effect as well as design proposals how to minimise detrimental effect of instationary, multi dimensional cylinder flow.

The tasks of this project are:

Explore the time dependent, compressible flow within a compressor cylinder shortly before the end of the compression cycle using a CFD code.

Study effects on:

Flow losses

In cylinder pulsations

Eccentric piston load

Derive design rules

Since high speed compressors become more and more popular results of this project could be of major signification for the design of future compressors. Therefore this project has been awarded to TU Dresden which has got long-term experience in CFD modelling, has access to powerful computer equipment required to perform the complex time dependent, multidimensional flow calculations and in depth knowledge of reciprocating compressor design.

### Simulation of multistage compressors

Predicting compressor failures already in early stages reliably is a prerequisite for condition based maintenance strategies. Currently this task is completed by measuring operating parameters and comparing the measured values against predefined “good” conditions. Good conditions are either defined empirically by taking snapshots of the operating parameters when the compressor plant is running well or theoretically applying rather crude process models. Since both methods do not account for transient effects and other disturbing influences alarm thresholds must be set rather conservatively to avoid false alarms. Thus failures detection is neither very sensitive nor fast.

Handling of multiple operating conditions resulting in different sets of good conditions is another challenge, which is addressed by only few commercially available condition monitoring systems.

State of the art systems should support failure identification as well. Integrated expert systems organising the knowledge gained through past experience may help users to locate the position of failure.

However, another promising approach to:

identify failures and  
locate the cause of failures

based on a detailed physical model accounting for transient effects, potential component failures and variation of operating conditions has been proposed by TU Dresden.

After careful assessment of the prior state of the art the EFRC has awarded TU Dresden to start a feasibility study exploring the potential of this approach.

A model of a multistage compressor has been programming using the Matlab Simulink programming environment. First results indicate that with state of the art PC computing equipment (Pentium IV, 1.5 Ghz) a full dynamic simulation can run with at a speed of 1/10 of real time. With the fast increase in computing power it is rather likely

that in the foreseeable future real time simulation of a multistage compressor is possible.

Furthermore results indicate that it is possible to identify different failures causes – e.g. discharge valve failure in second stage – by comparing the timely development of temperature and pressure patterns.

### **Rod Load Sensor**

Direct measurement of rod load via strain gauges and telemetry would be a useful tool to protect compressors under very critical operating conditions or to analyse special compressor failures (e.g. repeated liquid slug induced damages and/or repeated breakage of rods). For standard applications currently applied methods suffice to protect machines from overload. In case direct rod load monitoring would be required, the result would allow relatively fast implementation of this technology.

A project aiming for a cost efficient methods to continuously monitor rod load has been assigned to Prognost Systems GmbH.

Technology screening has been completed. Feasible solutions have been identified. Provided successful passing of some commercial and technical criteria, the EFRC will start the development of a related product.

### **Optimisation of separators in respect to effects of pulsating flow**

Liquids are a main cause of compressor failures. The presence of liquids can cause damages on valves or even the piston rod can breakdown. Therefore, separator vessels are installed upstream to prevent liquid inflow into the compressor cylinders.

These separators are dimensioned based on a maximum and minimum steady gas flow. However, pulsations generated by the compressor can cause large velocity fluctuations in the separator vessel even in the case that these fluctuations are damped by a pulsation damper. Often reversed flow can

occur. As the periodic time of the velocity pulsations are in the same order of the liquid residence time, it is to be expected that the separation efficiency is affected. The pulsations can also cause already separated liquids to be re-entrained into the main gas flow due to droplets being sheared of unstable, wavy liquid films.

An inventory is made by TNO TPD, Delft, to what extent precautions are taken during the design phase of gas/liquid separators to prevent these effects. The major separator manufacturers do not take into account the pulsating flow in the design phase. Neither with respect to the effects on the performance, nor to the effects on the mechanical integrity of the separator vessel internals. However, all manufacturers agreed that flow reversal should be avoided.

The study by TNO TPD is intended to explore the occurrence of compressor failures due to liquids and to check the feasibility of future liquid prevention and system optimisation projects.

### **How to participate**

Under EFRC statutes, one of the purposes of EFRC is to promote research on reciprocating compressors. To pursue this goal in an effective way that involves both the Executive Committee and the members, an R&D Working Group has been set up in accordance with the provisions below:

- (1) Membership in the R&D Working Group is open to all EFRC members.
- (2) Membership registrations can be filed directly with the Chairman of the R&D Working Group.
- (3) Registration for the R&D Working Group shall be binding on registering members for at least one work year of the R&D Working Group or longer if the registration indicates a longer period.

The working group decides upon:

annual work program  
annual membership fee

Project results are available to the members of the R&D working group under the following provisions:

(1) The EFRC shall be entitled to all rights, in particular exploitation rights to the work results of the R&D Working Group, as well as incorporeal rights (rights to intellectual property) to the extent permitted in law.

(2) Members who have belonged to the R&D Working Group for the duration of a given project and who have rendered their contributions in full shall receive a documentation of the results and shall be granted the corresponding license rights free of charge.

(3) Members who have not belonged to the R&D Working Group for the duration of a given project shall have the opportunity to acquire these license rights the same as the members who have belonged to the R&D Working Group for the duration of a given project by rendering a mutually agreed upon monetary contribution or contribution in kind to EFRC.

(4) Licenses granted to the members in this way shall be non-transferable. The member shall therefore not be entitled without the written approval of EFRC to pass these licenses on in full or in part to third parties. No member has an automatic claim to receive such approval from EFRC.

---

<sup>1</sup> Peters M.C.A.M.: Evaluation of low frequency pulsation damping devices. EFRC conference on Life Cycle Costs - Reciprocating Compressors in the Focus of Function, Economics and Reliability, May 17th / 18th, 2001, The Hague

<sup>2</sup> Machu, E.: Increased power consumption of high speed, short stroke reciprocating compressors caused by pocket losses and gas inertia effects, Compressor Tech<sup>two</sup>, März – April 1999

<sup>3</sup> Böswirth, L.: Strömung und Ventilplatten-bewegung in Kolbenverdichterventilen, erweiterter Nachdruck 1988, Eigenverlag, Wien





## Fundamentals

---

E. Huttar, V. Kacani / Leobersdorfer Maschinenfabrik AG

- **Simulation of leakage through piston rings on reciprocating compressors**

G. Vetter, Friedrich / Alexander-University Erlangen

N. Feistel / Burckhardt Compression AG

- **Investigation of the operational behaviour of dry-running piston-rod sealing systems in crosshead compressors**

B. Howes, D. Derksen, K. Eberle / Beta Machinery Analysis Ltd.

- **API 618 Forced Response Studies**

A. Eijk / TNO TPD

G. Samland, N. Retz, D. Sauter / Burckhardt Compression AG

- **Economic benefits of CAD-models for compressor manifold vibration analyses according to API 618**

A. J. Smalley, R. E. Harris, C. M. Gehri, G. W. Weilbacher / Southwest Research Institute

- **Dynamic characteristics of large high-speed reciprocating compressor systems**

A. Thönnissen / VSP-Aachen GmbH

- **Multidimensional simulation of pulsations with a new adaptive cartesian flow-solver**

A. Brighenti, A. Pavan / S.A.T.E. S.r.l.; M. Maffei / SIAD

- **Investigation on the influence of pressure pulsations on multistage reciprocating compressors - Comparison between test and simulation results**

G. Will, G. Flade / TU Dresden

- **Simulation of the flow in ring valves**

G. Samland, N. Retz / Burckhardt Compression AG

- **Thermal and structural analysis of a reciprocating compressor cylinder**



# **Simulation of leakage through piston rings on reciprocating compressors**

**by:**

**Ernst Huttar, Vasillaq Kacani  
Leobersdorfer Maschinenfabrik AG  
Leobersdorf  
Austria**

## **Reliability and economics of compression systems – recent trends in the market of reciprocating compressors**

**March 27<sup>th</sup> / 28<sup>th</sup>, 2003 Vienna**

### **Abstract:**

In this paper a simple calculation model for the simulation of leakage through piston rings on reciprocating compressors will be presented. The flow through the rings will be modelled using an equivalent orifice (for the ring gap) and a channel flow (for the ring side clearance). Depending on the stage pressure ratio, the orifice flow is either subsonic or sonic, and through the channels the flow is either laminar or turbulent. Each chamber between the rings is assumed to have uniform pressure. For the simulation we state a set of differential equations for the active cylinder compartments (crank and head end) and for all annular chambers between the piston rings. For k-piston rings the number of equations is  $4+2(k+1)$ . The equations are solved using an integration method of the 4<sup>th</sup> and 5<sup>th</sup> order.

## 1 Introduction

The calculation of leakage is the subject matter of the theoretical and experimental research of various authors [2], [3], [4], [5]. A more exact summary of the work done in this field is given in [5].

This paper will provide a physical and mathematical model of the leakage flow through the piston rings of the piston compressor, after which the results of the simulation will be presented. Particular attention is paid to the extent to which loss through leakage depends on compressor speed, molecular weight and the number of piston rings.

## 2 Symbols and subscripts

$c_p$	specific heat
$k$	number of piston rings
$\dot{m}_{i,S}$	mass flow through suction valve
$\dot{m}_{i,D}$	mass flow through disch. valve
$\dot{m}_{j,L}, \dot{m}_{j,R}$	leakage through piston ring
$\dot{m}_{j,RS}$	mass flow through the channel
$\dot{m}_{j,RD}$	mass flow through the ring gap
$p_i$	pressure cylinder compartment
$p_S, p_D$	pressure, cylinder passage
$p_i$	pressure, annular ring chamber
$T_i$	temp. annular ring chamber
$t$	time
$u$	internal energy
$A_{1S}, A_{2S}$	area, suction valve
$A_{1D}, A_{2D}$	area, discharge valve
$A_{j,RD}$	area of ring gap
$N$	compressor speed
$M$	molecular weight
$R$	specific gas constant
$T_i$	temperature
$T_S, T_D$	temperature, cylinder passage
$V_i$	momentary compartment volume
$Z$	compressibility
$\alpha$	orifice contraction coefficient
$\omega$	angular velocity
$\lambda_i$	angular velocity
$\rho_i$	angular velocity
$\kappa$	isentropic exponent
$\tau$	period
$\psi$	flow function
$\Pi_{j,R}$	pressure ratio ring j
1	head end compartment
2	crank end compartment
S,D	suction, discharge
R	annular compartment
k	number of piston rings
j	annular chamber

v  
L valve  
leakage

## 3 Description of the physical model

The flow through the active cylinder compartments in the piston compressor is influenced mainly by the volumetric efficiency, the heat coefficient (heat generated) and the losses due to the pressure at the suction end being less than the stage pressure, as well as by the amount of leakage through the piston rings and valves.

This paper examines leakage through the piston rings only. This is defined by the equation:

$$\lambda_{i,L} = 1 - \frac{(\dot{m}_{i,D})_{\text{Gap Area} > 0}}{(\dot{m}_{i,D})_{\text{Gap Area} = 0}}$$

The model will be explained using a double-acting cylinder as example. The direction of the leakage flow depends on the difference between the pressures  $p_1$  and  $p_2$  (head end and crank end compartments).

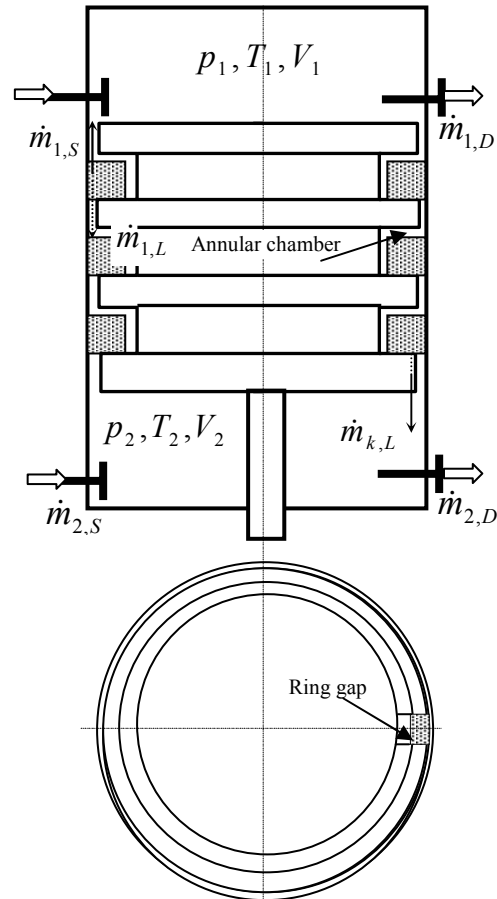


Fig. 1: Double-acting cylinder, physical model.

During one revolution of the crankshaft, the sign of the pressure difference  $p_1 - p_2$  changes and the direction of the leakage flow changes correspondingly.

Figure 1 shows the physical model.

The pressures and temperatures in the active cylinder compartments (head end and crank end) and in the annular chambers between the rings, constitute the unknown independent variables. They depend on the position of the crankshaft and consequently also on the time 't'. These periodic functions are linked by physical laws (equation of state, balance of mass and energy conservation). The stage pressures, both on the suction and on the discharge sides, are assumed to be constant.

#### 4 Differential equations

From the equation of state and the balances of masses and energy [1], we obtain the time rate of the temperatures and pressures  $dT/dt$ ,  $dp/dt$  in the cylinder compartments and in all the ring chambers.

$$\begin{aligned} p \cdot V &= m \cdot Z \cdot R \cdot T \quad (Z, R = \text{const.}) \rightarrow \\ dp \cdot V + p \cdot dV &= Z \cdot R (dm \cdot T + m \cdot dT) \\ dm &= dm_v + dm_L \\ -p \cdot dV + c_{p,v} \cdot T_v \cdot dm_v + c_{p,L} \cdot T_L \cdot dm_L &= \\ d(m \cdot u) \end{aligned}$$

We obtain the following differential equations for the active cylinder compartments - head end and crank end.

$$\left\{ \begin{aligned} \frac{dT_i}{dt} &= \left[ (\kappa T_{i,v} - T_i) \dot{m}_{i,v} + (\kappa T_{j,L} - T_i) \dot{m}_{j,L} - \right. \\ &\quad \left. - \frac{p_i}{c_{v,i}} dV_i \right] \cdot \frac{1}{m_i} \\ \frac{dp_i}{dt} &= \left[ ZR\kappa T_{i,v} \dot{m}_{i,v} + ZR\kappa T_{j,L} \dot{m}_{j,L} - \right. \\ &\quad \left. - p_i \left( \frac{ZR}{c_{v,i}} - 1 \right) \cdot dV_i \right] \cdot \frac{1}{V_i} \\ i &= 1 \rightarrow HE, \quad i = 2 \rightarrow CE - \text{Compartment} \end{aligned} \right.$$

The mass flow rate  $\dot{m}_{i,v}$  is the flow through the suction/discharge valve and is an algebraic

discontinuous function. During the expansion/compression phases, it is zero, and during suction/discharge it can be determined from the valve parameter and the pressure difference at the valve.

Accordingly, for the annular chambers:

$$\left\{ \begin{aligned} \frac{dT_{j,R}}{dt} &= \left[ (\kappa T_{i,R}^U - T_{j,R}) \dot{m}_{j,R,L} + \right. \\ &\quad \left. (\kappa T_{j+1,R}^O - T_{j,R}) \dot{m}_{j+1,R,L} \right] \frac{1}{m_{j,R}} \\ \frac{dp_{j,R}}{dt} &= \left[ ZR\kappa T_{i,R}^U \dot{m}_{j,R,L} + ZR\kappa T_{j+1,R}^O \dot{m}_{j+1,R,L} \right] \frac{1}{V_{j,R}} \\ j &= 1, 2, \dots, k \end{aligned} \right.$$

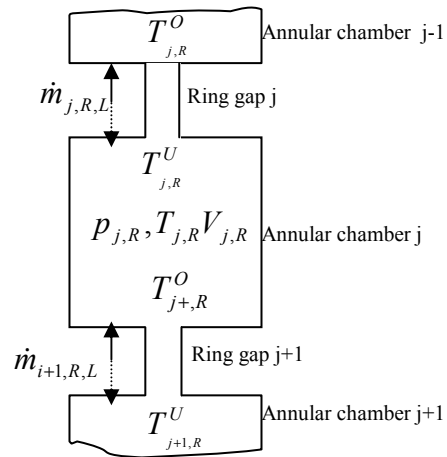


Abb. 2: Annular chamber.

The mass flow rate  $\dot{m}_{j,R,L}$  is made up of the mass flow through the ring gap  $\dot{m}_{j,RD}$  and the mass flow through the channel (ring side clearance)  $\dot{m}_{j,RS}$ .

The mass flow rate through the ring gap (depending on the pressure ratio and the pressure difference in the neighboring annular chambers) is calculated as follows [1]:

$$\frac{dm_{j,RD}}{dt} = \text{sgn}(p_{j,R} - p_{j+1,R}) A_{j,RD} \psi_{j,R} \alpha \sqrt{2p_{j,R} \rho_{j,R}}$$

The discharge function  $\psi$  depends on the flow ratio at the ring gap..

$$\psi_{j,R} = \begin{cases} \sqrt{\frac{\kappa}{\kappa-1}} \cdot \sqrt{\Pi_{j,R}^{\frac{2}{\kappa}} - \Pi_{j,R}^{\frac{\kappa+1}{\kappa}}} & \text{subsonic flow} \\ \sqrt{\frac{\kappa}{\kappa+1}} \left( \frac{2}{\kappa+1} \right)^{\frac{1}{\kappa-1}} & \text{sonic flow} \\ \Pi_{j,R} = \frac{\max(p_{j,R}, p_{j+1,R})}{\min(p_{j,R}, p_{j+1,R})} & \text{pressure ratio} \end{cases}$$

Formulae for the flow rate through the ring channel can be taken from [4].

For 'k' piston rings, a system with  $4+2(k-1)$  differential equations is obtained. The unknowns can be grouped together in a common periodic vector  $y(t)$ .

$$y(t) = \begin{pmatrix} T_1 \\ p_1 \\ T_2 \\ p_2 \\ T_{1,R} \\ p_{2,R} \\ \vdots \\ T_{k,R} \\ p_{k,R} \end{pmatrix} = \begin{pmatrix} y_1 \\ y_2 \\ y_3 \\ y_4 \\ y_5 \\ y_6 \\ \vdots \\ y_{n-1} \\ y_n \end{pmatrix}, n = 1, 4 + 2(k-1)$$

$$y(t) = y(t + \tau) \quad \tau = \frac{\pi \cdot N}{30}$$

To this, the equations for the mass flow rates through the valves and the piston rings still have to be added.

The integration of the differential equation systems is carried out numerically over a period  $\tau$  using an approximation of the 4<sup>th</sup> and 5<sup>th</sup> order, as described in [6].

## 5 Results

Simulation calculations were carried out for various compressor speeds and molecular masses. Leakage is greater at lower compressor speeds. The same behavior can be obtained by varying the molecular mass. The calculated curves can also be approximated using polynomials. Thus, without

much calculation, which is expensive, the results can be used in the selection and the recalculation of compressors.

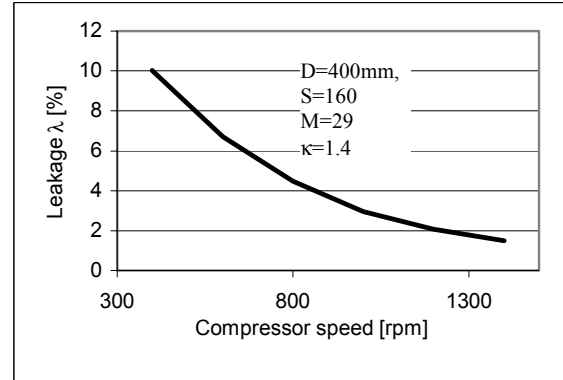


Fig. 2: Leakage versus compressor speed

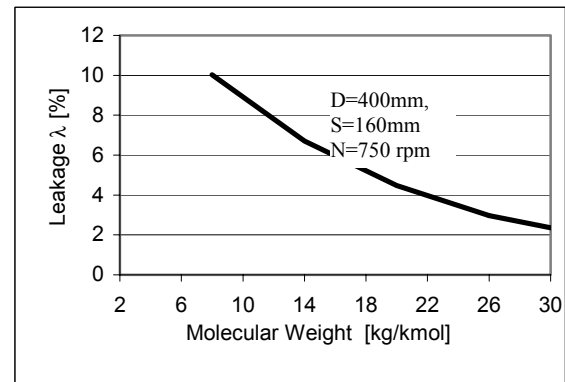


Fig. 3: Leakage versus molecular weight

- [1] Baehr H.D.: Thermodynamik, Berlin-Heidelberg-New York 1981.
- [2] Eweis M.: Reibungs- und Undichtigkeitsverluste an Kolbenringe. Forschungsheft 371, Ausgabe B, Band 6, März/April 1935.
- [3] Tang-Wie Kuo, Mark C. Sellnau, Mark A. Theobald, John D Jones.: Calculation of flow in the Piston-Cylinder-Ring Crevices of a Homogeneous-Charge Engine and Compression with Experiment. SAE Technical Paper Series, 890838, International Congress and Exposition Detroit, Michigan, February 27 1989.
- [4] Trutnovsky K.: Berührungsfrei Dichtung, VDI-Verlag, Düsseldorf 2.Auflage 1964.
- [5] Lutz B.: Beitrag zur Bestimmung der Leckverluste im Arbeitszylinder eines Kolbenkompressors. Diss. Karlruhe, 1968.
- [6] Engeln –Müllgas G., Reuter F.: Formelsammlung zur numerischen Mathematik mit Standard Fortran 77 Programmen. Bibliographisches Institut Mannheim/Wien/Zürich, B.I. Wissenschaftsverlag.



# **Investigation of the operational behaviour of dry-running piston-rod sealing systems in crosshead compressors**

by:

**Prof. G. Vetter, Friedrich-Alexander-University Erlangen-Nuremberg,  
Erlangen, Germany**

**Dr. N. Feistel, Burckhardt Compression AG,  
Winterthur, Switzerland**

**Reliability and economics of compression systems -  
recent trends in the market of  
reciprocating compressors  
March 27<sup>th</sup> / 28<sup>th</sup>, 2003 Vienna**

## **Abstract:**

Great demands are placed today on the reliability of dry-running process-gas compressors, due to the extraordinarily high costs resulting from any production losses. A simultaneous increase in the requirement for higher load parameters - particularly in terms of the pressure difference to be sealed and the average piston velocity - and longer maintenance intervals has led to a more frequent dimensioning of dry-running sealing systems at the limits of stable operation. However, it is not easy to define these limits, due to the special operational characteristics of gastight frictional seals, which differ notably from those of the comparatively leaky non-contact seals. The expression "gastight" is used to describe elements which provide complete (i.e. axial and radial) covering of all ring joints normally present inside piston-rod sealing systems (packings). Accordingly, the processes taking place in such sealing systems are to be investigated by conducting experiments on a specially equipped crosshead compressor.

## 1 Introduction

The components of a crosshead compressor which mainly impose restrictions on its maintenance intervals include the compressor valves and, not least of all, the sealing and guiding elements. For reasons related to costs, energy and the environment, preferred use is made today of oil-free compression by a dry-running compressor, the cylinders of which do not require the usual external lubrication. Operators would like to see dry-running compressors gradually assume the tasks presently being performed by lubricated machines.

Due to the large number of parameters, however, it is not easy to define the limiting range in which dry-running seals can still be operated dependably. A prerequisite for reliable design is a detailed knowledge of the tribology of dry-running frictional systems<sup>1,2</sup> and the loads exerted on the individual sealing elements during operation. However, the load parameters imposed on such a sealing system can only be established at its borders through known compression and ambient variables. In contrast, the spatial and temporal distribution of the pressure difference within a serial arrangement of sealing elements, and the effects of this distribution on the sealing characteristics of the various combinations of sealing-element design and dry-running material are not fully known.

The experimental investigations conducted so far on oil-lubricated sealing systems<sup>3,4,5</sup> consisting mainly of metallic sealing elements do not provide a

consistent representation of the processes taking place inside sealing systems of crosshead compressors; this is attributable primarily to the different boundary conditions prevailing during the experiments. In spite of the consequently restricted comparability of individual experimental results, however, the pressure distribution over a serial arrangement of sealing elements is evidently not uniform.

## 2 Function, design and characteristics of dry-running sealing systems

A dry-running sealing system of a crosshead compressor is intended to seal a pressure difference in the presence of reciprocating motion, during which process it is necessary to ensure constant and minimal leakage over the longest possible operating periods. In the case of frictional sealing elements possessing the characteristic of wear compensation, operational behaviour is decisively influenced by the degree of wear as well as other parameters, as shown schematically in Fig. 1.

The expression "gastight" is used to describe elements which provide complete (i.e. axial and radial) covering of all ring joints. Gastight sealing elements are typically used in piston-rod sealing systems – so-called packings – requiring elaborate joint covering to prevent a release of process gas to the environment. Gastight piston rings of different designs are also employed in cylinders intended, for example, to compress gases of a low molecular weight to high pressures.

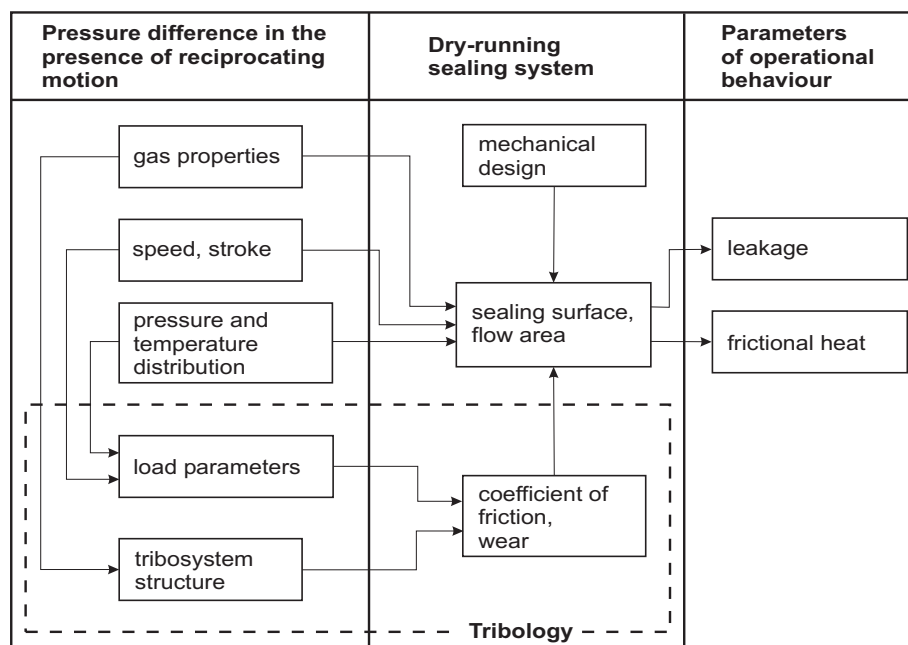


Fig. 1: Parameters influencing the operational characteristics of a dry-running sealing system in a crosshead compressor

Prof. G. Vetter, Dr. N. Feistel: Investigation of the operational behaviour of dry-running piston-rod sealing systems in crosshead compressors

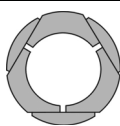
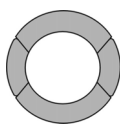
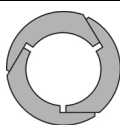
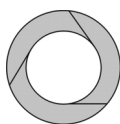
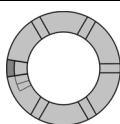
Design	Definition	Wear	Class	Shape	Cover ring
	<b>S1</b> six-piece, tangential cut	limited by design	segmental sealing rings	symmetric	necessary
	<b>S2</b> four-piece, unequal segments	unlimited			
	<b>S3</b> three-piece, step bridge (penguin style)	limited by design		asymmetric	
	<b>S4</b> three-piece, tangent to internal diameter (TID)	unlimited			not required
	<b>S5</b> twin ring	limited by design	one-piece rings		

Table 1: Characteristics and classes of various sealing-element designs

The wide spectrum of piston-rod sealing elements, designed similar to piston rings in some cases, is especially suitable for describing the various design features involved. The different designs can be classified roughly into sealing elements consisting of either several individual segments, or one or more one-piece rings. This distinction is of particular significance to the type of wear compensation, which is achieved through a radial or tangential shift of individual segments in the case of segmented sealing elements, and through elastic/plastic deflection of a curved beam in the case of one-piece rings. In addition to various segmented packing rings, Table 1 accordingly also shows a combination of two one-piece rings bearing a close resemblance to the twin piston ring. The twin packing ring similarly consists of an L-shaped and a rectangular ring section which are joined to form a sealing element. However, a difference in the case of the twin packing ring (simply

termed twin ring in the following) is that the L-shaped ring

constitutes the main wearing element, while the rectangular ring is used to seal the step cut joint in the radial direction and mount the garter spring. The step cut joint eliminates the need for an additional cover ring usually required for axial joint sealing. The elaborate combination of step cut joint and integrated radial cover ring used for sealing this single joint results in a very tight design which serves to elucidate the differences between the typical, segmented packing seals and the piston sealing elements.

### 3 Experimental approach and test packing set-up

To allow an investigation of the influence of parameter variations on the pressure and temperature distribution inside the sealing system and its leakage, the parameters need to be measured during operation and evaluated subsequently. In principle, such measurements can be performed inside the cylinder<sup>4</sup> and on the piston rod<sup>3,5</sup>. Since a transmission of signals from the reciprocating piston can only be achieved through techniques which are not only complex but also susceptible to errors, and because variations in the configuration of the sealing system are severely restricted, a decision was made in favour of investigating piston-rod seals.

A horizontal process-gas compressor operated with nitrogen and converted specially for the purpose of measuring a packing's leakage and internal distribution of pressure and temperature<sup>8,9</sup> was used as a basis for experimental investigations of the operating characteristics of dry-running sealing systems in a crosshead compressor. All the measured pressure signals are represented as excess levels with respect to the ambient pressure (gauge pressure). A piston rod made of 34 CrAlMo 5 nitrided steel and having a diameter of 50 mm,

hardness of 900 HV and a surface roughness of  $0.12 \leq R_a \leq 0.25 \mu\text{m}$  was used as the opposing body for the sealing elements. Fig. 2 shows the principle design and dimensions of the test packing.

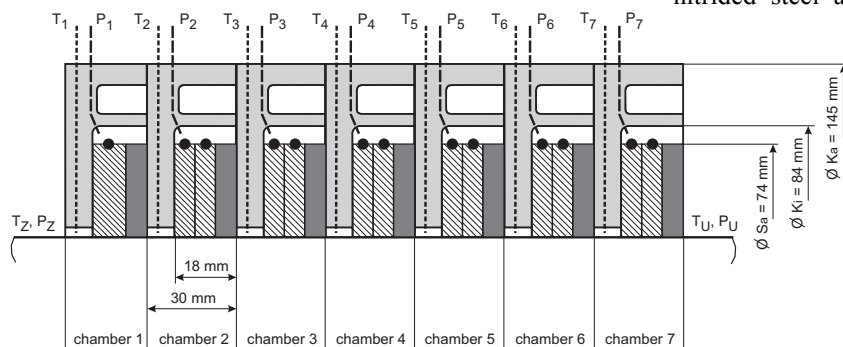


Fig. 2: Design and geometric dimensions of the test packing

#### 4 Special operating characteristics of gastight sealing systems

For the experimental investigations to provide clearly analysable results within a restricted time period, demanding operational conditions were to be created without causing any overloading. For this reason, a suction pressure of 2.5 MPa and final pressure of 6.0 MPa were selected to generate the pressure difference, the average piston velocity being 4.0 m/s. The test object for determining the load parameters comprised a packing consisting of six six-piece sealing elements made of PTFE filled with carbon/graphite and each equipped with a three-piece, radially cut cover ring and an one-piece, uncut anti-extrusion ring made of sintered iron. As is the case in most piston-rod sealing systems, the frictional sealing elements were preceded by a so-called throttle ring designed as a contactless gap seal.

After a brief, initial period of stable operation, the selected load parameters started to cause overloading. The measured values in Fig. 3 indicate that the temperature in certain chambers rose notably after just a few hours; on attainment of a peak value of 180 °C in chamber 6 after slightly less than 24 hours, the experiment finally had to be stopped. It is clearly evident that the highest temperatures occurred not at the packing inlet, but in the chambers located furthest away from the compression chamber. It is only following step-by-step reductions in the suction pressure to 1.6 MPa, the final pressure to 4 MPa and the average piston velocity from 4 to 3.19 m/s that stable operation was achieved at low temperatures of around 80 °C.

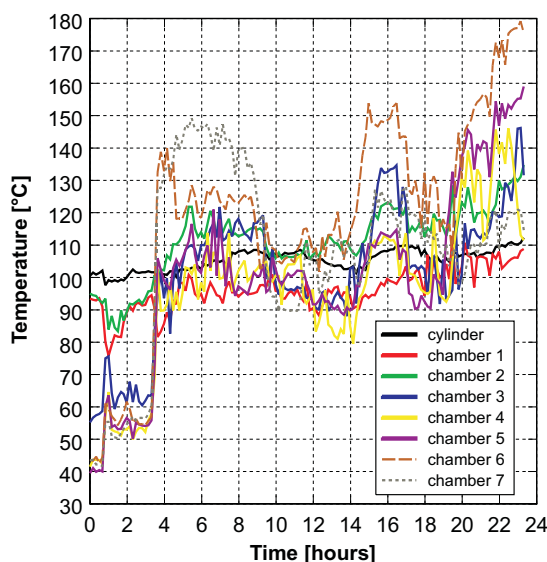


Fig. 3: Overloading of the test packing resulted in a rapid temperature rise, the peak values being measured in the sealing element chambers located furthest away from the compression chamber

Fig. 4, top shows the pressure curves measured inside the individual ring chambers during stable operation as a function of the crank angle. Clearly, the throttle ring does not contribute significantly toward sealing the pressure difference. The first frictional sealing element adjoining the throttle ring seals the remaining part of the pressure component varying between the suction and final levels, termed dynamic pressure component in the following. The residual, static pressure component of the total pressure difference is equal to the suction pressure of 1.6 MPa. This part is only sealed by the last of the sealing elements located furthest away from the compression chamber. No pressure drop is measurable across the flow through sealing elements three to five, i.e. the sealing efficiency of these elements is negligible compared with the sealing elements under instantaneous load. These different sealing effects are attributable to the varying flow area, which depends mainly on the prevailing pressure difference - a characteristic of gastight contact seals.

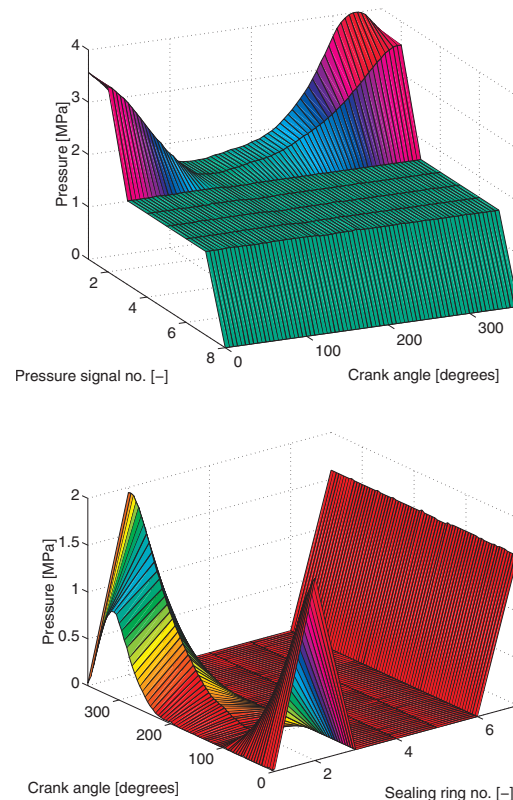


Fig. 4: Measured pressure distribution (top) and characteristics of the individual pressure components (bottom) sealed by the individual sealing elements for a packing consisting of one throttle ring and six six-piece sealing elements

Representing the measured pressures in the form of pressure differences sealed by the respective sealing elements as a function of the crank angle results in the characteristics shown in Fig. 4, bottom. Here, it is evident that although the first frictional sealing element seals the largest numerical pressure difference, it only does this over a small range of crank angles. In contrast, element 6 which seals the suction pressure is subjected to a constant load during any complete rotation of the crankshaft. This explains why the highest temperatures in the previously described overload experiment were measured in the vicinity of the packing outlet.

## 5 Influence of sealing-element design

The experiments with sealing elements of various designs were intended to demonstrate their typical operating characteristics until stable conditions in the run-in state are reached. PTFE filled with carbon/graphite was used as a dry-running material for all sealing-element designs investigated as part of this experiment series. Use of a throttle ring was avoided in order to ensure clearly identifiable conditions under which the dynamic pressure component would act on the contact seals. Every test packing accordingly comprised six sealing elements of the design under investigation. For the load parameters values of 1.6 MPa for the suction pressure, 4.0 MPa for the final pressure and 3.19 m/s for the average piston velocity were selected which had resulted in stable operating conditions in the preliminary experiments.

The pressure and leakage curves ascertained for the various packing ring designs can be used to demonstrate the principal differences in the operational behaviour of gastight sealing elements. While in the case of all designs investigated the sealing of the dynamic pressure component was performed entirely by the first sealing element right next to the compression chamber, differences were revealed concerning the sealing of the static pressure component. Designs with a slightly higher leakage rate tend to seal the static pressure component by means of the last sealing element located furthest away from the compression chamber. This type of pressure distribution achieves a high stability, and designs which typically exhibit this condition immediately after having been started in the new state turn out to possess a highly reproducible operational behaviour. Fig. 5, top shows the temporal pressure distribution for a packing comprising six six-piece sealing elements with symmetrically cut segments. The relatively

constant leakage rate was calculated as having an average value of  $0.97 \text{ sm}^3/\text{h}$ .

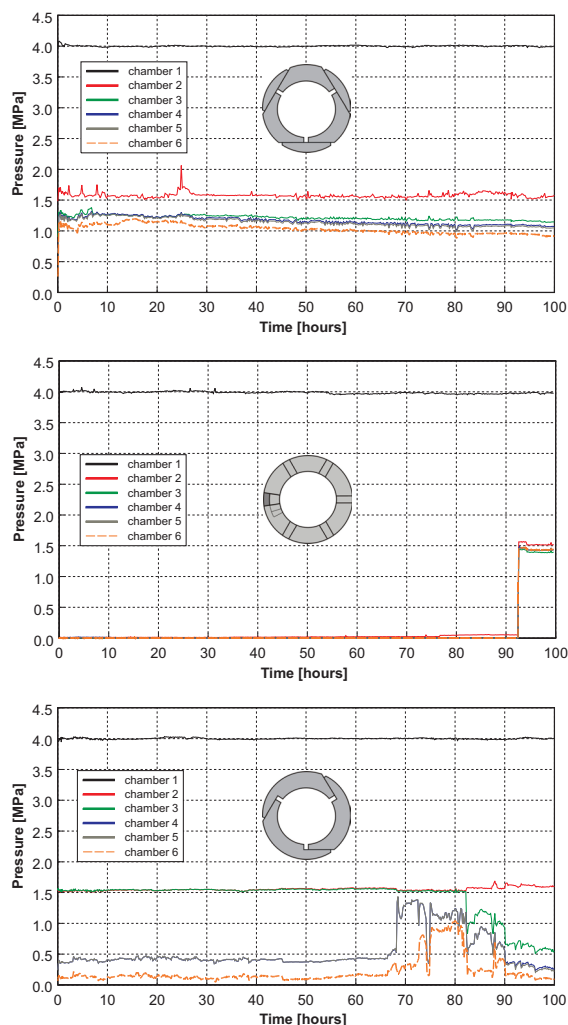


Fig. 5: Pressure distribution vs. time of six sealing elements of the designs designated six-piece „S1“ (top), twin-ring „S5“ (centre) and three-piece, step bridge „S3“ (bottom)

In the case of designs which exhibit a very low leakage due to a more effective joint sealing, the element activated for sealing the static pressure component depends, above all, on differences in production quality and deviations from the optimal alignment to the piston rod during installation. Understandably, it is difficult to predict which element will seal the suction pressure component, and the reproducibility of operational behaviour is correspondingly poor here.

The higher the sealing efficiency, the greater the tendency to seal the suction pressure in the proximity of the compression chamber, as demonstrated by the twin-ring design incorporating a sole, elaborately sealed joint (Fig. 5, centre). Over



Prof. G. Vetter, Dr. N. Feistel: Investigation of the operational behaviour of dry-running piston-rod sealing systems in crosshead compressors

a period of 90 hours, the first element of the twin-ring packing sealed both parts of the total pressure difference: dynamic and static pressure components (average leakage:  $0.15 \text{ sm}^3/\text{h}$ ). In view of the desired increase in the performance of dry-running

sealing systems, however, this concentration of the entire pressure difference on a single sealing element proves to be a highly unfavourable operating characteristic, even if it does not yet result in overloading in the case of the load parameters used here.

In addition to systems exhibiting a stable sealing of the pressure difference by one or two sealing elements, investigations were also performed of sealing systems exhibiting a continuously variable pressure distribution. In this case, the three-piece, step bridge design with its asymmetrically cut segments turns out to have a special behaviour (Fig. 5, bottom). A brief transient phase exhibiting a stable pressure distribution essentially among two sealing elements (average leakage:  $0.19 \text{ sm}^3/\text{h}$ ) was abruptly followed by a fluctuating phase in which the remaining sealing elements also contributed briefly and to different degrees to the sealing effect. However, the dynamic pressure component continued to be sealed stably by the first element. The rapid, stochastically changing pressure distribution also influences the leakage rate, whose average value was ascertained as being  $0.62 \text{ sm}^3/\text{h}$  in this case.

A comparison of the average pressure differences determined for the individual sealing elements over the entire duration of the experiments with the wear ascertained after the experiments shows that the dynamic and static pressure components result in differing wear characteristics depending on the design in use. If the average wear of a sealing element is expressed with respect to the average, sealed pressure difference and the sliding distance, one obtains a characteristic parameter similar to the wear coefficient commonly used in tribology. In this case, however, it is necessary to consider the fact that the external pressure applied to the sealing element does not describe the actual load exerted on the sealing surface.

Fig. 6 shows the wear coefficients calculated accordingly for the sealing elements subjected to the highest dynamic and static pressure components in the case of all investigated designs. This representation reveals notable differences in the dynamic and static wear characteristics of the various designs, in spite of their identical sealing-ring material. The three-piece, step bridge design

(S3) exhibits the lowest value under static load. With a dynamic load value almost five times as high, however, this design possesses a high sensitivity to the pulsating pressure component, similar to the four-piece ring with unequal segments (S2) and the three-piece ring cut tangentially with respect to the internal diameter (S4). The twin ring (S5) as the sole representative of the one-piece design turned out to have the most favourable wear characteristics under dynamic load.

The different effects of the dynamic and static pressure components on the wear characteristics of the individual sealing-element designs can be used to optimize sealing systems during their practical configuration. Depending on the composition of the pressure difference to be sealed, it might be advisable to replace the usually homogeneous sealing system with a combination of two or more designs. For example, twin rings and a three-piece, step bridge design are suitable respectively for sealing dynamic and static pressure components.

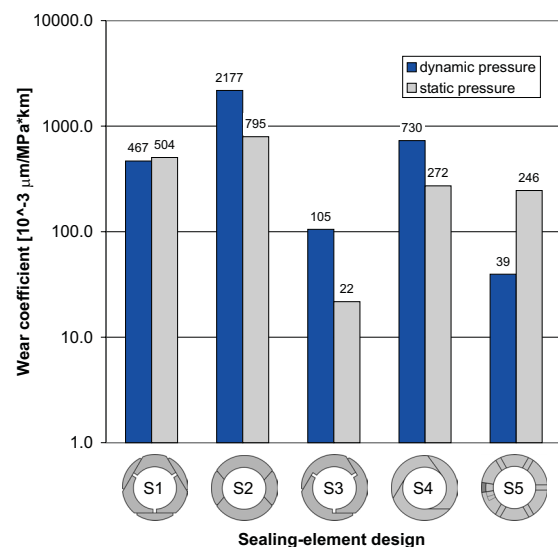


Fig. 6: Wear coefficients of various sealing-element designs subjected to static and dynamic pressure

## 6 Effect of the pressure difference to be sealed

The previously described experiments on the six-piece sealing elements revealed a stable and reproducible pressure distribution at both ends of the sealing system. Fig. 7 shows that new, six-piece sealing elements comprising filled PTFE exhibit this typical pressure distribution over a wide range



of suction/final pressure combinations between 0.4/1.0 and 4.0/10.0 MPa. The displayed pressure distributions consist of average values obtained during measurements lasting roughly four hours in each case. During the last load step, however, the high static load exerted by a suction pressure of 4.0 MPa led to a rapid temperature rise in the vicinity of the packing outlet, so that this experiment had to be stopped after two hours.

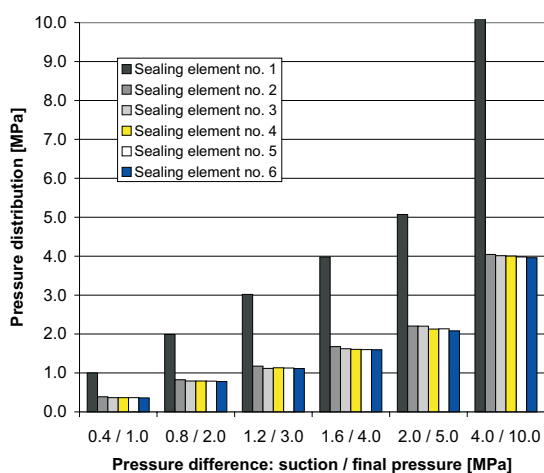


Fig. 7: Pressure distributions in a packing with six six-piece sealing elements (S1) for various combinations of suction pressure and final pressure ( $cm = 3.19$  m/s)

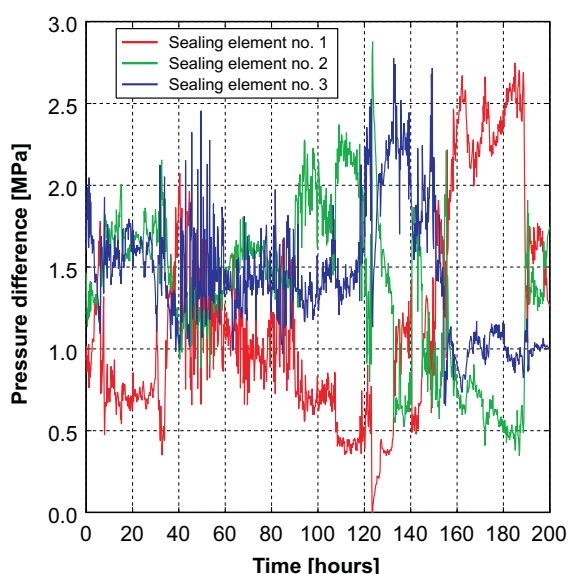


Fig. 8: Pressure differences vs. time of a packing comprising three sealing elements of the step bridge design (S3) consisting of filled PTFE,  $p_s = p_d = 4$  MPa,  $cm = 3.19$  m/s (scanning rate: 300 s)

In the case of the six-piece design, a further increase in the pressure difference is consequently

limited by sealing of the suction pressure component by means of a single sealing element and the high temperatures resulting therefrom. This also applies to nearly all the other investigated designs. However, the three-piece, step bridge design exhibits favourable characteristics for sealing static pressure differences. The special behaviour of this type of element when sealing static pressure was therefore investigated more closely in a separate experiment. For this purpose, three sealing elements comprising filled PTFE were subjected to a purely static pressure difference of 4.0 MPa. Fig. 8 shows that the distribution of the suction pressure also changes continuously under these experimental conditions. Averaging the pressure components corresponding to the three rings results in low load levels (Table 2), so that no temperature rise occurred during the entire experiment.

	S3 no. 1	S3 no. 2	S3 no. 3
average pressure load	1.18 MPa	1.37 MPa	1.44 MPa
average wear of ring segments	0.27 mm	0.19 mm	0.26 mm
wear in the middle of the segments	0.50 mm	0.33 mm	0.49 mm
average wear at the segment ends	0.16 mm	0.11 mm	0.14 mm

Table 2: Average pressure load and wear of three sealing elements of the step bridge design (S3) consisting of filled PTFE after 200 hours,  $p_s = p_d = 4.0$  MPa,  $cm = 3.19$  m/s

This special operating characteristic is due to an uneven material removal over the individual segments, the maximum wear occurring typically in the middle of each segment (Table 2). Although an uneven loss of material from the frictional surfaces was established in the case of all sealing-element designs, it has special consequences for the sealing function of the three-piece, step bridge ring. With this design, radial joint sealing is also achieved by the main segments, so that an uneven removal of material opens the sealing surfaces between the individual segments (Fig. 9). While this often leads to failure by fracture in the case of materials with a low ductility, pressure differences applied to materials with a strong tendency to creep result in elastic/plastic deformations of the bridge pieces, accompanied by changes in the flow areas and consequential alterations in the pressure distribution inside the sealing system.

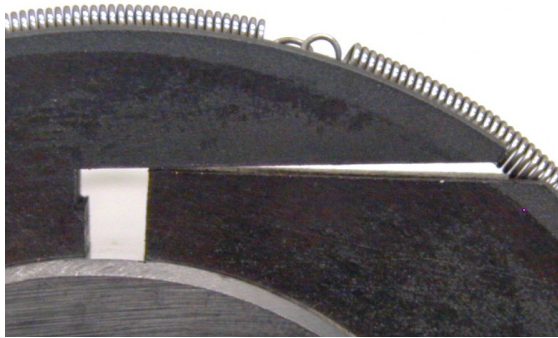


Fig. 9: Formation of gaps around the joint of a step bridge design (S3) comprising filled PTFE, resulting from an uneven material removal, the maximum wear occurring in the middle of each segment

## 7 Influence of the sealing-element material

The carbon/graphite-filled PTFE used as material for the sealing elements in the previously described experiments possesses good lubrication properties as well as a high ductility, but only average to poor strength and a strong tendency to creep, thus restricting its suitability to applications involving relatively low load parameters. Demanding applications involving high pressure differences and / or high temperatures are therefore realized mainly using high-temperature polymers modified specially for dry-running by means of solid lubricants. PEEK, a typical representative of this material class, is filled with PTFE, carbon fibre and graphite. As shown in Table 3, the modulus of elasticity determined at 150 °C in the bending experiment in accordance with DIN 53 452 is more than 7 times higher than the value for PTFE with a carbon/graphite filling. In addition to filled fluorocarbon and modified high-temperature polymers, polymer blends are also used specially for extremely dry gases. A frequently employed variant of such a polymer blend is a PTFE/PPS mixture, filled with graphite and carbon fibre, and characterized by a much lower ductility compared with carbon/graphite-filled PTFE.

	carbon/ graphite- filled PTFE	PTFE/ PPS- polymer blend	modified PEEK
elongation after fracture, RT	16.4 %	6.3 %	3.4 %
elongation after fracture, 150 °C	15.7 %	7.4 %	7.5 %
flexural modulus of elasticity, RT	1285 MPa	2137 MPa	3856 MPa
flexural modulus of elasticity, 150 °C	309 MPa	408 MPa	2304 MPa

Table 3: Mechanical properties for typical representatives from the three main groups of material for dry-running sealing elements, obtained from bending experiments in accordance with DIN 53 452

The effects of the sometimes notably different physical/mechanical properties of the various materials on the operating characteristics of sealing systems are to be demonstrated using a step bridge design (S3) as an example. For this purpose, a number of experiments involving six sealing elements comprising filled PTFE, polymer blend and modified PEEK were conducted, in each case at an average piston velocity of 3.19 m/s, suction pressure of 4 MPa and final pressure of 10 MPa. Fig. 10 shows the pressure signals measured in the individual chambers of the packing under these conditions. Whereas in the case of all three investigated materials, the dynamic pressure component is sealed by the first element in a manner typical of gastight designs, material-related differences were observed during the distribution of the static pressure component among several sealing elements.

In the case of the design comprising filled PTFE, the distribution of the suction pressure fluctuated rapidly among the remaining five sealing elements, so that the average value of the measured pressure signals results in an almost ideal, stepped reduction in suction pressure, as shown in the bar chart. The leakage rate, which fluctuated notably, was calculated as having an average value of 2.5 sm<sup>3</sup>/h. In the design involving the polymer blend, however, the suction pressure was initially sealed fully by the last element, as in the case of the six-piece design. Only after a test duration of approximately 30 hours there was an abrupt transition to an even and stable distribution of the suction pressure between the second and the last sealing elements, and an almost constant leakage rate with an average value of just 1 sm<sup>3</sup>/h.

The step bridge design exhibited the least favourable operational characteristics in the design comprising modified PEEK, which also achieved a stable but uneven distribution of suction pressure among the last three sealing elements. The average value of the measured pressures shows that the largest part of the suction pressure was sealed by the last element. In addition, the high flexural modulus of elasticity and creep resistance of modified PEEK prevent the applied pressure difference from causing an elastic/plastic reduction of the joint gap, as in the case of filled PTFE, as a result of which high leakage rates between 5 and 7  $\text{sm}^3/\text{h}$  were measured here.

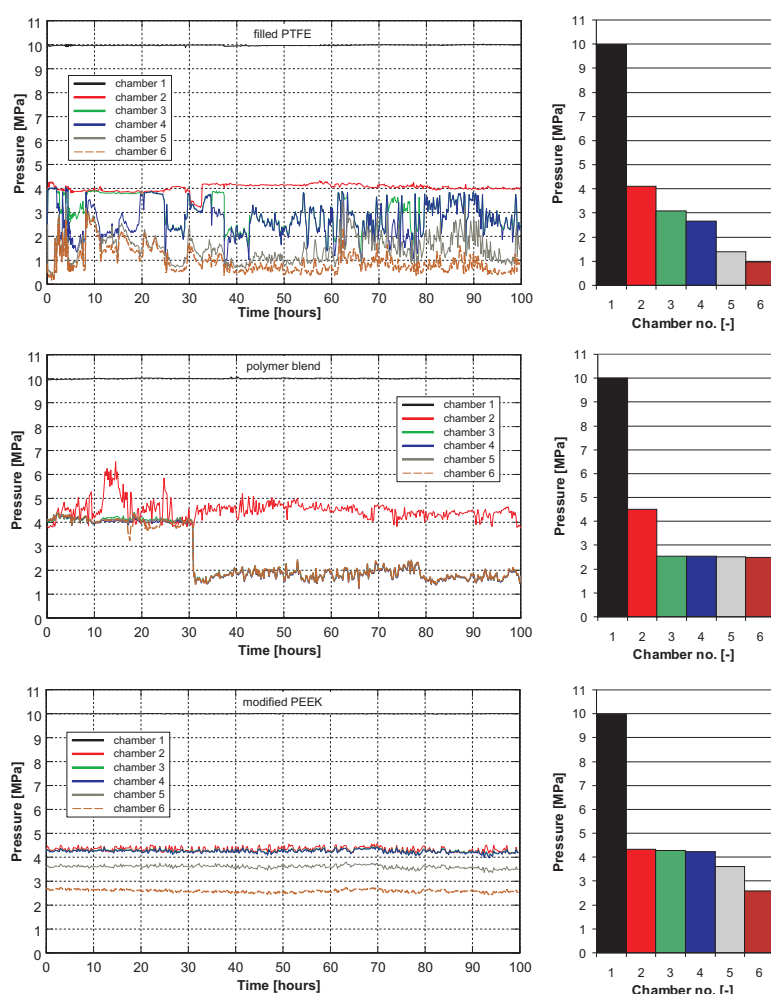


Fig. 10: Pressure vs. time and average values (bar charts) for packings consisting of six sealing elements of the step bridge design (S3) made of filled PTFE, polymer blend and modified PEEK,  $p_s = 4.0 \text{ MPa}$ ,  $p_d = 10.0 \text{ MPa}$ ,  $cm = 3.19 \text{ m/s}$

## 8 Effect of piston velocity

The piston velocity has a complex effect on the tribological quantities friction and wear of plastics; due to the partly high degree of heating of the frictional surfaces, dependencies similar to those in the case of temperature variations can be established in extreme cases<sup>6</sup>. In addition to significantly increasing the wear of the sealing elements, high average piston velocities can therefore also damage a dry-running sealing system by raising the temperatures of the frictional surfaces to impermissibly high levels. Moreover, a series of experiments conducted at different speeds showed

that an increase in the average piston velocity can also have a negative effect on the pressure distribution inside a sealing system.

As shown in Fig. 11, a distribution of the dynamic and static pressure components at both ends of a sealing system was measured at an average piston velocity of  $2.53 \text{ m/s}$  ( $474 \text{ min}^{-1}$ ) in an experiment lasting one hour. A rise in the average piston velocity brought about by increments in rotational speed led to a reduction of 50 % in the suction pressure on the last sealing element, the remaining suction-pressure component being sealed by the first element already subjected to the dynamic pressure component. Finally, at a rotational speed of  $756 \text{ min}^{-1}$ , nearly the entire pressure difference was sealed by the first element. The high load resulted in a rapid temperature rise, so that the experiment had to be stopped before its scheduled duration of one hour.

The additional concentration of the suction pressure on the first sealing element already subjected to the dynamic pressure component is due to an increasing sealing efficiency with increasing speed. The theoretically and

experimentally investigated increase in the sealing efficiency accompanying a rise in the pressure pulsation frequency is described in<sup>7</sup> for unsteady labyrinth flow. Accordingly, the improved sealing efficiency in the case of the gastight contact seals investigated here is also more likely a result of the increased frequency of the dynamic pressure component than the rise in the average piston velocity. For this reason, higher average piston

velocities in the case of gastight sealing systems should be achieved preferably through longer strokes instead of higher rotational speeds.

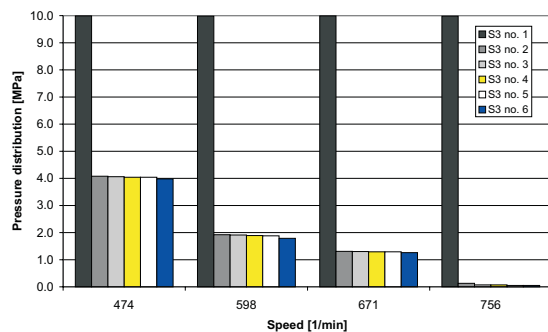


Fig. 11: Influence of compressor speed on pressure distribution of a packing consisting of 6 sealing elements of the step bridge design (S3) made of polymer blend (stroke = 160 mm),  $p_s = 4.0$  MPa,  $p_d = 10.0$  MPa

## 9 Summary

The experimental investigations made it evident that the heterogeneous, partly contradictory images of the pressure distribution in gastight contact seals are caused mainly by the vague conditions prevailing during sealing of the static pressure component. Whereas in the case of all investigated designs, the dynamic component of the pressure difference to be sealed is handled almost entirely by the first element located right next to the compression chamber, the sealing of the static pressure component depends on a large number of parameters. In the case of sealing elements with a particularly elaborate joint sealing, there is a danger of the dynamic and static pressure components being concentrated on the first sealing element, which can result in overload. This unfavourable behaviour is encouraged by high frequencies of the dynamic pressure component, in view of which high average piston velocities should be realized preferably through long strokes instead of high rotational speeds.

The split-up of the pressure difference into dynamic and static components results in differing wear characteristics in the case of the various sealing-element designs; this should be accounted for systematically in order to achieve the desired performance enhancement. Depending on the composition of the pressure difference to be sealed, it might be advisable to replace the usually homogeneous sealing system with a combination of two or more designs. For example, twin rings and a three-piece, step bridge design are suitable

respectively for sealing dynamic and static pressure components.

The experimental investigations also show that the operating behaviour of gastight contact seals is influenced to a large extent by the properties of the dry-running materials used. The often substantial differences which can occur among various dry-running materials given otherwise identical conditions are attributable mainly to the dependence of the wear compensation on the modulus of elasticity, ductility and creep resistance.

## Notation

P	pressure sensor
T	temperature sensor
c	piston velocity [m/s]
p	pressure [MPa]
s	suction
d	discharge
m	average
Z	cylinder
U	ambient conditions
PTFE	poly tetra fluoro ethylene
PEEK	poly ether ether ketone
PPS	poly phenylene sulphide

## References

- <sup>1</sup> Vetter, G.; Tomschi, U.: Zur Tribologie der Trockenlaufdichtungen von Hubkolbenverdichtern Pumpen + Kompressoren 1, 1995, S. 66 – 78
- <sup>2</sup> Tomschi, U.: Verschleißverhalten von Trockenlaufwerkstoffen für Abdichtelemente in Kolbenkompressoren Dissertation Universität Erlangen-Nürnberg, 1995
- <sup>3</sup> Scheuber, K.: Dynamische Druckverteilung in der Zylinderdichtung von Höchstdruckkompressoren Technische Rundschau Sulzer (1980) 3
- <sup>4</sup> Beckmann, W.: Ermittlung von Einflußfaktoren auf das Betriebsverhalten trockenlaufender Kolbenringdichtungen Dissertation TU Dresden, 1985
- <sup>5</sup> Raubenheimer, D.: The Behaviour of Reciprocating Compressor Piston Rod Packing I MechE 1990-7
- <sup>6</sup> Uetz, H.; Wiedemeyer, J.: Tribologie der Polymere München/Wien: Carl Hanser Verlag 1985

Prof. G. Vetter, Dr. N. Feistel: Investigation of the operational behaviour of dry-running piston-rod sealing systems in crosshead compressors

---

<sup>7</sup> Trutnovsky, K.; Komotori, K.:  
Berührungsfreie Dichtungen  
4. Auflage, VDI-Verlag, 1981, S. 24 – 44, S. 282

<sup>8</sup> Feistel, N.:  
Bestimmung der Kolbenstangen-Oberflächen-  
temperatur eines trocken laufenden Kreuzkopf-  
kompressors  
Industriepumpen + Kompressoren 3, 2001

<sup>9</sup> Feistel, N.:  
Beitrag zum Betriebsverhalten trocken laufender  
Dichtsysteme zur Abdichtung der Arbeitsräume  
von Kreuzkopfkompressoren  
Dissertation Universität Erlangen-Nürnberg, 2002

# API 618 Forced Response Studies

by:

**Brian C. Howes, M.Sc., P.Eng.**

**Derrick D. Derksen, M.Sc., P.Eng.**

**Kelly Eberle, P. Eng.**

**Beta Machinery Analysis Ltd., Calgary, Canada**

**Reliability and economics of compression systems –  
recent trends in the market of  
reciprocating compressors**

**March 27<sup>th</sup> / 28<sup>th</sup>, 2003 Vienna**

## **Abstract:**

API 618, 4th Edition, Design Approach 3, requires that the vibration and stress levels in compressor manifolds and piping be calculated. Studies M.6 and M.7 are described. However, many would insist that this type of analysis is impractical or ineffective.

In fact, there are uncertainties associated with the behaviour of the final system versus the modelled system. Most of these uncertainties are related to construction and installation variations.

This paper attempts to demonstrate that mechanical modelling is valuable in the design of compressor installations. Good design, however, must be combined with attention to detail in the implementation stage. At best, all vibration problems can be avoided at start-up. At worst, tuning the system, after start-up, to reduce vibrations can be achieved with minimal impact. This efficient tuning of the system is achieved through an understanding of the sensitivity of the system to added mass, and by the strategic provision of places for stiffening braces and supports.



## Introduction

API 618 contains specifications for modelling bottles and piping associated with reciprocating compressors. There are many reasons to do such modelling, but there are detractors who believe that the process has no value. We have found, however, that users of compressors who have experienced vibration problems after startup generally agree that forced response studies in the design stage are a good idea.

It is said that all models are wrong. This is true, but at issue is to what degree is a model wrong. Is there sufficient accuracy to provide useful information? There are limitations in the design stage regarding one's knowledge of the exact configuration of a system. After the design is completed, construction does not always conform to the design for various reasons. As a result, there will be differences between predicted and actual behavior of a system.

We see benefits from the modelling process, nonetheless. Examples are given that demonstrate what can be achieved with modelling.

## API 618 Specifications

An API 618 4<sup>th</sup> Edition, Design Approach 3 analysis specifies that the requirements outlined in Studies M.2 through M.8 be met. The most significant change in the 4<sup>th</sup> Edition from previous versions of API 618, and the level of analysis commonly performed in industry, is the requirement to determine vibration and stress levels in the compressor manifolds and piping (Studies M.6 and M.7).

From API 618 4<sup>th</sup> Edition, Appendix M:

**Study M.6 - Compressor Manifold System Vibration and Dynamic Stress Analysis:** Predict vibration and stress levels on pulsation bottles and closely coupled piping due to pulsation-induced unbalanced forces and cylinder gas loads.

**Study M.7 - Piping Dynamic Stress Analysis:** Predict vibration and stress levels in critical areas on piping and vessels away from the compressor due to significant pulsation-induced unbalanced forces. Areas will be defined as critical by the mechanical design and predicted unbalanced force levels.

Predicting vibration and stress levels in the compressor manifold area (Study M.6) is often more complex than predicting vibration and stress levels away from the compressor (Study M.7). Pulsation-

induced unbalanced forces can be obtained from an acoustical model. In the immediate compressor area it is important to not only include the pulsation-induced forces across the pulsation bottle or manifold and the close coupled piping, but the acoustical force acting between the pulsation bottle and cylinder gas passage on the suction and discharge side of the cylinder.

Cylinder gas loads that are to be included in a M.6 Study are often more influential than the pulsation-induced forces, especially for a reasonably designed acoustical system. Cylinder gas loads occur at all orders of run speed with the force at the fundamental order being the largest. Generally the lower orders are more significant than the higher orders. The relative magnitude of the harmonic components is a function of not only pressures but of cylinder loading. Whether or not a clearance volume pocket is fully open or closed, or if a cylinder is single acting or double acting can have a significant effect on the amplitude of the gas force at the different harmonics. For this reason it is critical to consider the full range of operating conditions in a M.6 Study and not just the design point of the compressor.

Note that the M.6 Study does not include the compressor residual unbalanced forces and moments. The scope of the analysis can be increased to include these excitation sources, but the model must be extended to include the frame, skid structure, and possibly the foundation.

## Goals of modelling

There are several goals of modelling the dynamic mechanical response of compressor systems. The obvious goals are

- Avoidance of mechanical resonance with known excitations [such as cylinder gas loads, pressure pulsation-induced shaking forces, and unbalanced forces and moments due to reciprocating inertias], though this is often not possible, such as with variable speed systems;
- Avoidance of excessive vibrations [see discussion of vibration problems below]; and
- Avoidance of stresses that could cause fatigue failures.

Less obvious goals are to provide

- suggestions for modifications to permit simple changes after start-up to correct vibration problems,
- a relationship between vibration and stress,
- an understanding of stress gradients in the vicinity of where a strain gauge might be installed,

- feedback to the designer of the pulsation control system when it could be better to reduce pulsations than to change the mechanical system response,
- understanding of the variations in vibrations with respect to operating conditions and load steps on the compressor. This information is particularly useful during start-up verification testing. It is necessary to compare the vibrations at the start-up condition with the vibrations that will occur when the system reaches the “worst vibration” condition and load step.

It would be interesting to predict the effect of pipe strain on vibrations and stresses in a system. However, this is a topic reserved for the installation and start-up verification testing. Suffice to say that pipe strain can have a negative effect on vibration characteristics of a piping system.

## Results of modelling

The results of model studies must be evaluated. A forced response study will provide predictions of mechanical natural frequencies, vibrations, and stresses. However, the designer needs to be prepared to decide if a vibration problem or a stress problem will exist. This process is not as straightforward as it might seem.

## Diagnosing a vibration problem

In the design stage:

- Use of vibration guidelines can provide an answer. However, vibration guidelines are empirical and are intended to be conservative. The chart shown in Figure 1 has two sets of guidelines that are more or less empirically derived. Inexperienced users need to use guidelines such as these with caution. Generally, stresses will be acceptable even if vibrations exceed the vibration limits.
- Sometimes vibrations are perceived as a problem after a compressor is put into operation even though stresses are not dangerous [e.g., damaged gauges, loosening bolts, uncomfortable to stand on the grating, visually unsettling movement of piping or vessels, etc.] In the design stage, previous experience from measuring vibrations on operating compressors should be used to help assess the need to reduce vibrations even though the associated stresses are predicted to be low enough.
- Appendages are excited by the vibration of the pipe. Absolute vibrations on the end of an appendage may be worse than differential movements relative to the pipe. Elimination of appendages or proper design of appendages will help to avoid problems predicted by the model.

- Relationships between vibrations and stress are geometry dependent. Consequently, no one guideline can be valid for an entire system.
- Stress is proportional to displacement. Overall true peak displacements must be used to compare to stresses, unless a single frequency is present. Use of RMS Overall vibration levels leads to under-predicting actual displacements, particularly around reciprocating machinery, where many harmonics are contained in vibration signatures.

In the operating system:

- Vibration guidelines are conservative so that they provide a screening tool. If vibrations are above guideline, consider the stress levels, or reduce vibrations.
- Meeting a vibration guideline does not guarantee the absence of a problem but risk is normally reduced to acceptable levels.
- It is useful to have predictions of vibration operating deflected shapes (ODS) and resultant stress to augment empirical guidelines. Compare measured ODS with the predicted ODS to ensure the validity of the predictions. This is more important at higher frequencies.
- Closely spaced natural frequencies can have distinctly different mode shapes leading to radically different stress levels for the same absolute vibration amplitude.

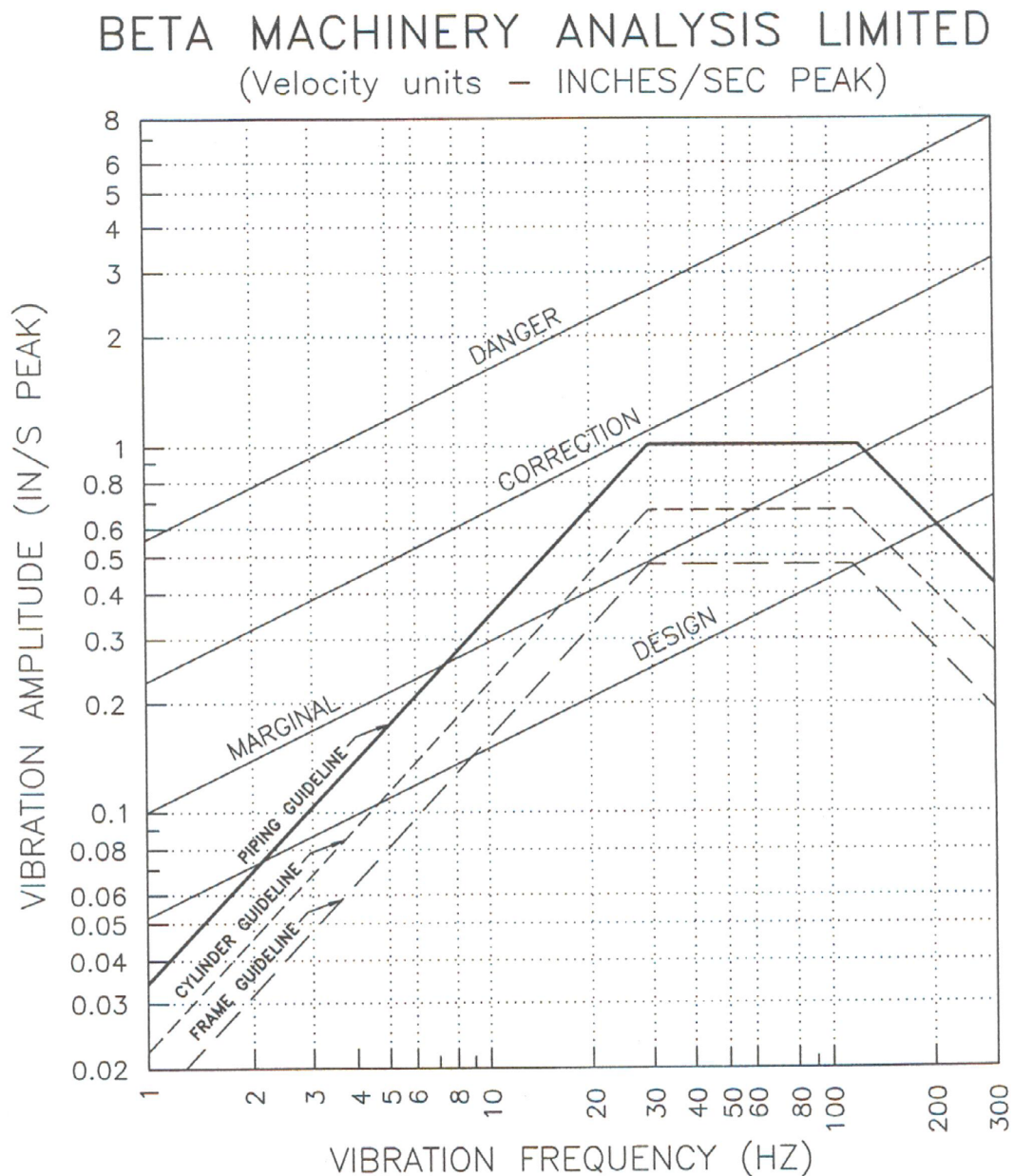
## Diagnosing a stress problem

- Guidelines for allowable stress are less empirical than guidelines for vibrations. Assumptions remain related to residual static stresses and stress concentration factors.
- Since residual weld stresses are indeterminate, stress relieving welds reduces the uncertainties associated with predicted stresses by making the endurance limit predictable.
- Stress measurement or prediction includes the effects of macro geometry (unlike vibrations compared to an empirical guideline), but is still affected by micro geometry (such as weld surface treatments).
- Assumptions regarding measurements are still implicit (Is the strain gauge at the point of highest strain? If not, what is the highest strain?)
- One can use empirical guidelines for allowable strains derived from experience. See Reference 1, for example.

## Use of mechanical natural frequency (MNF) predictions

- MNFs are faster and simpler to calculate than forced response studies [see Case History 1]

- Avoiding MNFs at 1X, and 2X shaft speed close to a compressor is generally viewed as a good idea, regardless whether a forced response study is done. (Most compressors have unbalanced forces and moments inherently due to reciprocating and rotating inertia.)
- Limit the analysis to MNF predictions until the system looks acceptable based on good engineering judgement and experience. Then do a forced response study.
- Determine the sensitivity of MNFs to mass and stiffness variations. This sensitivity informa-



### TYPICAL GUIDELINES FOR HIGH SPEED (1200RPM MAX.) SEPARABLE COMPRESSORS

The BMA\* guideline for piping vibration indicated by the solid bold line is based on the lesser of the following limits for piping:

- 10 MILS PEAK TO PEAK displacement
- 1 INCH/SEC PEAK velocity
- 2 G's PEAK acceleration

\* Adapted from SWRI and extensive vibration troubleshooting experience.

05-011-002  
02 REV. B 7/98  
D:\Office\QA\05\05011002.dwg

Figure 1

tion is of use in the field after start-up to de-tune resonances that have crept into the system for whatever reason [see Case History 2 for examples of variations in construction details].

- Provide an understanding of the location of MNFs relative to orders of run speed (using an interference diagram). If an MNF is predicted to be close to an order that has a propensity to cause high vibrations (either due to magnitude of the forces or the phase relationships), then checking ways to avoid such a resonance can be done at this stage. Consider adding welding pads to vessels or providing space for outboard cylinder supports in case additional supports are required after start-up. Changes to the bottles may be an alternative depending on the critical path of the project. Decisions to make such major changes should be made after evaluation of the forced response study's predicted stress or vibration.

### Usefulness of forced response studies

- Sometimes the forces and moments at 1X or 2X crankshaft speed are high enough to create high vibrations even though the system is non-resonant [see Case History 3]. A forced response model is the only way to predict such an eventuality.
- Sometimes cylinder gas forces at 3X or 4X are high enough to cause excessive resonant vibrations of the bottles. We have developed empirical rules to estimate the likelihood of such an occurrence, which helps when deciding to do a forced response study. However, only a forced response model will confirm a problem in the design stage. Changes to bottles may be required to solve such a problem, but bottle changes are not usually agreed to without compelling evidence.
- Operating conditions and load steps [hence forces] can vary. At start-up, it may be impractical to test the system over the entire range of conditions that are expected over the life of the unit. Therefore, it is useful to predict the vibrations and stresses for the system over the range of conditions that the unit will see. Due to the complex phase relationships among the many forces in a system, there is no other way to assess the various operating conditions to determine the worst case for stresses and vibrations.
- Tuning analyses can be done for fixed speed units. If vibrations or stresses are predicted to be high, changes in MNFs can be made to eliminate resonances. If a resonance does occur after start-up, the model will have provided an understanding of how to quickly and efficiently get rid of it.

### The modelling process

- Fast track work makes communications difficult. Some projects have a very short timeline. Difficulties with communication in both directions can occur. Careful planning of the project is required to avoid these problems.
- Detailed models of the vessels are required [brick and plate elements as opposed to beam models]. Beam elements can be used to model piping.
- Predictions of vibration and stress at resonance depend on damping, which does vary between systems. Experience with actual systems is the basis for deciding what value of damping to use in a model. We know of no way to predict system damping.

### Case histories

The first case demonstrates the need for accurate boundary condition information.

The second case shows that small construction variations can make a large difference to vibrations.

The third case demonstrates that forced response models are sometimes required to predict a problem.

#### Case history 1

The first Case History discusses a situation wherein the assumptions regarding the boundary condition at the base of a pair of scrubbers were wrong in the design stage. It had been assumed that the steel beams under the scrubber would be located such that they would transfer maximum stiffness from the concrete foundation to the base of the scrubber. High vibrations resulted after start-up due to resonance of the mechanical natural frequencies of the scrubbers with moments in the compressor acting at twice crankshaft speed.

Pictures of the finite element analysis models of the actual base are shown in Figures 2 and 3. The skid beams below the scrubber are modeled in great detail. The scrubber is modelled with plate or brick elements, rather than with beam elements.

The results of the new as built model were found to closely simulate the field measured mechanical natural frequencies, see Table 1. Then, after adding more anchor bolts, putting gussets on the skirts and filling the void under each scrubber with grout, the predicted results were acceptable. Refer to the table below for the comparative numbers for one of the scrubbers.



Description	Horizontal MNF (Hz)	Axial MNF (Hz)
Shop test “as built”	10	12
Field test “as built”	11	12.8
Model: scrubber without skid (rigid base)	15.4	15.4
Model: scrubber with skid	10.4	11.3
Model with modifications	15.2	15.3
Field test with modifications	15.3	17.8

Table 1: Predicted and Measured Scrubber MNFs

### Discussion:

Highlights from this case study are:

- Actual boundary conditions are required for accurate mechanical models.
- If the actual boundary conditions are modelled correctly, accurate results can be predicted by the model.
- The model results gave everyone involved the confidence to install the changes.
- The first set of changes was sufficient to resolve the problem. Trial repairs were not required.

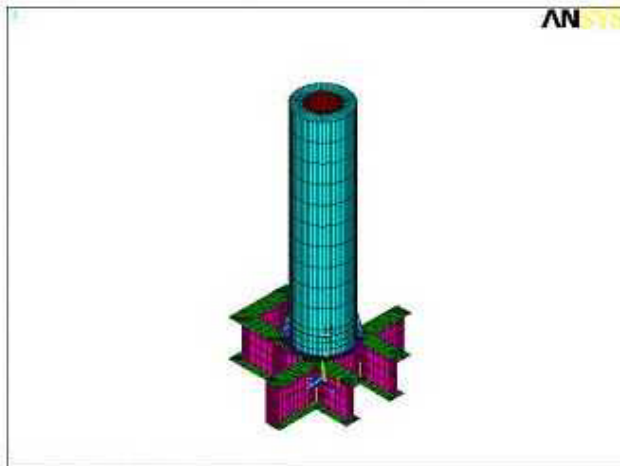


Figure 2: Scrubber and skid finite element model

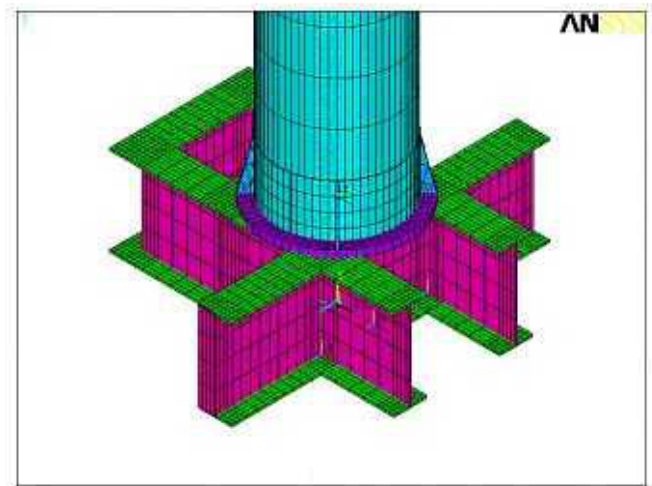


Figure 3: Detail View

### Case history 2

This Case History is included to point out the significance of small variations in construction details.

As discussed beside the photographs, there were variations in the construction of the supports (up-right location relative to the flange set, and cross-brace details). Superficially, these three support structures are the “same”. In practice they behave quite differently.

Tuning of the MNFs was required to obtain acceptably low vibrations. This was done with the aid of tuning masses designed with the assistance of a computer model. A limited amount of experimenting was needed to get the required MNFs.

Photographs of support structures for 3 separate “identical” compressors:



Note the differences in the locations of the cross-braces between the top unit and the other two. Extra flexibility was created by putting the brace in the middle of the upright as well as below the top of the upright.

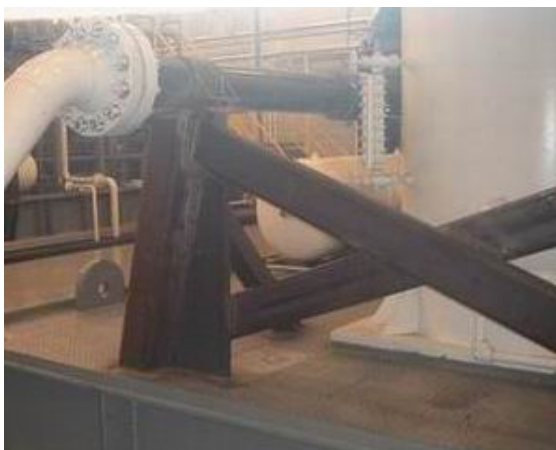
Another difference among the three units is the distance from the flange set to the clamp. The difference was not large, but was significant.

The top unit required several tuning weights to lower the MNF of the section of the piping to the left of the clamp. It had to be moved from near the top of 4 times run speed to near the bottom of 4<sup>th</sup> order.



The middle unit required a tuning mass to lower its MNF to just above the top of 4<sup>th</sup> order.

The bottom unit required no tuning mass to keep its MNF above 4<sup>th</sup> order.



### Case history 3

This Case History is included to demonstrate the need for forced response calculations in some cases. The original model of the frame and pedestal was done in the design stage. The mechanical natural frequency of that system was calculated and found to be above twice crankshaft speed. Avoidance of resonance with the couple at twice crankshaft speed

was considered to be sufficient to avoid vibration problems.

In operation, it was found that vibrations were too high at the first order of crankshaft speed. The unbalanced couple about a vertical axis was very



large. Vibrations increased with the square of the speed and peaked at the top of run speed.

Stresses were not considered a problem, although some discussions regarding the possibility of failure of the grout did occur. Our opinion was that as long as oil was not allowed to get between the grout and the steel, no problems would have occurred with the grout. A protective layer over the grout

was recommended to prevent oil contacting the grout.

The vibration was, in effect, a quasi-static response. The frequency of the couple at run speed was low compared to the MNF of the frame and pedestal. Inadequate static stiffness of the system was at fault, combined with the large couple in the compressor.

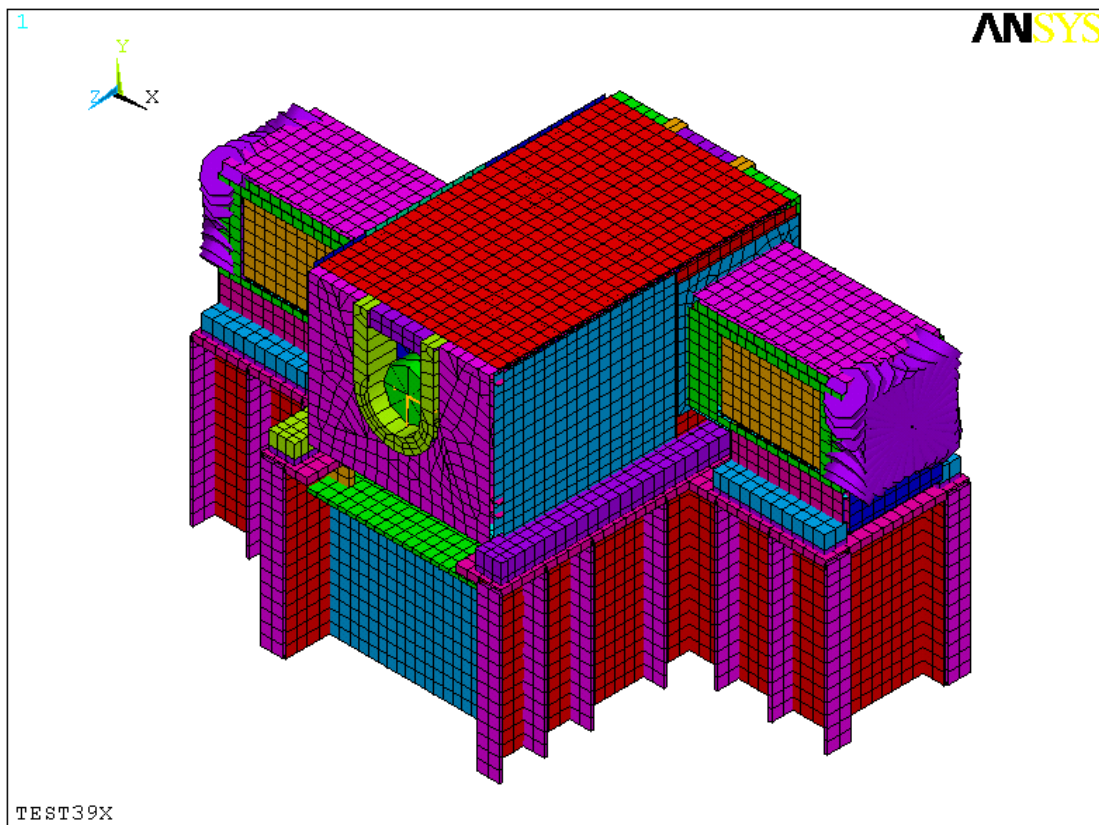
A new model was created of the pedestal and the frame. Forces from cylinder gas loads as well as the couple caused by the reciprocating and rotating weights were used to excite the system. Predicted vibrations were quite close to the field measurements. The need to include gas forces was surprising. If the frame were rigid, the gas loads would cancel. Flexibility in the frame results in additional movements of the frame and pedestal due to the gas loads.

Several changes were modelled. The first set of modifications made (steel plates on the ends of the pedestals and rotating counterweights on the crankshaft to reduce the vertical couple) was successful in reducing the vibrations to the guideline level supplied by the manufacturer. Several additional modifications (knee braces) had been suggested, but these were not required, as predicted by the model. A large incremental effort would have been required to introduce the additional changes. The model results gave us the confidence to do the limited set of modifications. Without the model, it is likely that the additional modifications would have been installed “just in case”.

The model of the compressor frame and the pedestal are shown below. The model included details of the compressor frame, compressor dog-house, compressor crankshaft, the grout layer between the frame and the pedestal, and the frame anchor bolts.

## Conclusions

1. API 618 mandated forced response studies can provide valuable insights into the performance of a reciprocating compressor system.
2. Experience has shown that not all risk of a dynamic force excitation related problems will be



eliminated by doing a forced response study. The risk of failure due to dynamic force excitation will be reduced to acceptable levels if a forced response study is conducted.

3. One key to conducting a meaningful forced response study is including sufficient detail in the models

## Reference

Acoustic Fatigue Involving Large Turbocompressors and Pressure Reduction Systems, by David E. Jungbauer and Larry E. Blodgett, Southwest Research Institute, San Antonio, Texas.

## Author biographies

### **Brian C. Howes, M.Sc., P.Eng. Chief Engineer**

Brian graduated from the University of Calgary with a Master of Science in Solid Mechanics. His thesis was entitled *Acoustical Pulsations in Reciprocating Compressor Systems*.

Brian has worked with Beta Machinery Analysis since 1972. In his present position as Chief Engineer for Beta, he has traveled all over the world, troubleshooting as far abroad as India, China and Venezuela.

Brian has many technical papers to his credit. The range of machinery problems they cover includes all manner of reciprocating and rotating machinery and piping systems, balancing and alignment of machines, finite element analysis, modelling of pressure pulsation torsional vibration testing and modelling, flow induced pulsation troubleshooting and design, pulp and paper equipment such as pulp refiners, etc. He has worked on hundreds of reciprocating compressor installations.

### **Kelly Eberle, P.Eng. Senior Project Engineer**

Kelly Eberle is a Senior Project Engineer for Beta Machinery Analysis Ltd., Calgary. His experience includes 14 years of troubleshooting problems and design for a wide range of equipment, with a primary focus on reciprocating compressor installations. He has a Bachelor of Science in Mechanical Engineering from the University of Saskatchewan.

### **Derrick D. Derksen, M.Sc., P.Eng. Project Engineer**

Derrick graduated from the University of Saskatchewan with a Master of Science in Mechanical Engineering in 1993. His thesis was entitled *The Effect of Wind on the Air Intake of Cooling Towers*.

Previous employment with Atomic Energy of Canada Limited and contract work with the University of Saskatchewan has developed his experience in experimental measurement, dimensional analysis, fluid dynamics, flow-induced vibration, acoustics, and finite element modelling.

Derrick has worked with Beta Machinery Analysis since 1997. In his present position as Project Engineer for Beta, he works on digital acoustic simulation, thermal analysis, and dynamic finite element analysis of reciprocating compressor packages. Developing analysis techniques and practical application of technology are an integral part of his daily duties.



**Burckhardt Compression**

# **Economic benefits of CAD-models for compressor manifold vibration analyses according to API 618**

**Eijk, A.**

**Flow and Structural Dynamics (PULSIM)**

**TNO TPD**

**Delft, The Netherlands**

**Samland, G.**

**Retz, N.**

**Sauter, D.**

**Research & Development**

**Burckhardt Compression AG**

**Winterthur, Switzerland**

## **Reliability and economics of compression systems - recent trends in the market of reciprocating compressors March 27<sup>th</sup> / 28<sup>th</sup>, 2003 Vienna**

### **Abstract:**

Reciprocating compressors, including pulsation dampers and the connected pipe system, are often the heart of an installation and should therefore operate reliable. Compressor manifold vibrations can contribute to fatigue failure of the system which can lead to unsafe situations, loss of capacity and increase in maintenance as well as repair costs.

To avoid these situations a compressor manifold analysis has to be carried out at a very early stage of the design of an installation. A compressor manifold analysis is an optional analysis in the 4<sup>th</sup> edition of the API Standard 618. However, in the 5<sup>th</sup> edition of the API Standard 618 this analysis is mandatory in a Design Approach 3 analysis.

In this paper it will be demonstrated that a compressor manifold analysis can be carried out in an accurate and economic way by means of a finite element substructuring technique, using FE models generated from CAD models. The accuracy of these models has been validated by means of a modal analysis.

## 1 Introduction

Reciprocating compressors are used in the field of oil refining, chemical and petrochemical industries, air separation as well as gas transport and storage. The compressor, including pulsation dampers and connected pipe work, often is the heart of an installation and should therefore operate reliably. Pulsation and vibrations may disturb safe and reliable operation.

To avoid vibration problems and to optimise the dynamic behaviour, it is common practice to carry out a so-called pulsation and mechanical analysis during the design stage of an installation<sup>3,1,9</sup>. These analysis includes the investigation of compressor manifold vibrations, which are the vibrations of compressor cylinders, distance pieces, crosshead guides, pulsation dampers and piping near the compressor. Especially for larger compressors, compressor manifold vibrations are important as the mass of compressor parts and pulsation dampers increases, which leads to low-resonance frequencies which may be excited by pulsation forces, by gas loads in the compressor cylinder, and by unbalanced forces and moments of the compressor<sup>4</sup>. Several actual cases have been encountered, in which pulsation forces have excited compressor manifold vibrations and caused fatigue failure.

In the 4<sup>th</sup> edition of the API Standard 618<sup>1</sup> the compressor manifold analysis is an option (option M5+M6 of appendix M). However, in the 5<sup>th</sup> edition of the API Standard 618<sup>2</sup>, this analysis is mandatory if a Design Approach 3 analysis has been specified. To keep the costs to a minimum, economic models have to be used to analyse the compressor manifold vibrations accurately.

In this paper it will be demonstrated that it is possible to use CAD models of compressor parts in an economic way for an accurate compressor manifold analysis. The method is based on finite element models of compressor parts, which have been achieved from CAD models. Despite large and complex finite element models, the method is efficient and easy to use and more accurate than usual analytical methods. Before going into detail on this method, a short overview of the pulsation and mechanical analysis will be given, followed by a description of the kind of compressor manifold vibrations which may occur. The procedure to achieve accurate finite element models from CAD models will be discussed. Examples of finite element models of a vertical and a horizontal compressor of equal size will be shown.

To validate the accuracy of finite element models, a modal analysis has been carried out for both the horizontal and the vertical compressor. The effect of boundary conditions will be discussed.

Finally the power and accuracy of the substructure technique will be presented.

## 2 Compressor manifold vibrations

### 2.1 General

Compressor manifold vibrations are a specialised and complicated form of vibration of a part of the piping, pulsation dampers and compressor parts such as cylinders, distance pieces and crosshead guides. Figure 2.1.1 shows an example of a compressor manifold.

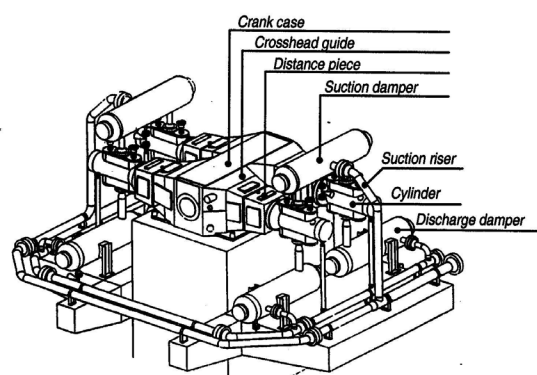


Figure 2.1.1: Example of a compressor manifold

If not properly controlled, these vibrations can cause fatigue failure of the system because compressor manifold mechanical natural frequencies can be excited by gas loads in the cylinder, by pulsation-induced forces in the cylinder and/or pulsation dampers and by mechanical loads of the compressor.

Some of the common compressor manifold vibrations have special names and are summarised as follows<sup>5</sup>:

- Low mode
- Rotary mode
- Cylinder resonance mode
- Suction damper cantilever mode
- Suction damper angular mode

The compressor manifold vibration modes as mentioned above, only occur in systems without connecting piping. In most practical cases, a part of the connected pipe system will also contribute to compressor manifold vibrations.

## 2.2 Compressor manifold analysis according to the API Standard 618

The procedure of a compressor manifold analysis according to the API Standard 618 is as follows<sup>3</sup>:

The first step in the analysis is to generate the mechanical model of the pipe system. The second step is to generate mechanical models of the compressor parts. These parts will be assembled and the lower mechanical natural frequencies will be calculated. For those cases where acoustical and mechanical natural frequencies coincide (worst-case situations), a forced response analysis must be carried out to calculate:

- Vibration levels of compressor and piping
- Cyclic stress levels in piping and pulsation dampers

Vibration and cyclic stress levels must be compared with allowable levels and in case of exceeding, modifications have to be investigated to finally achieve acceptable levels. The procedure is also indicated in the flowchart in figure 2.1.2. This paper will focus further on modelling and not on calculations.

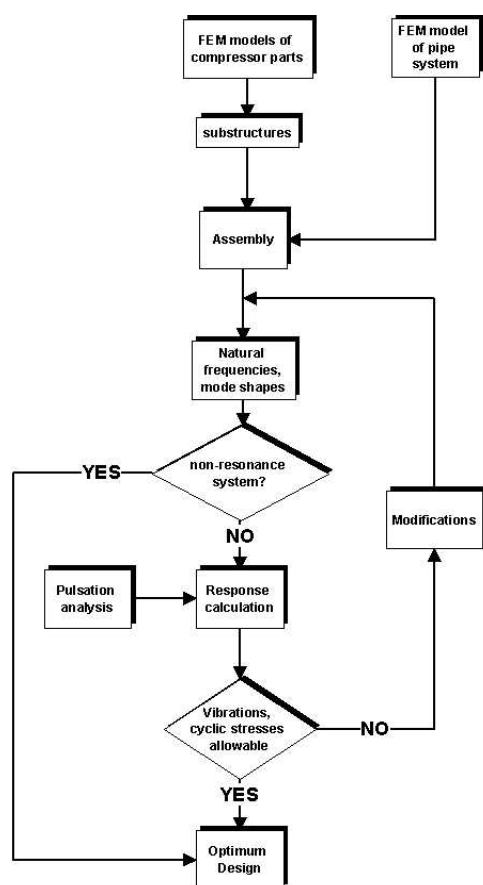


Figure 2.1.2: Flowchart of the API 618 compressor manifold analysis

## 2.3 Modelling

### 2.3.1 Pipe system

The pipe system as well as the structure on which the supports are mounted, can be modelled normally with Timoshenko beam-type elements. Some components of the pipe system, such as flanged<sup>6</sup> and branch connections, always require special attention because the flexibility of these parts can have a distinct influence on the natural frequencies of some compressor manifold vibration modes, such as suction bottle cantilever modes, suction bottle angular modes and cylinder resonance modes<sup>7</sup>.

Branch connections can be modelled by means of three translation and three rotation springs. For accurate calculation of spring constants and stress intensification factors (SIF's), a finite element model of the branch connection has to be made which is built up with shell elements. Calculated spring constants and SIF's are used then in beam type models of the pipe system.

### 2.3.2 Compressor parts

The flexibility and mass distribution of compressor parts such as cylinder, distance piece, crosshead guide and crankcase, are very important, because these parameters determine some of the possible compressor manifold vibration modes as described previously.

It strongly depends on the construction of the machine what parts have to be included in the calculations. In many cases, the distance piece is the most flexible part of the compressor. Together with the relative heavy mass of the cylinder these two parts determine the most important vibration modes. However, for compressor configurations the flexibility of the crankcase also plays an important role in some compressor manifold mode shapes. In this case the crankcase has to be included in the calculations.

Most cylinders can be modelled by means of concentric, relatively stiff pipe elements. Other parts can be modelled in several ways. An overview how dynamic properties (mass and stiffness) of compressor parts can be determined, is given below:

**Method 1:** Finite element models with only beam, spring and mass type elements

This method is the easiest way to model the compressor parts but is in most cases the less accurate modelling. Stiffened parts, such as crosshead gui-



des, are difficult to model with beam type elements and especially if the (local) flexibility of the crankcase and/or the crosshead guide have an important effect, these models will be less accurate.

Another complicated factor with this modelling is that field measurements have shown that the flexibility of the connection of some parts (cylinder/distance piece and distance piece/crosshead guide) can have an important effect on the natural frequencies of some compressor manifold vibration modes. To determine these effects, extensive measurements have to be carried out. Therefore it is not advised to use these models.

**Method 2:** *Finite element models with shell type elements only*

To overcome the disadvantages of the models of method 1, shell type finite element models can be used. Shell type models are far more accurate than beam type models but require more modelling effort than beam type models.

The disadvantage of shell type models is that some parts of the structure, such as the cylinder/distance piece and distance piece/crosshead connection and the foundation parts of the crankcase do behave rather as solid structures than as shell type structures, which can be source of an inaccuracy.

**Method 3:** *Finite element models with a combination of shell and solid type (and sometimes also spring) elements*

To overcome the disadvantages of the models of method 2, shell type finite element models in combination with solid type elements can be used. This requires some more modelling time but is more accurate. Without the usage of CAD models these are the most frequently used models for compressor manifold analyses.

**Method 4:** *Finite element models with solid type elements only*

The compressor parts can also be built up with solid type elements. However, this method requires much more modelling effort than the other methods and is normally not used when CAD models are not available. However, if CAD models are available the most logic step is to use this method.

### 3 CAD models of compressor parts

#### 3.1 Background

The traditional engineering approach is also known as "Serial Engineering". This conventional product development process has been largely sequential in

nature and segmented with some very hard breaks between the process phases i.e. each discipline performs its own individual function and passes the results to the next discipline in the serial chain. This conventional way of redesigning a product leads to rework, iterations with non-value-added changes and recalls, which can easily use up the profit margins of a new product.

If the work is done using an integrated development environment, a reduction of the design cycle time and a product value improvement at the same time is possible<sup>10</sup>. The Concurrent Engineering (CE) approach encourages teamwork and forces to focus on the expertise from all disciplines that are involved to work closely together in parallel right from the early stage of the product design and development stage.

The virtual, digital product is a substantial prerequisite for the concurrent or simultaneous engineering. On the basis of a central (CAD) data model the virtual product development is able to consider all aspects from the concept to the implementation phase.

#### 3.2 Current situation

Actually all revised, optimised or new compressors and their specific components are stored in the digital product database. Figure 3.2.1 shows the digital mock up of different components for a vertical compressor. In principle, these parts are accessible to a Finite Element Analysis (FEA). The analyses performed so far range from simple linear static analyses to complex, non-linear, transient dynamic analyses as well as to Computational Fluid Dynamics (CFD) analyses.

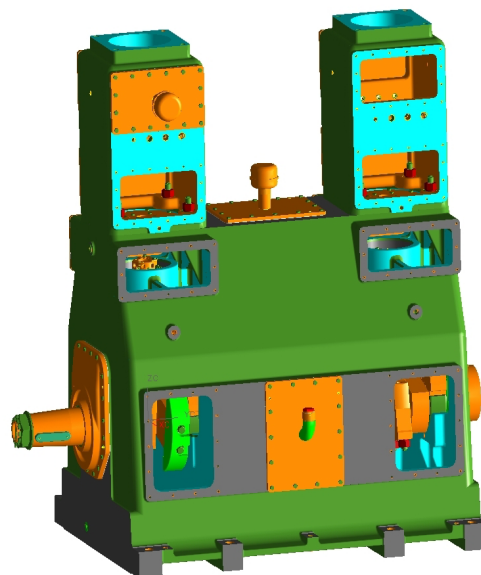


Figure 3.2.1: Digital mock up



As mentioned above CAD models are available for new types of compressor components. The appropriate CAD models are not available for older parts. But the experience over the past years in generating CAD models for the digital product database and transferring them to FE programs has led to the fact, that it is possible to provide these models in a very short time. If it is clear from the outset that the CAD models are only used for a FEA, the time for generation of the models can be further reduced. Appropriate simplifications are made from the beginning. Therefore, it is possible to provide a complex component like a compressor frame within one working day.

## 4 Conversion from CAD models to FE models

### 4.1 Basics

As a prerequisite, standardised methods how to build up the CAD model are a necessity to guarantee the further use of the models for various CAX techniques. The quality of the CAD-model has to be improved by these standardised methods in an early stage of the process. Another important factor for success are the CAD engineers themselves. The CAD user should have a common understanding of CAE in order to prepare the model in such a way that it can be used for further investigations. Preparing a model means for example neglecting threads in the model or very small radii for an optimisation run to reduce the time for the analysis.

There are special tools available in order to transfer CAD models into the FE program database. These tools either use a standard product data exchange for the translation between CAD/CAM systems (like IGES or STEP) or they translate the data through specific CAD interface programs.

In the present case the CAD models were built using the Unigraphics (UG) CAD System. Finite element analysis was performed with the ANSYS program. Initially, a specific UG interface program was used within ANSYS. Because of the number of errors and translation problems, the overall performance was not satisfactory. Better and stable conditions were obtained using the Parasolid interface. Parasolid is a core solid modeller and is used in a wide diversity of leading CAD/CAM/CAE systems. The CAD models are stored in UG in appropriate Parasolid files. These Parasolid models can then be converted into an ANSYS volume model and can be meshed without any problems.

Components with complex geometrical shapes like a compressor frame cannot be meshed usually with a mapped mesh, resulting in a brick shaped element mesh. Special second order tetrahedrons have to be used to mesh these volumes. These 10-node tetrahedrons have a quadratic displacement behaviour and are well suited to model irregular meshes such as produced from various CAD/CAM systems.

In the past large and/or complex volumes could only be meshed with first order tetrahedrons due to computer hardware reasons. This led to doubtful results by an artificial reinforcement of these elements. As a result of the increased computer capacity today only second order elements should and must be used. Comparisons of the results for different element types showed the appropriate accuracy.

The model in figure 4.1.1 is ready for the CAE. Details are removed and the model is reduced to the characteristics necessary for a FEA e.g. a modal analysis.

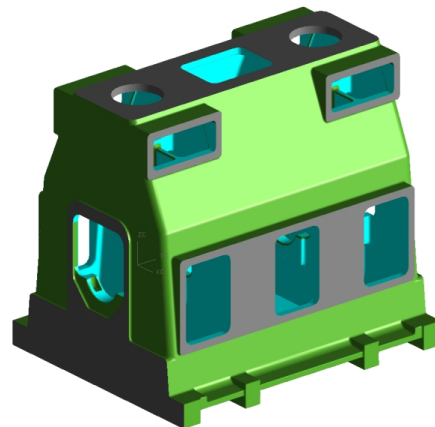


Figure 4.1.1: CAD-model ready for CAE.

## 4.2 Examples of modal analysis calculations

### 4.2.1 Compressor frame

For the modal analysis numerous calculations were accomplished. On the one hand, it has to be verified that the used element types as well as the number of the elements and/or nodes lead to the required accuracy. On the other hand, shell and solid models were compared to each other. The advantages of direct data transfer from CAD models should be pointed out by this comparison. As the foundation part of the frame does not behave like a shell structure, solid elements were used in this region. The

shell element model as well as the solid element model for the vertical compressor frame are shown in figure 4.2.1. Table 4.2.1 shows the calculated natural frequencies for the two different element types. The boundary conditions for the frame are fixed degrees of freedom (DOF) in the region of the hold down bolts. The results of the two models agree well (difference of the results for the first six modes < 3.5%). This means that both models could be used for an accurate modal analysis. However, as explained before solid models can be generated more easily with CAD models. Therefore, all further calculations have been carried out with solid element models derived from the CAD models.

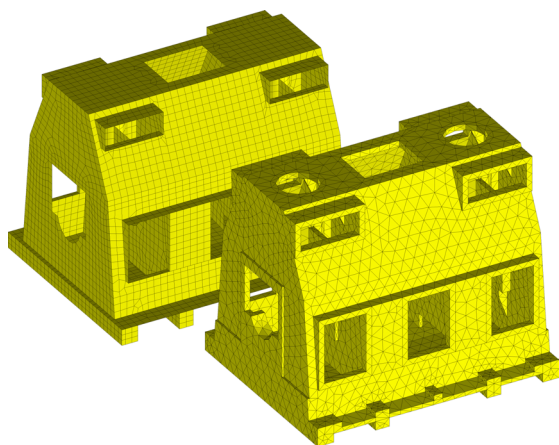


Figure 4.2.1: Shell/solid (left) and solid model (right) for the vertical compressor frame

Mode shape No.	Frequency [Hz]	
	Shell/Solid Element Model	Solid Element Model
1	126.2	123.9
2	150.3	155.9
3	157.3	158.4
4	159.2	160.2
5	187.1	187.6
6	187.8	188.8

Table 4.2.1: Natural frequency comparison between shell/solid element and solid element model (vertical compressor frame)

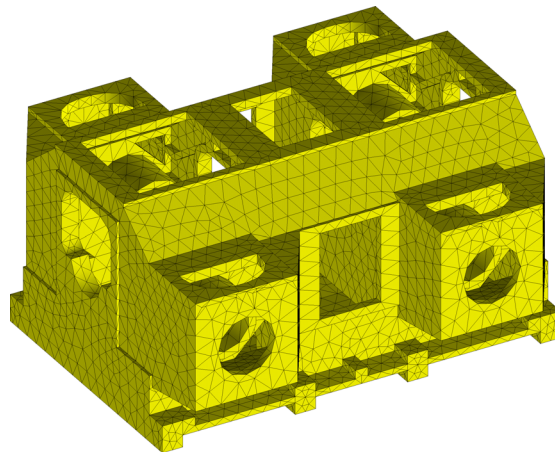


Figure 4.2.2: Solid element model of a horizontal compressor frame

In figure 4.2.2 another example of a solid element model of a horizontal 4-cylinder compressor frame is shown. The results of the natural frequency calculation of this model for different fixations have been summarised in table 4.2.2. The results clearly show the influence of a fixed or free foundation.

Mode shape No.	Frequency [Hz]	
	Fixed foundation	Free foundation
1	180.2	133.8
2	190.3	218.8
3	216.4	220.7
4	223.5	239.7
5	227.8	258.0
6	251.5	278.3
7	264.1	279.4

Table 4.2.2: Natural frequencies for the horizontal compressor frame with fixed / free foundation (solid elements)

#### 4.2.2 Complete compressor

The frame of the vertical compressor has been extended with distance pieces, covers and cylinders to model the complete compressor. The distance pieces were generated from the CAD model in the same way as for the frame. The cylinders of the machines can be regarded as rigid components and could therefore be substituted by a square-cornered block volume with the correct mass distribution. The appropriate supports were also taken into account, see figure 4.2.3. Table 4.2.3 shows the results of the natural frequency calculation of the most important mode shapes which have a large effect on the compressor manifold vibrations. This means that natural frequencies of internal parts such as bearing houses are not shown because in most of

the cases they do not have an important effect on the compressor manifold vibrations. Figure 4.2.3 also shows a plot of a mode shape at 24.8 Hz.

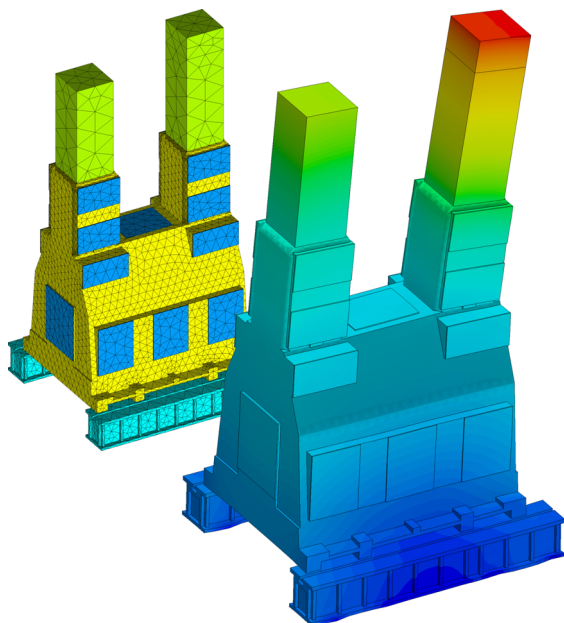


Figure 4.2.3: Complete compressor model (solid elements) including detailed supports for test bed run and corresponding mode shape at 24.8 Hz

Mode shape	Frequency [Hz]
1	24.8
2	25.3
3	34.9
4	35.2

Table 4.2.3 Table with natural frequencies for the complete vertical compressor (solid element model)

## 5 Validation measurements

### 5.1 General procedure

In order to validate the accuracy of the finite element models, an experimental modal analysis has been carried out for both the horizontal and the vertical compressor. The purpose of an experimental modal analysis is the determination of the modal parameters (natural frequencies and corresponding mode shapes), which can easily be compared with the modal parameters obtained from a Finite Element Analysis.

The compressors have been excited mechanically by means of an impulse hammer and the resulting transient motion has been measured at several positions on the compressor. For the measurement of the spatial motion, triaxial piezo-electric accelerometers have been used which are attached to the objects by means of magnets. The force applied by the hammer during the impact has been measured by a piezo-electric load cell inside the hammer. The signals of the accelerometers as well as the signal of the load cell have been amplified by charge amplifiers. The data acquisition has been carried out by Labview and for further analysis Matlab was used.

In addition to the pulse hammer excitation method, an Operating Deflection Shape (ODS) measurement has been executed. The motions of the running compressor have been measured at different rotational speeds of the crankshaft. If the difference in step size between the rotational speeds is not too large all natural frequencies are excited and the corresponding motion will show appropriate amplitudes. With this method it is possible to identify the most important compressor manifold natural frequencies and mode shapes without using any additional exciter (e.g. an impulse hammer). It appears that the mechanical loads of the compressor are strong enough to excite the different mode shapes.

### 5.2 Pulse hammer excitation results for the compressor frames

The first measurements have been carried out for the bare compressor frames. The frames of a vertical and a horizontal compressor type have been mounted to the ground in different ways. The following measurements were carried out for the frames:

- Fixed to the ground with four clamping devices
- Fixed on different assembly supports

Figure 5.2.1 shows the location of the measuring points for the vertical and horizontal compressor frame. In Figures 5.2.2 examples of two mode shapes for the vertical compressor frame, fixed to the assembly supports, are shown.

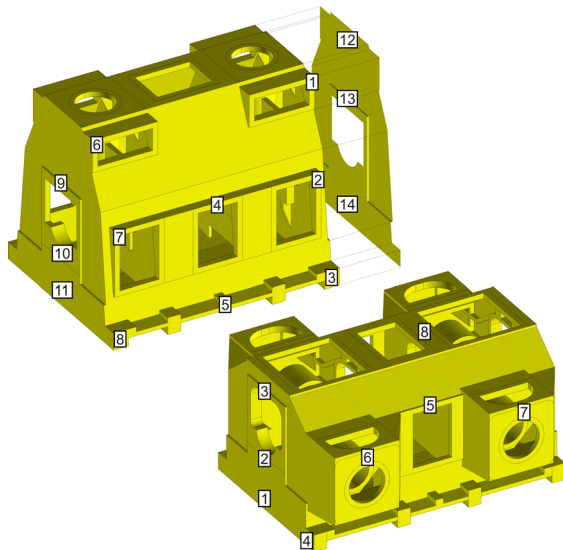


Figure 5.2.1: Location of measuring points for the vertical and horizontal compressor frame

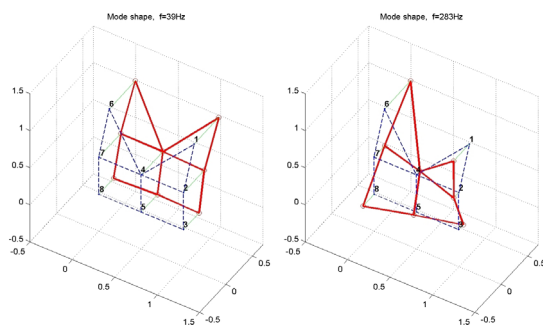


Figure 5.2.2: Mode shape (left) at  $f=39$  Hz (mainly rigid body motion) and mode shape (right) at  $f=283$  Hz (torsion) for the vertical compressor frame

The measured mode shape at 39 Hz shows that the foundation fixing is more or less elastic and differs from an assumed rigid fixing of the frame in the Finite Element model. It is time consuming to achieve the same boundary conditions in the FE model and the test situation. Therefore, it is difficult to compare the results of the FE analysis and the measurements.

In many cases the results of FE modal analysis differ much from experimental results. This is due to different boundary condition effects. In order to compare the results, the boundary conditions must be the same for both systems. This can be achieved in two ways:

1. The given support of the machine has to be modelled in such a way that it matches the shop test configuration. As indicated earlier this can be time consuming.

2. The effects of the boundary conditions which have an important influence on the modal parameters both in the model and shop test can be excluded by mounting the compressor on very flexible mounts.

If none of these two methods is feasible, one must try to find the mode shapes where the influence of the boundary conditions can be neglected. This is the case for mode shapes without motion at the support locations. The mode shape as shown in figure 5.2.3, where mainly point 10 is moving, could be used for this purpose. For this case the comparison between the FE model ( $f=183$  Hz) and the experimental modal analysis (EMA) results ( $f=193$  Hz) show an acceptable agreement.

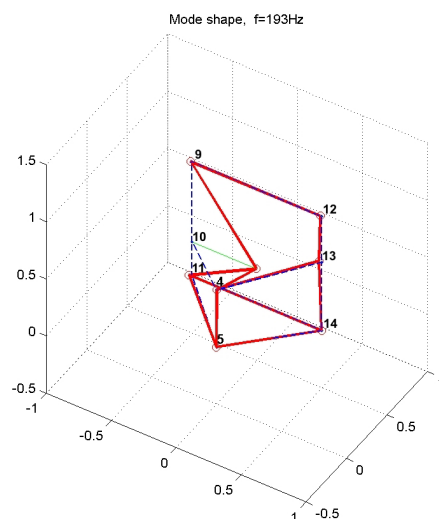


Figure 5.2.3: Mode shape at  $f=193$  Hz (mainly point 10 is moving) for the vertical compressor frame

The fact that an infinitely rigid restraint is not present for most of the measurements is also valid for the horizontal compressor frame. Thus e.g. the mode shape as shown in figure 5.2.4 can be used to compare the results with the FEA analysis. For this mode shape mainly point 2 and 5 are moving and not the support points. The comparison between the FE model ( $f=261$  Hz) and the experimental modal analysis results ( $f=262$  Hz) agree very well.



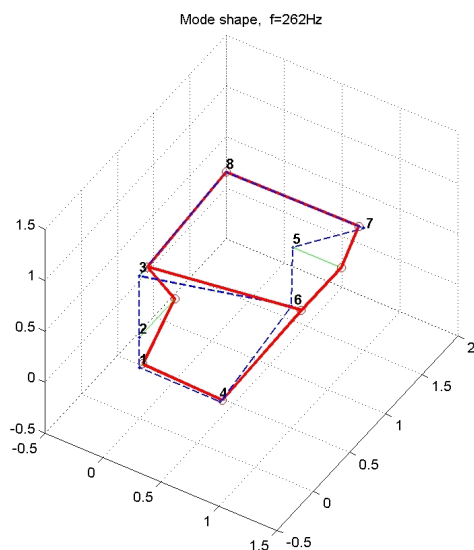


Figure 5.2.4: Mode shape at  $f=262$  Hz (mainly point 2 and 5 are moving) for the horizontal compressor frame

In order to improve the results of the FEA the actual clamping device including the jigs, where the frames are clamped onto, have been modelled. Figure 5.2.5 shows some of the model details such as buckle and two different assembly jigs. With these details included in the models the results of the FE modal analysis match the measured results quite well. Table 5.2.1 shows the comparison of different measured and calculated values for both the horizontal and vertical compressor frame. For the vertical compressor frame it was not possible to achieve reasonable results for Mode A and B. Depending on the simulated fixation, the FEA results of especially the first two modes, vary in a wide range (values in brackets: weak support of the frame). The influence of the fixation is reduced by the mass of the frame. This can be seen from the results of the horizontal compressor frame which has a larger mass.

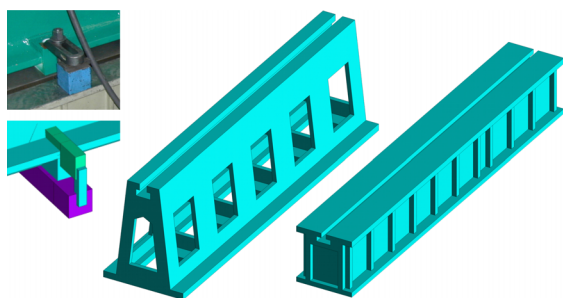


Figure 5.2.5: Details for simulating the fixation of a compressor frame on the test stand

Mode	Vertical compressor frequency [Hz]		Horizontal compressor frequency [Hz]	
	FEA	EMA	FEA	EMA
A	113(44)	39	61	74
B	161(66)	131	103	121
C	162	172	164	134
D	183	193	184	192
E	187	201	261	262
F	303	283	279	288

Table 5.2.1: Comparison of calculated and measured frequencies for the vertical and horizontal compressor frame

## 5.3 Results of complete compressor

### 5.3.1 Operation Deflection Shape (ODS) method for the vertical compressor

In this chapter the ODS measurements for the vertical compressor are discussed. The location of the measuring points is shown in figure 5.3.1 for the vertical compressor. The crankshaft speed and its higher order harmonics can be found very easily in figure 5.3.2. At 22 Hz an additional resonance is found which is quite remarkable. It can be concluded that for a given rotational speed, the natural frequencies are not only excited at frequencies which are harmonics of the crankshaft speed, but also at other frequencies. This means that other mechanism, leading to a wide-band excitation must be present. Impulses from the support of the machine or from assembling points may be the cause.

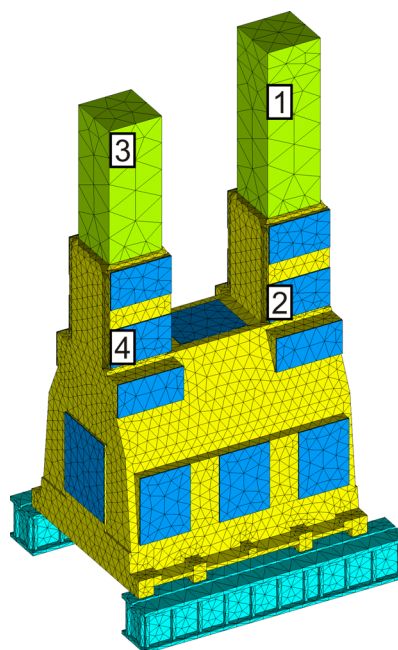


Figure 5.3.1: Location of the measuring points for the complete vertical compressor



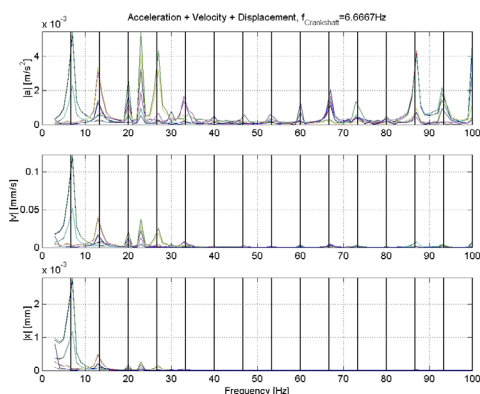


Figure 5.3.2: Transfer function for the vertical compressor

To get a quick overview a waterfall plot showing the acceleration amplitudes as a function of the crankshaft speed and frequency has been used (see figure 5.3.3). In such a plot the natural frequencies can be detected through vertical lines.

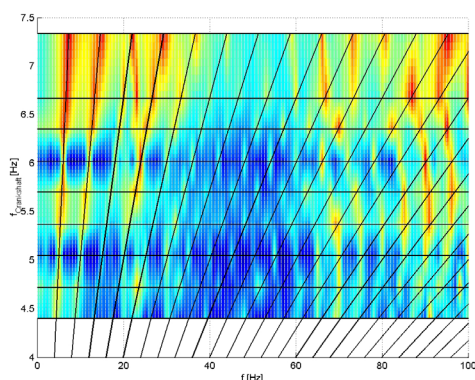


Figure 5.3.3: Waterfall plot showing the acceleration amplitudes as a function of the crankshaft speed and frequency

Table 5.3.1 shows the measured and calculated natural frequencies for the complete vertical compressor. The difference between the FE models and the measurement results is smaller than for a bare compressor (see table 5.2.1). This is due to the larger mass of the complete compressor.

Mode shape	Frequency [Hz]	
	FE model	ODS
1	24.8	22
2	25.3	25
3	34.9	30
4	35.1	33
5	97.2	87

Table 5.3.1: Comparison of natural frequencies between the FE model and the ODS data

### 5.3.2 Pulse hammer excitation method and ODS method for the complete horizontal compressor

The location of the measuring points is shown in figure 5.3.4.

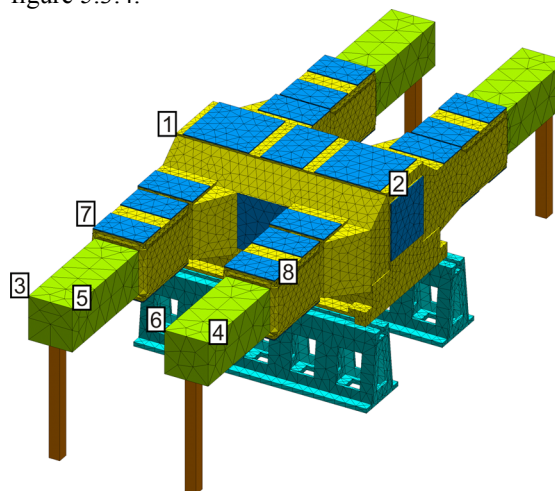


Figure 5.3.4: Location of measuring points

The absolute values of the transfer function for the horizontal compressor are shown in figure 5.3.5. The plot contains the data of all measuring points in three directions (x, y, z). The transfer function is the complex ratio between the acceleration measured at a certain point and the excitation force of the impulse hammer. In figure 5.3.5 the natural frequencies can easily be detected. The first two mode shapes with natural frequencies of 22 Hz and 32 Hz are shown in figure 5.3.6. In table 5.3.2 the first three measured natural frequencies are listed and compared with the corresponding mode shapes of the FEA. An ODS has also been carried out and the results are listed in table 5.3.2. The results of the two measurement methods agree very well with the determined natural frequencies obtained by the FEA.

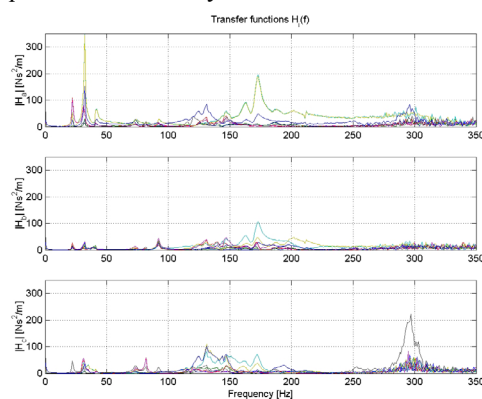


Figure 5.3.5: Transfer function for the horizontal compressor

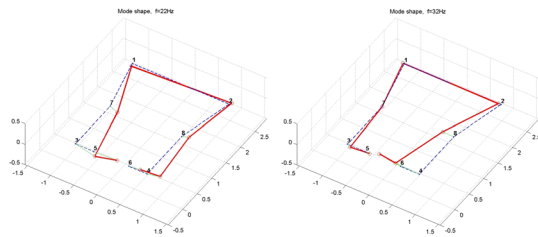


Figure 5.3.6: Mode shape at  $f=22$  Hz (left) and  $f=32$  Hz (right)

Mode shape	Frequency [Hz]		
	FE model	EMA	ODS
A	20	22	22
B	28	32	29
C	89	92	87

Table 5.3.2: Comparison of natural frequencies between the FE model and the experimental modal analysis for the horizontal compressor frame

## 6 Substructuring techniques

### 6.1 Introduction

In compressor manifold vibration studies, cyclic stresses in compressor parts are not calculated and models of compressor parts can therefore be kept relatively simple. Nevertheless, the number of degrees of freedom of compressor parts is very large (50,000-100,000) in comparison with the number of degrees of freedom of the pipe system. The number of responses to be calculated can also be considerable (1,500 responses is no exception). This leads to unacceptable computation times, which is the reason why it is not feasible to include the shell or solid element models in the pipe system model. One solution is the use of so-called substructures.

Substructuring<sup>5</sup> is a technique that simply condenses a group of elements into a single element represented as a matrix. This single matrix element is called a substructure or super element. The number of degrees of freedom of the super element (called master degrees of freedom: MDOF) is much less in comparison the complete FE model with preservation of accuracy of stiffness and mass.

Prestressed bolted joints can be included in the substructures if necessary. The general purpose finite element code ANSYS<sup>8</sup> uses the Guyan (or static) reduction in the substructure technique, which is only applicable for linear systems. Substructures can be included easily in the beam type model of the pipe

system using a procedure that has been developed especially for this purpose.

The advantage of the substructure technique is that each substructure of a compressor part is stored in a central database and can be employed by several users in various projects.

### 6.2 Examples

In this chapter two examples will be given. The substructures have been calculated with finite element models which have been derived from CAD models. The first example is a crankcase of a vertical compressor with two cylinders. The finite element model consists of 49742 quadratic 10 nodes tetrahedron elements and is shown in figure 4.2.1 (total number of degrees of freedom: 295,200). The second example is a crankcase, including the crosshead guide, of a horizontal compressor with four cylinders as shown in figure 4.2.2. The finite element model consists of 42541 quadratic 10 nodes tetrahedron elements (total number of degrees of freedom: 251,000).

From these models, several substructures have been generated with different master degrees of freedom (MDOF). Table 6.2.1 and 6.2.2 give an overview of the natural frequencies of the substructures with different MDOF. From table 6.2.1 it can be seen that for both compressors the most important natural frequencies of the substructures with only 1500 MDOF differ less than 1% from the natural frequencies of the original finite element models. This means that with these substructures accurate natural frequencies can be calculated with a large reduction in computer calculation time.

It should be noted that the boundary conditions of these models differ (models have not been fixed to a supporting structure) from the models discussed in the other chapters. Therefore the results of the natural frequencies cannot be compared with these of the other models.

Mode shape No.	Master degrees of freedom MDOF				Original model
	500	1000	1500	2000	
1	156.9	156.6	156.5	156.5	156.4
2	160.3	159.9	159.8	159.8	159.7
3	182.9	182.6	182.4	182.3	182.0
4	192.8	192.1	191.8	191.6	191.2
5	219.1	218.0	217.8	217.6	217.4
6	241.5	239.5	239.0	238.8	238.4
7	287.4	282.1	279.9	278.8	276.6
8	296.5	294.6	291.8	290.4	287.5
9	302.7	294.9	293.9	293.6	293.0
10	312.4	309.0	307.6	307.0	305.8

Table 6.2.1: Natural frequencies [Hz] as a function of MDOF of the vertical compressor

Mode shape No.	Master degrees of freedom MDOF				Original model
	500	1000	1500	2000	
1	137.8	137.8	136.9	136.6	136.5
2	224.5	224.4	223.9	223.7	223.5
3	227.1	227.1	226.1	225.5	225.3
4	248.0	248.0	244.5	242.9	242.1
5	270.7	270.7	267.1	266.0	265.3
6	291.8	291.8	284.6	282.0	280.9
7	297.7	297.7	290.0	288.0	287.2
8	311.2	311.2	302.3	300.0	298.2
9	325.6	325.6	318.5	316.1	314.8
10	343.6	343.6	339.6	337.2	335.8

Table 6.2.2: Natural frequencies [Hz] as a function of MDOF of the horizontal compressor

## 7 Summary and conclusions

Reciprocating compressors, including pulsation dampers and connected pipe system, are often the heart of an installation and should therefore operate reliable. Compressor manifold vibrations can contribute to fatigue failure of the system which can lead to unsafe situations, loss of capacity, increase in maintenance and repair costs.

To avoid these situations a compressor manifold analysis has to be carried out in an early stage of the design. In the 5<sup>th</sup> edition of the API Standard 618 such an analysis is mandatory in a Design Approach 3 analysis.

In this analysis the dynamic properties (stiffness and mass) of compressor parts have to be modelled in a proper way to accurately predict the natural frequencies and consequently the dynamic response

(vibrations and cyclic stress levels) of a compressor manifold.

The easiest way is to model the compressor parts with beam type finite element models. However, these models are not very accurate and should not be used for this purpose.

The most accurate way to model the dynamic properties is to use shell and/or solid type finite element models. Finite element models, which are built with solid elements, require the most modelling effort. To minimise the modelling effort the compressor parts are therefore normally built up with shell type elements. In most cases the bottom of the crankcase, to which the foundation bolts are connected, is often modelled with solid type elements.

However, if CAD models are available, the modelling effort can be further reduced considerably. In the past the transformation from CAD models to finite element models did not work properly and the generated finite element models has to be “repaired” before they could be used. The “repairing” process was sometimes time consuming and the advantage of using CAD models was waved away. Efficient programs are available nowadays to generate accurate finite element models from CAD models. This method is therefore far more economic than other methods.

The disadvantage of finite element models is that they require a large amount of computer calculation time. One solution is to use a substructure technique, which reduces the computer calculation time dramatically but preserves the accuracy of the dynamic properties such as mass and stiffness.

The accuracy of the used finite element models has been validated with a so-called modal analysis. With this technique the natural frequencies and mode shapes of the construction are measured by means of a pulse hammer excitation and a so-called operation deflection shape measurement (ODS) on the test rig in the factory. The advantage of the ODS measurements over the pulse hammer method is that the measurements can be carried out in less time.

It is known that the natural frequencies and modes shapes strongly depend on the boundary conditions such as the foundation holding down bolts with which the compressor is tightened to the foundation. In a finite element analysis the model is normally restrained for all dynamic motions at these points. However, the foundation of the test rig is most of the times not infinitely stiff and differences between

the calculated and measured results will occur. These effects should therefore be included in the finite element models for a comparison between the models and reality. The measurements showed a good agreement with the finite element results.

This leads to the final conclusion that accurate finite element models can be generated from CAD models in such a way that economic and accurate compressor manifold analyses according to the API Standard 618 can be carried out. This procedure also is an additional element for the virtual product development method and therefore supports the efforts of continuously improving the reliability and efficiency of reciprocating compressors.

## 8 Acknowledgement

This project has been sponsored by Burckhardt Compression and TNO TPD. The authors would like to thank both organizations for the admission to publish the results and all employees for their contribution.

## 9 References

- <sup>1</sup> API Standard 618, 4<sup>th</sup> edition, June 1995, "Reciprocating Compressors for Petroleum, Chemical and Gas Industry Services".
- <sup>2</sup> Pyle, A., Eijk, A., Elferink, H., "Coming 5<sup>th</sup> edition of the API Standard 618, Major changes compared to the API 618, 4<sup>th</sup> edition", 3<sup>rd</sup> EFRC Conference, 27-28 March 2003, Vienna
- <sup>3</sup> Egas, G., "Building Acoustical Models and Simulation of Pulsations in Pipe Systems with PULSIM3", Workshop Kolbenverdichter, 27-28 October 1999, Rheine, pp 82-108.
- <sup>4</sup> Palazzolo, A.B., Smalley, A.J., and Lifshits, A. "Recent Developments in Simulating Reciprocating Compressor Manifolds for Vibration Control", ASME 85-DET-179, presented at the ASME Design Engineering Division Conference and Exhibit on Mechanical Vibration and Noise, Cincinnati, Ohio, September 10-13, 1985.
- <sup>5</sup> Eijk, A., Smeulers, J.P.M., Egas, G., "Cost-effective and detailed Modelling of Compressor Manifold Vibrations", Pressure Vessel and Piping Conference, Montreal, Canada, July 1996. PVP-Volume 328, pp 415-424
- <sup>6</sup> Lifson, A. and Smalley, A.J., "Bending Flexibility of Bolted Flanges and Its Effects on Dynamical Behaviour of Structures", Volume III, Journal of Vibration, Stress and Reliability in Design, October 1989, pp. 392-398.
- <sup>7</sup> Tseng, J.G., and Wickert, J.A., "On the vibration of bolted plate and flange assemblies", Journal of Vibration and Acoustics, Volume 116, 1994, pp.468-473.
- <sup>8</sup> ANSYS Users' Manuals Vers. 6.1, SAS IP, 2002
- <sup>9</sup> Lifson, A., and Dube, J.C., "Specifying Reciprocation Machinery Pulsation and Vibration Requirements Per API-618", DT-66, American Gas Association Operating Section Proceedings, 1987, pp. 50-58.
- <sup>10</sup> Samland, G. et al. "Virtual Product Development - A Method for Increasing the Reliability and Efficiency even in the Reciprocating Compressor Industr", 2<sup>nd</sup> EFRC Conference, 17-18 May 2001, The Hague, NL, pp. 227-235.



# **Dynamic characteristics of large high-speed reciprocating compressor systems**

by:

**Smalley, A. J., Harris, R. E., Gehri, C. M., and Weilbacher, G. W.**

**Mechanical and Fluids Engineering Department**

**Southwest Research Institute®**

**San Antonio, Texas**

**USA**

Session 5

**Reliability and economics of compression systems –  
recent trends in the market of  
reciprocating compressors  
March 27<sup>th</sup> / 28<sup>th</sup>, 2003 Vienna**

## **Abstract:**

This paper presents predicted and measured dynamic characteristics of high-speed high-power reciprocating compressors. It describes and demonstrates the analyses necessary to ensure their dynamic integrity. Increasing size and power tends to decrease acoustic and mechanical natural frequencies, but increases the frequency of strong excitation energy. The paper shows the capabilities and limits of plane-wave acoustics, and where 3D acoustics is needed. The paper identifies the existence of system modes and how 3D finite element analysis can predict these modes and their response.



## 1 Introduction

A family of large slow-speed integral reciprocating compressors dominates the US gas as transmission industry. These are an aging fleet of compressors, which operate in the 270 to 330 rpm range. Increasingly, horsepower replacement projects, typically driven by emission requirements are considering high horsepower designs (4000 to 8000 HP) operating in the speed range of 750 rpm. These modern separable units are driven either by lower emission 4-stroke engines or electric motors. Capacity control is a key component to flexible operation required of US gas transmission stations. Capacity control is used to maintain required pressure ratios across the station, while operating the drive at an optimal torque level. Typically, turn-down ratios of up to 50% are required in modern installations. Capacity control options include speed control, traditional volume pockets, or modern schemes including stepless unloader designs like the Hoerbiger Hydrocom.

A large US pipeline company recently undertook an ambitious horsepower replacement project, involving both fixed-speed electric-drive compressors with stepless unloader technology, and variable speed engine-driven units with pockets and pneumatic valve lifters. Several firsts or near firsts, as described in Table 1, were achieved in this effort. Figure 1 shows a Siemens motor-driven fixed-speed 8000 HP Ariel unit, while Figure 2 shows a similar six-cylinder unit driven by an 8000 HP Wartsila engine. These installations include 18.5 inch cylinders, large 48-inch primary pulsation control bottles, and dual nozzles on all suction and discharge cylinders with vertical secondary bottles. On the outboard cylinders on the fixed speed units, electro-hydraulic controllers act as stepless unloaders. The design speed range on the engine drive units was 550 to 775 RPM. Motor drive speeds are 720 RPM.

Several key features of the design should be noted. Large pulsation control vessels were installed to control low frequency pulsations/vibrations, and to minimize flow losses. Use of side-by-side dual nozzles (instead of a single larger diameter nozzle) by the compressor manufacturer reduces the size of the cylinder casting required to achieve comparable pressure drop of a large single nozzle; however, the two penetrations in each chamber of the pulsation dampener add a source of excitation not present with a single nozzle. The use of stepless unloaders achieves seamless capacity control over a wide flow range, but requires careful engineering to control

pulsation responses under part load. The large size increases the inertia of the compressor, cylinders, and attached bottles with the potential for vibration modes in which these inertias interact with each other and the support structure.

Table 1. Project Firsts or Near Firsts

- 8000 HP; Up to 775 RPM (Only 6% of installed recip base in gas transmission >4,000 HP!)
- 1333 HP/cylinder and 1.3 ratio.
- 48-inch bottles and 50 MMSCFD per cylinder.
- Stepless capacity control on a fixed speed high-speed low ratio unit.
- 8000 HP engine drive.
- Above plus dual nozzles.



Figure 1: Typical 8,000 HP Fixed Speed Motor-Driven Unit



Figure 2: Typical 8,000 HP Variable Speed Engine-Driven Unit

## 2 3D Acoustics

Figure 3 presents a 3D solid model for one of the primary suction bottles, including internals. It shows the double nozzle configurations feeding three chambers, each separated by ellipsoidal head

baffles. Internal choke tubes connect two of the chambers to a common chamber at one end. An external discharge choke tube connects this common chamber to a vertical secondary bottle. On top of the bottles, Figure 3 shows two inspection ports with overhung flanges, which proved vulnerable to induced bottle vibration.

Figure 4 shows a 3D acoustic finite element model of the primary and secondary discharge bottles, developed using ANSYS. Figure 5 shows a nozzle resonance mode shape for the common chamber predicted by 3D analysis. This mode, easily predicted by 1D modeling, preserves its planar nature in the nozzles, and in the choke tubes. Note, however, the significant pressure levels that can arise for this mode in the bottle chambers, particularly for the common chamber. Roughly 30% of the dynamic pressure behind the valves remains in the common bottle chamber. In this mode, high nozzle response levels can produce large dynamic forces on the bottle walls, potentially exciting mechanical shell resonances of the bottle, or resonances of small fittings attached to the bottles.

Figure 6 shows (based on plane wave prediction of response to cylinder excitation) that without a nozzle orifice, the pulsation pressure in the suction nozzle would reach 76 PSI at 40% capacity. The predictive acoustic model includes a detailed treatment of the unloader mechanics, involving valve plate inertia and dynamic response of the plate under gas, and inertia forces. With a nozzle orifice installed, the predicted pulsation drops to 21 PSI—field data showed pulsation of 14 PSI. Figure 7 shows a qualitatively similar trend for the discharge nozzle on the fixed speed units. On the discharge side, the magnitude of predicted pulsation without an orifice is lower, and installing the orifice causes less reduction in predicted pulsation. The trade-off between pulsation control, capacity control, and flow efficiency is most apparent from the results for the suction nozzles.

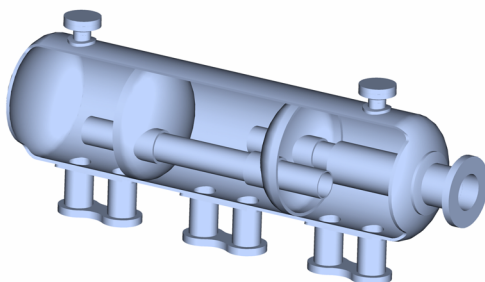


Figure 3. Solid Model—Suction Bottle showing Internal Geometry, Dual Nozzles, and Inspection Ports

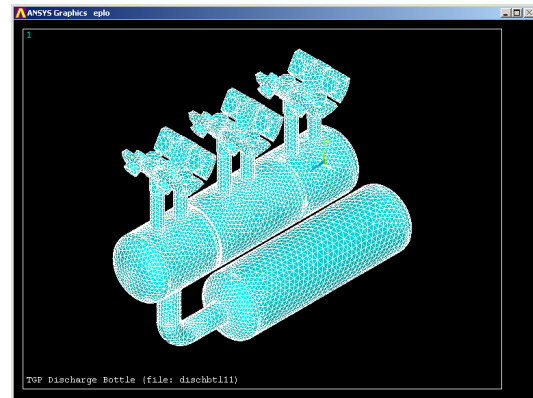


Figure 4. 3D Acoustic Model of Primary and Secondary Discharge Bottles

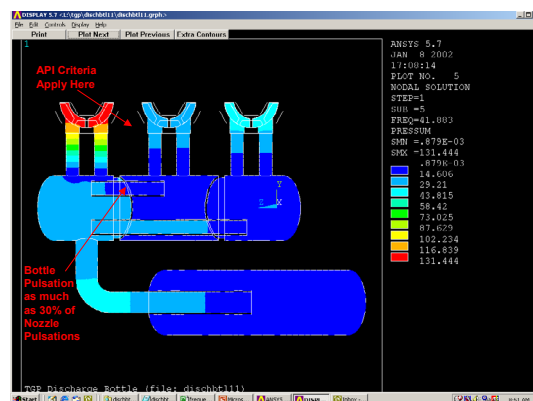


Figure 5. Nozzle Resonance Predicted by 3D Acoustic

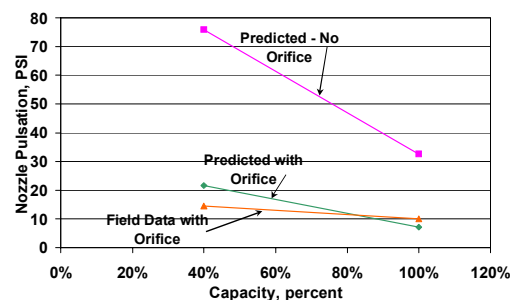


Figure 6. Influence of Unloading on Suction Nozzle Pulsation, Fixed Speed Unit

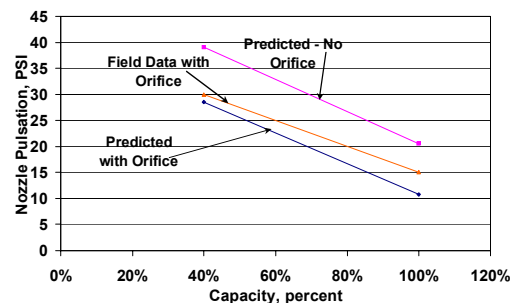


Figure 7. Influence of Unloading on Discharge Nozzle Pulsation, Fixed Speed Unit

Table 2 compares the frequencies of a number of important acoustic modes as predicted by plane wave analysis (Interactive Pulsation-Performance Simulation - IPPS), and by 3D acoustic analysis (ANSYS). It shows that for frequencies below 250 Hz, the 3D analysis closely reproduces the modes predicted by plane wave analysis.

Table 2. Acoustic Filter Frequencies

ANSYS	IPPS	Definition of Response
6.14	6.10	Helmholtz Freq., $f_H$ End Chamber to Sec Bot
7.73	7.90	Helmholtz Freq., $f_H$ Middle Chamber to Sec Bot
15.29	15.20	Helmholtz Freq., $f_H$ Short Internal Choke
41.88	41.50	Nozzle
42.46	41.80	Nozzle
57.46	58.80	Choke Length
79.17	79.30	Internal Long Choke
150.57	149.50	Middle Chamber Length
154.02	156.60	End Chamber Length
155.37	155.80	Internal Short Choke

Figure 8 illustrates another of the modes predictable by either method—a nozzle chamber length resonance at 150 Hz, one of several similar modes associated with the different chambers. These modes are excited by the dual nozzle configuration. By locating all connecting pipe or nozzles at the center of the bottle chamber length, it is normally possible to force any flow modulation to enter the bottle at a node of the first chamber length resonance, and thereby to avoid excitation of the chamber length resonance. Dual nozzles without pipe-backs allow for excitation of this baffle-to-baffle mode. Note that nozzle orifices have little effect on the chamber length resonant response. These baffle-to-baffle modes do not necessarily create large unbalanced shaking forces in the lengthwise direction of the bottle, due to the symmetry of the bottle construction. However, they can create a large radial forced response on the bottle walls, and produce significant vibration of small attachments and inspection ports. Field tests revealed significant vibrations on the inspection ports at the twelfth and thirteenth multiples of running speed (orders closest to the baffle mode resonance). These responses were severe enough to require field bracing of the inspection ports. Ultimately, the inspection ports were completely removed due to crack initiation at the welds on the inspection port bracing.

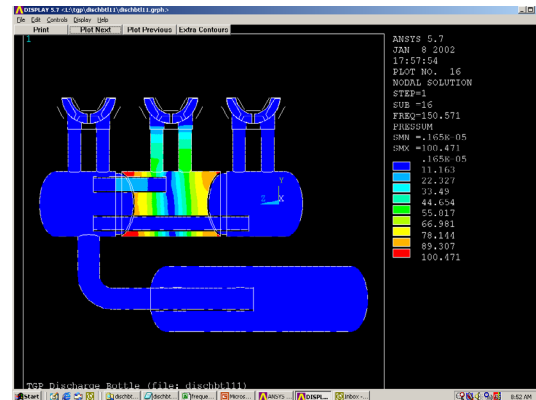


Figure 8. Chamber Length Mode Predicted by 3D Acoustic Analysis

Figure 9 shows one alternative solution to using internal pipe backs for dual nozzle cylinders. The transition piece preserves the dual nozzle connection at the cylinder, but combines the flow from the dual nozzles into a single connection with the bottle, and so avoids off-center excitation of the associated chamber length resonance.

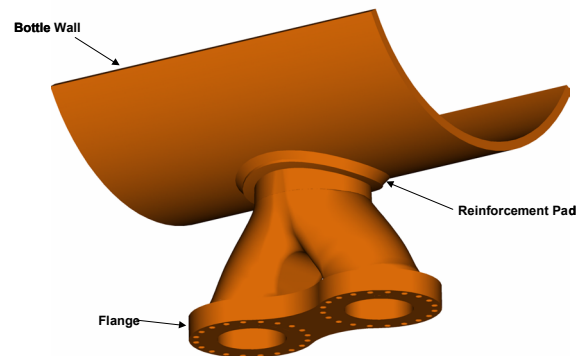


Figure 9. Constant Area Transition Nozzle for Center Feeding Bottle from Dual Cylinder Ports

As discussed earlier, 3D acoustic analysis accurately reproduces those modes predicted by plane wave analysis. However, at 250 Hz and above, additional acoustic modes associated with the bottle diameter occur, as illustrated graphically in Figure 10. These acoustic cross modes have the potential to excite bottle vibration shell modes, which involve both circumferential and axial deformation. Figure 11 presents bottle pulsation and bottle surface vibration predictions, showing significant levels around the 250 Hz region, and illustrating the potential for significant response.

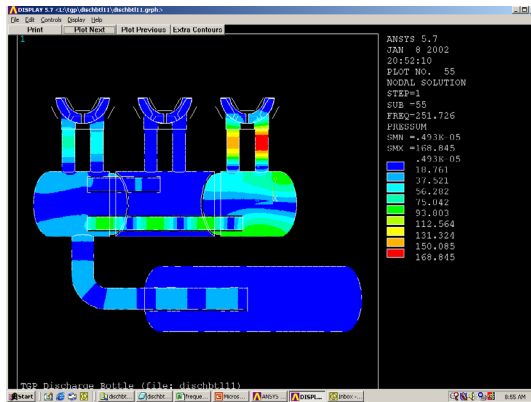


Figure 10. Bottle Chamber Cross-Mode Predicted at 252 Hz

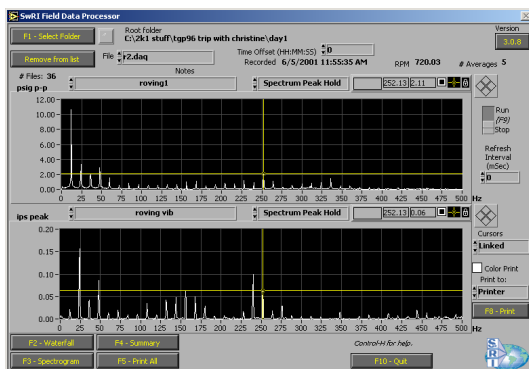






Figure 13. Cross-Brace to Neutralize Opposed Cylinder Excitation of SB Cantilever Mode

As mentioned, modeling approaches can have a significant impact on the predicted key frequencies. Figure 15 presents predictions of the suction bottle cantilever mode for a number of alternative modeling assumptions or degrees of model completeness. The various analyses included:

- A beam model with flexibility factors at nozzle-to-bottle joint based on circular pad reinforcement; no attached piping.
- As for the previous case, but with attached piping.
- Shell model of the bottle without attached piping, and bottle internals represented by their mass only (no internal stiffening).
- Shell model with bottle internals included in structural model.
- Shell model with bottle internals and attached piping.
- Solid model with bottle internals (10-node tetrahedrons).
- Beam model with flexibility factor calculated for deformation of the nozzle to shell joint for a dual pad under moment loading induced by a lateral force at the nozzle flange.

These different analyses have shown that the bottle internals have a significant stiffening effect for such large bottles, and neglecting this stiffening in a shell model will lead to unrealistically low predictions of natural frequency (in this case by 5 Hz or 27%). Beam models ultimately rely on the accuracy of joint flexibility factors to accurately predict key frequencies. The results summarized in Figure 15 also show that with an appropriate flexibility factor, the beam model predicts a natural frequency which agrees closely with the shell model; however, using a flexibility factor developed for more conventional circular pad reinforcement, and only with pad diameter twice the nozzle diameter, can

unrealistically stiffen the model for a dual nozzle with reduced pad area, and can over-predict the suction bottle cantilever mode. In practice, beam models with flexibility factors can provide a cost-effective screening method, but such models must be used with caution. Recent work has clearly shown that the accuracy of flexibility factors in predicting resonant frequencies is strongly dependent on the general agreement between the mode shape that is being predicted, and the deflected shape used in extracting the flexibility factor.

## Bump Test



## Resonance at 24 Hz

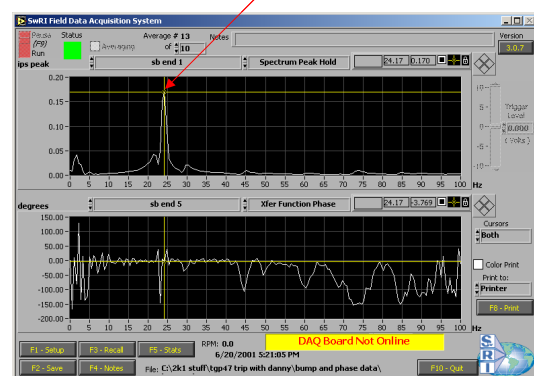


Figure 14. Bump Test for Suction Bottle Resonance with Cross-Brace Removed

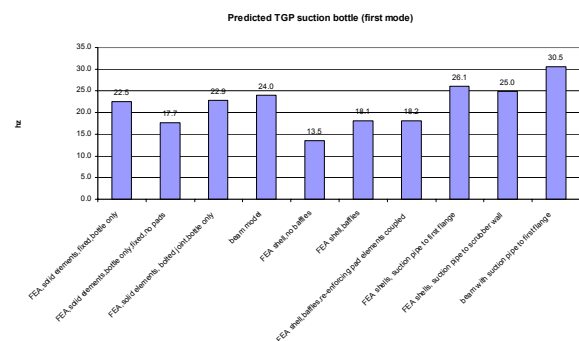


Figure 15. Predicted Frequencies with Various Models and Configurations



Figure 16 shows the deformation of the bottle and nozzle for the predicted suction bottle cantilever mode without attached piping, as predicted by the shell model, and clearly shows the key deformation occurring at the nozzle bottle connection, not in the nozzle element itself.

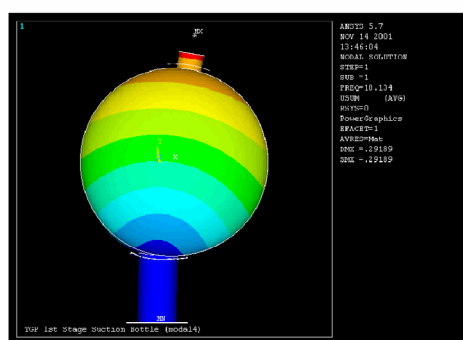


Figure 16. Combined Nozzle and Bottle Deformation Predicted by 3D Shell Model for Suction Bottle Cantilever Mode

For high horsepower/high-speed units, higher modes can also contribute significantly to vibration and stress conditions. Testing of the large bottles during operation revealed high peak-to-peak dynamic strain in the bottle wall near the reinforcing pad, and high vertical vibration on the top of the bottle under part-flow conditions. Figure 17 shows the location of strain gages 3 and 4 relative to the pad. Figure 18 makes clear that strain increases at reduced flow conditions (45% flow), reaching close to twice that at 100%. Figure 19 shows the frequency content of corresponding measured strain for gage 3. The data (bottom trace) indicates a significant strain component at about 132 Hz (eleventh order of running speed), and lesser contributors at 144 Hz and 156 Hz. This suggests the excitation of a natural frequency in this frequency range. Figure 20 shows the response of the same strain gage (No. 3) to a vertical bump test with the unit not running, revealing a clear resonance at 144 Hz. It appears that the vertical cylinder motion drives the bottle vibration, rather than pulsation in the bottle. As shown in Figure 21, vertical vibration on the cylinder and at the top of the bottle increases with reduced capacity in a similar manner to the strain data, with levels at the top of the bottle roughly twice those of the cylinder.



Figure 17. Measured Microstrain as a Function of % Maximum Capacity—Gages 3 and 4

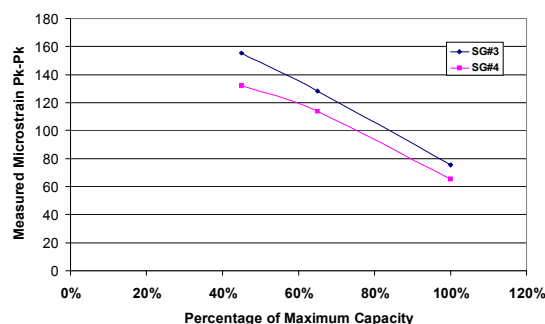


Figure 18. Strain as a Function of Capacity Setting—Gages 3 and 4

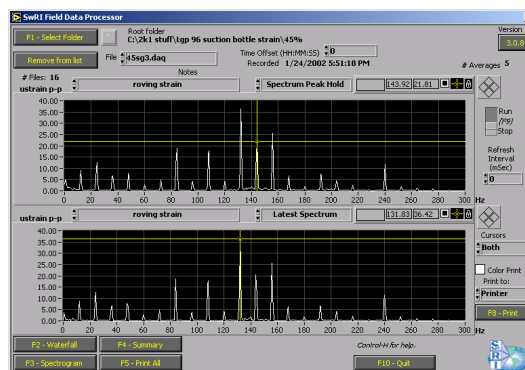


Figure 19. Typical Response Spectrum (45% Capacity; Gage 3)

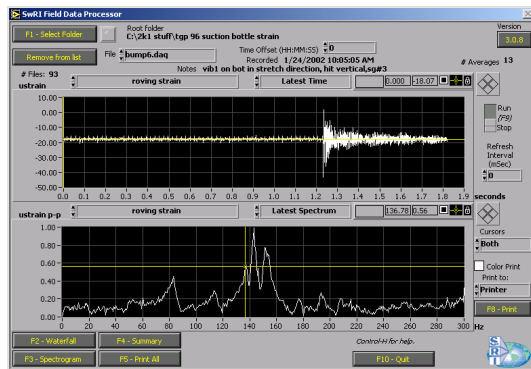


Figure 20. Strain Gage Bump Test; Response of Gage 3 to Vertical Excitation of Bottle

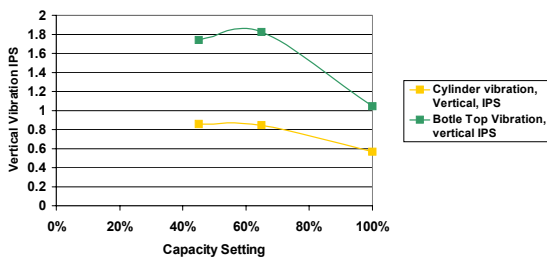


Figure 21. Vertical Vibration as a Function of Capacity Setting—on Cylinder, and on Top of Suction Bottle

Using the 3D-shell model of the suction bottle, the vertical response mode shown in Figure 22 was predicted. The mode shape is consistent with the locations of high strain measurements and with the ratio of measured vibration levels. Although predicted at 110 Hz, the presence of this mode and the response data illustrate both the difficulty in predicting these higher modes, and the potential importance of these higher modes in generating high stress conditions.

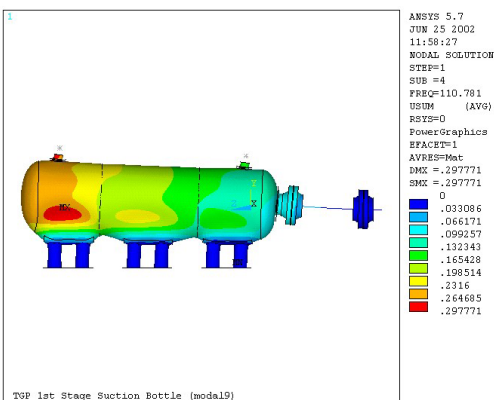


Figure 22. FE Graphic of Vertical Bottle Mode Excited at 110 Hz

The presence of shell modes starting at 150 Hz or below implies that for high-speed/large bottle applications, a number of shell modes can exist in the range between this frequency and 300 Hz. Strong potential also exists for high mechanical response near resonance when pulsations attributable to 3D acoustic modes are also predicted to occur in a similar range—e.g., starting at 250 Hz. The need exists for a criterion to identify and guard against excessive bottle dynamic pressure pulsations, which incorporates dynamic pressure and bottle wall area. At present, no such criterion exists; the API 618 criteria apply either in the compressor nozzle or in the attached piping, and imply that if these criteria can be met, the pulsation damper system which accomplishes these levels must be satisfactory. In fact, high radial forces can exist when high pulsations in the bottle combine with a large wall area.

## 4 Compressor Frame Mechanical Response

In addition to the modes involving bottle motion and deformation discussed above, the compressor frame of a large, high-speed compressor unit can experience resonant vibration under certain conditions. Field-testing indicated that limiting operation to axially symmetric loading conditions significantly reduced the vibration levels, while unsymmetric loading contributed to a strong 100 Hz response. Figures 23 and 24 present measured data of vibration on the cylinder in the stretch direction. The first of these figures is for load step 5 (unsymmetrical), and the second is for load step 1 (symmetrical). The frame resonance is clearly apparent in the frame vibration signal at 100 Hz (Figure 23), but the symmetrical loading (Figure 24) greatly reduces the response at 100 Hz. The data for either loading condition shows an additional resonant frequency at about 158 Hz. This vibration has an amplitude of 0.2 to 0.4 ips on the frame, and 0.9 to 1.1 ips at the end of the cylinder, indicating the cylinder stretching over its length, with some lateral stretching of the frame. The finite element predictions of Figure 25 show a mode at 100 Hz, which involves predominantly rigid body motion of the frame symmetrically about a central vertical axis, with deformation of its mounts and skid, and some additional motion of the bottles relative to the cylinder. It is clear from the large-scale finite element modeling of the compressor/skid system that no longer are resonances of significance limited to the piping system. The compressor system with attached pulsation bottles can now form a mechanical system coupled with the flexibility of its mounting system. This mechanical system has the

potential for natural frequencies at a low enough frequency to be excited by energy generated in the cylinders.

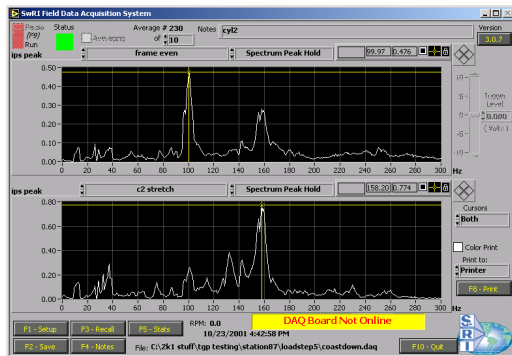


Figure 23. Speed Sweep Response—Frame and Cylinder Vibration in Stretch Direction—Load Step 5 (unsymmetrical)

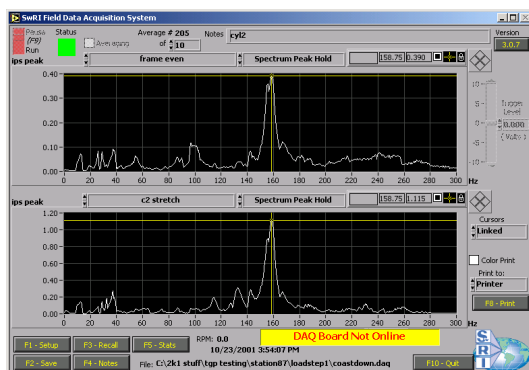


Figure 24. Speed Sweep Response—Frame and Cylinder Vibration in Stretch Direction—Load Step 1 (symmetrical)

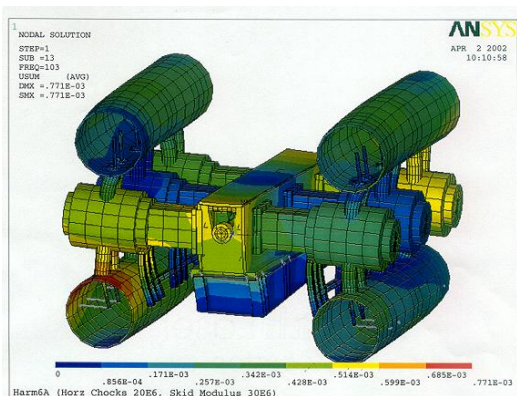


Figure 25. Predicted Mode Shape at 100 Hz, with Flexible Mount

## 5 Torsional Analysis

To ensure integrity of any compressor package with compressor-driven through a coupling, the torsional dynamics of the system must be considered. As

discussed by Harris and Smalley<sup>1</sup>, failures of couplings, crankshafts, motor shaft, and auxiliaries have been observed in a number of such installations. Variable speed motors, high-power, and stiff couplings appear to aggravate the potential. While soft couplings avoid torsional resonance at running speed, they can be subject to wear and high transient loads during start-up. Engine drives and fixed-speed installations are not immune from torsional vibration problems. Careful analysis, including critical speed and forced response, must be performed to predict dynamic stress accounting for local stress concentration factors with conservative application of torsional strength criteria.

## 6 Conclusions

Installation of high horsepower, high-speed reciprocating compressors will require advanced acoustic/mechanical analysis to accurately predict and avoid detrimental resonance and forced response conditions. As the size of high-speed compressors and their pulsation control vessels grow, the characteristics of acoustic and mechanical modes change. Frequencies for classes of modes previously of little or no concern now approach or overlap frequencies of excitation from the compressor at which energy exists to cause significant response. Plane wave acoustic modeling combined with selective 3D finite element approaches can provide an accurate and powerful analysis tool for predicting coincidence of pulsation order and key acoustic modes. Experience with this new class of compressors suggests that there is a need for a criteria to limit bottle shell responses, excited by pulsation levels in the bottles, supplementing the traditional unbalanced shaking forces calculated along the length of the bottles. For large bottle systems, finite element analysis, including bottle wall flexibility, will be required to resolve key resonance frequencies and avoid coincidence of acoustic cross modes with mechanical shell modes. It is apparent from the field test data and finite element analysis that compressor frame flexibility and the quality of the skid design and connection can contribute to overall vibration levels. A systems approach to design analysis will become increasingly important. Finally, vibration levels for this class of machines will be significantly higher than on the older large capacity slow-speed machines. Vibration levels in the 0.5 to 1.5 ips range will require higher levels of unit maintenance. Bottle designs of the type described in this paper should not have small attachments and fittings or large inspection ports. In the 1 ips vibration

Smalley, A. J., Harris, R. E., Gehri, C. M., and Weilbacher, G. W.: Dynamic characteristics of large high-speed reciprocating compressor systems

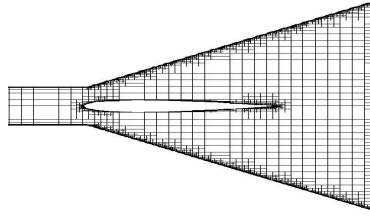
---

environment, the traditional approach of field repairs through addition of support and gusset can introduce more problems than they solve.

---

## **1 References**

<sup>1</sup> Harris, R.E. and Smalley, A.J., "Proposed Consensus Document for Torsional Vibration Analysis of High-Speed Reciprocating Compressor Installations," presented at the GMRC Gas Machinery Conference (GMC), October 7-9, 2002, Nashville, Tennessee.



# **Multidimensional simulation of pulsations with a new adaptive cartesian flow-solver**

by:

**Amin Thönnissen**  
**VSP-Aachen GmbH**  
**Aachen**  
**Germany**

**Reliability and economics of compression systems -  
recent trends in the market of  
reciprocating compressors  
March 27<sup>th</sup> / 28<sup>th</sup> , 2003 Vienna**

## **Abstract:**

A new time dependent flow solver was developed to evaluate 3-dimensional pulsations in pipingsystems of Reciprocating Compressors. Special boundary-conditions and the implementation of an **Adaptiv-Meshrefined-Solver** results in the advantage of fast gridgeneration and optimized numerical solutions for low cellnumbers at highest efficiency. The simulation will focus on the special behaviour of multidimensional wavereflection for internal dampingsystems, like orifices and pulsationvessels. Nonreflecting (absorbing) boundary conditions will guarantee a precise research of internal damping systems, which are not constraint to physical variables.



## 1 Introduction

Although the variety of complex internal flows that computational fluid dynamics can analyse continues to increase, the solution to complex unsteady flows are desired. Especially multidimensional wavereflection may influence the pulsation-amplitudes and -frequencies in a way, that structural resonances might appear. Dependent on geometric complexity and the amount of numerical operations, the multidimensional simulation process is a difficult task. Many different techniques still require significant user input to generate a computational grid for each new configuration. Modern techniques increasingly automate this process. These traditionally unstructured-grids, that are in use by the aerodynamic community today, are typically based upon triangular (in 2 dimensions) or tetrahedral (in 3 dimensions) elements. This means, that the grid-generation process now entails specifying the bounding surfaces and filling the domain with these elements. The volume grid is generated, so that the cells on the boundaries of the domain have faces coincident with the boundaries. In this sense, the volume grid is constrained by the boundary discretization. This method requires the resulting volume grid to match the surface mesh where the volume cells are adjacent to the boundaries, which makes the surface discretization the controlling factor for the grid resolution and quality near the body. For complicated geometries and flows, this brings the user back into the grid generation process, discretizing the surface, which is often a timeconsuming task (see fig. 1.1).

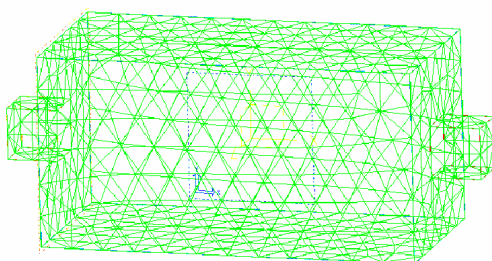


Fig. 1.1: Tetrahedral unstructured volume-grid

The **cartesian-cell-based** approach presented here, generates a volume grid automatically when giving the functional or discrete description of multiple bodies and domains. In addition, due to the special data structure used to store the grid and flow data, **adaptive-mesh-refinement** is a natural extension of this approach. The novelty of the Cartesian-Cell method arises from the application of cartesian cells to non square domains. In addition to the geometric flexibility afforded with the cartesian approach in particular, is the ability to perform **solution-**

**adaptive-mesh-refinement**, which results in a better efficiency of numerical operations, using the minimum of necessary cells. This means, that cells are added locally to regions, where an increased resolution is desired. Fig. 1.2 shows an example of a mesh-refinement-process including the tree-datastructure.

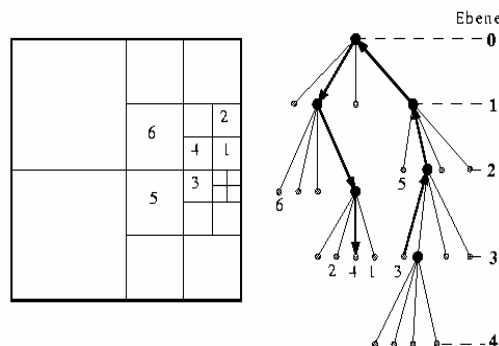


Fig. 1.2: Isotropic refinement and Data-Tree

Cartesian grid methods are based on the idea, that a body is „cut“ out of a „background“ grid made up of cells with purely horizontal and vertical faces. The „cut“ is determined by examining the interaction of a cell and the body. This procedure allows grids to be automatically generated for arbitrarily geometries. Cartesian grids have multitude advantages, including ease of grid generation, simpler flux-formulations, simplifications of the data-structure and an excellent cancellation of truncation errors in regions where the grid is regular. Cartesian methods integrate the governing equations using a uniform, orthogonal discretization of space. This guarantee of mesh quality suggests improved accuracy for a given difference schema. Improved accuracy translates into lower discretization error for a given number of cells. This can also be interpreted as an efficiency claim, since a smaller number of cells will be required to achieve a specified level of numerical accuracy.

## 2 Unstructured cartesian grids

In this method the cartesian implementation is based on fully unstructured data. In this context, „unstructured“ means, that hierarchical information is not used to infer mesh topology. Instead, connectivity is explicitly stored. Data structures from **Finite-Element-Methods** are implemented much the same way that they are for unstructured approaches on tetrahedral meshes. Such structures provide much more flexibility since they easily incorporate the possibility of anisotropic refinement of cartesian cells. The simplifications of using

cartesian grids leads to an extremely compact data structure. In this algorithm the mesh is described by a list of cell faces, that point to the cartesian cells on either side. Despite the unstructured framework, the cartesian nature of the hexahedra volume permit cell and face structures to be stored with approximately 9 words per cell.

The mesh generation process begins with an initial coarse mesh or even a single cell, covering the domain of interest (see fig. 2.1). This mesh is then repeatedly subdivided to resolve the boundary of the geometry. After each refinement, cells which lie completely outside the body, are removed from the mesh. Only when the generation of the volume mesh is complete, the algorithm computes the cut-cell intersections with the surface geometrie. The domain is subdivided with  $M_j$  possible coordinates in each dimension,  $j = (0,1,2)$ . Thus each node in the mesh may be specified exactly by the integer vector  $i$ , and the cartesian coordinates,  $x_i$ . The use of integer coordinates makes it possible to compare vertex locations and leads to compact storage schemes.

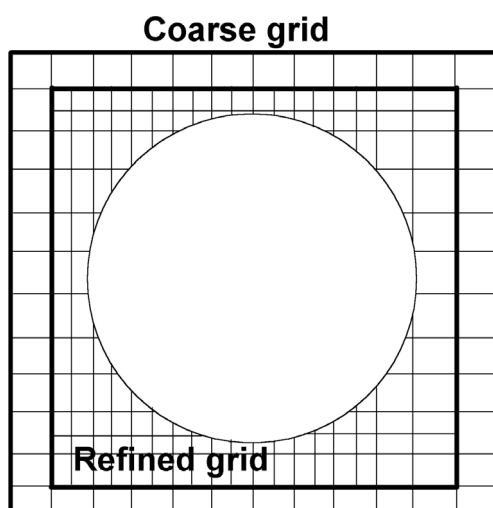


Fig. 2.1: Gridrefinement of a curved body

All surface intersecting cartesian cells in the domain are initially automatically refined a specified number of times. Further refinement is based upon a curvature detection strategy, which first detects angular variation of the surface normal within each cut cell and then examines the average surface normal behaviour between adjacent cut cells.

For angular variations more than  $20^\circ$  the cells and their neighbour-cells will be tagged for refinement. A cell is refined by dividing it in two equal parts in any direction of  $x$ ,  $y$  and  $z$  coordinates. Thus, it is possible to refine a cell in more than one direction, as shown in fig. 2.2. For practical reasons,

limitations are imposed on the minimum cell-size and the maximum number of cells. Grid coarsening is performed by removing the interface between cell  $i$  and its neighbor  $j$ . In general, a cell may be candidate of coarsening in more than one direction.

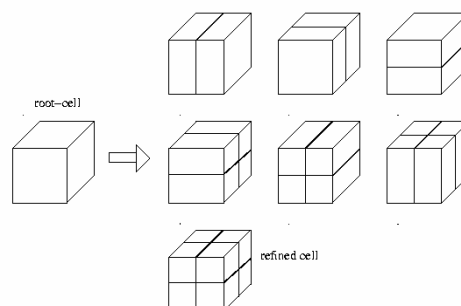


Fig. 2.2 Anisotropic Cell-Refinement

After a grid is coarsened and refined, it will contain cells of various size and aspect ratio. In general the grid may not be smooth. This means, that a cell may have any number of neighbours, and it may degrade solution accuracy. Hence, it is required to smooth out the grid by limiting the number of neighbouring cells per cell. In this algorithm, the criterion for grid smoothness is, that at most two neighbouring cells exist along any of  $x$ ,  $y$  and  $z$  directions on a cell face. If this condition is violated, the cell is divided into two cells in the direction of too many neighbours. Fig.2.3 shows a grid smoothing-process for two neighbour cells.

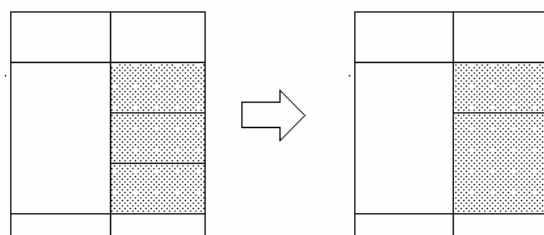


Fig. 2.3: Grid-smoothing

As an example, fig.2.4. shows an anisotropic mesh generation for a curved geometry.

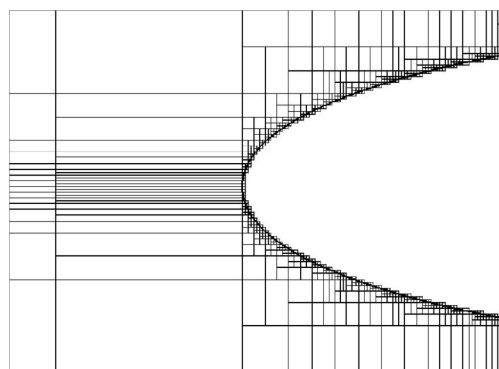


Fig. 2.4 Anisotropic cartesian refinement of a curved geometry

### 3 Flow-solving

An explicit second-order finite-volume unstructured flow solver is used for the computation of pulsations. The unsteady flow is simulated, solving the *Euler-equations*, which describe conservation of mass, momentum and energy for an ideal compressible inviscid fluid in three dimensions. These equations are often written as:

$$\frac{\partial \vec{Q}}{\partial t} + \frac{\partial \vec{F}}{\partial x} + \frac{\partial \vec{G}}{\partial y} + \frac{\partial \vec{H}}{\partial z} = 0$$

Where „ $\vec{Q}$ “ is the state vector and „ $\vec{F}, \vec{G}$  and  $\vec{H}$ “ are the fluxes in the  $(x, y, z)$ -directions respectively:

To complete the system, the ideal gas law as the equation of state is used:

Hence:

The Flow-Solver which is described here, consists

$$\rho E = \frac{p}{\gamma - 1} + \frac{1}{2} \rho \cdot q^2, \rho H = \frac{\gamma \cdot p}{\gamma - 1} + \frac{1}{2} \rho \cdot q^2$$

of three primary components:

1. a linear reconstruction method for obtaining accurate limited values of the flow variables at face midpoints

$$p = (\gamma - 1) \rho \epsilon$$

$$\vec{Q} = \begin{pmatrix} \rho \\ \rho u \\ \rho v \\ \rho w \\ \rho E \end{pmatrix}$$

$$\vec{F} = \begin{pmatrix} \rho u \\ \rho u^2 + p \\ \rho uv \\ \rho uw \\ \rho uE \end{pmatrix}, \vec{G} = \begin{pmatrix} \rho v \\ \rho uv \\ \rho v^2 + p \\ \rho vw \\ \rho vH \end{pmatrix}, \vec{H} = \begin{pmatrix} \rho w \\ \rho uw \\ \rho vw \\ \rho w^2 + p \\ \rho wH \end{pmatrix}$$

2. an upwind-Scheme for computing the flux through the cell-faces
3. and a multistage time-stepping scheme for advancing the solution

### 3.1 Reconstruction and limiting

In order to evaluate a flux through a cellface, flow-quantities are required at both sides of the face. To achieve higher order accuracy, solution gradient information must be used. A linear reconstruction method is used to determine a second order approximation to the state at the face midpoints, based on the cells in the neighbourhood of the face. It relies on a suitable weighted *least-squares-method* about the cell of interest for the

$$\vec{Q}_k = (\rho, u, v, w, p)^T$$

reconstructed primitive variables:

Once the gradient of  $\vec{Q}_k$  is known in each cell, the value of  $\vec{Q}_k$  can be found anywhere in the cell from:

whereas  $\vec{Q}_{k,c}$  is the value of  $\vec{Q}_k$  at the cell centroid, and  $d\vec{r}$  is defined as the distance vector:

$$d\vec{r}_x = x - x_c, d\vec{r}_y = y - y_c, d\vec{r}_z = z - z_c$$

Exemplarily, the values at the face midpoints of an uncut cell in two dimensions are simply:

$$\vec{Q}_{k, \text{left}} = \vec{Q}_{k,c} - \frac{1}{2} \cdot \Delta x_c \cdot \nabla_x \vec{Q}_k$$

$$\vec{Q}_{k, \text{right}} = \vec{Q}_{k,c} + \frac{1}{2} \cdot \Delta x_c \cdot \nabla_x \vec{Q}_k$$

$$\vec{Q}_{k, \text{top}} = \vec{Q}_{k,c} + \frac{1}{2} \cdot \Delta y_c \cdot \nabla_y \vec{Q}_k$$

$$\vec{Q}_{k, \text{bottom}} = \vec{Q}_{k,c} - \frac{1}{2} \cdot \Delta y_c \cdot \nabla_y \vec{Q}_k$$

$$\vec{Q}_k(x, y, z) = \vec{Q}_{k,c} + \nabla \vec{Q}_k \cdot d\vec{r}$$

If the full gradient is used in reconstructing the values at the face midpoints, the computed values could fall outside the bounds of the data. To avoid

$$\vec{Q}_k(x, y, z) = \vec{Q}_{k,c} + \Phi \cdot \nabla \vec{Q}_k \cdot d\vec{r}$$

$$\hat{u} = \frac{\sqrt{\rho_L u_L} + \sqrt{\rho_R u_R}}{\sqrt{\rho_L} + \sqrt{\rho_R}}$$

$$\hat{p} = \sqrt{\rho_L \rho_R}$$

$$\hat{a}^2 = (\gamma - 1)(\hat{h} - \vec{v} \cdot \vec{v} / 2)$$

this, the computed gradients are limited through the equation:

Where  $\phi$  is a limiter, with a value between zero and one. In regions where  $\phi=1$ , a linear reconstruction is being used, and the truncation error is  $O(h^2)$ . In regions where  $\phi=0$ , a piecewise constant reconstruction is being used and the truncation error is  $O(h)$ .

### 3.2 Flux-formulation

A finite-volume method needs a flux function to compute the solution to the unsteady problem at each interface between the cells in the grid. Here, an approximate Riemann-solver, which is described in [8], will be used for a proven upwind-scheme. The interface flux will be computed as:

$$\vec{F} = \frac{1}{2}(\vec{F}_L + \vec{F}_R) - \frac{1}{2} \sum_{i=1}^5 \lambda_i \cdot \vec{\alpha}_i \cdot \vec{r}_i$$

where  $F_L$  and  $F_R$  are the fluxes for the left and right state, and  $\lambda_i$  are the wave-speeds. The right eigenvectors  $r_i$  of the Roe-Matrix are:

where the Roe-averaged speed is:

and the wave strengths are:

$$\lambda = \begin{pmatrix} \hat{u}-\hat{a} \\ \hat{u} \\ \hat{u} \\ \hat{u} \\ \hat{u}+\hat{a} \end{pmatrix}$$

$$R = \begin{pmatrix} 1 & 0 & 0 & 1 & 1 \\ \hat{u}-\hat{a} & 0 & 0 & \hat{u} & \hat{u}+\hat{a} \\ \hat{v} & 1 & 0 & \hat{v} & \hat{v} \\ \hat{w} & 0 & 1 & \hat{w} & \hat{w} \\ \hat{h}-\hat{u}\hat{a} & \hat{v} & \hat{w} & \frac{1}{2}\hat{q}^2 & \hat{h}+\hat{u}\hat{a} \end{pmatrix}$$

$$\hat{q}^2 = \hat{u}^2 + \hat{v}^2 + \hat{w}^2$$

$$\alpha = \begin{pmatrix} (\Delta p - \rho \hat{a} \Delta \hat{u}) / 2 \hat{a}^2 \\ (\hat{a}^2 \Delta \rho - \Delta p) / \hat{a}^2 \\ \hat{\rho} \Delta v \\ \hat{\rho} \Delta w \\ (\Delta p + \hat{\rho} \hat{a} \Delta u) / 2 \hat{a}^2 \end{pmatrix}$$

The state quantities  $u, v, w, h$  are evaluated at the Roe-average state:

### 3.3 Time stepping scheme

The time-like evolution of each cell is computed according to a multistage Runge-Kutta time stepping method, where  $m$  is the number of stages:

$$\vec{Q}^{(0)} = \vec{Q}^{(n)}$$

$$\vec{Q}^{(k)} = \vec{Q}^{(0)} + \nu \alpha_k \frac{\Delta t}{V} \text{Re } s(\vec{Q}^{(k-1)}), \quad k = 1 \dots m$$

$$\vec{Q}^{(n+1)} = \vec{Q}^{(m)}$$

The residual,  $\text{Res}(\vec{Q})$  is defined with  $i$  loops over the faces of each cell,  $F_i$  is the computed flux between the current cell and its  $i$ 'th neighbour, and  $A_i$  represents the interface area:

$$\text{Re } s(\vec{Q}) = \sum_i \vec{F}_i A_i$$

Finally, the time step is computed based on the maximum wave speed within the cell, given by the *CFL criterion*.

$$\frac{\Delta t}{V} = \frac{CFL}{\sum_i (\hat{a} + |\hat{u}|) A_i}$$

## 4. Boundary conditions

Direct simulation of compressible unsteady flows requires an accurate control of wave-reflections from the boundaries of the computational domain. This is not the case, when acoustic damping systems have to be calculated without any physical or numerical reflection. It is worth noting, that the mechanisms by which acoustical waves are eliminated in many codes is somewhat unclear and very often due to numerical dissipation. As direct simulation algorithms strive to minimize numerical viscosity, acoustic waves have to be eliminated by another mechanism, such for example by using the so called *non-reflecting* or *absorbing* boundary conditions. A useful technique for specifying boundary conditions for hyperbolic systems is to use relations based on *characteristic lines*, i.e., on the analysis of the different waves crossing the boundary. However, it seems reasonable to avoid any kind of extrapolation method. Knowing which

physical boundary conditions have to be imposed, is not enough to solve the problem numerically. When the number of physical boundary conditions is less than the number of primitive variables (this is always the case at an outflow), the nonspecified variables have to be found by the (*soft*) numerical boundary conditions. They are called “*soft*”, when no explicit boundary condition fixes one of the dependent variables, but the numerical implementation requires some specification of this variable. To avoid overspecifying the boundary conditions by using extrapolation methods, a more rigorous method is, to use the conservation equations themselves on the boundary to complete the set of physical information. By other words, variables which are not imposed by physical boundary conditions are computed by solving the same conservation equations as in the domain. All the incoming waves of the hyperbolic system can be estimated from the original choice of the physical boundary and can be expressed in terms of the outgoing wave amplitudes, which can be computed by a one sided *upwind-differencing-scheme*. This procedure gives the missing terms in the conservation equations and allows the advance in time of all variables which are not fixed to physical boundary conditions. Using the characteristic solution of the *Euler-equations*, the amplitudes  $L_i$  of the characteristic waves, which associate with each characteristic velocity  $\lambda_i$ , can be found by:

$$\begin{aligned} L_1 &= \lambda_1 \cdot \left( \frac{\partial p}{\partial x} - \rho a \frac{\partial u}{\partial x} \right) \\ L_2 &= \lambda_2 \left( a^2 \frac{\partial \rho}{\partial x} - \frac{\partial p}{\partial x} \right) \\ L_3 &= \lambda_3 \frac{\partial v}{\partial x} \\ L_4 &= \lambda_4 \frac{\partial w}{\partial x} \\ L_5 &= \lambda_5 \left( \frac{\partial p}{\partial x} + \rho a \frac{\partial u}{\partial x} \right) \end{aligned}$$

where  $\lambda_1$  and  $\lambda_5$  are the velocities of sound waves moving in the negative and positive directions,  $\lambda_2$  is the convection velocity (the speed at which entropy waves will travel) while  $\lambda_3$  and  $\lambda_4$  are the velocities at which  $v$  and  $w$  are advected in the  $x$  direction. The  $L_i$ 's can also be defined as the amplitude variations of the characteristic waves crossing the boundary. The approach used in this technique is to infer values for the wave amplitude variations in the multidimensional case by examining a *local associated one-dimensional problem*, which is called **LODI-system**. At each point on the boundary the relations obtained by this method are not “physical” conditions, but should be viewed as

compatibility relations between the choices made for the physical boundary conditions and the amplitudes of waves crossing the boundary. In terms of the primitive variables, the **LODI-system**

$$\begin{aligned} \frac{\partial \rho}{\partial t} + \frac{1}{a^2} \left( L_2 + \frac{1}{2} (L_5 + L_1) \right) &= 0 \\ \frac{\partial p}{\partial t} + \frac{1}{2} (L_5 + L_1) &= 0 \\ \frac{\partial u}{\partial t} + \frac{1}{2 \rho a} (L_5 - L_1) &= 0 \\ \frac{\partial v}{\partial t} + L_3 &= 0 \\ \frac{\partial w}{\partial t} + L_4 &= 0 \end{aligned}$$

is:

The previous relations may be combined to express the time derivatives of all other quantities of interest, like temperature, flow rate, entropy or enthalpy.

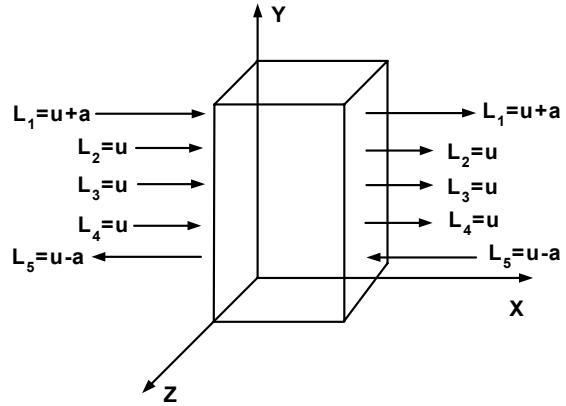


Fig. 4.1: Waves leaving and entering the boundary of the computational domain

#### 4.1 Inlet and outlet boundary

To evaluate the pressurefluctuation and the amount of damping through orifices or pulsation-vessels, a harmonic Mach-number fluctuation is defined at the inlet boundary. The obvious conclusion is, that density- and pressure-waves will travel with their characteristic speed towards the outlet boundary, which is defined nonreflective. Body-surfaces inside the computational domain are described as nonabsorbend ( $\alpha=0$ ). There for, pressure waves will be reflected, which results in an interference with forward travelling waves. The validation of the nonreflective boundary condition is printed in fig.4.1.1 and fig. 4.1.2, where a sinusoidal pressure wave travels in a straight pipe from the inlet to the outlet.





Fig. 4.1.1: Pressure-waves for nonreflecting boundaries.

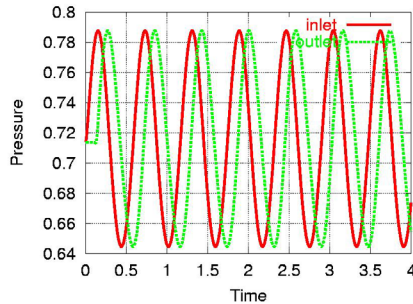


Fig. 4.1.2: Time signal at 600 Hz oscillation

## 4.2 Results of a venturi-damper

The method described above, has been tested on several internal flows. The testcase was chosen to show the fidelity of results for complex geometries. The steady-state conditions for the initial flowfield was computed for a maximum Mach-number of  $Ma=0.05$ . The pressure waves where induces by a sinusoidal oscillation frequency of 555 Hz. To resolve the complete venturi-geometrie, the initial mesh was refined based on curvature-functions. The pulsating flowsolution are pictured in *fig.4.2.1* and *fig.4.2.2* To point out the efficiency of an orifice-damper, the venturi was equipped with an additional orifice. *Fig.4.2.3* and *fig.4.2.4* display the time-dependent pressure signals and the pressure-field at a certain time-step. Comparing the results of the venturi with and without orifice, it can be determined, that the orifice leads to an additional reduction of the amplitude. As a result of body-reflected waves, higher harmonics appear in the time-signal.

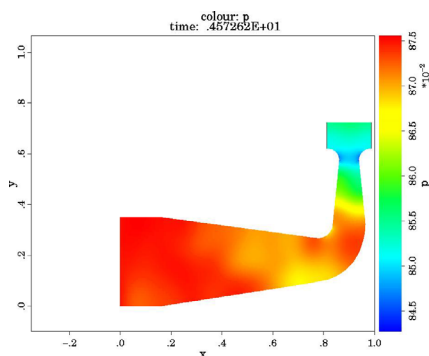


Fig. 4.2.1: Pressure waves at 555 Hz oscillation.

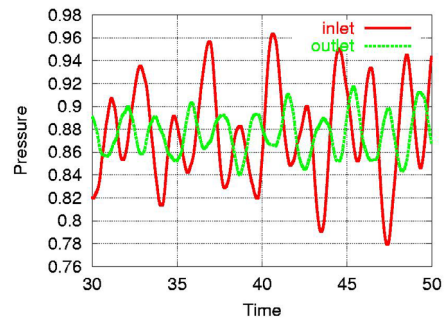


Fig. 4.2.2: Time signal at 555 Hz oscillation.

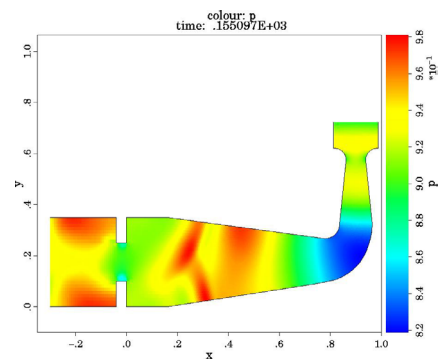


Fig. 4.2.3: Pressure waves at 555 Hz oscillation

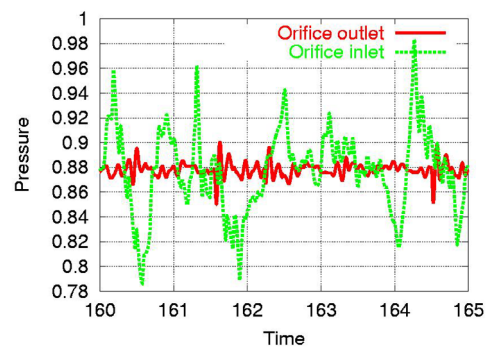


Fig. 4.2.4: Time signal at 555 Hz oscillation

## 4.3 Acoustic approach

If the Mach-number and the pressure-fluctuations are in the range of acoustically noise, the multidimensional Euler-problem can be linearised to the acoustic equations. The examination of sound attenuation can be simulated in a couple of hours, even for complicated geometries. Exemplarily *fig.4.3.3* and *fig.4.3.4* display the results of soundpressure for a typical pulsation-vessel. Additionally the simulated attenuation function is printed in *fig.4.3.5* for a wide range of frequencies.

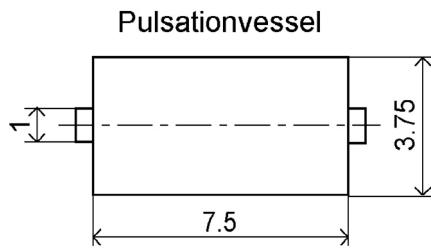


Fig. 4.3.1: Dimensions of the pulsationvessel

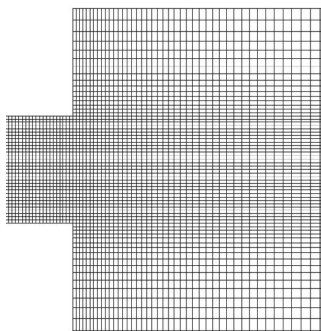


Fig. 4.3.2: Cartesian Mesh at the inlet of the pulsationvessel

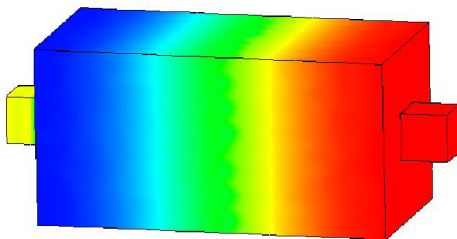


fig. 4.3.3: Soundpressure at 298 Hz oscillation

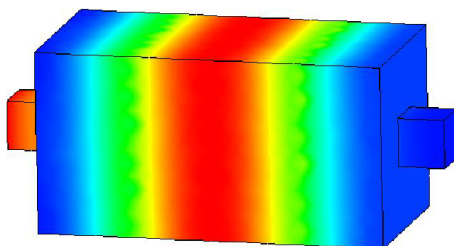


Fig. 4.3.4: Soundpressure at 580 Hz oscillation

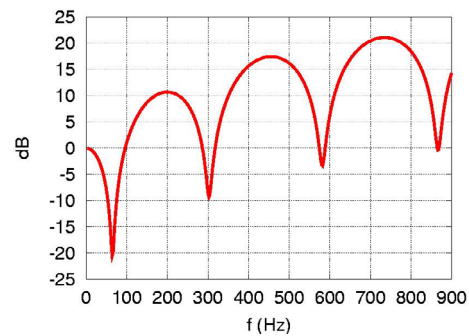


Fig. 4.3.5: Attenuation versus frequency

## 5 Conclusion

An adaptive cartesian mesh algorithm has been successfully tested to obtain nonsteady pulsations for internal flow-configurations. The testcases included both, the solution of the Euler-equation for a venturitype channel, as well as the acoustical approach for a pulsation-vessel.

Geometric refinement effectively enhance resolution of regions of high body curvature. Considering nonreflecting boundary conditions at the inlet and outlet, results in an accurate simulation of propagating waves. This method avoids numerical high frequency-waves which could propagate upstream and induce false inlet-oscillations.

For the practical use of this simulation, the future work will be expanded to the implementation of a one-dimensional reciprocating compressor model, which will simulate the unsteady flow-variables at the inlet boundary of a multidimensional grid.

## 6 References

- 1 T.J. Barth, in Computational Fluid Dynamics, Lecture Series 1990-04 (von Karman Institute for Fluid Dynamics. 1990)
- 2 K. Nakahashi, *An Automatic Grid Generator for the unstructured Upwind Method*, AIAA 9<sup>th</sup> Computational Fluid Dynamics Conference, 1989.

- 3 B. van Leer, C.H. Tai and K.G. Powell, *Design of optimally smoothing Multistage Schemes for the Euler-Equations*, AIAA 9<sup>th</sup> Computational Fluid Dynamics Conference, 1989.
- 4 B. Epstein, A.L.Luntz and A. Nachshorn. *Multigrid Euler-Solver about Arbitrary Aircraft Configurations with Cartesian Grids and Local Refinement*. AIAA 9<sup>th</sup> Computational Fluid Dynamics Conference, 1989.
- 4 M.J. Berger and R.J. LeVeque. *An Adaptive Cartesian Mesh Algorithm for the Euler-Equations in Arbitrary Geometries*. AIAA 9<sup>th</sup> Computational Fluid Dynamics Conference, 1989.
- 5 T.J. Poinsot, *Boundary Conditions for Direct Simulations of Compressible Viscous Flows*, Journal of Computational Physics 101, 104-129 (1992).
- 6 M.J. Berger and R.J. LeVeque. *An Adaptive Mesh Refinement using Wave-Propagation Algorithms for Hyperbolic Systems*, SIAM J. Numer. Anal., July, 1997
- 7 J.Bonet *An Alternating Digital Tree Algorithm for 3D Geometric Searching and Intersection Problems*, In. Journal for Num. Methods in Eng., Vol.31 (1991), pp.1-17.
- 8 C.Hirsch *Numerical Computation of Internal and External Flows*, John Wiley & Sons, (1988).

# **Investigation on the influence of pressure pulsations on multistage reciprocating compressors - Comparison between test and simulation results**

by:

**Ing Attilio Brighenti,  
Ing. Andrea Pavan  
S.A.T.E. S.r.l.  
Venezia  
Italy**

**Ing Massimo Maffeis  
SIAD Macchine Impianti S.p.A.  
Bergamo  
Italy**

**Reliability and economics of compression systems -  
recent trends in the market of  
reciprocating compressors  
March 27<sup>th</sup> / 28<sup>th</sup>, 2003 Vienna**

## **Abstract:**

The response of a reciprocating compressor piping system to predefined disturbance signals, generated at any interface with the gas flow, can be analysed by a digital computer model, which includes all the components of the compressor and piping system.

This allows the intrinsic piping response and flow resonance attitude in the frequency and time domain to be analysed, as a function of pressure or mass flow rate signals that can be calculated when the interaction between the machine thermodynamics, the valves mechanics and the fluid exchange process are taken into account together with the piping flow dynamics.

This paper, after a brief summary of the mathematical modelling approach, concentrates on the presentation of the results and the interpretation of experimental and simulation work, applied to a real industrial high-pressure compressor.

## 1 Introduction

Mathematical modelling of reciprocating compressors is an activity in increasing demand in industrial projects for the verification of pressure pulsations in piping, e.g. to verify the compliance of an installation with the API 618<sup>1</sup> rules. In particular approach 2 therein, requires the interaction between the machine and the piping dynamics with which the same is connected to be considered; in particular the cylinder gas thermodynamics, the valves mechanics, the compressible fluid exchange process and the piping flow dynamics.

This requirement stems from the fact that, while the piping dynamics have a linear behaviour in typical correct design conditions (Mach lower than 0.2 and pressure pulsations amplitudes close to the acceptable limits), which allow the application of the well-known electro acoustic analogy, the disturbing signals at the interface with the piping are determined by several non linear phenomena and by the afore mentioned interactions.

The objective of creating a set of practical design and verification tools suitable to fulfil all the necessary steps for a complete dynamic analysis required the following stages of development, started in 1994:

- Developing and analytically/numerically validating **ACUSYS**<sup>2,3,4</sup>, the linear analysis tool and piping subsystems block builder.
- Developing and analytically/numerically validating **ACUSCOMP**<sup>5,6</sup>, a non-linear model of multi-cylinder reciprocating compressors incorporating plena, non-linear flow restrictions, valves and linear piping subsystems.
- Enhancing the modelling capability of **ACUSCOMP** to incorporate models of leakages through suction and discharge valves, piston ring and rod seals of the compressor.
- Setting up portable instrumentation for in-cylinder measurements and comparing the results of simulations with test data on a real commercial compressor.

The paper illustrates the overall theoretical basis of the tools developed showing the preliminary results from the last of the above step, still in progress, and the potential applicability of these tools also for

on/off-line diagnostics of reciprocating compressor installations.

## 2 Mathematical model

The machine elements considered in the overall compressor plant model are:

- *Piping state space matrixes*, i.e. the overall dynamic characteristics of each piping side (suction, discharge or interstage) connected to one or more cylinders.
- *Single or double effect cylinders*, which include:
  - *Cylinder thermodynamics*, which include both the open phase (exchange with the piping) and closed phase (closed valves).
  - *Suction and discharge valve shutter dynamics*, as a function of either mechanical commands (e.g. cam shaft or rotary actuators) or differential pressure drive, between the cylinder and the plant side (both dynamically calculated).
  - *Suction and discharge valve gas flow dynamics*, as a function of the instantaneous valve opening and gas conditions at their inlet and outlet sections.
  - *Flow dynamics through narrow gap leakages*, i.e. through valves seats, piston rings and rod seals.
- *Plena*, representing the buffer volumes that are at the interface of the machine, between valves and piping.
- *Restrictions*, representing equivalent pressure loss elements that can be used in place of the entire piping state space blocks to analyse the behaviour of a machine without the multimodal dynamic behaviour of the piping (this can be a preliminary step during a new machine or installation design)

The following sections summarise the mathematical basis of the above model components.



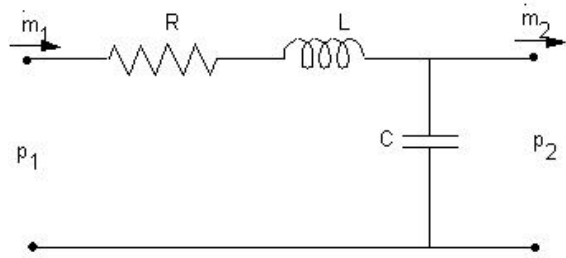
### 3 Piping model and pulsation propagation

The model of a plant, implemented in **ACUSYS**, is essentially a finite elements model of a mono-dimensional field of propagation.

This hypothesis of plane wave propagation is valid when the wavelength is sufficiently greater than the tube diameter or than the characteristic dimension orthogonal to the propagation direction, namely when:

$$f < 0.6 \frac{c}{D} \quad (1)$$

In Eq. 1  $f$  is the frequency (Hz) of a generic signal component,  $c$  the sound speed inside the fluid pipe (m/s), corrected to account for the pipe hoop compliance and  $D$  the maximum pipe cross section dimension, orthogonal to the propagation direction of the sound waves (m). This condition is usually verified inside compressors piping. For example for a piping having a diameter of 240 mm and a sound speed of 450 m/s this cut-off frequency is of 135 Hz, while the compressors speed fundamental typically ranges from 10 to 20 Hz. Viscous effects and sound wave scattering dampen the higher frequencies.



Picture 1: Electro-acoustic analogy adopted in **ACUSYS**

Besides the plane wave propagation model, associated to the range of frequencies studied, **ACUSYS** runs under the hypothesis of a linear relationship between amplitudes of pressure variations and local fluid velocities, valid as long as the latter and the mean fluid velocity are small enough compared to the sound speed. Such hypothesis leads to the electro-acoustic analogy<sup>7</sup>, represented in *Picture 1*.

$$R\dot{m}_1 + L \frac{d\dot{m}_1}{dt} = p_1 - p_2 ; \quad (2)$$

$$L = \frac{\Delta x}{A} ; \quad R = \frac{\lambda}{2} \frac{\Delta x}{D} \frac{\dot{m}_0}{\rho_0 A^2}$$

$$C \frac{dp_2}{dt} = \dot{m}_1 - \dot{m}_2 \quad (3)$$

$$C = \frac{A \Delta x}{c^2}$$

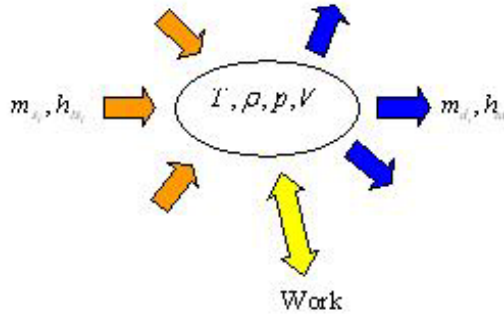
In Eqs. (2) and (3), which respectively represent the continuity and momentum balance after the above-mentioned approximation, the following notations and definitions are applied (in S.I. units):

- $R$ : equivalent resistance derived from the linearisation of the turbulent friction relationship (Eq. 4),
- $L, C$ : equivalent inductance and capacity of the element respectively
- $\dot{m}, p$ : flow rate and pressure of the fluid at sections 1 and 2
- $t$ : time
- $A$ : pipe cross section area
- $\Delta x$ : element length
- $c$ : sound speed of the fluid in the element
- $\lambda$ : friction head loss factor per unit length
- $D$ : pipe diameter
- $\rho$ : mass density of the fluid
- $_0$ : subscript indicating the mean value in a period of time (e.g. the period of the 1<sup>st</sup> harmonic component)

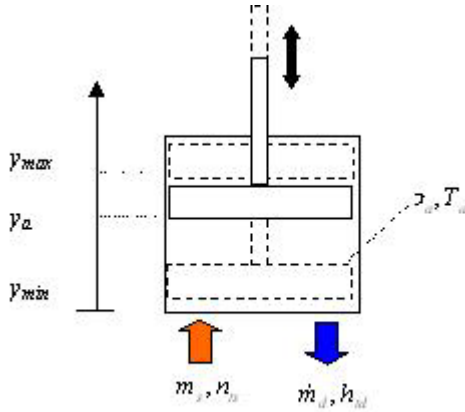
$$\Delta p_0 = (p_1 - p_2)_0 = \lambda \frac{\Delta x}{D} \frac{\dot{m}_0^2}{2\rho_0 A^2} \quad (4)$$

where:  $\dot{m}_{10} = \dot{m}_{20} = \dot{m}_0$

## 2.2 Cylinders and plena



Picture 2: General mass-energy balance of an element with fixed or variable volume



Picture 3: Mass-energy balance representation for a cylinder

In the **ACUSCOMP** model of a compressor, elements with fixed volume, like plena, and with variable volume, like cylinders, are both considered, as represented in

In general the mass balance for a single element can be written as in Eq. (5), where  $\rho$  is the fluid density in the volume  $V$  and the subscripts  $s$  and  $d$  refer to the suction and discharge ports respectively.

$$\frac{d\rho}{dt} = \frac{1}{V} \left( \sum_{i=1}^{n_s} \dot{m}_{s_i} - \sum_{i=1}^{n_d} \dot{m}_{d_i} - \rho \frac{dV}{dt} \right) \quad (5)$$

Eq. (6) is instead the general expression of the energy balance, where  $U$  is the total internal energy,  $h$  is the specific enthalpy of the gas flows and  $L$  the work performed by the gas in the adiabatic volume.

$$\frac{dU}{dt} = \sum_{i=1}^{n_s} \dot{m}_{s_i} h_{ts_i} - \sum_{i=1}^{n_d} \dot{m}_{d_i} h_{td_i} - \frac{dL}{dt} \quad (6)$$

In the case of a real gas with compressibility factor  $z$ , assumed as constant for the gas conditions at the temperature and pressure in the volume  $V$ , the expressions of the specific internal energy  $u$  and enthalpy  $h$  can be written like for an ideal gas, as in Eqs. (7) and (8) respectively.

Considering the work performed by the gas in the volume  $V$ , see Eq. (9), and the real gas state equation (10) and combining together Eqs. (6), (7), (8), (9) and (10), the final Eq. (11) of the energy balance inside  $V$  can be obtained; in this equation  $\gamma = c_p/c_v$  and  $m$  are respectively the isentropic and the polytropic exponent. The latter is defined in terms of a polytropic efficiency that can take into account internal thermodynamic losses and heat exchange with the boundary surface (e.g. cylinder wall).

$$u = \frac{U}{\rho V} = c_v T \quad (7)$$

$$h = c_p T \quad (8)$$

$$dL = p dV \quad (9)$$

$$\frac{p}{\rho} = \bar{z} R T \quad (10)$$

$$\frac{dT}{dt} = \frac{m-1}{\gamma-1} \left[ \gamma \frac{1}{\rho V} \sum_{i=1}^{n_s} \dot{m}_{s_i} T_{ts_i} - T \left( \gamma \frac{1}{\rho V} \sum_{i=1}^{n_d} \dot{m}_{d_i} + \gamma \frac{1}{V} \frac{dV}{dt} + \frac{1}{\rho} \frac{d\rho}{dt} \right) \right] \quad (11)$$

For a cylinder, as represented in Picture 3, the volume  $V$  depends only on the piston stroke. Thus, calling  $A_a$  the piston area,  $y_a$  the piston position,  $T_a$  the temperature and  $\rho_a$  the density inside the cylinder, the Eqs. (6) and (11) can be rewritten as (12) and (13).

$$\frac{d\rho_a}{dt} = \frac{1}{A_a y_a} \left( \dot{m}_s - \dot{m}_d - A_a \rho_a \frac{dy_a}{dt} \right) \quad (12)$$

$$\frac{dT_a}{dt} = \frac{m-1}{\gamma-1} \left[ \frac{\gamma}{A_a \rho_a y_a} \dot{m}_s T_{ts} - T_a \left( \frac{\gamma}{A_a \rho_a y_a} \dot{m}_d + \gamma \frac{1}{y_a} \frac{dy_a}{dt} + \frac{1}{\rho_a} \frac{d\rho_a}{dt} \right) \right] \quad (13)$$

A plenum is an element of fixed volume interfaced with the piping (or restriction) on one side and the valves (suction or discharge), on the other, which is put in communication with the cylinder volumes when the valves open. In double effect cylinders a single plenum can surround a pair of valves of the same type (suction or discharge). Eqs. (14) and (15) are derived from (6) and (11) deleting the derivative term of  $V$ , which is constant.

$$\frac{d\rho}{dt} = \frac{1}{V} \left( \sum_{i=1}^{n_s} \dot{m}_{s_i} - \sum_{i=1}^{n_d} \dot{m}_{d_i} \right) \quad (14)$$

$$\frac{dT}{dt} = \frac{m-1}{\gamma-1} \left[ \gamma \frac{1}{\rho V} \sum_{i=1}^{n_s} \dot{m}_{s_i} T_{s_i} - T \left( \gamma \frac{1}{\rho V} \sum_{i=1}^{n_d} \dot{m}_{d_i} + \frac{1}{\rho} \frac{d\rho}{dt} \right) \right] \quad (15)$$

### 2.3 Valves and restrictions

**ACUSCOMP** calculates the opening of each compressor valve solving the single degree of freedom equation of the shutter position. The forces considered are those due to the pressure difference between the cylinder and the adjacent plenum, acting on the effective shutter area, the restoring force by non-linear springs and friction damping. End stroke shock constraints are modelled too, which yield bouncing behaviour to be visible, when occurring, in the resulting plots. Based on the above balance the valves open only when a positive pressure difference exceeds the spring preload and the friction forces.

The mass flow through the valves orifices is calculated as a function of the instantaneous valve opening, the pressure upstream and downstream and the temperature upstream of the valve, i.e. in the cylinder or plenum, based on well-known orifice gas dynamic relationships<sup>8</sup>: Eqs. (16) through (19). This calculation procedure is based on the commonly accepted assumption that the head losses along the fluid accelerated stream, from the intake (subs. "1") to the vena contracta (subs. "a"), are negligible compared to the expansion losses in the decelerated stream, i.e. from the vena contracta to the outlet section (subs. "2") and that the intake Mach number is also low enough (less than 0.2)

$$\dot{m} = X_v A_v \Psi \sqrt{p_{t1} \rho_{t1}} \quad (16)$$

$$A_v = \sqrt{2} \cdot \Phi = \sqrt{2} \alpha A = A \sqrt{\frac{2}{\zeta}} \quad (17)$$

$$p_a = p_{t1} - \frac{p_{t1} - p_{t2}}{1.2 \cdot 10^{-3} C_1^2} \quad (18)$$

$$\Psi = 0.0244 C_1 \sqrt{\frac{\frac{2\gamma}{\gamma-1} \left[ \left( \frac{p_{t1}}{p_a} \right)^{\frac{\gamma-1}{\gamma}} - 1 \right]}{\left( \frac{p_{t1}}{p_a} \right)^{\frac{\gamma+1}{\gamma}}} } \quad (19)$$

The following other notations and definitions are applied in the above equations (S.I. units):

- $\rho$ : gas density (kg/m<sup>3</sup>),
- $X_v$ : instantaneous valve opening, derived by the shutter motion equation (not shown here for brevity),
- $A$ : valve flow area (m<sup>2</sup> in S.I. units, at full opening) provided by valve manufacturers.
- $A_v$ : valve flow coefficient (m<sup>2</sup> in S.I. units, at full opening) provided by valve manufacturers after incompressible flow tests,
- $\alpha$ : flow area contraction ratio (dimensionless),
- $\zeta$ : head loss factor (dimensionless),
- $C_1$ : gas correction factor (dimensionless)<sup>8</sup>.
- Subscript "t" indicates the *total* or stagnation quantities as opposed to the *static* ones, following the common convention in gas dynamics.

The generalised orifice model above allows the calculation of both the flow through compressors valves, which is normally sub critical, and that through any other restrictions, e.g. equivalent obstructions or loss elements that can be used in place of an entire piping. This allows the analysis of complex plants dynamics with process control and choke valves whose flow is strongly non linear or also to approximate pipelines by equivalent lumped restrictions (quasi-steady non linear model), in order to make rapid preliminary analyses of the behaviour and indicated cycle of a compressor, checking the pre-sizing of the compressor valves, while neglecting pressure pulsations.

## 2.4 Leakage sources

The same orifice compressible flow model is the basis for the dynamic calculation of leaking flows through seals or valve seats, which can be choked, as a function of the instantaneous gas conditions on the two sides of the orifice (e.g. the pressure in the two volumes of a double effect cylinder).

The modelled leaking pseudo-orifices considered in each **ACUSCOMP** two effect cylinder model are the following four pairs:

- piston ring seal (leaking to/from either effects)
- piston rod seal (leaking to/from crankcase)
- suction valve (leaking from each effect to the suction plenum)
- discharge valve (leaking from the discharge plenum into each effect)

Implementing these modelling features proves essential to better approximate the indicated ( $p$ - $V$ ) diagram of real compressors, avoiding the rough approach of using equivalent polytropic exponents, which should instead be calculated from appropriate realistic values of the polytropic efficiency during compression and expansion, regardless of the leaks.

The leakages influence the pressure inside the cylinders, at any given position along the piston stroke. The inter-stage pressure settlement is consequently affected depending on the input/output flow at the two ends, i.e. on the shape and duration of the valves flow duty cycle. All these factors impact on the consequent pressure spectra at the ends of the interconnecting piping and the piping dynamics, which ultimately provide a dynamic feedback to the valves, influencing the actual flow rate to/from the cylinder. All these complex interactions, which ultimately do affect the compressor performance, are difficult to evaluate unless by fine numerical modelling.

Another reason for separating the modelling of leaking flows from the thermodynamics is that by this method it is possible to evaluate the effects of increasing leakages on the  $p$ - $V$  diagram and plena pressure spectra. Having this knowledge in advance allows the support of monitoring and diagnostic activities during the compressors lifetime, which could rely on robust algorithms for the evaluation of

trends of specific signal features, associated to pre-analysed fault levels and faults/signals cause-effects relationships.

## 3 Experimental apparatus

### 3.1 Compressor

A three-stage air compressor produced by SIAD Machine Impianti S.p.A. has been used in the subject development programme (*Picture 4*), in order to gain experience in data acquisition in a real industrial environment. Its nominal characteristics are the following:

• Mass flow rate	0.3843	kg/s
• Suction pressure	1.013	bar a
• 1 <sup>st</sup> interstage pressure	3.6	bar a
• 2 <sup>nd</sup> interstage pressure	12.5	bar a
• Discharge pressure	41.0	bar a
• Revolution speed	1185	rpm

The compressor is a three, double effect cylinder type. In the test installation it delivers air to a discharge pipe ending with a choked valve set manually to stabilise the flow at the desired test pressure.

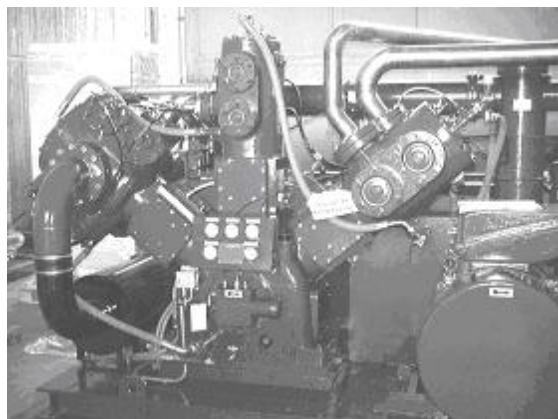
Downstream of each stage the compressed air passes through a pulsation damper and a shell and tube water cooler which brings its temperature down to +35°C.

### 3.2 Data acquisition system

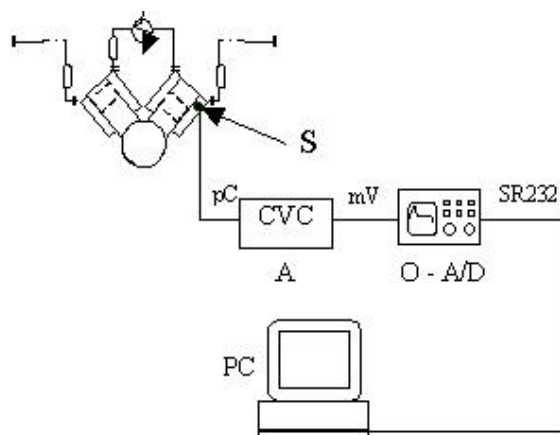
The measurements recorded during the tests are the following:

- Average gauge pressure at the discharge plenum of each stage.
- Dynamic pressure by means of a piezoelectric transducer having the following characteristics:
  - Resolution: 0.028 kPa
  - Dynamic range 34500 kPa
  - Max. Static pressure 69000 kPa
  - Frequency range 5-50000 Hz
- Temperature at six points (suction, discharge inlet/outlet of the interstage coolers).
- Flow rate at the compressor discharge.

The TDC is triggered by means of an encoder, having an accuracy of  $\pm 1^\circ$ ; data are sampled at 20 kHz frequency.



Picture 4: Three-stage air compressor used for test



Picture 5: Scheme of the data acquisition system.

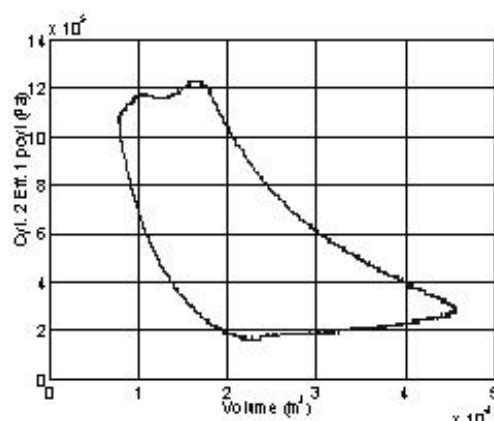
The data acquisition system is shown in Picture 5, with particular reference to the measurement of the dynamic pressure. The dynamic pressure, whose average value is zero, is converted into absolute pressure values during data post-processing, after having accounted for average pressure bias and the sensor gain sensitivity to gas temperature. Simulations on the sensor thermal dynamics, based on ACUSCOMP results, proved that this gain can be considered constant throughout a cycle, as the thermal inertia and the small convective surface of the sensor prevents it from following the ca. 20 Hz frequency of the gas temperature changes. Therefore the gain of the sensor can be calculated based on the average in-cylinder gas temperature, calculated on its own by means of cycle simulations or by other measurements. In the future the in-cylinder temperature could also be added to the experimental setup, to enhance the accuracy. The pressure sensor is mounted centrally at the top of the cylinder head, with no modifications of the

standard components, exploiting the existing plugged bore, foreseen to access the piston head for mounting. Therefore the transducer senses without delay the pressure changes in the real compressor cylinder. During this first phase of the development programme, which has the purpose of exploring the applicability and reliability of the test method, only one piezoelectric sensor was available. Therefore the tests had to be performed by shutting-down/restarting the compressor from/to the same conditions, to allow pressure readings in each cylinder.

## 4 Results

### 4.1 Experimental data

To date the measurements recorded during the test sessions were sufficiently indicative only for the second stage cylinder, which shall be illustrated here below (Picture 6). It should be noted that the measurements recorded were affected by earthing noise at 50 Hz, generated by surrounding industrial installations. This noise frequency is within the range of the phenomena of interest, which spans from the fundamental harmonic at 19.75 Hz (corresponding to the shaft speed) up to ca 300 Hz, to appropriately include the valves dynamics.



Picture 6: Experimental  $p$ - $V$  diagram of the 2<sup>nd</sup> stage – 1<sup>st</sup> effect cylinder of the tested compressor

It may clearly be seen that both the suction and discharge pressures are lower than the nominal values of respectively 3.6 and 12.5 bar or even to the 3.4 and 11.7 bar that corresponds to the test delivery pressure of 40 bar absolute. This difference can be due either to an actual different settlement of the inter-stage pressures or due to measurement errors that are being investigated.



Despite this discrepancy this plot is taken as the reference background (dashed line in all the pictures), for the comparisons made in the following section with the simulation results. This helps illustrate the sensitivity to various physical phenomena.

## 4.2 Simulation results

Many simulation runs have been performed during this phase of the work, in order to gain sensitivity to the importance of the many phenomena and parameters that affect the performance of a real compressor. Among others the following model set ups are presented:

- a) Model with quasi-steady piping, i.e. with non linear restrictions (see sec. 2.3)
- b) Model with dynamic linear piping, i.e. with full state-space piping subsystems (see sec. 2.1)
- c) Model like (a) but with leakages (see sec. 2.4) through:
  1. Piston rings (0.1 % of piston bore)
  2. Suction valves (50  $\mu\text{m}$  equivalent lift for the 1<sup>st</sup> and 2<sup>nd</sup> stage, 20  $\mu\text{m}$  for the 3<sup>rd</sup> stage, out of a lift of 2.2 and 1.6 mm respectively)
- d) Model like (b), but with the same added leakage sources as model (c).

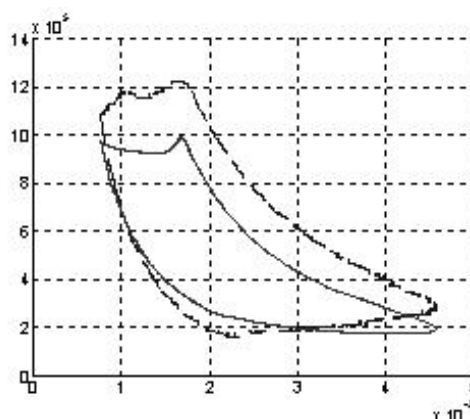
All the other parameters were maintained constant throughout the above simulations, complying with the nominal data of the compressor and the reference test, performed at 40 bar discharge. Other parameters of interest are:

- Polytropic efficiency on both compression and expansion: 90 %
- yielding:
- Polytropic exponent on compression: 1.47
- Polytropic exponent on expansion: 1.35

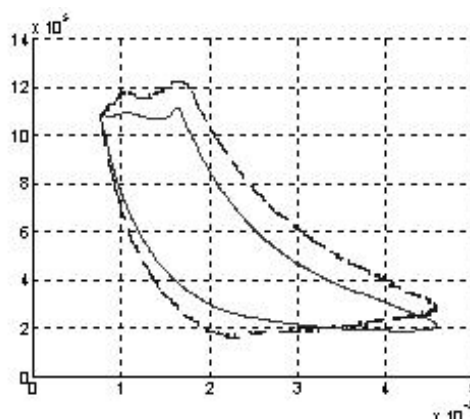
## 4.3 Discussion

The comparison of the simulation results from models (a) and (b) from Picture 8 and Picture 10 shows the great importance of dynamic pressure

pulsations in the piping, as to the settlement of the inter-stage pressures, even if the inlet and outlet average values are as expected (Picture 12 vs. Picture 14). But another influencing factor that must be accounted for in compressors modelling is the leakage, e.g. through the piston rings and the valves. Despite the relatively low values used for the examples provided in this paper, it is clear that adding these factors to the base models (a and b) approaches reality more closely.



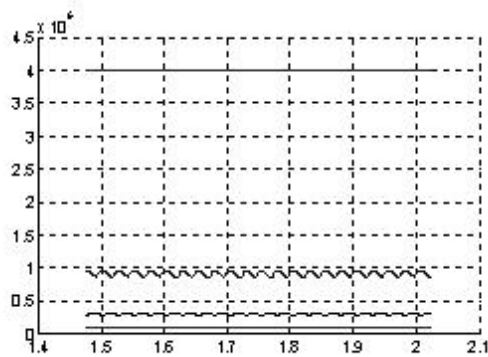
Picture 7: Simulated  $p$ - $V$  diagram of the 2<sup>nd</sup> stage – 1<sup>st</sup> effect cylinder of the tested compressor – model (a): quasi-steady non linear piping - no leakages.



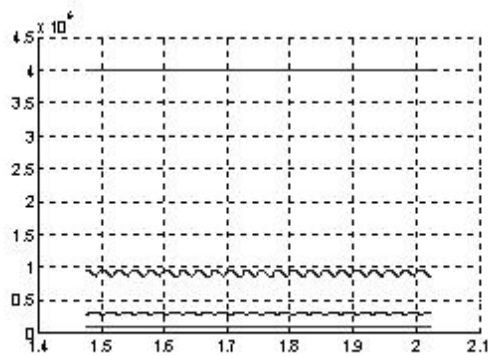
Picture 8: Simulated  $p$ - $V$  diagram of the 2<sup>nd</sup> stage – 1<sup>st</sup> effect cylinder of the tested compressor – model (b): dynamic linear piping – no leakages.

A direct comparison between Picture 16 and Picture 18 shows that simulation results present a better match with the experimental ones when the leakage factors are added, respectively to the model on quasi-steady piping and that on the dynamic piping. In both cases the effect is to increase the inter-stage pressure, as could be expected, to compensate for the reduced net flow rate. In the case of the dynamic piping the discharge pressure tends to be

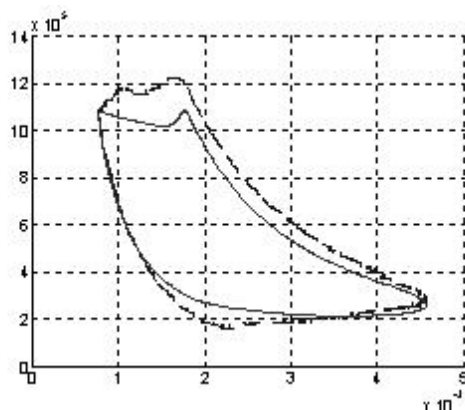
overestimated, with the given parameters. Other leaking elements have yet to be simulated at the time of writing this paper, as the work is still ongoing. However it is evident from these examples that exploring, by modelling the main factors shown herewith helps the understanding of the influence of some components on the overall performance.



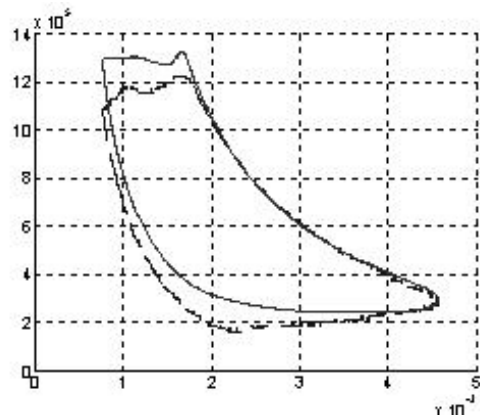
Picture 9: Simulated plena pressures – model (a): quasi-steady non linear piping – no leakages.



Picture 10: Simulated plena pressures – model (b): dynamic linear piping – no leakages.



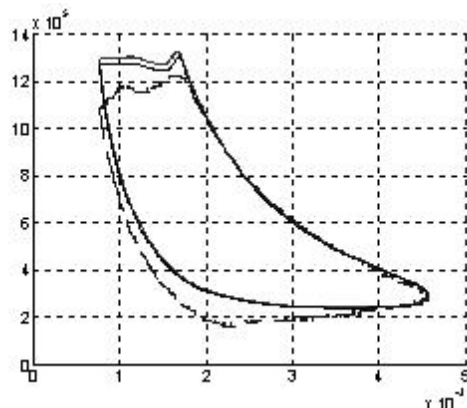
Picture 11: Simulated  $p$ - $V$  diagram of the 2<sup>nd</sup> stage – 1<sup>st</sup> effect cylinder of the tested compressor – model (c): quasi-steady non linear piping – with leaking piston rings and suction valves.



Picture 12: Simulated  $p$ - $V$  diagram of the 2<sup>nd</sup> stage – 1<sup>st</sup> effect cylinder of the tested compressor – model (d): dynamic linear piping – with leaking piston rings and suction valves.

#### 4.4 Potential for diagnostic applications

The last result worthy of mention, from the work done so far, is the possibility to detect failures from clear signals changes. If the simulation with the model (d) is repeated with a leakage area increased by just 30% through the suction valve of the 1<sup>st</sup> effect of the 2<sup>nd</sup> stage, the  $p$ - $V$  diagram changes again, showing a decreased discharge pressure on this effect, as shown in Picture 20, where the black line indicates the failed compressor cycle, overlapped to that of Picture 18 (solid line) and the experimental one (dashed line). This is just an example as previous work done on a different compressor demonstrated that the changes spread over all the signals, i.e. even plenum pressures and cylinders not affected directly by the failure.



Picture 13: Simulated  $p$ - $V$  diagram of the 2<sup>nd</sup> stage – 1<sup>st</sup> effect cylinder of the tested compressor – model (d): dynamic linear piping – with leaking piston rings and suction valves. Increased leakage

through the suction valve of the 1<sup>st</sup> effect of 2<sup>nd</sup> stage cylinder (black line).

## 5 Conclusion

The work presented in this paper shows the possibility to predict and evaluate in quantitative terms the magnitude of pressure pulsations and their importance on the performance of reciprocating compressors, making simulations a valuable tool not only to assess a plant according to API 618 rules, but also to ensure a correct and efficient performance throughout its lifetime.

The influence of these dynamic factors and engineering parameters goes through various direct and indirect phenomena modifying the  $p$ - $V$  diagram and valves flows of all the cylinders of a multistage compressor. Performances are also greatly influenced by leakages through e.g. the valves shutters, the piston rings and, though not explored in this work so far, through the rod seals.

The parallel activity on a real industrial compressor shows a reasonable match between simulated and test data, considering the uncertainties that are still pending on the measurements. The experimental work is also providing valuable specific experience about the problems to be encountered in the industrial environment, in the management of dynamic signals. A thorough critical analysis and new tests are pending at the time of writing this paper.

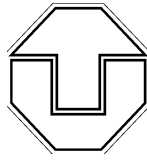
Finally this work shows the great potential of simulations in view of diagnostic applications. Indeed generating signal patterns from models of the normal operating conditions of a compressor, to be stored in a database together with other patterns generated on simulated faulty conditions, would allow faster symptoms detection and early warning on potential breakout. When a monitoring system is already installed on a facility the addition of diagnostic tools based on models would add only offline decision support software functionalities with no intrusion into the equipment hardware or controllers operation.

## 6 Thanks

The authors wish to thank the EFRC 2003 organization, particularly Mr. Johannes Wunderlich for accepting the publication and presentation of this work.

## References

- <sup>1</sup> API STANDARD 618 *Reciprocating Compressors for Petroleum, Chemical and Gas industry Services*, 4th Ed., June 1995
- <sup>2</sup> Brighenti A., Osti P.: *ACUSYS - Application of MATLAB-SIMULINK for the simulation of acoustic pulsation in plants* (in Italian), 1st Italian MATLAB Conference, Bologna, 14 Oct. 1994
- <sup>3</sup> Brighenti A.: *ACUSYS - Application of MATLAB-SIMULINK for the simulation of acoustic pulsation within plants* (in Italian), 23rd Congress of the Italian Acoustic Association, Bologna, 12-14 Sep 1995
- <sup>4</sup> Brighenti A., Contiero D.: *Preliminary validation of ACUSYS to analyse instabilities in the non linear combustion zone – plant acoustic interaction*, ISMA 21st Noise and Vibration Engineering Conference, Leuven, 18-20/9/96
- <sup>5</sup> Brighenti A., Pavan A.: *ACUSCOMP and ACUSYS – A powerful hybrid linear/non linear simulation suite to analyse pressure pulsations in piping*, ISMA2002 International Conference on Noise and Vibration Engineering – Leuven (Belgium) 16-18 Sep. 2002
- <sup>6</sup> Veronese G.: *A Cross-Model Comparison of Potential Pipeline Hazards Caused by Emergency Shutdown of Large-Scale Gas Plants* EUROFLAM Report No. 2943, Nov 2002, Cardiff Univ., School of Engineering.
- <sup>7</sup> Munjal M.L.: *Acoustics of Ducts and Mufflers*, John Wiley & Sons, Inc. 1987
- <sup>8</sup> Miller, D.S. "Internal flow systems", BHRA, 2<sup>nd</sup> ed.



TECHNISCHE  
UNIVERSITÄT  
DRESDEN

# **Simulation of the flow in ring valves**

by:

**Prof. Dr.-Ing. habil. Gotthard Will / Dipl.-Ing. Georg Flade**  
**Professorship of Pumps, Compressors and Apparatuses**  
**Technische Universität Dresden**  
**Dresden**  
**Germany**

**Reliability and economics of compression systems –  
recent trends in the market of  
reciprocating compressors  
March 27<sup>th</sup> / 28<sup>th</sup>, 2003 Vienna**

## **Abstract:**

The gas flow influences the opening and closing behaviour of compressor valves importantly. Therefore it influences the service life of these parts.

The usual way of valve designing using one-dimensional calculation needs empirical determined coefficients.

Using CFD simulation no additional experimental investigations are necessary. This report informs about the approach to predict the valve operation with stationary and transient CFD solutions.

## 1 Objectives of the analysis

The automatic valves are those compressor components which are the most delicate. Their reliable function is the most decisive factor for operational safety of compressors, their life time determines the maintenance cycle of compressors. The total pressure loss over the valves influences the energetic efficiency decisively. The optimal design of the valves is therefore a central task in developing a reciprocating compressor.

Trying to minimize the total pressure loss arouses the demand for large products of opening time and opening area for the exchange of the gas charge.

Intending to minimize construction volumina of compressors requires valves with a small increase of cylinder clearances bearing high working frequencies.

These opposing demands require valve developing to create an optimal compromise. The antecedence is a reliable calculation of valve functions.

The usual way of this is to predict valve operation with a numerical solution of motion equations [cf. Pohlenz, Bauteile für Pumpen] for the valve plate (1) using empirical approaches for the flow force.

$$F_{\text{Flow}} - F_{\text{Inertia}} - F_{\text{Spring}} = 0 \quad (1)$$

In general the flow force is related to a fictive force using a force coefficient  $\Psi$ . This fictive force results from the total pressure difference over the valve and its seat (2).

$$F_{\text{Flow}} = A_{\text{Seat}} \cdot \Delta p \cdot \psi \quad (2)$$

To calculate the total pressure difference  $\Delta p$  there is used a general approach (3) with a flow resistance coefficient which is determined empirically as well. These two coefficients usually have to be determined experimentally for every design type of valves. Here only a stationary flow through the valve at variable stroke positions is investigated.

$$\Delta p = \rho \cdot \frac{1}{2} \cdot c_{\text{Gap}}^2 \cdot \zeta_{\text{Gap}} \quad (3)$$

Flow forces being caused by the valve motion are described with a gas spring- and gas inertia effect respectively in current literature [cf. Böswirth, Strömung und Ventilplattenbewegung in Kolbenverdichterventilen]. These flow forces cannot be considered in the formula above.

A recent research cooperation of TU Dresden with Hörbiger Ventilwerke Wien aims at predicting valve functions based on a transient flow solution

for the exchange of the compressed gases. That indicates basically two advantages:

1. A experimental determination of the force- and flow-coefficient is not necessary.
2. The consideration of the transient gas forces is possible.

The following contribution reports the approach to this task and first results for the prediction of the opening behaviour of a ring valve.

## 2 The simulation model for the Navier-Stokes-code TASCFLOW

Ring valves have a complicated three-dimensional geometry, their exact modulation for Navier-Stokes solver (CFD) requires an immense expenditure which is not necessary. If the disturbances induced by the narrow connections bridging the ring grooves are not taken into consideration, the flow through the valve is symmetrical around the axis of the valve.

That is why the calculation model can be reduced to a narrow sector of the valve having only two cell layers.

The chosen example is the suction valve of the second stage of a hydrogen compressor. For this valve, results of measurements were available showing the stroke curves and flow coefficients.

The following table shows the most important data of the compressor and the valve.

Valve		
Stroke	1	mm
Mass valve plate	50	g
Area valve plate	77.3	cm <sup>3</sup>
Number of springs	8	
Spring constant (1spring)	2.115	N/mm
Tension of the springs (closed)	5.5	mm
Compressor		
Manufacturer	Ingersoll Rand	
Type	2-HHE-FB-2	
Stage 2:		
Piston diameter	215.9	mm
Piston stroke	254	mm
Length of connecting-rod	625	mm
Rpm	508	1/min
Cylinder clearance	24.2	%
Suction pressure	2.88	MPa
Output pressure	5.88	MPa
Suction temperature	309	K

Table 1: Data of the compressor including the valve



The calculations were made using the commercial Navier-Stokes solver TASCFLOW. (Producer: AEA)

Figure 1 shows the boundaries of the modelled space. The dimensions of the model were chosen thus, that the suction chamber and the cylinder room during the opening phase of the valve are existent.

Because of that, the storage capacity of these rooms is taken into consideration and the constraints of the boundary conditions are outside of the valve.

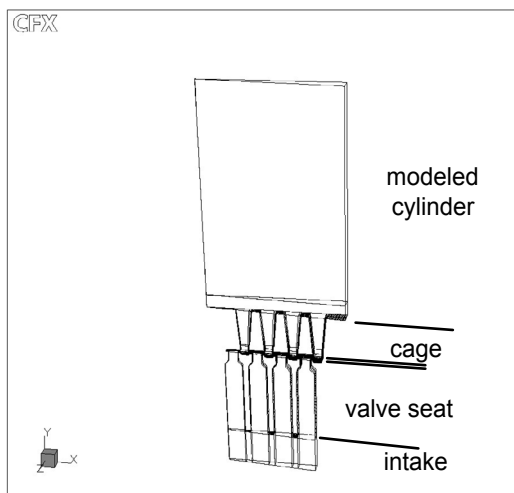


Figure 1a: Wireframe of the modelled sector

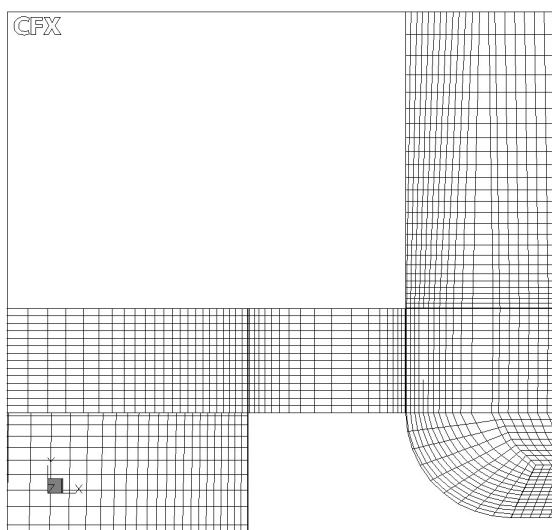


Figure 1b: Part of the mesh near the gap

The meshing of the computational area was made using hexagonal elements. They can be deformed to reflect the time dependent geometry around the valve plate.

To predict the impact velocity of the plate against the cage, the simulation of the opening phase is sufficient. (Figure 2)

First the time dependent stroke of the valve was prescribed in advance with a constant plate velocity of 2m/s. Figure 2 shows the forces acting on the valve plate.

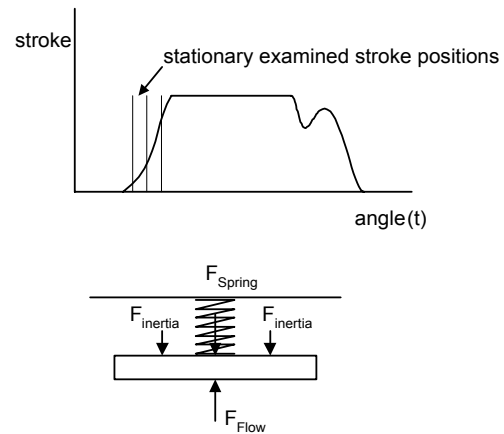


Figure 2: Opening phase of the valve and acting forces on the plate

The calculation of the transient flow cannot start with a closed valve. While the grid moves the topological structure of the mesh remains constant. That is why in the case of a closed valve there are cells having an infinite small width, and this limiting case is not predictable.

For that reason the calculation is started at the moment where the gap has a width of 10 % of the maximum plate stroke. To make a transient flow simulation the initial flow field has to be known. It can be predicted approximately by a stationary flow solution on a grid having this initial gap width.

The pressure difference determined by the spring tension of the closed gap was set as boundary condition of this calculation. To take the velocity of the valve plate at the initial gap width into account, the boundaries of the calculation area at the under-side and the topside of the valve plate are defined as outlet region and as inlet region respectively.

At these regions the fluid velocity is dictated to the presumed plate velocity.

The boundary conditions of the transient simulation are the constant inlet pressure of the suction chamber, the outlet velocity corresponding to the movement of the piston and a presumed plate velocity.

To predict the crank position and the velocity of the piston the moment the valve opens was determined.

The time step duration of the CFD calculation was set so that the opening phase (duration 0.4 ms) is divided into 100 equal time steps.

### 3 Simulation results of the complete sector mesh

The transient flow solution is intended for predicting the time dependent flow force acting on the valve plate.

Firstly the stationary calculated results of an intermediate stroke position should be visualized.

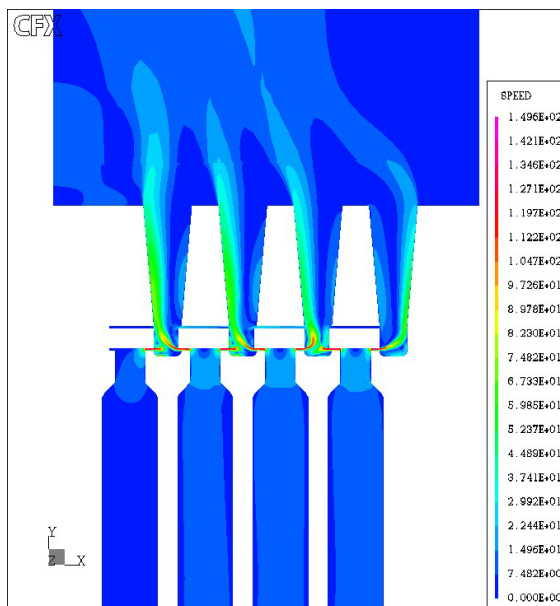


Figure 3: Stationary calculated speed distribution at 50 % of stroke

Figure 3 shows the lines of constant velocity (isotachs). Because only a sector of the valve was modelled, the figure shows only the right part of the complete valve section. The axis of rotation is located on the left boundary of the figure.

The speed distribution of all gaps is comparable and the coming out jets are positioned at the inner sides of the channels located in the cage. The impulse of the jet coming out of the outer gap of a channel is higher than the impulse of the belonging inner jet due to different mass flows. As expected, the jet coming out of the last gap on the right is positioned at the outer boundary of the channel.

Figure 4 visualizes the flow condition shortly before the maximum stroke is reached in showing velocity-vectors. Apart from the jets flowing out of the opposite valve gaps, which are surrounded by several vortexes, a conspicuous jet like flow comes out of the gaps between the valve plate and the cage which are getting smaller.

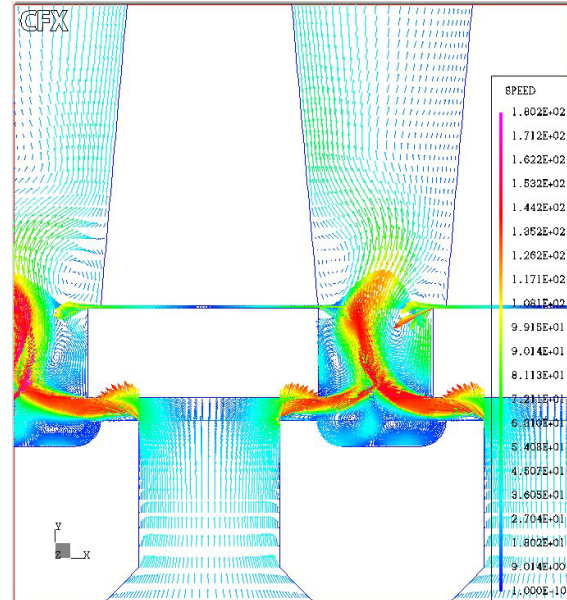


Figure 4: Vector field shortly before the maximum stroke is reached

Based on the calculated pressure distribution around the valve plate, a stroke dependent flow force can be determined. The result plotted in figure 5 firstly shows an increasing flow force. Due to shock waves this force is fluctuating.

In the second half of the valve stroke the force decreases, shortly before the plate stops, the force changes their direction.

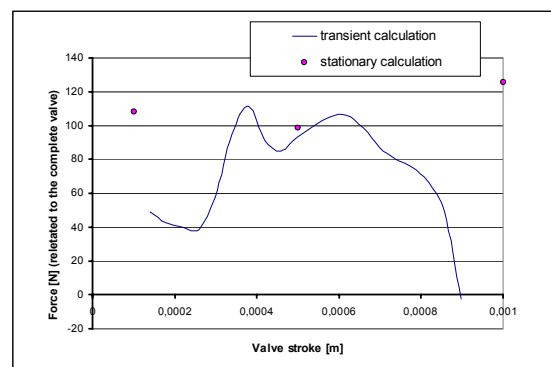


Figure 5: Flow forces transient/ stationary calculation

The figure contains the stationary calculated flow forces at 10 %, 50 % and 100 % of the valve stroke. The comparison of transient and stationary determined forces shows that there are big differences, especially before the plate stops.

#### 4 Force controlled movement of the singular ring

The results shown above for transient flow solutions in a valve having several plates indicate that the differences in the structure of the flow solution between the different channels are less important. But these results show as well, that the time dependent alteration of the flow force cannot be neglected.

For that reasons it seems advisable to reduce the calculation area to a single valve ring including the belonging channels and on the other hand to calculate the plate movement based on the influence of the changing flow force.

The computational area can be simplified further. Since the breadth of the plate ring is small in comparison with its radius, the differences between the inner and outer gap areas can be neglected. With this assumption the problem can be regarded as symmetrical. Therefore we can proceed with a planar examination.

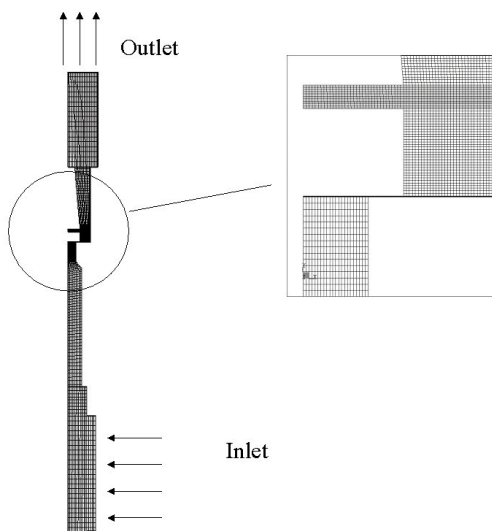


Figure 6: Computational grid of the singular valve ring

The chosen computational domain which is based on the thoughts above is shown in figure 5. Its dimension in flow direction is chosen with the points of view explained above for the complete valve sector. The boundary conditions at the inlet and the

outlet are the same too. The side boundaries are defined as symmetrical borders.

The nodes of the grid have a constant distribution along the x-axis, otherwise the mesh is destroyed by the CFD-program while adapting the mesh to the time dependent geometry.

The initial conditions were determined by a stationary calculation at a 5 % stroke position. In order to renounce assumptions about the stroke curve no initial plate velocity is preset. When the simulation starts the plate is regarded to be stationary. The resulting misrepresented balance of the acting forces leads to a higher acceleration of the plate. Therefore the calculated stroke curve approximates the real stroke curve very fast.

The simulation method uses an extern procedure, which determines the flow force acting on the plate by integration of the pressure distribution. To predict the position of the plate after each time-step this procedure calculates their acceleration based on the summa of flow-, spring- and mass-force.

Figure 7 shows the time dependent stroke and velocity of the plate. The time dependent flow force and the cylinder pressure are marked in figure 8.

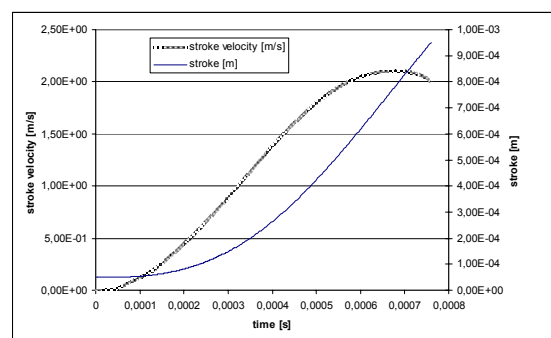


Figure 7: Valve stroke and stroke velocity

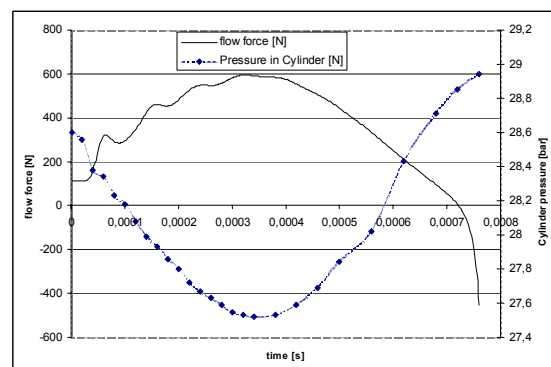


Figure 8: Pressure in cylinder and flow force acting on the plate

## 5 Further actions in the analysis of the fluid-dynamic dependent operation of the valve

The experience with the examples above shows, that the expenditure to predict the transient opening-behaviour of ring valves is acceptable if the geometry is as simplified as possible. The calculation of the time dependent stroke can be connected with the flow solution to consider the transient share of the flow force. There were no further assumptions necessary for this calculations. This prediction method is physical more exact than the prediction based on stationary determined force coefficients. On the other hand it is more comprehensible than the calculation including additional models describing the inertia of the gas or the spring effect of gas volume in narrow gaps.

Despite that some uncertainties of the shown examples have to be considered. The initial condition at the beginning of the time interval is regarded as a fundamental uncertainty. Because it is not possible to carry out the prediction of the conditions in a closed valve using the available Navier-Stokes-solvers, it seems advisable to start the analysis with an one-dimensional-solution. The result of the one-dimensional solution can be used as initial condition for the two-dimensional CFD calculation.

To validate the results of the theoretical analysis, parallel calculations and measurements are planned using the valves of a non-lubricated experimental air compressor located at TU Dresden.

The presented analysis of the opening behaviour covers only a part of the complete operation cycle of the valve. Therefore it suggests itself to analyse the closing behaviour. In the case of poor fitted springs a flow field having larger transients can be expected.

The influence of possible shock waves between valve ring, seat and cage has to be analysed.

## Reference

Pohlenz, W.: Bauteile für Pumpen, Verlag Technik Berlin, 1983

Böswirth, L.: Strömung und Ventilbewegung in Kolbenverdichterventilen, Eigenverlag Wien 2002

AEA-Technology, TASCFLOW Vers. 2.9 User Documentation Volume I - III, 1999

# **Thermal and structural analysis of a reciprocating compressor cylinder**

by

**Georg Samland**

**Nicole Retz**

**Research & Development**

**Burckhardt Compression AG**

**Winterthur**

**Switzerland**

**Reliability and economics of compression systems -  
recent trends in the market of  
reciprocating compressors  
March 27<sup>th</sup> / 28<sup>th</sup>, 2003 Vienna**

## **Abstract:**

Heat transfer does not just affect the performance, operation and reliability, but also the design of compressors. Apart from a structural analysis, it is possible to improve reciprocating compressor cylinders by taking thermal and fluidic effects into account. These improvements as well as casting and manufacturing considerations can be incorporated into an integrated development process. The results of the redesigned cylinder show that it is possible to use the present understanding of the phenomenon of in-cylinder heat transfer for analysing and designing better, cost-effective and efficient cylinders, even with API requirements such as an active cylinder cooling. The redesigned cylinder consists of three parts and the cylinder liner. The shape and location of the new cooling water cavity have completely changed, resulting in a straightforward casting pattern for the complete cylinder.



## 1 Introduction

Product and process technology in the surrounding field of the reciprocating compressor industry is rapidly evolving. Customers are placing an increasing emphasis on quality and reliability, at the same time looking for a cost-effective compressor.

There is no doubt that product quality is of greatest importance for a reciprocating compressor manufacturer to survive in the competitive global market. To respond to the increasingly dynamic and challenging market demands, the manufacturers have to modernise their products and product lines. Therefore, the ageing but proven products, strongly grown casting pattern and casting pattern variations are consequently requiring a complete redesign of the products.

Most of the compressor manufacturers are working on the subject of the cylinder, one of the known cost determining components of a reciprocating compressor. Depending on the point of view, the task is solved in different ways. The activities range from pure thermal analysis to structural analysis and to computational fluid dynamic (CFD) analysis.

## 2 Cooled or non-cooled cylinders?

Years ago, considerable research work, discussions and publications [1,2,3,4] about the extent of influence of heat transfer (specially for the cylinder) on compressor performance could be noticed. On the theoretical side, in addition to a basic research for understanding the phenomenon of unsteady heat transfer inside compressor cylinders, some in-cylinder heat transfer correlation have been developed for use in compressor simulation models in order to account for heat transfer effects on overall compressor performance. The most important effect appears to be the heating up of the suction gas which has a direct effect in reducing volumetric efficiency and an indirect effect in increasing power requirements. On the experimental side, improvements in sensor and instrumentation technology have helped in making simultaneous measurements of in-cylinder temperature, pressure and heat transfer rates.

Recently the main activity is focused on a more or less pragmatic way to deal with the cylinder subject. The latest publications [5,6,7] do not refer to the above mentioned investigations. The efforts for an economic manufacturing and therefore a cost reduction for the cylinder are the main focus of many compressor manufacturers. Among other

activities, such a cost reduction can be realised by omitting the active cylinder cooling completely. Thus, cooling of the cylinder is done through natural convection on the external surface of the cylinders. References are made to the experiences from the so-called high-speed compressors used so far. However, API demands are consciously not taken into consideration.

But, the results found in the literature, indicate that heat transfer plays a very important role in efficient operation of reciprocating compressors. According to [4] heat transfer can account for as much as 10 percent in compressor volumetric and thermodynamic efficiencies.

Summarizing these points does not lead to the question, whether cooled or non-cooled cylinders should be used. The question is: Is it possible to use the present understanding of the phenomenon of in-cylinder heat transfer in order to transfer the knowledge to designers for analysing and designing better, cost-effective and more efficient cylinders?

The current investigation gives first answers to this question. But the results also show that there is a need for further research in this area.

## 3 Objective of the current investigation

Objective of the investigation was a concept revision of the currently used cylinder design regarding thermal, fluidic and structural aspects.

Requirements that have to be considered are:

- API conform design i.e. cooled cylinder, cylinder liner
- Cost effective design
- Manufacturing point of views
- Proof of life cycle fatigue
- Design verification of the cooling water cavities
- Maintainability

Thus, these requirements led to a number of analyses. In addition to a basic thermal analysis, a CFD calculation of cooling water cavities has been carried out. Finally, a structural analysis was performed.

Some of the compressor manufacturers only use the maximum allowable working pressure (MAWP) as a static criterion for their cylinder design. This leads to a conservative and massive cylinder design with

e.g. burst pressure for nodular cast iron of 8\*MAWP and for grey cast iron of 10\*MAWP.

In the present case, the following loadcases for the structural analysis are considered:

- Preload due to assembly conditions
- Pressurised cylinder during inspection
- Suction pressure
- Discharge pressure

The latter two cases are important in order to determine the fatigue life aspects of the components due to alternating suction and compression conditions. Complex calculations are necessary in order to answer the question of life cycle and fatigue behaviour. An in-house developed program based on the FKM guideline /10/ is used to evaluate and optimise the fatigue behaviour.

## 4 Analysis

### 4.1 Thermal Analysis

#### 4.1.1 Background

Accurate information about heat transfer processes play a significant role in simulation and design of reciprocating compressors. The heat transfer process that takes place in the interface between the working fluid and the cylinder walls is one of the most relevant effects regarding reciprocating compressor performance.

For a reciprocating compressor cylinder, the heat transfer that influences the efficiency could be divided into two parts: The heat transfer in the suction passage and the heat transfer in the cylinder (regenerative heating).

The high temperature of gas in the discharge passage and the gas temperature in the cylinder cause the metal to heat and this, in turn, increases suction gas temperature as it flows through the suction passage. This increases temperature of the trapped gas and decreases compressor capacity. The pV-diagram and compressor power are unchanged by this heating. Therefore, the compressor efficiency is reduced. The amount of this heating depends on discharge temperature, cylinder design and cooling effectiveness.

Liner or cylinder wall temperature in an operating compressor will be between suction and discharge gas temperatures. During the high pressure part of

the cycle, heat will be transferred from the gas to the cylinder wall. During the low pressure part of the cycle, heat will be transferred from the cylinder wall to the gas in the cylinder. Thus, fresh gas will be heated in the cylinder before it is compressed. This increases trapped temperatures and decreases compressor capacity. Heat transfer decreases compressor power requirement, but not as much as reduction in capacity. Thus, there is a small loss in compressor efficiency. This effect is affected by cylinder cooling and depends on the heat transfer coefficient between the cylinder wall and the gas in the cylinder. This, in turn, depends on the gas properties which are relatively well known, and gas flow velocity and pattern in the cylinder as function of time which are not well known.

#### 4.1.2 Procedures

There are three possible approaches to carry out a thermal analysis:

- Fixed temperature distribution as a boundary condition for in-cylinder surfaces and other exterior areas
- Bulk temperatures and convection film coefficients applied to in-cylinder surfaces and other exterior areas
- Conjugate heat transfer analysis to determine the convection boundary conditions implicitly

The first approach is applied if accurate information regarding detailed temperature distribution is available. It is only reasonable to use these boundary conditions for single parts in order to calculate displacements and stress due to a temperature field. This approach gives compressor designers little or no insight into the mechanism of heat transfer, and the design changes that can improve compressor performance.

The second approach uses simple energy and mass balances based on the first law of thermodynamics to predict bulk thermodynamic properties of the gas in the cylinder. Heat transfer between the cylinder walls and the gas is calculated with widely used correlation for the heat transfer coefficient.

The third approach solves the unsteady continuity, momentum and energy equations for the gas in the cylinder using, for example, a finite difference technique. No heat transfer coefficient is needed in this model. The main disadvantage is that this method requires tremendous calculation capacities.

The work described afterwards uses the second approach. It is an effective way to get first results. The necessary bulk thermodynamic properties can be gained from the experience with advanced reciprocating compressor simulation programs and perhaps with existing experimental results.

### 4.1.3 Heat transfer modeling

A large number of experimental and theoretical studies have been performed in the field of instantaneous heat transfer between the in-cylinder gas and the solid walls. The main objective of all these works was to develop simple correlation to predict the Nusselt number for the gas-cylinder interface as a function of global properties. As a result, more or less sophisticated models are available to be used for reciprocating compressor simulation. Straightforward models use a correlation assuming that heat transfer follows Newton's law. Other models take into consideration that the instantaneous heat transfer is out of phase with the difference between bulk gas and wall temperature. Heat transfer out of phase with temperature difference can be described using a complex Nusselt number. Heat transfer is then expressed as the sum of one part proportional to temperature difference and another part proportional to the rate of change of temperature.

In the present case, the model suggested by Liu and Zhou /8/ supplied the best results for an overall compressor simulation. According to this model, the global Nusselt number for the cylinder is a function of the Reynold and Prandtl number

$$Nu_Z = A \cdot Re_Z^b \cdot Pr_Z^c$$

with the constants  $A=0.75$ ,  $b=0.8$ ,  $c=0.6$  for the process gas compressor under study. Different compressor designs, e.g. labyrinth piston compressors, lead to different values for the constants.

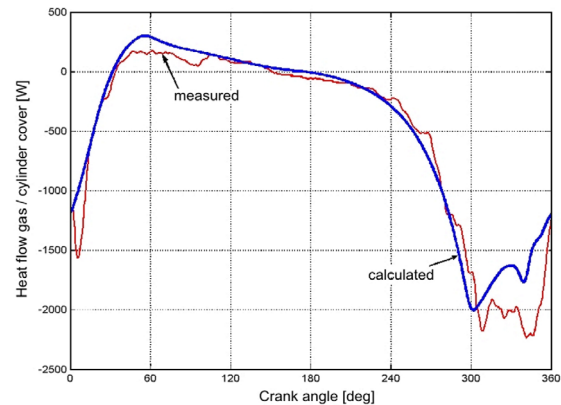


Figure 4.1.1: Measured and calculated heat flow

However, heat flux values measured in the cylinder cover differ from the results obtained by the simulation. If the heat transfer is predicted using a complex Nusselt number model suggested by Lawton /9/, the measured and calculated heat flux agree well. But in this case, the calculated piston temperature is typically too high for this model. These results show, that there is a need for further research in this area. Figure 4.1.1 shows the measured heat flow for the cylinder cover and the calculated heat flow according to Lawton.

Nevertheless, these models are accurate enough to get a first view inside the cylinder. Therefore, the calculated bulk thermodynamic properties of the gas in the cylinder were used as input for the following thermal analysis. Figure 4.1.2 and 4.1.3 show an example of calculated bulk temperatures and appropriate convection film coefficients for one cycle in a nitrogen compressor (suction pressure 1.2 MPa, discharge pressure 4.2 MPa).

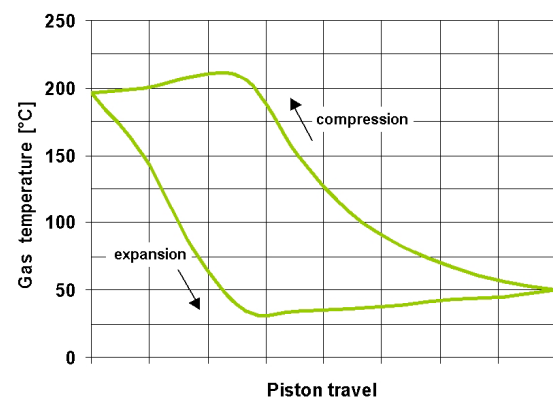


Figure 4.1.2: Example of calculated bulk temperature for one cycle

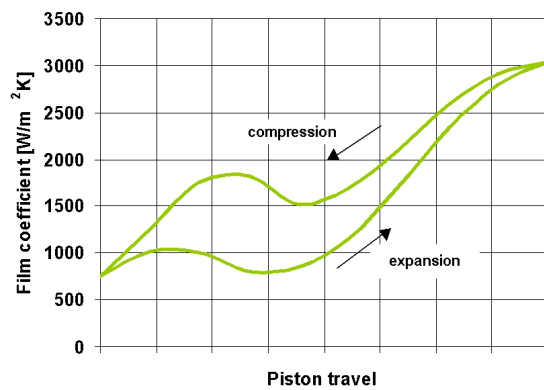


Figure 4.1.3: Example of calculated convection film coefficients for one cycle

#### 4.1.4 Results

The following results are a short excerpt from extensive parameter studies. Figure 4.1.4 shows the CAD model of a standard cylinder. It is a proven cylinder design with longstanding operational experience in many applications.

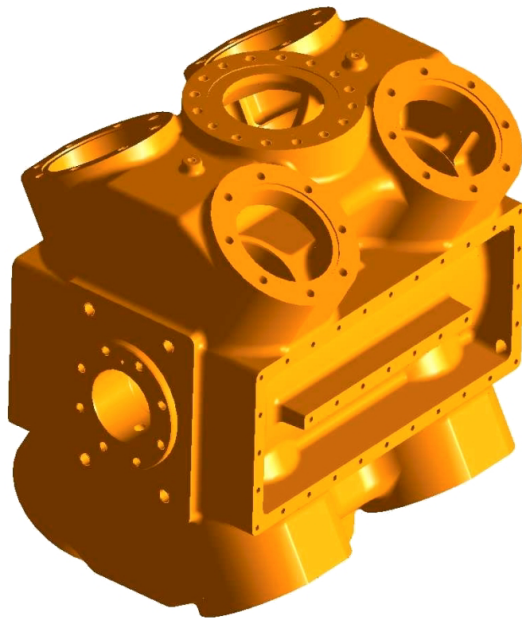


Figure 4.1.4: CAD model of a cylinder

This type of cylinder design is symmetric and therefore, the corresponding volume model for the FEA can be reduced to a half-model. Figure 4.1.5 shows such a half model of the cylinder with cylinder liner and cylinder cover. Details are removed and the model is reduced to the characteristics necessary for a Finite Element Analysis (FEA). The

corresponding finite element mesh is shown in figure 4.1.6.

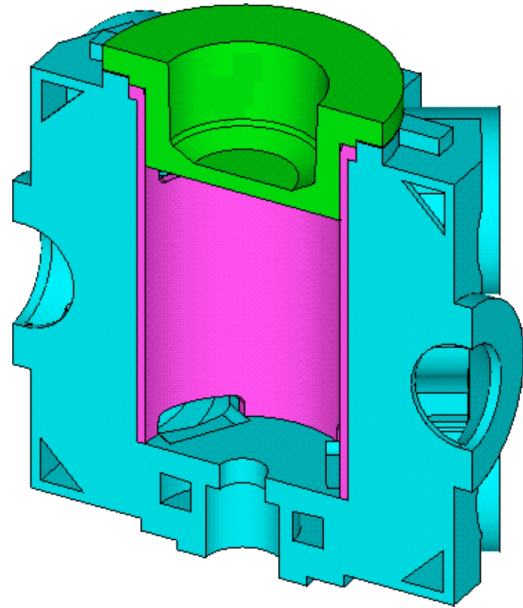


Figure 4.1.5: Volume half-model of the cylinder including cylinder liner and cover

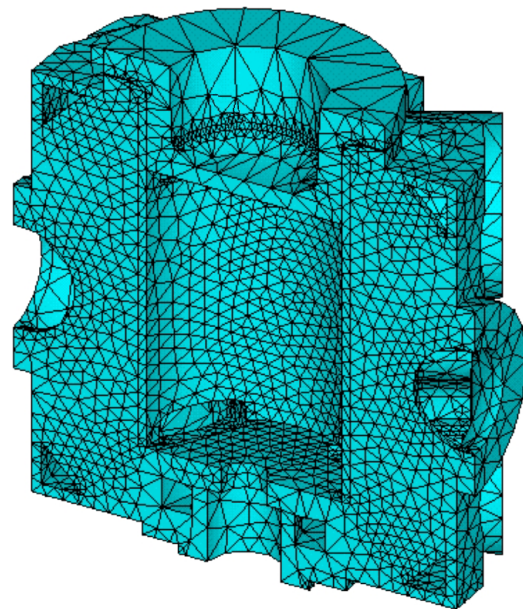


Figure 4.1.6: Finite element model of the cylinder including cylinder liner and cover

For the thermal analysis the boundary conditions according to figures 4.1.2 and 4.1.3 were used. Figure 4.1.7. shows exemplarily the film coefficient for the cylinder liner surface. With the corresponding bulk temperature, a temperature field as shown in figure 4.1.8. was calculated. The hot



discharge side can clearly be seen. Also, a non uniform temperature distribution along the cylinder circumference is visible. This agrees with the experimental results showing that the cylinder wall and/or cylinder cover temperature is temporally constant and locally variable in a steady state system.

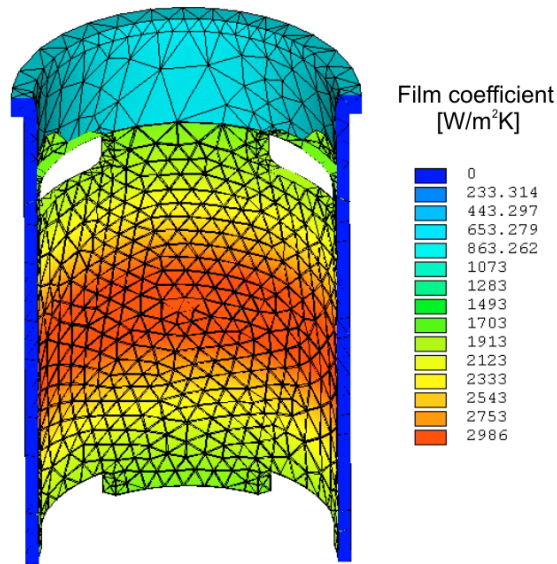


Figure 4.1.7: Film coefficient for the cylinder liner surface

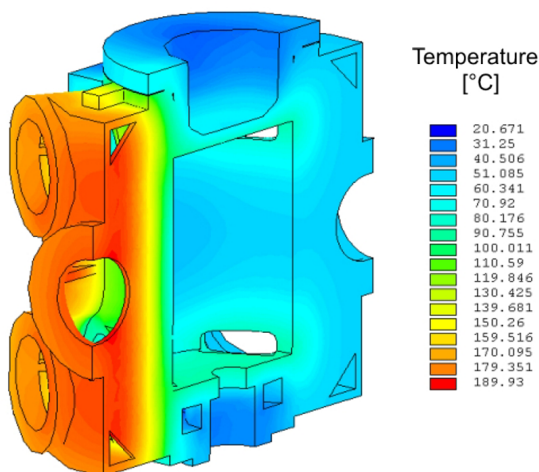


Figure 4.1.8: Temperature field for the cylinder

A sensitivity study with parameter variation was made in order to get information about the influence of various heat transfer conditions on the overall temperature and heat flux distribution. With these studies e.g. it is possible to determine the effects of direct or indirect cylinder cover cooling.

Figure 4.1.9 shows the heat flux distribution for the cylinder liner. There is a remarkable heat flux into

the cylinder gas chamber in the region of the discharge side. This leads to a heating up of the trapped gas which, as above-mentioned has a direct effect in reducing volumetric efficiency.

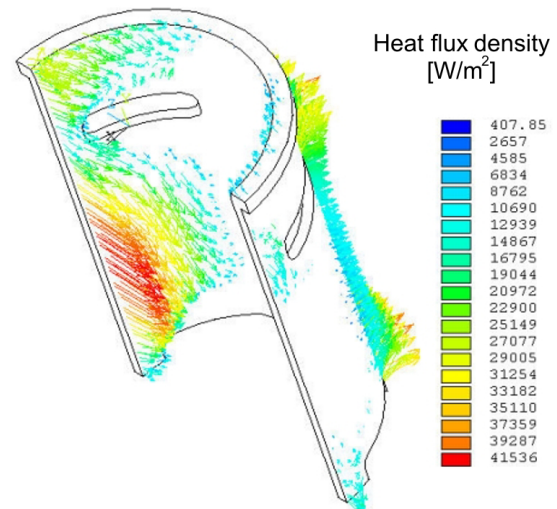


Figure 4.1.9: Heat flux distribution for the cylinder liner

As mentioned, this is a first approach to understand and determine the heat transfer process in the cylinder in three dimensions. It is also a first approach to visualise the local heat flux distribution in the cylinder which could help to improve the cylinder design. Provided that sufficient computer capacity is available, the next reasonable step should be a conjugate heat transfer analysis. In a conjugate heat transfer problem, the temperature equation is solved in a domain with both fluid and non-fluid (that is, solid material) regions.

#### 4.1.4 Conclusion from the thermal study

The thermal study showed the following, partly trivial and known results:

- Asymmetric temperature field
- Cooling is important on the discharge side of the cylinder. Cooling on the suction side is not necessary.
- Discharge gas chamber has to be separated or isolated from the compression chamber especially the middle section of the cylinder.
- Active cooling in the actual design takes place in between the suction and discharge side with unsatisfactory results.



These are aspects from the thermal point of view. From an economic point of view it is not possible to put these ideas into practice. Due to the casting process it is better to have symmetric parts. Separating the entire discharge gas chamber from the cylinder is also not a practicable way.

These considerations and manufacturing/casting point of views led to a complete redesign of the cylinder. Now, the new cylinder consists of three parts and the cylinder liner, figure 4.1.10. Packing cooling is no longer directly integrated in the cooling cycle.

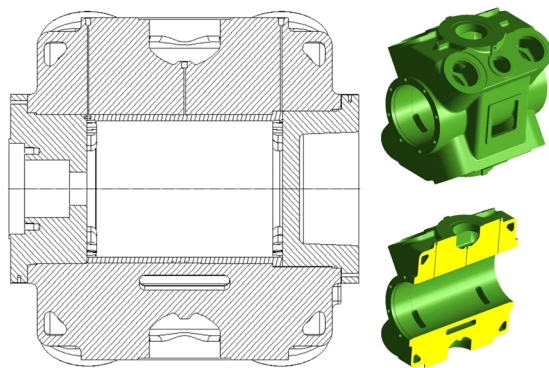


Figure 4.1.10: Redesigned cylinder including cylinder liner and covers

Figure 4.1.11 shows the standard (left side) and new (right side) design of the cylinder (top) and the actual and new design of discharge/suction gas chamber (middle) as well as the cooling water cavities (bottom). The shape and location of the new cooling water cavity has been completely changed and is utilised to separate the hot discharge gas chamber from the compression chamber inside the cylinder. A further advantage is the resulting straightforward casting pattern.



Figure 4.1.11: Comparison of standard (left side) and new (right side) cylinder design - complete cylinder (top), discharge/suction gas chamber (middle), cooling water cavities (bottom)

## 4.2 Computational fluid dynamics analysis

In order to analyse the three-dimensional fluid flow field of the cooling water through the cylinder, a simple Computational Fluid Dynamics (CFD) analysis was carried out. The aim of such an investigation was the comparison between the former and the new geometry of the cooling water cavity with respect to the fluid flow characteristics. The fluid flow problem is defined by the laws of conservation of mass, momentum, and energy. These laws are expressed in terms of partial differential equations which are discretised with a finite element based technique. The elements are of the 8 noded 3D fluid-thermal type.

As for all the other analyses, the model was built using the data of a CAD model. Figure 4.2.1 shows

the streamlines of the flow for the cooling water cavity of the standard cylinder design. Due to the geometry of the large cooling water cavity, location of inlet and outlet flanges and the according boundary conditions of the cooling water flow (e.g. pressure, temperature at the in- and outlet) an unsymmetrical flow characteristic can be noticed. Especially in the lower part of the cavity, the main flow through the packing cooling could be seen on one side.

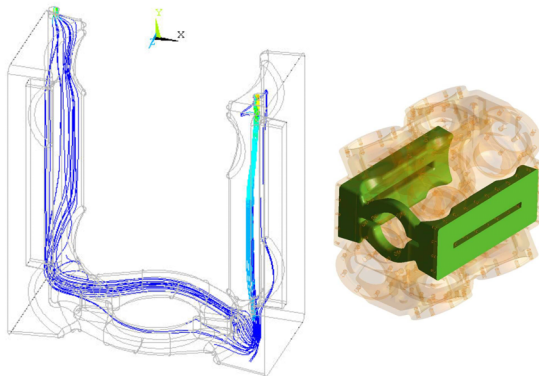


Figure 4.2.1: Fluid flow through the cooling water cavity of the standard cylinder

For the new cylinder design, the cooling water flow (Fig. 4.2.2) is evenly distributed, specially in the region where the hot discharge side is separated from the compression chamber.

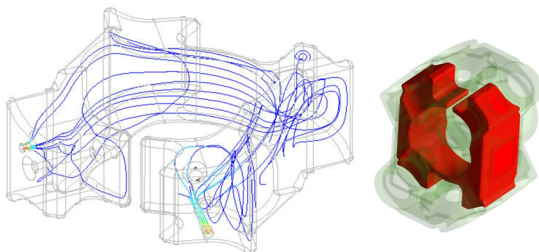


Figure 4.2.2: Fluid flow through the cooling water cavity for the new cylinder design

### 4.3 Structural analysis

For the structural analysis, the FE model shown in figure 4.1.6 could be used. Four loadcases were taken into consideration:

- Loadcase 1: Pressurised cylinder (gas chamber and cooling water cavity) as used for the inspection
- Loadcase 2: Preload under assembly conditions
- Loadcase 3: Pressure under operating conditions during suction phase
- Loadcase 4: Pressure under operating conditions during discharge phase

Complex calculations are necessary in order to answer the question of the life cycle fatigue behaviour of different components. An in-house developed program based on the FKM guideline /10/ is used to evaluate and optimise the fatigue behaviour.

Safety factors or load carrying capacity factors respectively, are therefore determined using a reduced Haigh diagram (Figure 4.3.1). Reduction is made on the “amplitude axis” with respect to surface roughness, size of raw material, loaded volume etc. Then, the calculated service stress is checked for the position in the “safe area” and the equivalent safety factors are calculated.

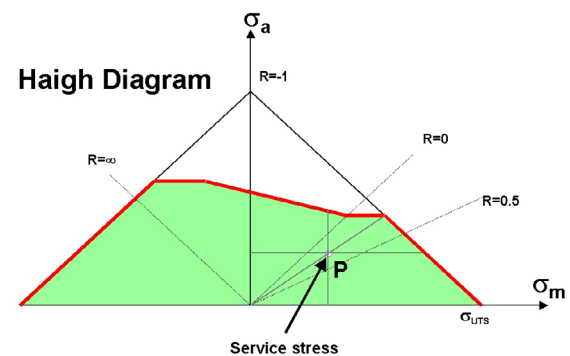


Figure 4.3.1: Reduced Haigh diagram

A load capacity of 100 percent corresponds to the maximal admissible load if appropriate safety factors are built in. The maximum load is considered in the static load carrying capacity, while in the cyclic load carrying capacity the mean stress and the corresponding stress amplitude were taken into account.

First of all, the equivalent loadcases for the minimum and maximum loads are calculated to determine the mean stress and the stress amplitude for the components. Figure 4.3.2 shows an example of the equivalent stress distribution for the standard cylinder (right) and for the redesigned cylinder (left) under an increased maximum pressure load of

12.8 MPa. Especially the critical regions, like some ribs in the discharge gas chamber or the valve chamber, were optimised, improving thus the fatigue behaviour. Figure 4.3.3 shows a cut view of the quarter model of the cylinder. The critical regions for the non-optimised, standard design are clearly to be recognised. The resulting cyclic load carrying capacity for the redesigned cylinder is shown in figure 4.3.4.

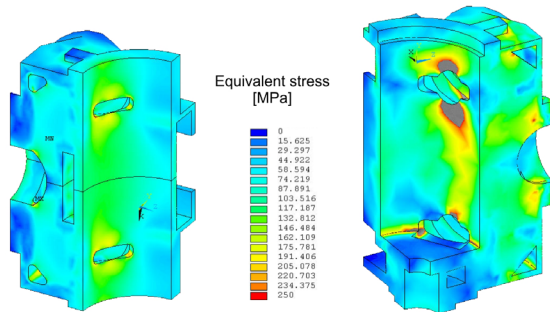


Figure 4.3.2: Equivalent stress for the standard cylinder (right) and for the redesigned cylinder (left)

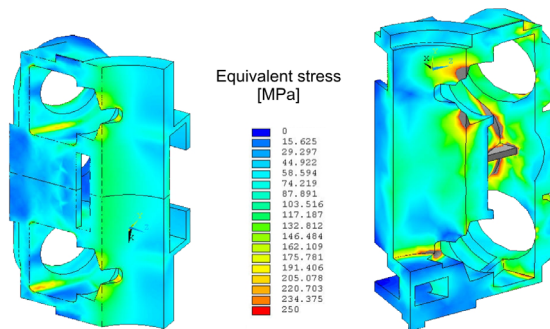


Figure 4.3.3: Equivalent stress for the standard cylinder (right) and for the redesigned cylinder (left) - cut view

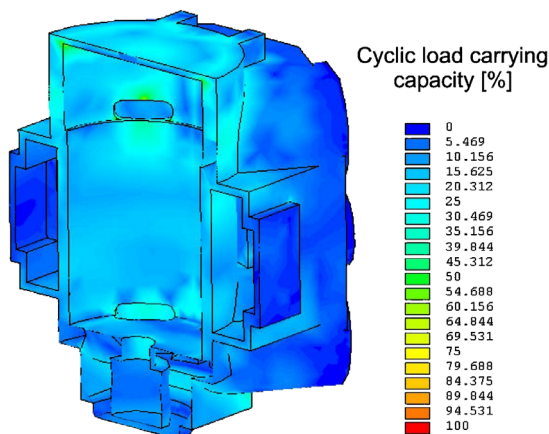


Figure 4.3.4: Cyclic load carrying capacity for the redesigned cylinder

## 5 Next Steps

The next important step will be the verification of such a redesigned cylinder by means of experimental data. For example, strain gauge measurements will be used for the verification of the structural integrity. Temperature measurements could be used to validate the calculated temperature distribution.

The heat transfer models still have room for improvement. Therefore, further measurements specially with the heat flux sensor are necessary in order to get more detailed information about the local and temporal temperature and heat flux field inside the cylinder.

Finally, performing a conjugate heat transfer analysis would be another important step. It would help to understand the phenomenon of heat transfer in the cylinder and would give further information to the designers, on how to improve the cylinder design.

## 6 Conclusions

Heat transfer does not just affect the performance, operation and reliability but also the design of compressors. Apart from a structural analysis, it is possible to improve the design of reciprocating compressor cylinders if thermal and fluidic effects are taken into account. These results, together with casting and manufacturing considerations can be incorporated into an integrated development process.

The results for the redesigned cylinder show that it is possible to develop a cost effective design even with API requirements such as cooled cylinder and cylinder liner.

The new cylinder design consists of three parts and the cylinder liner. Packing cooling is no longer integrated directly in the cooling cycle. The location of the new cooling water cavity has completely changed and is utilised to separate the hot discharge gas chamber from the compression chamber inside the cylinder.

The results show that it is possible to use the present understanding of the phenomenon of in-cylinder heat transfer in order to transfer the knowledge to designers for analysing and designing better, cost-effective and more efficient cylinders. But the results also show, that there is a need for further research in this area.

## 7 References

- /1/ Brok, S.W., Toubert, S. and Van Der Meer, J.S.  
Modelling of cylinder heat transfer – large effort, little effect?, Proc. 1980 Purdue Comp. Tech. Conf., pp. 43-50.
- /2/ Shiva Prasad, B.G.  
Fast response temperature measurements in a reciprocating compressor, Proc. 1992 Purdue Comp. Tech. Conf., pp. 1385-1395.
- /3/ Fagotti F., Prata A.T.  
A new correlation for instantaneous heat transfer between gas and cylinder in reciprocating compressors, Proc. 1998 Purdue Comp. Tech. Conf., pp.
- /4/ Gerlach R.C, Berry R.A.  
Effect of heat transfer and related variables on compressor performance, Proc. of the Fourth Annual Reciprocating Machinery Conf., San Antonio, TX, USA, 1989
- /5/ Cierniak S.V.  
High Speed -API 618– Prozessgas-Kolbenverdichter- die optimale Lösung zur Kostenbeherrschung, Kötter - Workshop Kolbenverdichter, Rheine /Germany, 2002, pp.77-93
- /6/ Hoff K.H.,  
Entwicklungsschwerpunkte des Schnellläufers 320hs, Kötter - Workshop Kolbenverdichter, Rheine /Germany, 2002, pp.169-184
- /7/ Käyser C.C.H.  
Kühlung der Verdichterzylinder – Wahrheiten und Unwahrheiten, Kötter - Workshop Kolbenverdichter, Rheine /Germany, 2002, pp.185-193
- /8/ Liu, R. and Zhou, Z.  
Heat transfer between gas and cylinder wall of refrigerating reciprocating compressor, Proc. 1984 Purdue Comp. Tech. Conf., pp. 110-115.
- /9/ Lawton, B.  
Effect of compression and expansion on instantaneous heat transfer in reciprocating internal combustion engines, Proc. ImechE, Vol. 201 (1987), No. A3, pp. 175-186.
- /10/ Theorie der FKM-Richtlinie und deren Anwendung, Seminarunterlagen, Richtlinie, Abschlussbericht, IMA Dresden, D, 1999.





## Selection and Sizing

---

A. Pyle / Shell Chemical LP; A. Eijk / TNO TPD

H. Elferink / Thomassen Compression Systems

- **Coming 5th Edition of the API Standard 618**  
**Major changes compared to the API 618, 4th edition**

G. Kopsick / Ariel Corporation

- **Comparison of moderate and low-speed API-618 reciprocating compressor designs for petroleum, chemical and gas industry services**

S. Cierniak / HGC Hamburg Gas

H. Funke, D. Wendt / ALSTOM Power Conversion GmbH

- **Optimizing the drive system for variable speed electric motor driven reciprocating compressors**

H. S. Gujral / PCA; S. Cierniak / HGC Hamburg Gas

- **Economizing the engineering costs of packaging reciprocating compressors to diverse customer specifications: some methods and strategies**

N. Feistel / Burckhardt Compression AG

- **Influence of piston-ring design on the capacity of a dry-running hydrogen compressor**

J. Greven, K. Hoff / Neuman & Esser GmbH & Co. KG

- **Reliable high-pressure-CO<sub>2</sub>-compression by means of well-aimed compressor design**

W. Wirz / Dresser-Rand Company

- **High speed separable compressors – an alternative for slow speed integral-engine compressors for natural gas transmission and gas storage**





Shell Chemicals



# Coming 5<sup>th</sup> Edition of the API Standard 618

Major changes compared to the API 618, 4<sup>th</sup> edition

Pyle, A

Engineering Services-Mechanical Equipment

Shell Chemical LP, Deer Park Plant

Houston, USA

Eijk, A

Flow and Structural Dynamics

TNO TPD

Delft, The Netherlands

Elferink, H

Thomassen Compression Systems B.V.

Compressor Technology

Rheden, The Netherlands

## Reliability and economics of compression systems – recent trends in the market of reciprocating compressors

March 27<sup>th</sup> / 28<sup>th</sup>, 2003 Vienna

### Abstract:

This paper will present the highlights of changes that will be found in the 5<sup>th</sup> Edition of API 618, which is expected to be published in late 2003 or early 2004. Approximately every 5 years the API Standards are revised in such a way that the latest field experiences and proven designs are included to achieve more efficient, reliable and safe systems. For this purpose a task force group of the API Standard 618 was formed and has been working on the 5<sup>th</sup> edition since the end of 1999. Another important issue was to write the 5<sup>th</sup> edition so that it would be accepted by the ISO. In the future, it is expected to become ISO 13707 and then become the world standard for reciprocating compressors for petroleum, chemical and gas industry services.

The paragraph handling Pulsation and Vibration control has had major changes. Three different design philosophies are used in the world for pulsation and vibration control each leading to the same result: avoiding problems with vibration, performance, reliability and flow measurement errors. These different design philosophies are now accepted by the API committee and are included in the 5<sup>th</sup> edition. A new API document, RP 688 will be issued to give more clarification to this subject.

This paper mainly discusses and highlights the most important changes in the area of pulsation and vibration control, both in API 618 and in RP 688. However, the other main changes and improvements are also summarized.

## 1 Introduction

API 618<sup>1</sup> has been used to specify reciprocating compressors for the oil, gas and chemical industries for almost 40 years. As this document has been developed in the USA all references are related to US standards and practices. ISO 13707<sup>2</sup> will fulfill the same need. However, it contains where available, ISO standards and other outside US proven practices.

As these companies have globalised, it has become apparent that having single, internationally accepted standards would greatly simplify the specification, design and procurement process for users, designers and suppliers alike.

Section 2 will explain in more detail the process that API and ISO have undertaken to harmonize their standards into one single standard for each application. It will also specifically address the process and timeline for API 618 and ISO 13707.

In Sections 3 and 4, the changes that have been made to the 5<sup>th</sup> Edition<sup>3</sup> of API 618 will be reviewed. One of the most significant changes that will be found in the 5<sup>th</sup> Edition of API 618 is in the paragraphs that define the requirements for pulsation and vibration control. These changes will be explained in Section 3 while the non-pulsation and vibration related changes will be covered in Section 4.

## 2 Background on API 618 and ISO 13707

API, in the early nineties took the initiative to have their API documents adopted and published by ISO. As a result of this, the ISO organization has formed working groups to review the API documents for preparing ISO documents based on the existing API's. The ISO documents would become the global working documents for machinery in the Petroleum, Chemical and Natural Gas Industry.

The ISO working group was instructed to minimize their changes, with respect to the existing API paragraphs, and to make essential changes only and not to include additional paragraphs except where it was felt to be absolutely necessary.

The working group TC 67/118 SC6 WG 2 was formed and started in 1992 preparing a draft ISO 13707, based on the draft 4<sup>th</sup> edition of API 618. The API Task Force continued simultaneously their work on the 4<sup>th</sup> edition of API 618 and completed

their work in 1995 and the document has been published in June 1995.

The ISO working group completed their draft ISO 13707 also early 1995. This document could however not be published at that time since ISO documents in general are “normative” whereas the ISO 13707, derived from API 618, wasn't. It took some time within the ISO organization to get a “guideline” accepted as an ISO document. This created an enormous delay in the publication of the ISO documents. Finally the ISO 13707 was published in 2000 (5 years after the 4<sup>th</sup> edition of API 618 was published).

API proceeded, according their rules, and started a new Task Force in 1999 to prepare the 5<sup>th</sup> edition of API 618 for implementing all new experiences and proven developments.

During the 1<sup>st</sup> EFRC Conference in Dresden a paper<sup>4</sup> was presented by TNO TPD and South West Research Institute with suggestions for improvements and extensions to API 618 related to pulsation and vibration control.

The task force group for the 5<sup>th</sup> edition of the API 618 used this paper as a starting point. ISO was also invited to become member of this API Task Force.

It was agreed upon that the API would adopt in their 5<sup>th</sup> edition, as much as possible the deviations made and included in the ISO 13707. This also was the moment to make additions and modifications that ISO has not added in their first issue to be in line with API documents. On a number of paragraphs the European approach has now been added. In some cases the approach differs remarkably from the American approach. As both approaches show to be well developed they are included in this guideline.

The paragraph on “Pulsation and Vibration Control” is one of these paragraphs that shows the differences. This paragraph has been rewritten completely.

This paper will mainly concentrate on this subject. Other changes in the API 618 are mentioned but will not be discussed in this paper in detail.

The publication of the 5<sup>th</sup> edition of API 618 is expected late 2003. The 1<sup>st</sup> edition of ISO 13707 then becomes more or less out of date. To line up both documents again, the 5<sup>th</sup> edition of API 618 will be issued as a draft for the 2<sup>nd</sup> edition of ISO, the so-called ISO/DIS 13707. The comments on the DIS (Draft International Standard) will be compiled

and discussed. The necessary changes will be as much as possible implemented in the ISO 13707 and API 618. The intention is to publish the almost identical 2<sup>nd</sup> edition of ISO 13707 and the 6<sup>th</sup> edition of API 618 simultaneously.

The publication of the new 5<sup>th</sup> edition of API 618 is expected late 2003. This 5<sup>th</sup> edition will be issued as a draft of the 2<sup>nd</sup> edition ISO 13707. The intention is to publish the ISO 13707 2<sup>nd</sup> edition and the 6<sup>th</sup> edition of API 618, which should be almost identical, simultaneously.

Since the 5<sup>th</sup> edition of API 618 has not yet been published the authors cannot be held responsible for any changes that may be made to the material presented. Notes, belonging to the flowcharts and tables in this paper, have been eliminated for the sole purpose to reduce complexity.

It should however been recognized that the notes added in the final version of the API 618 5<sup>th</sup> edition and RP 688 contain valuable information.

### 3 Overview of Changes to Pulsation Control Requirements

When the taskforce first began to work on this section for the 5<sup>th</sup> edition, it established some objectives. Among these were:

- Improve the clarity of the requirements and provide better insight about the intent.
- Match the elements of each Design Approach to more accurately reflect what users request and experience indicates will work.
- Develop flowcharts to better illustrate the iterative design process.
- Update requirements to recognize the application of new technology.
- Expand the tutorial comment to help the user make more informed decisions.
- Ensure that each of the design philosophies used by the designers is accommodated in the specifications.

It is felt by the taskforce that the changes described in the following chapters have fulfilled these objectives.

### 3.1 Three Design Philosophies

There are three basic design philosophies that have been used for pulsation and vibration control in reciprocating compression systems. They are:

- Acoustic Control
- Shaking Force Control
- Vibration Control

It is beyond the scope of this paper to discuss the advantages and disadvantages of each philosophy. This will be explained in detail in API's new tutorial document, RP-688<sup>5</sup>.

#### 3.1.1 Acoustic Control

In API 618, the preferred philosophy has been and continues to be acoustic control. Acoustic control is provided by designing a system in compliance with the formulas that define the maximum allowable pulsation limits. Acoustic filtering is usually required to achieve these limits especially at higher frequencies, which can result in larger bottles and secondary bottles. At the 2001 Turbomachinery Symposium in Houston, Engineering Dynamics presented a paper<sup>6</sup> explaining the advantages of this philosophy in more detail.

Previous editions of API 618 have indicated that when this is not possible, the resulting shaking forces should be evaluated, but have provided no guidance for acceptable levels. Since the only other design limit that was provided was for maximum allowable cyclic stress, it has been interpreted to mean that when the pulsation limits could not be met, then the cyclic stresses had to be calculated. This was not the intent of the authors of the 4<sup>th</sup> edition.

In the 5<sup>th</sup> Edition, shaking force design guidelines will be provided. This not only provides a way to evaluate the impact of exceeding the pulsation limits, but also an end point for the analysis if the shaking force limits are met, without having to calculate the cyclic stresses. In addition, it enables the purchaser to select this philosophy for the design if they feel that its advantages outweigh its disadvantages.

#### 3.1.2 Shaking Force Control

This philosophy generally provides less pulsation control than the acoustic control philosophy,

especially at higher frequencies because the pulsation suppression devices usually do not utilize acoustic filtering. This often results in a more compact equipment layout, but also depends upon mechanical restraint to provided vibration control.

### 3.1.3 Vibration Control

Over the past 10-15 years a third design philosophy, vibration control, has evolved among the European designers. The pulsation suppression devices are sized and fabricated prior to the completion of the final piping design. During piping design, acoustical and mechanical tuning using forced response analysis is done to ensure that vibration levels and cyclic stresses in the combined system are acceptable. This philosophy has the greatest emphasis of the three on significant mechanical modeling and mechanical control.

## 3.2 Revisions and Clarifications for Each Design Approach

For each control philosophy, certain calculations have to be carried out which are specified in so-called design approaches. The design approaches should not be confused with the design philosophies. The 5<sup>th</sup> edition will be identical to the 4<sup>th</sup> edition in that there are three design approaches. Below a summary has been given for what is done in each design approach.

Design approach 1:

- Empirical suppression device sizing

Design approach 2:

- Empirical suppression device sizing.
- Pre-study (damper check) if piping design is not complete.
- Acoustic simulation including the piping if the piping design is complete.
- Completion of maximum piping span tables and vessel mechanical natural frequency calculations to meet separation margin criteria.

Design approach 3:

- As design approach 2 plus detailed mechanical analysis of piping and compressor manifold to ensure that the shaking force and separation

margin criteria are met or that the vibration criteria is met or that the cyclic stress criteria is met.

Unless otherwise specified, the design approach selection chart, which is shown in figure 1, shall be utilized to determine the design approach. For pressures above 350 bar, the purchaser and the vendor shall agree on the criteria for pulsation suppression.

3	3	3	200 bar ≤ P < 350 bar (3000 psi < P < 4500)	Absolute Discharge Pressure
2	3	3	70 bar ≤ P < 200 bar (1000 psi ≤ P < 3000 psi)	
2	2	3	35 bar ≤ P < 70 bar (500 psi ≤ P < 1000 psi)	
1	2	3	P < 35 bar (P < 500 psi)	
kW/Cyl < 55 (HP / Cyl < 75)		55 ≤ kW/Cyl < 220 (75 ≤ HP/Cyl < 300)	220 ≤ kW/Cyl (300 ≤ HP/Cyl)	
Rated Power per Cylinder				

Figure 1: Design approach selection chart

The design approaches provide the sequence of the analysis that is independent of which design philosophy is used. The following excerpt from the 5<sup>th</sup> edition explains the analysis sequence:

“To evaluate compliance with the basic criteria, the following hierarchy applies:

#### 1. Preliminary pulsation suppression device sizing

Determine pressure drop across the pulsation suppression device. The criteria as described shall be met. For Design Approach 1 analysis is completed.

For Design Approaches 2 and 3 next steps are applicable

#### 2. Pre-study of pulsation dampers (if required)

Determine pulsations at the compressor cylinder flanges, and at the line side nozzle of the pulsation damper. The criteria shall be met.

3. After the layout of the pipe system is completed, the pulsation analysis of the complete pipe system is undertaken.

4. Specify maximum piping spans and determine vessel mechanical natural frequencies.

If criteria are met Design Approach 2 will be completed.

If for Design Approach 2 the criteria under step 3 or 4 are not met then either a redesign or, step 5 and 6 shall be performed.

For Design Approach 3 next steps are applicable.

5. Develop a mechanical model and determine mechanical natural frequencies;

6. Determine the maximum allowable shaking forces and check whether these are higher than the acoustic shaking forces calculated by acoustic simulation. If criteria for steps 5 and step 6 are met, Design Approach 3 analysis is complete.

If the criteria in step 5 or step 6 are not met, either a redesign or, step 7 shall be performed.

7. Determine pipe vibrations based on the maximum calculated acoustic shaking forces.

If the vibration criteria in step 7 are-not met, either a redesign or step 8 shall be performed:

8. Calculate dynamic pipe stresses. Maximum allowable cyclic pipe stresses.

If criteria for step 7 or step 8 are met, Design Approach 3 analysis is complete. If the criteria are not met redesign is required.”

Figures 2, 3 and 4 are flowcharts that show in more detail design approaches 1, 2 and 3 respectively. Table 1 provides a summary of each of the design limits that are evaluated in the analysis.

The calculated levels for each design approach have to be compared with allowable levels. In the 5<sup>th</sup> edition additional items/calculations have been added, along with new allowable levels. A summary of the most important additions and allowable levels follows in the chapters below.

### 3.3 Addition of Speed of Sound Factor for Pulsation Criteria

As indicated in chapter 3.1, the allowable pulsation levels for the piping are intended to keep the pulsation-induced forces to low enough levels that minimal mechanical analysis is required in the piping outside the pulsation suppression devices. The formula for allowable pulsation levels was based upon natural gas applications.

From experience, designers have recognized that for gases with a different velocity of sound than for natural gas (e.g. Hydrogen or heavier hydrocarbons), a correction for allowable pulsation levels should be applied to avoid that too much or too little acoustic control is applied to the system to meet the API limits. Especially for Hydrogen systems with a much higher velocity of sound (approximately a factor 4 higher) than for natural gas, much higher pulsation levels can be allowed to achieve the same pulsation-induced forces on a pipe section. This can be demonstrated as follows:

In figure 5 a sketch is given of a pipe section with two bends. In the lower part a standing wave type pattern is given for a gas with a speed of sound of 300 m/s. The maximum pulsation-induced force occurs when a  $\frac{1}{2}$  wavelength ( $\frac{1}{2} \lambda$ ) just fits between the two bends. The reason for this is that the pulsations at the bends are exactly 180 degrees out of phase. At the same frequency, an acoustical standing wave will occur with a wavelength of 4 times the wavelength of a gas with a velocity of sound of 1200 m/s. However, from the figure it can be seen that for this gas the maximum pressure (and force) difference between the bends is 0.15 times the pressure difference of the gas with the lower velocity of sound.

For gases with a lower speed of sound the opposite will happen. Therefore, the following speed of sound correction term has been added to formula 7 in API 618 4<sup>th</sup> edition for the allowable pulsation levels of the piping as follows:

$$\sqrt{\frac{a}{350}} \quad \text{a is the speed of sound in m/s}$$

In table 1 the complete formula is given.



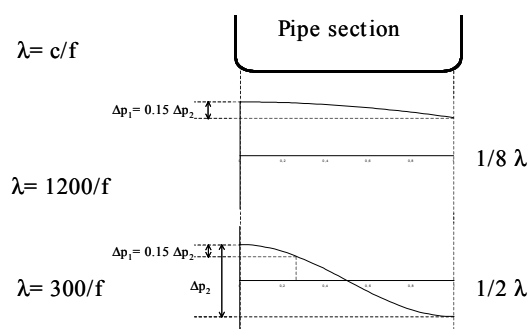


Figure 5: Pressure pulsations on a pipe section

### 3.4 Inclusion of Damper Check Option

Design approach 1 guides initial bottle sizing, which is intended to be used by vendors, to propose well-sized pulsation suppression devices.

With “initial bottle sizing”, only the volume of the pulsation bottles is determined to meet an allowable pulsation level at the line connection. In this way major mistakes in the dimensions and general arrangement will be avoided. This is important for the vendor to estimate the manufacturing costs of the dampers and reduces the risk of early purchase of long delivery materials.

Further, the end-user has some guarantee that the dampers have a sufficient size and that the quotations will be based on comparable sized dampers. This is what the phrase “for commercial sizing” means.

In case of more complex layouts of suppression devices (with or without internals) and complex cylinder passage volumes, internal resonances in the compressor manifold system can increase pulsation levels and pulsation-induced shaking forces. In that case a more accurate pre-design is required to reduce the chance of costly and time-consuming changes in a later stage of the project.

An acoustic pre-study (also called damper check or endless line check) of the pulsation suppression devices should be carried out now for Design Approaches 2 and 3. The pre-study should always be followed by a complete acoustic simulation study, which includes the pipe system. In a pre-study the following items have to be optimized:

- Damper volume to meet allowable API levels.
- Diameter and length of cylinder nozzles to avoid resonances between the damper and cylinder passage volume.

- Location of cylinder and line nozzles to minimize pulsation-induced shaking forces.
- Eventual dissipative damping devices in cylinder nozzles to meet API levels.
- If necessary, baffle plate and baffle choke tube (filter design) to meet API levels and/or to minimize pulsation-induced shaking forces.
- The ratio of surge volume length to internal diameter shall not exceed 4.0, to avoid excessive pulsation-induced shaking forces.

### 3.5 Addition of Shaking Force and Vibration Criteria

The formulas for the allowable shaking forces and a chart for vibration levels have been given in table 1. There are two formulas provided for piping and two for pulsation suppression devices. The first formula defines the allowable shaking force as a function of the effective restraint stiffness and the allowable design vibration level. The second formula provides a maximum shaking force, beyond which the strength of the restraint structure begins to govern instead of the stiffness.

The values represent a compromise between those historically used in acoustic control designs which are usually lower and those used in shaking force control designs which have usually been higher. This technique provides a criteria to implicitly provide pulsation and vibration control without rigorous mechanical modeling. It is extremely important to understand though, that these values are applicable for non-resonant conditions only.

At the 2001 Gas Machinery Council Conference in Austin, a paper was presented by Peerless Manufacturing<sup>7</sup> explaining the basis for not only the shaking force criteria but also for vibration and separation margins.

### 3.6 Addition of separation margins

The easiest way to avoid fatigue failures is keep the vibration and cyclic stress levels to a minimum. One of the possible solutions is to ensure that acoustical and mechanical frequencies do not coincide. For this reason a so-called separation margin criterion between acoustical and mechanical natural frequencies is added in the mechanical analysis in Design Approach 2 and 3 as shown in table 1.

### 3.7 Dynamic pressure drop considerations

For all design approaches an allowable pressure drop as a percentage of the mean static pressure has been specified up to now. The reason for this is to avoid too high fuel costs during the life cycle of the system or to avoid that the driver horsepower is not enough to handle the required flow.

However, at locations with high flow pulsations (e.g. inlet or outlet of large volumes) the so-called dynamic flow can be high and the dynamic pressure drop can become important. This means that the total pressure drop will be much higher than what will be calculated based upon the mean static flow.

Therefore, in the 5<sup>th</sup> edition it has been added that the limits for pressure drop shall be increased by a factor of 2 when the pressure drop is calculated using the total flow, where total flow is the sum of the steady flow plus dynamic flow components, provided that the static component still meets the criteria as specified (see table 1)

### 3.8 Addition of Criteria for Allowable Metering Error

Pulsations can have a significant impact on the accuracy of various types of measuring devices such as orifice, turbine, vortex and ultrasonic flow meters.

The systematic errors caused by a pulsating flow can be positive or negative and related to flow pulsation amplitude and frequency. In contrast to the criterion of pressure pulsation, as stated in API 618 in relation to pulsation forces, the flow pulsation amplitude (and frequency) determines the error in reading. This aspect should be taken into account in a pulsation analysis as per API 618 and errors in reading can be estimated based on the flow pulsations, calculated in the analyses at the flow meter location.

In the 5<sup>th</sup> edition this item has been added and an allowable measurement error has been specified for custody and non-custody transfer (see also an overview of allowable levels in table 1).

### 3.9 Appendices

The appendices for the pulsation and vibration control have also been changed. The most important changes are as follows:

Following the ISO format, the appendices will be called annexes in the 5<sup>th</sup> edition.

- The contents of Appendix M have been replaced by the Design Approach flowcharts found in figures 2, 3 and 4.
- All M items are deleted. M.1. through M.7. are implicitly covered in the new API Standard
- M.9 (valve dynamics) will be moved to the chapter “Valves and Unloaders”.
- M.8 (dynamic and static stresses on pulsation suppressor internals), M.10 (pulsation suppression device low cycle fatigue analysis) and M.11 (piping flexibility) are located in the normative clause.
- Annex N and O are identical to Appendix N and O of the 4th edition.
- The creation of a new Annex that contains informative material about the shaking force criterion.

### 3.10 Creation of RP-688 Tutorial on Pulsation and Vibration Control

The ISO standards have historically been entirely normative. When ISO 13707, 1<sup>st</sup> Edition was published, it contained some material that was not normative, since it was patterned from API 618, 4<sup>th</sup> Edition.

To try to streamline API 618, 5<sup>th</sup> Edition, it was a goal of the taskforce to try to remove as much of the informative material as possible. Due to the complexity of the pulsation and vibration control material, it was felt that additional tutorial or informative text was required, not less. API has previously used “Recommended Practice” documents to publish this type of information. The Subcommittee On Mechanical Equipment (SOME) chose this option to ensure that the 5<sup>th</sup> Edition is predominantly normative while also providing a tutorial document for the user to better understand the requirements and options that are available. Thus was born RP-688, “Recommended Practice for Pulsation and Vibration Control for Positive

Displacement Machinery in Petroleum, Petrochemical and Natural Gas Industry Services”.

The main topics that will be addressed in RP-688 are:

- Basic acoustic and mechanical theory.
- Acoustic, Shaking Force and Vibration Control methods.
- Expanded discussion of the design philosophies.
- Explanation of modeling methods.
- Commentary on the Pulsation and Vibration Control Clause in API 618.
- Explanation of reports provided by designers to the user.
- Field testing and troubleshooting guidelines.

The work on this document is still in progress with an anticipated publication date in 2004.

## 4 Other Changes to API618

### 4.1 Editorial Improvements

Editorial changes made in ISO 13707, 1<sup>st</sup> Edition to improve the clarity, have generally been accepted by the API 618, 5<sup>th</sup> Edition taskforce. Wording from the API Standard Paragraphs R22 has also been used where possible.

The format of the 5<sup>th</sup> edition has been changed so that it utilizes the ISO structure for numbering. The terminology also will change so that paragraphs will now be called clauses and appendices will be called annexes. Material that is redundant with other API standards has been either removed or abbreviated and the appropriate standard has been referenced. For example, paragraphs related to systems such as lubrication systems, control systems, piping and instrumentation are referenced to API 614 /ISO 10438 Part 1 and 2.

### 4.2 Technical Changes

Below a summary has been given of other significant additions and changes with deal with the mechanical design. These items will not be explained into detail.

- Hydraulic tightening of piston rods.

- Alternative methods of securing liners.
- Allowance for hydraulically operated unloaders.
- Alternative valve cover designs.
- More flexibility in piston rod coatings.
- Minimize threaded connections.

## 5 Conclusion

The 5<sup>th</sup> Edition of API 618 represents the culmination of almost 10 years of work by API and ISO to create a single international specification for reciprocating compressors. While the official, single standard in published form may still be several years away, the work done on both 5<sup>th</sup> edition of the API 618 and the 1<sup>st</sup> edition of ISO 13707 provides the majority of the content for that document. These documents are the result countless hours of work by many contributors from many different cultures. By working together to better understand each others needs and issues, compromises were possible that will enable this specification to be more frequently applied to reciprocating compressor applications around the world.

## 6 Acknowledgements

The authors would like to thank their companies for sponsoring their participation on the API 618 task force group. Further we would like to thank all members, and especially the chairmen, of the task force group for their contribution to the 5<sup>th</sup> edition of the API 618.

## References

- 1 API Standard 618, 4<sup>th</sup> edition, June 1995, "Reciprocating Compressors for Petroleum, Chemical and Gas Industry Services"
- 2 ISO 13707, 1<sup>st</sup> Edition, 1-12-2000 "Petroleum and Natural Gas Industries-Reciprocating Compressors"
- 3 API 618, 5<sup>th</sup> Edition Draft, "Reciprocating Compressors for Petroleum, Chemical, and Gas Industry Services"
- 4 Eijk, A., Smeulders, J.P.M., Blodgett L.E., Smalley, A.J., "Improvements and Extensions

to API 618 related to Pulsation and Mechanical Response Studies”, 1<sup>st</sup> EFRC Conference, 4-5 November 1999, Dresden, Germany

- 5 API RP-688, 1<sup>st</sup> Edition Draft, Recommended Practice for Pulsation and Vibration Control in Positive Displacement Machinery Systems for Petroleum, Petrochemical and Natural Gas Industry Services.
- 6 Atkins, K., Tison, J., “ The New Fifth Edition of API 618 for Reciprocating Compressors: Which Pulsation and Vibration Control Philosophy Should You Use? 37th Texas A&M Turbo Machinery Symposium, September 2001, Houston, Texas, USA
- 7 Rogers, P.E. “Rational Vibration, Shaking Force and Separation Margin Guidelines for Acoustical/Mechanical Analysis of Reciprocating Compressor Piping Systems”, Gas Machinery Council Conference, Austin, Tx., USA, October 2001.

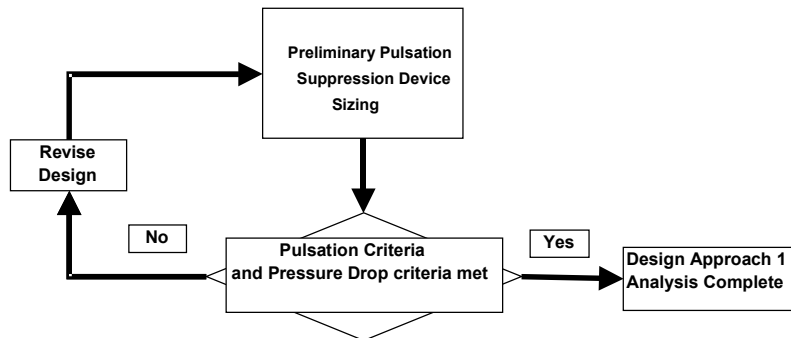
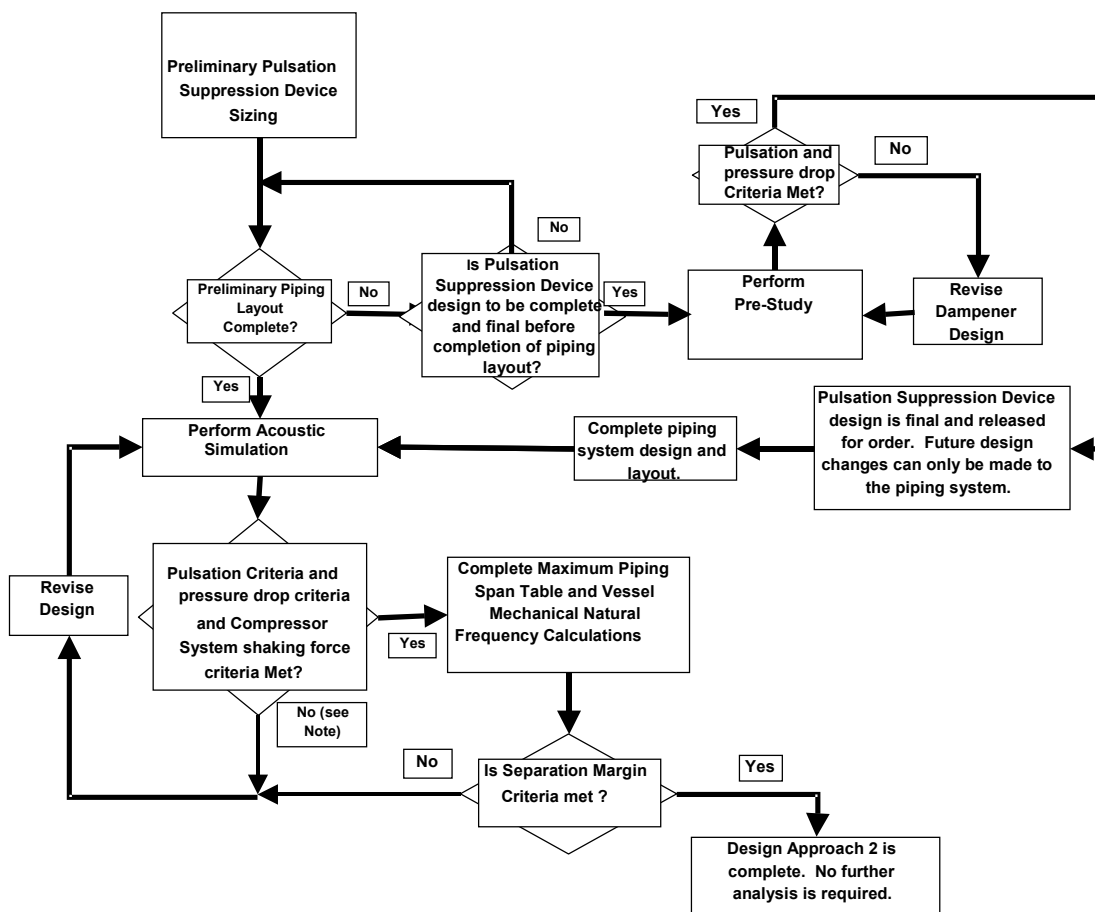


Figure 2: Pulsation and vibration workflow chart for Design Approach 1



Note - In the event that pulsation suppression device design is fixed, it may be necessary to accept higher pressure drop or perform a Design Approach 3 analysis.

Figure 3: Pulsation and vibration workflow chart for Design Approach 2



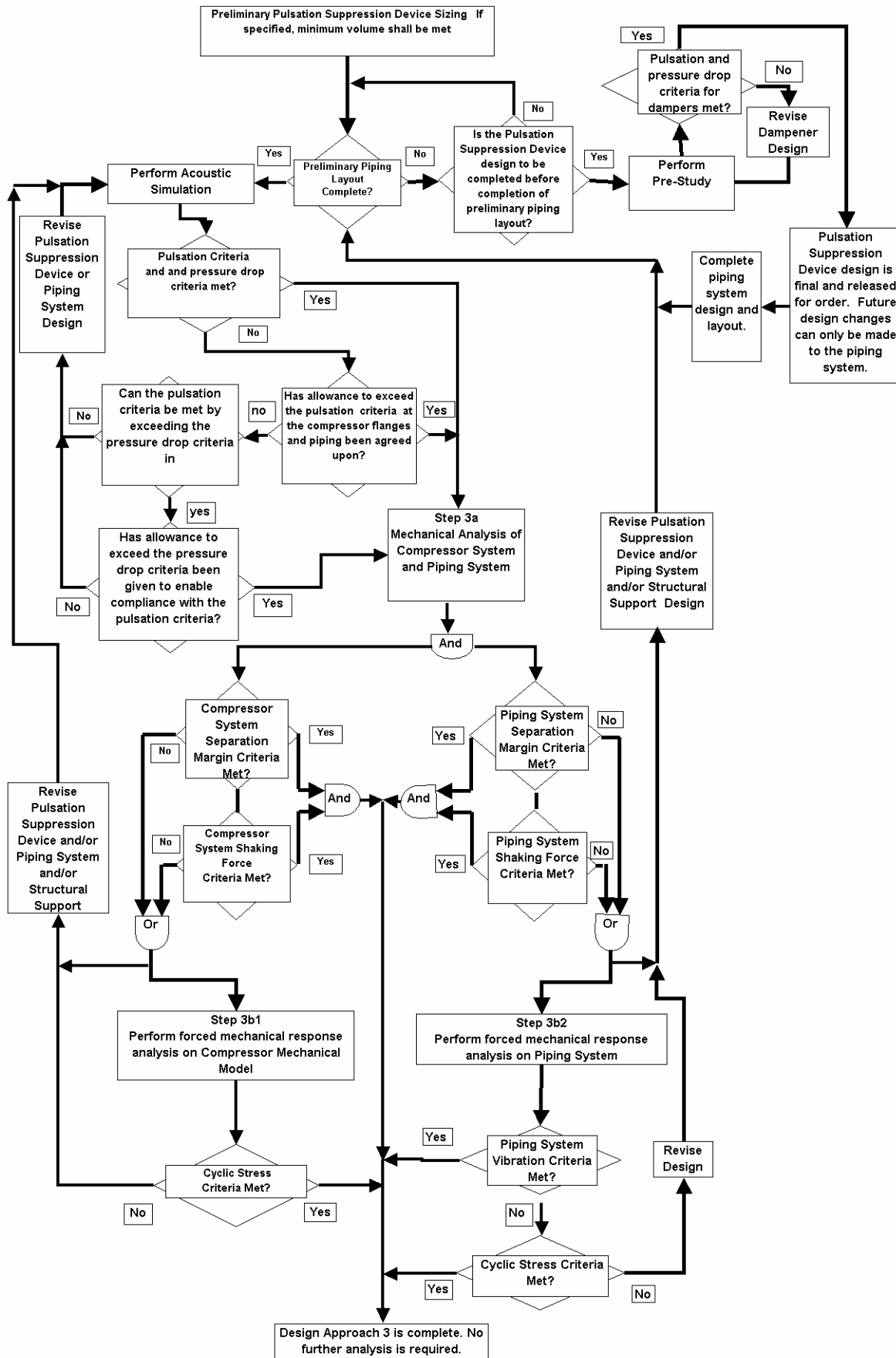
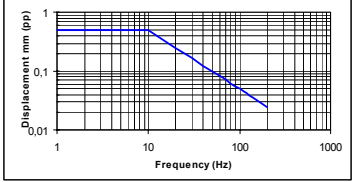


Figure 4: Pulsation and vibration workflow chart for Design Approach 3

Table 1: Overview of allowable levels for each design approach

Item	Design Approach 1	Design Approach 2	Design Approach 3
Initial damper sizing	<ul style="list-style-type: none"> <li><math>V_{\text{suction}} = 8.1 * PD(K * T_s/M)^{1/4}</math> (m<sup>3</sup>)</li> <li><math>V_{\text{discharge}} = 1.6 * (V_s/(R * 1/k))</math> (m<sup>3</sup>)</li> <li><math>V_{\text{suction}} \geq V_{\text{discharge}}</math></li> <li><math>V_s \geq 0.28 \text{ m}^3</math>, <math>V_d \geq 0.28</math> (m<sup>3</sup>)</li> </ul> <p> <math>V_s</math>= minimum required suction volume (m<sup>3</sup>)  <math>K</math>= isentropic exponent  <math>T_s</math>= absolute temperature (K)  <math>M</math>= molecular weight  <math>PD</math>= total net displacement per revolution of all cylinders to be pumped in the volume (m<sup>3</sup>) </p>	Not applicable	Not applicable
Pulsation levels in piping	$P = 4.1 / (P_L)^{1/3}$ (%) $P_L$ = line pressure (bar)	$P_{all} = \frac{400}{\sqrt{P_{mean} * D * f}} * \sqrt{a/350} \text{ [%pp]}$ <p> <math>P_{all}</math>= line side pressure (bar)  <math>D</math>= inside diameter (mm)  <math>f</math>= frequency (Hz)  <math>a</math>= speed of sound (m/s) </p>	Identical to DA 2
Pulsation levels at pre-study	Not applicable	<ul style="list-style-type: none"> <li>80% of piping allowable (DA 2) for single PSD (pulsation suppression device)</li> <li>70% for multiple PSD attached to common piping</li> </ul>	Identical to DA 2
Pulsation levels at compressor flange	7% <b>or</b> : $P_{cf} = 3 * R$ (%) whichever is lower $R$ =pressure ratio	Identical to DA 1	Identical to DA 2
Flow measurement error	Unless otherwise specified: <ul style="list-style-type: none"> <li>Non-custody transfer: &lt; 1.00 %</li> <li>Custody transfer: &lt; 0.125 %</li> </ul>	Identical to DA 1	Identical to DA 1
Pressure drop: Through a PSD based on static flow	<ul style="list-style-type: none"> <li>0.25% <b>or</b>:</li> <li><math>D_p = 1.67 * (R-1)/R</math> (%)</li> </ul> <p>           Whichever is higher  <math>R</math>=pressure ratio            Remark: limits shall be increased by a factor 2 when the pressure drop is calculated using the total flow (static + dynamic) provided that the static component still meets the criteria </p>	Identical to DA 1	Identical to DA 1
Pressure drop: When separator is an integral part of suppression device	<ul style="list-style-type: none"> <li>0.33% <b>or</b>:</li> <li><math>D_p = 2.17 * (R-1)/R</math> (%)</li> </ul> <p>           whichever is higher  <math>R</math>=pressure ratio            Same remark as for pulsation suppression device for dynamic flow </p>	Identical to DA 1	Identical to DA 1
Separation margin criterion	Not applicable	<ul style="list-style-type: none"> <li>Minimum NF: 2.4 times compressor speed</li> <li>NF separated minimum: 20% from dominant force frequency</li> </ul>	Identical to DA 2

Table 1: Continued

Item	Design Approach 1	Design Approach 2	Design Approach 3
Piping shaking force criterion	Not applicable	Not applicable	<ul style="list-style-type: none"> <li>• <math>SF_k = k_{eff} \cdot V</math> (N) <b>or</b>:</li> <li>• <math>SF_{pmax} = 10 \text{ NPS}</math> (N); whichever is smaller NPS= pipe size in mm</li> </ul>
Pulsation damper shaking force criterion	Not applicable	Not applicable	<ul style="list-style-type: none"> <li>• <math>SF_k = k_{eff} \cdot V</math> (N) <b>or</b>:</li> <li>• <math>SF_{pmax} = 45000</math> (N) whichever is smaller</li> </ul>
Vibration levels for piping in analysis Remark: For field measurements higher levels can be applied	Not applicable	Not applicable	
Vibration levels for compressors	Not applicable	Not applicable	In agreement with compressor manufacturer
Cyclic stress level in piping	Not applicable	Not applicable	180 N/mm <sup>2</sup> peak-peak



# **Comparison of moderate and low-speed API-618 reciprocating compressor designs for petroleum, chemical, and gas industry services**

by:

**George M. Kopsick  
Ariel Corporation  
Mount Vernon, Ohio  
U.S.A.**

## **Reliability and economics of compression systems – recent trends in the market of reciprocating compressors**

**March 27<sup>th</sup> / 28<sup>th</sup>, 2003 Vienna**

### **Abstract:**

API Standard 618, Reciprocating Compressors for Petroleum, Chemical and Gas Industry Services, is written to cover both moderate and low-speed reciprocating compressors for critical service applications but does not define the attributes of these two alternatives. This article reviews the basic design of both compressor types both to each other and API-618. Compressor application limits and their effects on reliability and expected operating time between maintenance are also discussed.

## 1 Introduction

The objective of this paper is to review the design of low and moderate-speed compressors in critical service applications relative to the requirements of API-618, Reciprocating Compressors for Petroleum, Chemical, and Gas Industry Services. Compressor application limits and their effects on reliability and expected operating time between maintenance are also discussed.

The API-618 specification is an accumulation of manufacturers' and users' knowledge and experience with reciprocating compressors. Its primary purpose is to provide minimum compressor design and application requirements so that safe, reliable compressor installations with long maintenance intervals can be achieved. The specification also serves as a standard against which different compressor offerings can be compared.

API-618 has become the international standard for defining requirements for all reciprocating compressors other than single-acting trunk-type piston designs, air or low-pressure plant services. Many companies use it as a base specification, which they amend with additions and deletions to create a specification that represents the firm's compressor requirements based on its own experience or specific project needs.

Reciprocating compressor specifications are continually updated to include additional knowledge and experience in an effort to improve the reliability of the equipment. The benefits gained from the use of the specifications have led to an expansion of their application to new or alternative compressor designs and additional industries. API-618 originally applied only to low-speed reciprocating compressors for refinery service. As new editions of the specification were written, the scope was expanded to include moderate-speed compressors as well as chemical and gas industry applications. Low and moderate-speed compressor designs were not defined in the specification because there was not a commonly accepted industry definition. Similarly, rotating and piston speed limits are not included in API-618 because they are dependent on the application and there are no commonly agreed upon limits.

The majority of API-618 is based on experience and knowledge gained from low-speed reciprocating compressor installations. Though most of the design requirements are applicable to all reciprocating compressor applications, some are more pertinent to either the low or moderate-speed variation. The general applicability of some specification

clauses to moderate-speed units is questionable when they are only appropriate for low-speed units.

## 2 Definition of Moderate and Low-Speed Compressors

API-618 states that it applies to low and moderate-speed compressors but does not define the meaning of either term. No commonly accepted definitions of these terms exist in the compressor industry. While some relate it to the piston speed, most people think of compressor speed as the rotating speed of the crankshaft.

Low and moderate-speed compressors are categorized by their rotating speed. The rotating speed range that identifies each type of equipment will always be a subject of debate, but is reasonably defined in the following table. Typical stroke lengths for each type are also shown.

	Low-Speed	Moderate-Speed
RPM	200 – 600	600 - 1200
Stroke mm (inch)	508 – 203 (20 – 8 )	203 – 76 (8 – 3)

*Chart 1: Low and Moderate Compressor Rotating Speeds and Stroke Length*

## 3 Basic Design Comparison of Low and Moderate-Speed Compressors

A design comparison of low and moderate-speed compressors, referenced and organized in accordance with Section 2 – Basic Design, API-618 is provided in this section. Other factors that affect reliability and operating time between maintenance are also included in the relevant sections.

### 3.1 General (API-618 Paragraph 2.1)

Low and moderate-speed compressor components are designed for a minimum service life of 20 years. Three years of uninterrupted service between maintenance intervals has been a goal put forth in API-618. It is equally obtainable with both low and moderate-speed designs in lubricated service if the process system design and the compressor component selections and application limits are appropriate. Three years of uninterrupted service in non-lubricated service is probably not attainable with current technology by any reciprocating compressor design other than a guided labyrinth piston with labyrinth packing.



## 3.2 Allowable Speeds (API-618 Paragraph 2.2)

Any discussion of allowable compressor speeds must be divided into two separate components: rotating speed and piston speed. Rotating speed is the rate at which the crankshaft is turning. Piston speed is the velocity at which the piston moves back and forth.

Rotating speed primarily affects cyclical (fatigue) life of components and the wear on rotating parts such as crankshaft main bearings. Piston speed affects the inertial forces and the forces and moments generated by the compressor as well as the expected life of wear components such as wear bands, piston rings, pressure packing elements, and valve plates. The practical limits of both rotating and piston speed are determined by available materials and technology.

API-618 states, “Compressors shall be conservatively rated at a speed not in excess of that known by the manufacturer to result in low maintenance and trouble-free operation under the specified service conditions. The maximum acceptable average piston speed (in meters per second or feet per minute) and the maximum acceptable speed (in revolutions per minute) may be specified by the purchaser where experience indicates that limits should not be exceeded for a given service.” It also states, “Generally, the piston speed and rotating speed of non-lubricated services should be less than those in equivalent lubricated services.”

The lack of any definitive piston and rotating speed limits has resulted in many users establishing limits in their specifications. In many cases these were established based on the limitations of materials and technology available at the time and have not been updated to represent current materials and technology. In other cases they were left unchanged based on the known low-speed designs at the time.

### 3.2.1 Piston speed

Piston speed is an important reciprocating compressor design parameter. The instantaneous piston speed varies from zero at the end of the stroke, to a maximum near the middle of the stroke, and back to zero. However, as a matter of practicality, “average” piston speed is used to establish limits, make comparisons between units and determine wear rates of wear components.

$$\text{Average Piston Speed (m/s)} = \frac{\text{Stroke (mm)} \times \text{RPM} \times 2}{60 (\text{s/min.}) \times 1000 (\text{mm/meter})}$$

or

$$\text{Average Piston Speed (ft/min)} = \frac{\text{Stroke (inch)} \times \text{RPM} \times 2}{12 (\text{inch/ft})}$$

*Chart 2: Average Piston Speed Calculation*

The maximum average piston speed that was known to provide reliable, long operating times between required maintenance at the time API-618 first was published (1964) was about 3.8 m/s (750-ft/min). Low-speed compressors typically had stroke lengths varying from about 508 to 203 mm (20 to 8 inch). The units were driven at synchronous speeds of less than 225 RPM for the long strokes and up to 514 RPM for the shorter strokes. A very common stroke length was 381 mm (15 inch) which was driven at 300 RPM, resulting in a 3.8 m/s (750-ft/min) piston speed. Because low-speed, long-stroke compressors were the only compressors used in refineries, people associated a low rotating speed such as 300 RPM with reliability. Operating at higher speeds resulted in reduced operating times between required maintenance because the piston speed exceeded the limits that provided long trouble free wear component life. Problems also resulted from the dramatic increase in unbalanced forces with speed. The misperceptions that the increased maintenance and vibration are due to RPM rather than piston speed and unbalanced forces and moments continue to this day.

Currently most manufacturers will offer lubricated compressors with average piston speeds up to 4.3 m/s (850 ft/min). Non-lubricated offerings are typically limited to 3.8 m/s (750 ft/min).

Piston speed affects the life of wear components such as wear bands, piston rings, pressure packings and to a lesser extent the piston rod. The wear rates of the non-metallic components are a function of:

- Lubrication
- Surface finish of the counterface material (coefficient of friction)
- Wear component velocity relative to the counterface material.
- Pressure loading on the wear part
- Non-metallic material selection
- Operating temperature
- Gas composition and any particulate

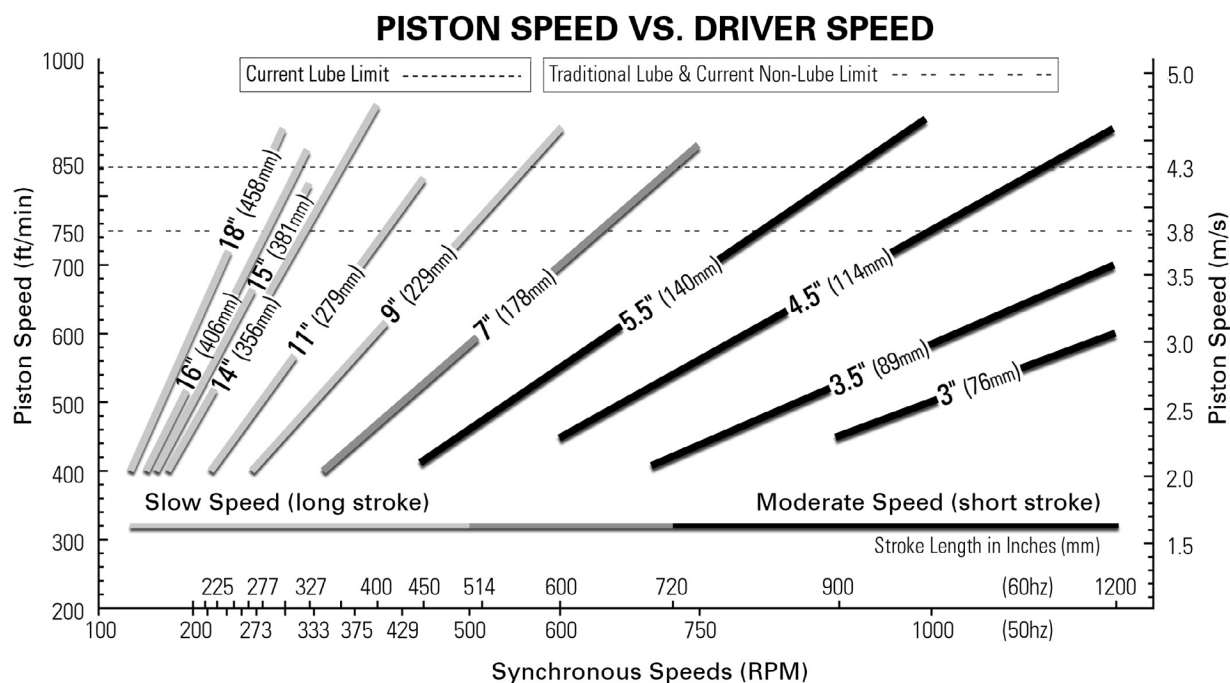


Chart 3: Piston Speed vs. Driver Speed

Low and moderate-speed compressors configured with similar materials and wear band loading should have the same wear component life for a given piston speed. Reducing the piston speed will provide increased wear component life, especially in non-lubricated services. The wear rate of a correctly selected non-metallic material in a non-lubricated service is relatively constant up to the point where its application temperature is exceeded. Operating the compressor at a low piston speed results in less wear material consumption per unit time and therefore longer time between required maintenance.

### 3.2.2 Rotating speed

The design of a reciprocating compressor is determined by the rotating speed at which it and the driver can operate reliably for the required time between maintenance intervals. As materials and technology have progressed both compressors and drivers have operated at increased drive speeds. This enables drivers to produce the same horsepower in smaller, lower cost sizes. This in turn has made it possible to design compressors with higher drive speeds with the benefit being equal throughput using smaller, lower cost compressors.

As driver speeds increased compressor strokes were shortened to maintain piston speeds that provide low wear rates. Units with higher drive speeds and

shorter strokes compared to low-speed designs are called moderate-speed compressors.

The rotating speed of a compressor can affect its reliability in a variety of ways including:

- Bearing wear rates
- Valve cyclic (fatigue) life
- Forces and moments created by the compressor and their effect on foundation life

Current materials and technology provide bearing designs, lubricating oils and forced feed lubrication systems that are capable of reliable operation at rotating speeds and bearing loads well over those employed on low and moderate-speed compressors. Both designs typically use precision fit tri-metal bearings. Aluminum bearings can be used in applications where hydrogen sulfide is present.

The majority of valves in both low and moderate-speed compressors use non-metallic materials. Non-metallic materials have finite cyclic fatigue life that is a function of impact velocity and bending stress. Impact velocity normally has a greater effect on valve life in most designs. While it is true that a valve operating at a given bending stress and impact velocity will operate for a longer time in a unit running at a lower cyclic rate (drive speed), current valve technology enables valves in moderate-speed compressors to provide 3 years of uninterrupted service. Cyclic fatigue of the valve plate material is no longer a major cause of valve failure. Factors that affect valve life are reviewed in the valve section of this document.

Low-speed units are built in horizontal, vertical and “Y-style” configurations. Initially low-speed units were not balanced to minimize the forces and moments created during operation. Later the horizontal configurations included provisions for balancing, but not to the level of balance provided in moderate-speed compressors.

Moderate-speed designs have horizontally mounted opposed cylinders. Opposing throws are component-balanced to within one or two kilograms.

The inertial force generated by one throw of a compressor can be calculated with the following formula:

$$F_{\text{Inertial}} = (m) (\omega^2) (R) (\cos \theta + R/L \cos 2\theta)$$

Where  $m$  = Mass of reciprocating components

$$\omega = (\text{RPM}) 2\pi / 60$$

$$R = \text{Crank throw (Stroke / 2)}$$

$$L = \text{Connecting rod center distance}$$

$$\theta = \text{Crank angle in degrees}$$

It can be seen from the equation that inertial force increases linearly with reciprocating mass and stroke length and to the square of the rotating speed.

For a compressor designed with horizontally opposed cylinders the inertial forces of the cylinders act in opposite directions and, to the extent that the reciprocating masses of the opposing throws are equal, cancel each other out. The actual unbalanced forces generated by the compressor will be the sum of the opposing forces. If the reciprocating masses of the opposing throws were the same the forces would cancel each other out and the unbalanced forces in the horizontal plane would be zero. Moderate-speed compressors component balance the reciprocating mass of opposing throws to within about a kilogram. This enables them to operate at higher rotating speeds without generating large forces. The inertial force equation can be used to show that a low-speed horizontally opposed compressor operating at a piston speed of 3.8 m/s (750 ft/min) at 300 RPM with a 381 mm (15 inch) stroke and a residue unbalance of 10 kg (22.2 lb.) will generate over three times the forces of a functionally equivalent moderate-speed unit operating at a piston speed of 3.8 m/s (750 ft/min) at 720 RPM with a 159 mm (6.25 inch) stroke and a residual unbalance of 1 kg (2.2 lb). The 10 kg residual low-speed compressor residual unbalance is a conservative estimate. Actual unbalance of 20 kg (44 lb) and higher is common. If the low-speed unit is a vertical or “Y-type” design the amount of unbal-

ance becomes very large causing a corresponding increase in forces and moments generated.

The forces created by a reciprocating compressor are handled by transmitting them to a sufficiently large foundation through large enough anchor bolt to prevent any relative motion between the compressor and the foundation. The larger the force, the larger the foundation’s mass needs to be and the more energy is transmitted through the foundation bolts. Reducing the forces and moments created by a compressor helps eliminate long-term foundation problems that occur as the concrete degrades over time due to age and the effects of a plant environment.

### 3.3 Allowable Discharge Temperature (API-618 Paragraph 2.3)

The discharge temperature application limits given in this section of API-618 apply equally to and are achievable by both low and moderate speed compressor designs. Knowing all the possible conditions at which the unit may be operated is important. An example of this is the requirement initially to operate a compressor designed for hydrogen service on nitrogen during the plant start-up. The discharge temperature in this start-up service can easily exceed the compressor design limits.

API-618 specifies the maximum allowable discharge temperature to be 150 degrees C (300 degrees F) for general service and 135 degrees C (275 degrees F) for hydrogen-rich services. The wear component life of units utilizing filled Teflon non-metallic materials can be increased significantly by lowering the stage discharge temperature through the addition of compressor stages on both low and moderate-speed units. Reducing the discharge temperature by 20 to 25 degrees C (36 to 45 degrees F) below these maximum limits can double the wear component life. The lower discharge temperatures are also helpful in reducing the fouling of water-cooled heat exchangers. The option of increasing the number of compressor stages to achieve these benefits is normally not explored due to the increased capital cost of the compressor. The higher initial cost can generally be returned a few times over through reduced maintenance and increased reliability.

### 3.4 Rod and Gas Loading (API-618 Paragraph 2.4)

The design requirements imposed by gas and inertial forces are the same for both low and moderate-speed compressors. These and the requirement for crosshead pin force reversal are well understood today. Both types of units provide robust designs.

The primary reason for rod load problems is operating the unit at an off design point that was not considered when the machine was designed. Modern compressor performance programs are capable of automatically calculating rod loads, crosshead pin reversal, basic valve dynamics, and stage performance over a large range of operating conditions. The compressor manufacturer is able to verify the suitability of the design for the intended application. This is a major step forward in insuring unit reliability over a few years ago and has resulted in decreases in valve and crosshead pin failures.

The inertial forces of the rotating components and the forces imposed by the gas on the piston constitute the forces created by the compressor. In all but some applications, such as units operating at high pressures or with single acting cylinders, the gas and inertial forces oppose each other. Reducing or eliminating the gas forces increases the net force applied to the reciprocating components. Compressor designs should be reviewed to see if they are suitable for all unloading steps and being brought up to full speed on start-up before gas loads are applied. The majority of horizontally opposed, moderate-speed reciprocating compressors are designed to handle the maximum inertia loads generated when rotated at full frame rated speed with no off setting gas loads. This should always be verified, particularly on low-speed units, which typically have larger reciprocating masses.

### 3.5 Critical Speeds (API-618 Paragraph 2.5)

A torsional analysis is equally important for both low and moderate-speed designs. A lateral study is typically not required for either design because of the inherent stiffness of the bearing support system. The main exception to this is a low-speed compressor with an engine type electric motor.

### 3.6 Compressor Cylinders (API-618 Paragraph 2.6)

Low and moderate-speed compressor designs are equally compliant with the majority of the API-618's cylinder design requirements. The two areas where the low and moderate-speed cylinder designs deviate are the inclusion of water jackets and cylinder liners. Low-speed, long-stroke compressors typically require water-jacketed cylinders to eliminate thermal distortion inherent to longer cylinders. Moderate-speed cylinders are shorter and can maintain dimensional stability as they heat up. Cylinder liners were used to provide an easy way to repair cylinder bore wear or damage due to bore distortion. The thermal stability of moderate-speed cyl-

inders in conjunction with the advent of the ability to harden cylinder bores for longer wear has eliminated the need for liners on moderate-speed machines.

#### 3.6.1 Water Jackets (Cylinder Cooling)

API-618 specifies that cylinders operating above stated discharge temperatures must have water jackets that are either static filled, have an atmospheric or pressurized thermosyphon or have forced liquid coolant depending on the discharge temperature. Additionally, any cylinder operating fully unloaded for extended periods of time shall have a water jacket with a forced liquid coolant.

There are two reasons for this requirement. The first is that water jackets were needed for the dimensional stability of the cylinder bore of long-stroke, low-speed compressors when API-618 was first written. The length of the cylinder and the casting quality available at that time resulted in the cylinder bore deforming as cylinder temperature increased. Water jackets were required to insure the heat effect was evenly spread around the cylinder bore to increase dimensional stability. This was critical in view of the use of metallic rings, and the fact that the bore of the cylinder was soft (approximately 25 Rc). If the cylinder bore distorted dimensionally, the piston rings would scrape the cylinder bore and damage it.

The second reason that water jackets were required was to carry away the heat generated by cylinders operating fully unloaded for extended lengths of time.

API-618 uses the term cylinder cooling for the water jacket. Inlet water temperature is specified to be a minimum of 6 degrees C (10 degrees F) above the gas inlet temperature to eliminate gas condensation, primarily during shutdowns. The static and thermosyphon designs will maintain bore stability but have no real mechanism to transport heat away from the cylinder. The inclusion of these designs reinforces the fact that water jackets are used to maintain bore stability rather than to transport heat away from the cylinder. The forced liquid cooled cylinder design specified in API-618 does transport heat away from the cylinder in the water. In operation the majority of the heat is picked up in the discharge passage of the cylinder where the maximum gas to liquid temperature differential exists. The amount of heat transferred from the surface of the bore is small. If the cylinder is viewed as a single pass shell-and-tube heat exchanger with a 381 mm (15 inch) long 'tube' of 25 to 35 mm (1 to 1.4 inch) cast iron having a mean gas to water differential temperature of 60 degree C (108 degrees F), it is apparent that little heat can be transferred from the cylinder bore. A forced liquid cooled cylinder does



provide enough heat transfer to reduce heating problems in extended periods of unloaded operation.

Moderate-speed compressor designs utilize cylinders with shorter stroke lengths. Current casting technology, the uses of non-metallic wear materials and the short bore length enable dimensional bore stability to be maintained without the need for water jackets. The reliability of these designs has been proven over the last thirty years in oil and gas production and gas transportation applications. Whereas previously water-jacketed cylinders were standard in these applications few if any are now utilized.

Cylinders that do not require water jackets have the benefit of eliminating the need for cylinder cooling water systems, the maintenance of those systems and the probability of bore distortion if cooling water flow is lost or the water jacket becomes plugged. Non-water jacketed cylinders do have the problem of not being suitable for operating totally unloaded for extended periods of time.

### 3.6.2 Cylinder Liners

API-618 specifies that cylinder liners be provided. Low-speed compressor designs are typically supplied with liners, while moderate-speed designs may or may not be available with them.

Originally long-stroke cylinders had problems with bore dimensional stability if the casting did not grow at the same rate as it increases in temperature. This in conjunction with the relatively hard rings used at the time API-618 was first published and the low bore hardness could result in damage to the bore's surface. Cylinder liners were included to help get a cylinder with bore damage back in service quickly and as cost effective as possible. A cylinder could be taken to a repair facility for liner replacement, and the unit would be back in operation within 5 to 7 days.

API-618 requires that piston rods be surface hardened in the packing area to increase their service life and help protect against damage. The option of hardening the surface of the cylinder bore to obtain these same benefits was a technology that did not exist at the time low-speed units were designed. Piston rods could be heat treated to increase their surface hardness while retaining suitable base material physical characteristics. A cylinder could not be heat treated to harden the bore surface because the base material at that time would not provide suitable pressure vessel characteristics.

The development of technologies such as ion-nitriding enables manufacturers to harden the surface of cylinder bores to 58+Rc without changing the base material characteristics. The hard surface provides the increase in life and resistance to damage that a hardened piston rod provides.

Moderate-speed cylinders can be obtained with liners, without liners and with hardened unlined bores depending on the manufacturer. The short stroke of moderate-speed cylinder designs enables bore stability to be better maintained than on a long-stroke design. The use of non-metallic rings and the improvement in casting technology eliminates problems with thermal growth causing the piston assembly scraping the cylinder wall.

The inclusion of a liner in a moderate-speed cylinder degrades the performance of the compressor because of the increased fixed clearance added in the valve area. For this reason most manufacturers do not include a liner unless the customer requests it.

A cylinder, either low or moderate speed, is still susceptible to bore damage due to particulate in the gas, lubrication problems or operating the unit with worn wear bands and/or piston rings. A hardened cylinder bore helps protect against bore damage and increases the life and reliability of the cylinder.

If damage does occur to the cylinder bore a liner can be replaced or the entire cylinder body can be replaced. Moderate-speed compressor manufacturers normally make the cylinder from castings with relatively high production volumes. Because of this castings are typically in stock. The cost of replacing a new moderate-speed cylinder body is about equal to the cost of taking a slow-speed cylinder to a machine shop, removing an interference-fit liner and replacing it with a new liner. This is possible because a moderate-speed cylinder is about half the size of the equivalent slow-speed cylinder and is produced with stock castings that are ordered in quantity. It takes about one week to replace a liner which is the same time required to obtain a new moderate-speed cylinder from a manufacturer that has stock castings.

Low and moderate-speed cylinders can also be damaged due to liquid slugs carried into the compressor or by ingesting a foreign object such as a valve part. A cylinder liner does not help place the unit back in service in either of these cases because other areas of the cylinder are often damaged. A new or rebuilt cylinder is typically required to correct these problems. Being able to source a new moderate-speed cylinder in a week eliminates much



of the downtime normally incurred in these situations.

### 3.7 Valves and Unloaders (API-618 paragraph 2.7)

The type of valves and their design and mounting in the compressor are equivalent for both low and moderate-speed compressors with the exception of the cyclic rate at which the valves open and close. Moderate-speed units run at higher drive speeds therefore the valves open and close more often per unit time. This is important because the majority of valves applied in downstream applications utilize non-metallic valve plates that have finite cyclic fatigue lives. A comparable designed and applied valve will operate for a longer period at a lower RPM than at a higher RPM. While this is true, running a compressor at a low drive speed of 300 RPM does not insure the valve will operate longer than one running at 900 RPM.

Paragraph 2.1 of API-618 states, “The equipment (including auxiliaries) covered by this standard shall be designed and constructed for a minimum service life of 20 years and an expected uninterrupted operation of at least 3 years. It is recognized that this is a system design criteria.”

Current valve technology enables valve for moderate-speed applications to achieve the 3 year uninterrupted operation criteria specified in API-618. Assuming that both the low and moderate-speed valves are correctly designed there are a number of other design requirements that have a larger impact on valve life than the cyclic life of the valve plate material. These include:

- Eliminating particulate matter and liquid carry-over in the process gas through inlet filters or separation.
- Selecting the most reliable type of valve design for the application.
- Defining all potential operating points and associated gas compositions.
- Conducting a dynamic analysis to define the correct valve components and insure the valve plate impact velocities are within conservative limits that enable the 3 year operating life criteria to be met.
- Selecting the correct valve plate, ring or poppet material for the application.

One or more of the above factors are typically the reasons for a valve not achieving its expected operating life. Inlet filtration and separation increases the initial cost of an installation but can have dramatic effects on the reliability of the compressor installation. New performance calculation software

that includes basic valve dynamic analysis is now available. Using it to verify the suitability of the valve design over a wide range of operating conditions and plot maps showing any areas that should be avoided helps eliminate problems.

API-618 compliant cylinder unloading is available on both low and moderate-speed compressors. Any application of unloaders or other types of capacity control devices should be reviewed to insure cross-head pin reversal requirements for the compressors are met under all conditions.

### 3.8 Pistons, Piston Rods, and Piston Rings (API-618 Paragraph 2.8)

Low and moderate-speed units offer components that meet the requirements of this section of API-618. Compressors that do not meet the requirements of this section are sometimes offered in an effort to lower the cost of the offering. Piston design should be reviewed to insure they include:

- Wear bands sized so that their bearing loads are no greater than 0.07 N/mm<sup>2</sup> (10 psi) for lubricated applications and 0.035 N/mm<sup>2</sup> (5psi) for non-lubricated applications.
- Wear bands designed to prevent underside pressurization. (The increased loading caused by wear bands being forced against the cylinder bore by underside pressurization will decrease their operating life.)
- Additional piston rings for low molecular weight applications.

Aluminum pistons are used for some large cylinders to decrease piston weights. This is done to decrease wear band loads and to reduce the inertial forces. While aluminum has been successfully employed for constructing pistons it has several disadvantages. First, the piston ring and wear band grooves must be made of wear resistant material or the motion of the rings in the grooves will open the ring clearances and lead to premature failure. Most companies eliminate this problem using a ring carrier made of iron or steel that is mated with aluminum components that form the ends of the piston. Secondly, the relatively large thermal expansion rate of aluminum compared to iron or steel can cause problems if the design is not properly engineered. For these reasons aluminum pistons should be avoided where possible.

### 3.9 Crankshafts, Connecting Rods, Bearings and Crossheads (API-618 Paragraph 2.9)

Low and moderate-speed compressor designs have crankshafts, connecting rods and bearings that are designed and built to the same design standards and materials. Moderate-speed crosshead designs typically differ from the API-618 specification and the low-speed designs that it is based on.

The manufacturing tolerances of large low-speed compressor components and the resulting large cumulative assembly dimensions require that the position of the crosshead be adjustable. The smaller size of moderate-speed compressors in conjunction with improvements in machining capability and the shorter stroke length eliminates the need for adjustable crossheads to position the rod correctly. One-piece crosshead designs eliminate assembly errors and the possibility of a multiple component assembly coming apart. Failure of the crosshead-bearing surface is rare. This and the fact that moderate-speed crossheads are available quickly and relatively economically eliminate the need for replaceable shoes.

### 3.10 Distance Pieces (API-618 Paragraph 2.10)

The type of distance pieces available and their design is the same for both low and moderate-speed compressors. The only real difference is the limitations API-618 places on the application of the Type C – long/long two-compartment distance piece. The specification states in a note to paragraph 2.10.1.3:

“Note: The Type C distance piece with two slingers, one in each compartment, is not normally used on process compressors. This type of distance piece is used only for special applications such as oxygen service. This distance piece design causes the overall length of the gas end assembly to become excessively large, thus causing the overall width of the compressors to become large, and therefore increasing foundation requirements. Uses of such distance pieces can cause piston-rod diameter to increase, because of the column effect of excessively long piston rods.”

While this is correct for low-speed compressors with long strokes, it is not correct for moderate-speed compressors with short stroke lengths. The difference in length between a Type C – long/long two compartment and Type D – long/short two

compartment distance piece on a moderate speed machine is small and has only minor effects on overall package size and foundation requirements. Type C distance pieces are commonly used on moderate-speed units because they provide increased ability to eliminate the ingress of frame oil into non-lubricated pressure packings. Additionally process gas can be better isolated from the environment.

### 3.11 Packing Case and Pressure Packing (API-618 Paragraph 2.11)

Low and moderate-speed units offer components that meet the requirements of this section of API-618.

### 3.12 Compressor Frame Lubrication (API-618 Paragraph 2.12)

Low and moderate-speed units offer components that meet the requirements of this section of API-618.

### 3.13 Cylinder and Packing Lubrication (API-618 Paragraph 2.13)

Low and moderate-speed units offer components that meet the requirements of this section of API-618. Low-speed compressors normally are fitted with point-to-point lubrication systems while moderate-speed units typically are supplied with divider block systems.

Point-to-point systems have the benefit of enabling the amount of oil supplied to each point to be individually adjustable while the unit is in operation. This is both good and bad. Though it allows oil flows to be changed while the unit is operating there is no real way to know how much (or less) oil is needed. A first approximation of the amount of oil needed is normally determined by knowing the volume of oil required per mm or inch of bore diameter. This volume is a function of gas composition and the compressor application. Counting how many drips per minute, as seen in a drip gauge, typically sets these flows. Small cylinder bores require less flow and are harder to properly set flow rates.

The use of too much cylinder lubrication is one of the major reasons for valve failure. If the lubrication rate is set too high the oil carries over into the valve. The presence of oil causes the valve plate to stick to the valve seat. This changes the dynamics of the valve plate and can lead to valve failure. This is not uncommon because most people believe

that more oil is better than less oil. If there is any question about the amount of cylinder lubrication oil, it is increased. The use of too much cylinder lubrication is a major reason for reduced valve life.

Divider block lubrication systems are common on moderate-speed compressors because the amount of oil required for each point is small. A divider block system enables this small amount of oil to be precisely metered. The amount of oil supplied by the total system can be changed while in operation. Changing the proportion of oil supplied to a single point requires that a different divider block be installed, which can only be done when the unit is not in operation. Eliminating the requirement to review the adjustment of multiple point-to-point flows can increase compressor reliability by eliminating the tendency to provide too much lubrication.

### **3.14 Materials (API-618 Paragraph 2.14)**

Low and moderate-speed units offer components that meet the requirements of this section of API-618.

## **4 Conclusion**

Reciprocating compressors for downstream applications must provide reliable, long operating periods between required maintenance intervals. API-618 and other reciprocating compressor specifications were written to capture and make available good compressor design practices that help make this goal achievable. The material and technology available at any point in time determine the design limits within which a compressor must be built. As materials improve and technology evolves the limits become less restrictive and the ability to develop new designs with additional benefits is available to those willing to make the investment in time and resources.

The first edition of API-618 was published in 1964. The material, technology and experience available at that time required that most reciprocating compressor for refinery applications be designed for drive speeds in the area of 300 RPM. Advances in these areas now enable reliable units to be built with drive speeds over 1000 RPM. These moderate-speed units offer the benefits of lower compressor, foundation and installation costs as well as smaller installation size. Additionally, units as large as 4.5 MW (6040 hp) can be supplied as assembled, pre-tested packages thereby reducing installation time and start-up delays.

API-618 and other reciprocating compressor specifications have been written and updated over time.

As they have independently evolved, inconsistencies and misapplications of some areas in the specification have occurred. Though the majority of design principles apply equally to both low and moderate-speed compressor designs, some design requirements apply only to one or the other.

Finally, the application of the API-618 specification to any installation does not insure a reliable compressor installation. There are many compressor application limits that are different for various applications. Many of these application limits are not included in API-618 or may be less than a maximum limit that is included in the specification. There are also a number of design decisions that may increase the operating periods between maintenance of an installation. Both of these design alternatives can be within the limits of API-618, but one typically at a higher first cost, will provide higher reliability. A classic example of this is adding another stage of compression to reduce stage discharge temperatures even though the alternative with fewer stages meets the discharge temperature limits of API-618. Using a four-stage rather than a three-stage compressor in a lubricated hydrogen application can sometimes double the Teflon based non-metallic wear material life. The reduced discharge temperatures can also reduce shell and tube cooler fouling problems encountered in installations with poor quality cooling water.

Both low and moderate-speed reciprocating compressors provide reliable service with equally long periods of operation between required maintenance.

# **Optimizing the drive system for variable speed electric motor driven reciprocating compressors**

by:

<b>Dr.-Ing. Siegmund Cierniak</b>	<b>Dr.-Ing. Hans Funke</b>	<b>Dipl.-Ing. Detlef Wendt</b>
<b>Compression Systems</b>		
<b>HGC Hamburg Gas Consult GmbH</b>	<b>ALSTOM Power Conversion GmbH</b>	<b>ALSTOM Power Conversion GmbH</b>
<b>Hamburg</b>	<b>Dresden</b>	<b>Berlin</b>
<b>Germany</b>	<b>Germany</b>	<b>Germany</b>

**Reliability and economics of compression systems –  
recent trends in the market of  
reciprocating compressors  
March 27<sup>th</sup> / 28<sup>th</sup>, 2003 Vienna**

## O. Abstract

Reciprocating compressor systems are today in Europe almost exclusively fitted with electric motors as main drives for the most varied applications. In the case of weak power grids – a situation which is particularly typical for "natural gas underground storages" because these locations are often found "in the middle of no-where" – this difficult case is of paramount relevance both for the equipment supplier (compressor and electric motor) and for the operator.

The average load torque of a piston compressor with an asynchronous motor drive is always subject to substantial oscillation torques. This leads to increased torsional stress of the complete shaft assembly and often to significant current fluctuations at the point of mains connection of the motor.

The oscillation problem of piston compressor drives has been known for many years, and was discussed in several publications. Initially, the motor was regarded as a delay element of the 1<sup>st</sup> order under control aspects. At a later stage, it was found that the motor must be regarded as an oscillating element, although it was not until the development of computer technology that it became possible to resolve the differential equations (voltage equations of the drive motor and motion equations) and to present all the oscillating parameters as a function of time.

This article presents a calculation program that permits the calculation of the electrical and mechanical oscillation parameters with sufficient precision, in particular, via the dynamic motor model. Variant calculations with different moments of inertia of the flywheel and different torsional rigidities of the coupling supply a design which features minimum oscillation exposure of shaft and grid (-> voltage flicker). The effect of oscillation damping is also described which can be implemented in the case of inverter-fed drives and which leads to a significant reduction of current and hence mains voltage oscillation. This fact is particularly important for compressor drives which must be connected to weak grids.

## 1. Introduction

Substantial oscillating torques are superimposed upon the average load torque of a piston compressor which are injected into the drive. This leads to increased torsional stress for the entire shaft

assembly and, as a result of speed fluctuations, to considerable torque and current pulsation in the motor. This is why it is important during the design phase to determine the electrical and mechanical operating parameters – in particular, torque, speed and current pulsation – with the maximum precision possible. These operating parameters must be determined from the point of view of the drive manufacturer because he is responsible for limiting system perturbation and mechanical stress of the motor. This means that the calculation of these operating parameters requires a model which simulates the motor with the maximum precision possible, whilst the so-called two-mass system is sufficient for representing the part of the coupled drive which is capable of torsional vibration.

The oscillation problem of piston compressor drives has been known for many years, and has been the subject matter of several publications. Initially, the motor was regarded as a *delay element of the 1<sup>st</sup> order* under control aspects. At a later stage, it was found that the motor must be regarded as an oscillating element, although stationary curves were sometimes still used for the motor torque characteristics and, above all, for the current characteristics. The differential equations were often linearized using the *method of small changes around a stationary operating point*. This approach provided closed solutions in the form of the *frequency or amplitude responses* (curve of the oscillation amplitudes vs. the frequency of the load torques [8; 11; 13; 14]). It was not until the introduction of computer technology that the demanding *dynamic presentation of the asynchronous motor* was introduced to practical design work. Using the familiar numerical methods, it was now possible to solve the differential equations (voltage equations of the asynchronous motor and motion equations) for changes of any size and to present all the oscillating parameters as a function of time.

This article presents a calculation program that permits the calculation of the electrical and mechanical oscillation parameters with sufficient precision, in particular, via the dynamic motor model. It is stated which simplifications of the model and of the presentation of the load torques (limitation of the ordinal number of the oscillating torques to be considered) are acceptable with a view to precision. The current pulsations are used as an example in order to compare the values calculated by stationary equations on the one hand and dynamic models on the other.

The practical procedure for dimensioning a compressor drive is illustrated on the basis of an



example. Variant calculations with different moments of inertia of the flywheel and different torsional rigidities of the coupling supply a design which features minimum oscillation exposure of shaft and grid (-> voltage flicker). In this context, the effect of oscillation damping is also described which can be implemented in the case of inverter drives and which leads to a significant reduction of current and hence mains voltage oscillation. This fact is particularly important for compressor drives which must be connected to weak grids. Finally, the usual general requirements for the maximum mechanical inertia possible and, when a certain limit value is no longer reached, for the "cyclic irregularity" are subjected to a critical review. In comparison to the fixed-speed asynchronous motor, some further advantages of the inverter feeder are explained. Besides simple adaptation of the working current to the respective requirement by the technology, it is, in particular, the fact of grid-compatible starting (nominal torque with starting current = nominal current throughout the entire starting range – important for weak grids!) and the stable bridging of short mains interruptions in conjunction with the avoidance of the dangerous opposition circuit which deserve special mention.

## 2 Calculation models

A strongly simplified signal flow diagram of the squirrel-cage induction motor can be used to explain the principles of the stationary and dynamic presentation of the drive (method of small changes in all variables).

### 2.1 Squirrel-cage induction motor as a delay element of the 1<sup>st</sup> order

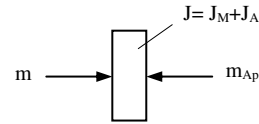
The rotating masses of the motor and compressor are combined to flywheel with the moment of inertia  $J = J_M + J_A$  at which the oscillating torque of the driven machine  $m_{Ap}$  and the motor torque  $m$  attack (Fig. 1). The general motion equation with the standardized speed  $\gamma = \Omega/\Omega_{0n}$

$$m - T_m \cdot \frac{d\gamma}{dt} - m_{Ap} = 0$$

becomes, on entering the Laplace range

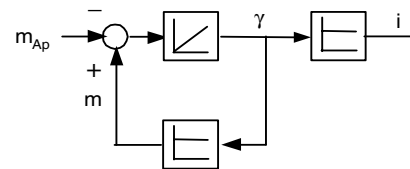
$$m - p \cdot T_m \cdot \gamma - m_{Ap} = 0$$

$$\gamma = \frac{1}{p \cdot T_m} \cdot (m - m_{Ap}) \quad (1)$$



Picture 1: Single mass torsional vibrating system

The simple signal flow diagram of the squirrel-cage induction motor can be expressed with (1). Due to the inertia of the mechanical system (I-element), a sudden change in load torque leads to a delayed change in speed  $\gamma$ . With a stationary view, one then assumes that the motor torque follows the speed deviation  $\gamma$  without delay – a transfer function  $m/\gamma = S$  (P-element where  $S$  – standardized rate of rise of the stationary M-n characteristic) corresponds to this assumption. The transformation of the closed circle and the usual approach of  $p = j\omega_p$  gives the amplitude response of the speed ( $\omega_p$  – radian frequency of the load oscillating torques):



Picture 2: Squirrel-cage induction motor, stationary

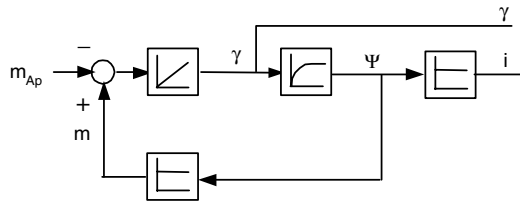
$$\frac{\gamma}{m_{Ap}} = \frac{1}{S \cdot \sqrt{1 + \left( \omega_p \cdot \frac{T_m}{S} \right)^2}} \quad (2)$$

This equation describes a delay element of the 1<sup>st</sup> order with the amplification factor  $1/S$ . In the case of a high rate of rise, i.e. with a small breakdown slip, the oscillating torque leads to a small speed deviation. The value for  $\omega_p \rightarrow 0$  is obtained from the stationary M-n characteristic. With increasing frequency, the speed deviation decreases continuously without any resonance sharpness occurring. It is hence not acceptable to neglect the electrical time constants, in particular, those of the rotor circuit because these lead to a delayed increase in motor torque.

### 2.2 Squirrel-cage induction motor as an oscillating element

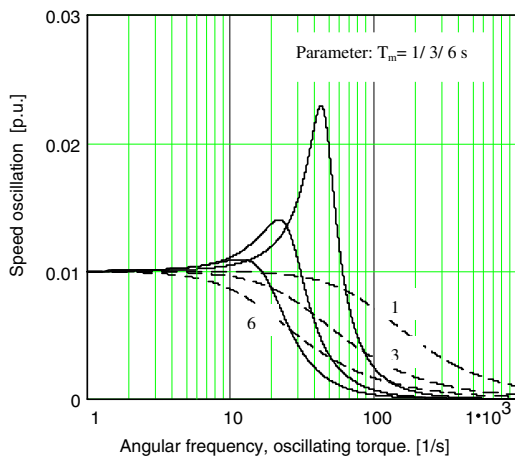
An important element for the real presentation of the squirrel-cage induction motor during dynamic

processes is the delayed change in rotor flux interlinking  $\psi$  as a consequence of a speed change. This relationship is considered in the signal flow diagram in Fig. 3 by a delay element of the 1<sup>st</sup> order. A P- element is used for the transfer function between the flux interlinking and the motor torque because no delay is effective here (the amplification factor  $S$  being retained for the purpose of approximation). The transformation of the signal flow diagram with the  $p = j\omega_p$  approach finally supplies an oscillating element for the amplitude response:



Picture 3: Squirrel-cage induction motor, dynamic

$$\frac{\gamma}{m_{Ap}} = \frac{1}{S} \cdot \frac{1}{\sqrt{\left(1 - \left(\frac{\omega_p}{\omega_e}\right)^2\right)^2 + \left(\frac{\omega_p}{\omega_e}\right)^2 \cdot \frac{T_m}{S \cdot T_2}}} \quad (3)$$



Picture 4: Frequency responses  $\gamma/m_{Ap}$

The curves according to (2) and (3) are shown in Fig. 4. The broken characteristics apply to the delay element of the 1<sup>st</sup> order – which can be clearly seen by the absence of a resonance curve. However, the reduction of the speed fluctuation above the knee-point frequency (delay element) and/or above the natural frequency (oscillating element) also differs from case to case: In the first case, the reduction proceeds according to  $1/\omega_p$  whilst in the case of the oscillating element, the reduction proceeds according to  $1/\omega_p^2$  whilst. In the case of the

stationary approach, one would thus always calculate excessively high values for the current, torque and speed oscillations in this range.

The characteristics of the oscillating element also show that an increase in mechanical inertia leads to a reduction of the motor's natural frequency and of the amplitudes at resonance and above.

This generalized view supplies a result which is not new, i.e. the fact that the calculation of the drive oscillations using the *stationary* motor characteristics in the interesting range of the interference frequencies often supplies excessively high oscillation values with the consequence that the resultant designs are unnecessarily massive and costly.

### 2.3 Calculation program for the complete drive suitable for practical application

The following requirements and assumptions had to be considered for programming:

1. The calculations focus on the stresses to which the motor, the inverter and the grid (flicker voltage), as well as the common shaft between motor and compressor and/or flywheel are exposed. The mechanical part is thus represented in a reduced form, i.e. as a two-mass system.
2. The coupling between the electrical and the mechanical parts must be considered, not just because of the determination of the shaft torque, but also because of the reciprocal influences of current and torque oscillations.
3. Use of a dynamic motor model. The differential equations DGL are solved on the PC using numerical methods rather than by the "method of small changes" in order to enable the calculation of the large-signal behavior.
4. The load torque of the compressor is available in the form of the *Fourier components* and is entered into the program as an interference variable (at least the torques up to an ordinal number of  $v = 10$  are considered).

$$(4a) \quad \frac{d\Psi_{Ld}}{dt} = -s_k \cdot \omega_{0n} \cdot \Psi_{Ld} + s_M \cdot \omega_{0n} \cdot \Psi_{Lq}$$

$$(4b) \quad \frac{d\Psi_{Lq}}{dt} = -s_M \cdot \omega_{0n} \cdot \Psi_{Ld} - s_k \cdot \omega_{0n} \cdot \Psi_{Lq} - s_k \cdot \omega_{0n} \cdot u_N$$

(4c)

$$\frac{ds_M}{dt} = \frac{1}{T_{mM}} \cdot \left[ \frac{c}{p \cdot M_n} \cdot (\delta_M - \delta_A) + 2 \cdot \Psi_{Ld} \cdot \frac{m_k}{u_N} \right]$$

(4d)

$$\frac{d\delta_M}{dt} = -s_M \cdot \omega_{0n}$$

(4e)

$$\frac{ds_A}{dt} = -\frac{1}{T_{mA}} \cdot \left[ \frac{c}{p \cdot M_n} \cdot (\delta_M - \delta_A) - m_A \right]$$

(4f)

$$\frac{d\delta_A}{dt} = -s_A \cdot \omega_{0n}$$

In the equation system shown opposite, the differential equations (4a) and (4b) apply to the flux interlinking of the rotor cage (the differential equations of the stator winding were linearized because their transient processes have no influence on the electromechanical transient processes discussed here), whilst the differential equations (4c) to (4f) apply to the mechanical system.

These differential equations show the course of action and the coupling between the electrical and the mechanical parts in a qualitative form. The oscillating torque of the compressor  $m_A$ , for example, leads to a change in slip  $s_A$  (4e) and hence in the angle  $\delta_A$  of the flywheel. This angle influences (4c) and changes the motor slip and hence, via the fluxes, the motor torque ( $m \sim \Psi_{Ld} - 2^{\text{nd}}$  summand in (4c)), and so forth. The slip speed  $s_A \cdot \omega_{0n}$  of the rotor of the driven machine is the differential speed in relation to the rotating-field speed (presentation of the rotor speed in the grid coordinate system):

$$s_A = \frac{\omega_{0n} - p \cdot \Omega_A}{\omega_{0n}}$$

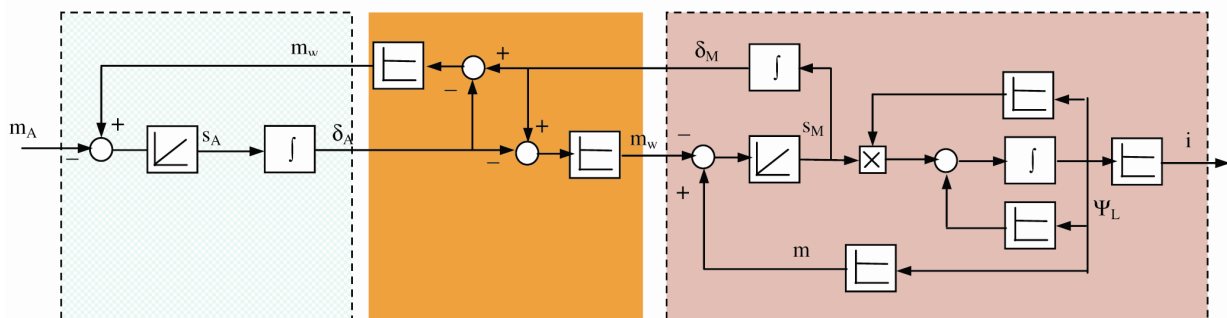
The torque of the shaft is proportional to the angle difference  $(\delta_M - \delta_A)$ . Fig. 5 shows the structure diagram belonging to differential equations (4),

however, with the electrical part being shown in a strongly simplified form. The input variable is the oscillating torque  $m_A$ , the output variable being the oscillating current  $i$  caused by the disturbing torque. It can be seen that the input signal, on its way to the output, passes through two important mechanical delay elements, i.e. the integrating elements with  $T_{mA}$  and  $T_{mM}$  and the delay element for flux generation, so that the current shows a partially smoothed curve (reduced amplitude) in the case of a conventionally designed drive with oscillating load. Furthermore, Fig. 5 also shows the coupling between driven machine and motor via the angles  $\delta_M$  and  $\delta_A$ . The calculation values and characteristics shown and referred to in the following sections were determined using this program.

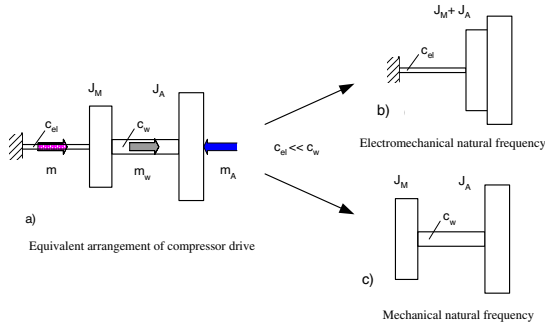
### 2.3.1 Natural frequencies

Due to the presentation of the mechanical system as a two-mass torsional vibrating system, two natural frequencies occur when this system is coupled with the squirrel-cage induction motor, i.e. the natural frequency  $f_{e10}$  which applies to the oscillations of the rotating masses at the "electrical" torsion spring [1] of the motor and the frequency  $f_{e20}$  which occurs during oscillation of the two masses in opposite directions at the mechanical torsion spring, i.e. the shaft. Fig. 6 shows a mechanical equivalent circuit where the effect of the air gap torque is represented by an equivalent torsion spring with the spring constant  $c_{el}$ . If the condition  $c_{el} \ll c_w$  is fulfilled, the coupled configuration can be broken down into 2 oscillating systems. In the first case, the two rotating masses oscillate in the same direction at the "electrical" spring, with its natural frequency being

$$f_{e10} = \frac{1}{2 \cdot \pi} \cdot \sqrt{\frac{c_{el}}{J_M + J_A}} \quad (5)$$



Picture 5: Simplified structure diagram of the squirrel-cage induction motor for disturbing torque at shaft



Picture 6: Mechanical equivalent arrangement

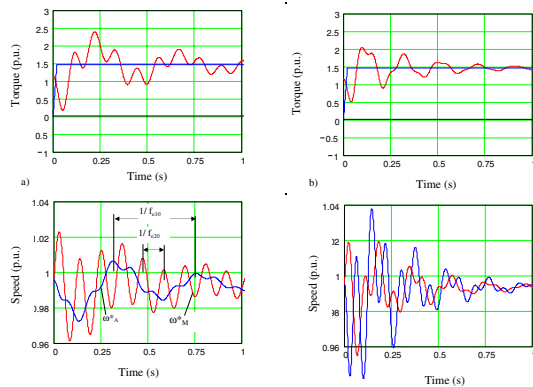
The mechanical natural frequency occurs during oscillation of the two masses in opposite directions at the torsion spring of the shaft:

$$f_{e20} = \frac{1}{2 \cdot \pi} \cdot \sqrt{\frac{c_w \cdot (J_M + J_A)}{J_M \cdot J_A}} \quad (6)$$

If the above-stated condition  $c_{el} \ll c_w$  is not fulfilled, then the complete solution for the arrangement shown in Fig. 6 must be used:

$$f_{e10,20} = \frac{1}{2 \cdot \pi} \cdot \sqrt{\frac{1}{2} \cdot \left( \frac{c_w}{J_A} + \frac{c_{el} + c_w}{J_M} \right) \cdot \left[ 1 \mp \sqrt{1 - \frac{c_{el} \cdot c_w}{J_M \cdot J_A} \cdot \frac{4}{\left( \frac{c_w}{J_A} + \frac{c_{el} + c_w}{J_M} \right)^2}} \right]} \quad (7)$$

The advantage of this equation is the fact that an overview of the positions of the possible resonant points is quickly obtained at the beginning of the design phase, and/or that the resonant points can be shifted to a desired range by changing  $c_w$  and  $J_A$ . However, the value of  $c_{el}$  is often unknown, so that it is at first necessary to resolve the system of the differential equations (4). Using the calculated natural frequency  $f_{e10}$  and the substituted value of  $(J_M + J_A)$ ,  $c_{el}$  is calculated from (5). The natural frequencies are determined from the *free oscillations* which are obtained by entering a surge torque  $m_A$  rather than an oscillating torque in (4e).



Picture 7: Free oscillations triggered by a surge

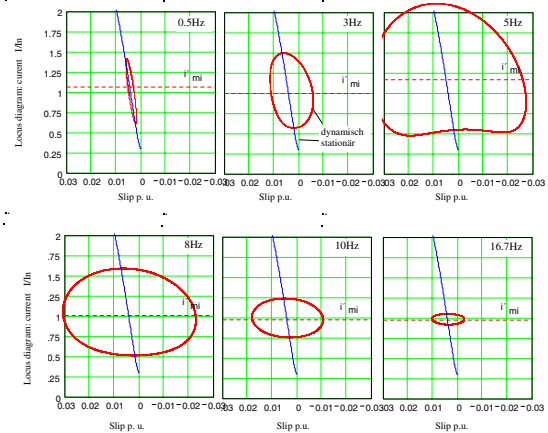
- a)  $J_A = 400 \text{ m}^2 \text{ kg}$ ;  $f_{e10} = 2.3 \text{ Hz}$ ;  $f_{e20} = 9.0 \text{ Hz}$   
b)  $J_A = 40 \text{ m}^2 \text{ kg}$

The other specifications of this drive are:  $P_n = 1800 \text{ kW}$ ;  $n_{0n} = 1500 \text{ min}^{-1}$ ;  $J_M = 120 \text{ m}^2 \text{ kg}$ ;  $c_w = 180,000 \text{ Nm/rad}$ . The natural frequencies in this example are determined most easily from the speed curves. Note that, because of  $J_A > J_M$ , the flywheel ( $J_A$ ) oscillates mostly with  $f_{e10}$ , whilst the rotor of the motor oscillates mainly with  $f_{e20}$  in relation to the flywheel.

With  $f_{e10}$ , one also obtains  $c_{el} = 174,000 \text{ Nm/rad}$ , so that it is then also possible to evaluate (7). The groups of curves according to (7) are shown in appendix A1.

### 2.3.2 Dynamic and stationary current/slip characteristics

Various calculation programs exist for compressor installations which consider the motor solely via its stationary current and torque characteristics. The program described was used to identify the pulsating-torque frequency up to which such a strongly simplified presentation is still acceptable. The results shown in Fig. 8 apply to the same motor as above and to the compressor according to the 1<sup>st</sup> design ( $J_A = 5 \text{ m}^2 \text{ kg}$ ;  $c_w = 500,000 \text{ Nm/rad}$ ). The disturbing torque used was the average compressor torque, including the fundamental-component oscillating torque ( $\Delta m_A = 0.4 = \text{constant}$ ;  $f_{p1} = 0.5$ ; 3; 5; 8; 10; 16.7 Hz). With  $f_{p1} = 0.5 \text{ Hz}$ , the dynamic characteristic differs from the stationary characteristic to a very small extent only, with the amplitudes being subject to the relationship of  $\Delta i \approx \Delta m_A = 0.4$ .



Picture 8: Dynamic and stationary current/slip characteristics

With increasing frequency, current pulsation also increases, and there is no longer any conformity with the stationary curve. The curve at 5 Hz shows substantial current and slip pulsation as a consequence of the resonance nearness (electrical natural frequency  $f_{e10} = 5.9 \text{ Hz}$ ). Above the resonant

frequency, current pulsation becomes increasingly smaller with increasing frequencies due to the effect of the mechanical inertia (the main axis of the elliptic current locus diagram is now horizontal). This means: In the case of very slow load changes, i.e. up to around 0.5 Hz in this case, the stationary characteristics can be used for the calculation – this range, however, is irrelevant for the piston compressor because its frequencies are significantly higher. In the resonant range, the stationary presentation inevitably always supplies excessively small values, whilst above the electrical natural frequency, the oscillating currents calculated by the stationary approach are always higher than the real values (refer also to Fig. 4). **Excessively high values calculated for the oscillating currents would hence in many cases lead to excessively large dimensions of the additional flywheels!**

The precise calculation of oscillating currents is of particular importance if the drive is connected to a weak grid. Even low oscillating currents would then lead to unacceptably high fluctuations of the busbar voltage. For the calculation of the system perturbation, it is thus necessary to use the dynamic motor model because utility companies today check very carefully whether the applicable specifications are adhered to.

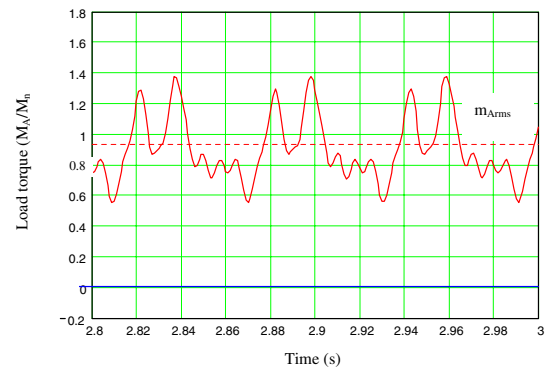
### 3 Design of a piston compressor drive

The individual design steps will be explained using the example of the drive implemented for the Reitbrook underground gas storage.

#### 3.1 Torques of the piston compressor

The manufacturer of the compressor specifies the torque diagrams and the Fourier components of the torque (mean value and superimposed oscillating torques). Since the compressor torque must be entered as a formula in equation (4e), this is determined using the Fourier components. Fig. 9 shows the torque as a function of time.

The RMS value of this curve is:  $m_{Arms} = 0.94$ , with the mean value being  $m_A = 0.92$  (not entered in the diagram: torque related to the nominal torque of the motor). Due to the relatively large mean component, the difference between the two values is small. In the case of a sufficiently high moment of inertia, the mean value of the torque of the compressor is relevant for selecting the rated power of the motor.



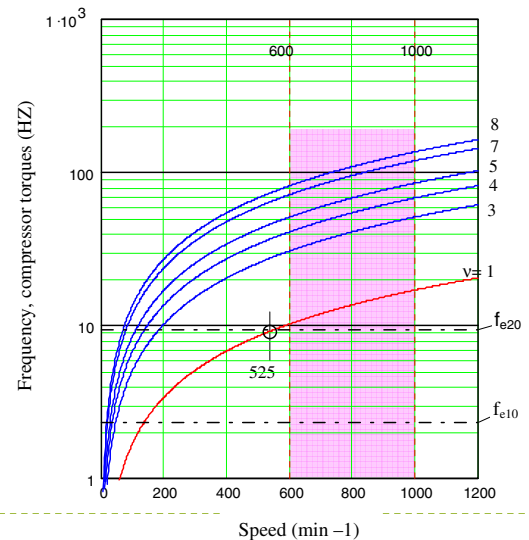
Picture 9: Torque of the piston compressor

#### 3.2 Frequencies of the oscillating torques of the compressor

The frequencies are subject to the relationship

$$f_{pv} = v \cdot \beta \cdot \frac{\Omega_{0n}}{2 \cdot \pi} \quad (8)$$

where  $v$  – ordinal number of the oscillating torque components;  $\beta = \Omega_0/\Omega_{0n}$ ;  $\Omega_{0n}$  – angular frequency of the synchronous nominal speed;  $\Omega_0$  – angular frequency of the synchronous speed set via the inverter (in the case of drives without inverter:  $\beta \approx 0.99$ ).



Picture 10: Oscillating-torque frequencies as a function of speed

In the case of the drive in question, the frequency of the fundamental-component torque at nominal speed is hence

$$f_{p1} = 1 \cdot 1 \cdot \frac{314}{2 \cdot \pi \cdot 3} \text{ Hz} = 16.7 \text{ Hz}$$

Besides the fundamental component, only the components with a sufficiently large amplitude are



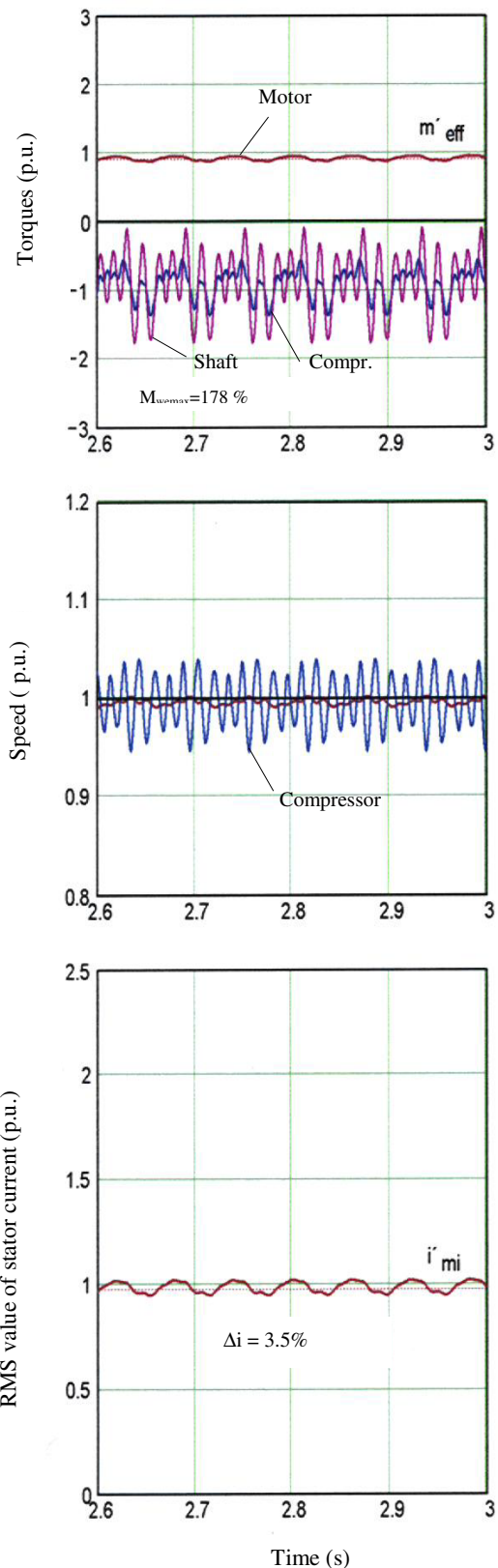
capable of triggering resonances. In the case of this compressor, these are the components with the ordinal numbers  $v = 1; 3; 4; 5; 7; 8$ . These torques are now used to check whether there are one or more frequencies near the natural frequencies within the planned speed setting range from 600 to 1000  $\text{min}^{-1}$ . A presentation of the type shown in Fig. 10 is a favorable approach. It can be directly seen that – in this case – the frequency characteristics of the higher-order components intersect the natural-frequency lines far outside the speed setting range. Only the characteristic with  $v = 1$  almost matches the mechanical natural frequency of  $f_{e20} = 9 \text{ Hz}$  (2<sup>nd</sup> design) at 525  $\text{min}^{-1}$ , i.e. near the lower operating speed limit. The solution of the equation system will indicate whether this distance of around 13% from the resonant frequency is still acceptable with a view to shaft stress and oscillating currents.

### 3.3 Calculation of current pulsation and of the motor and shaft torques

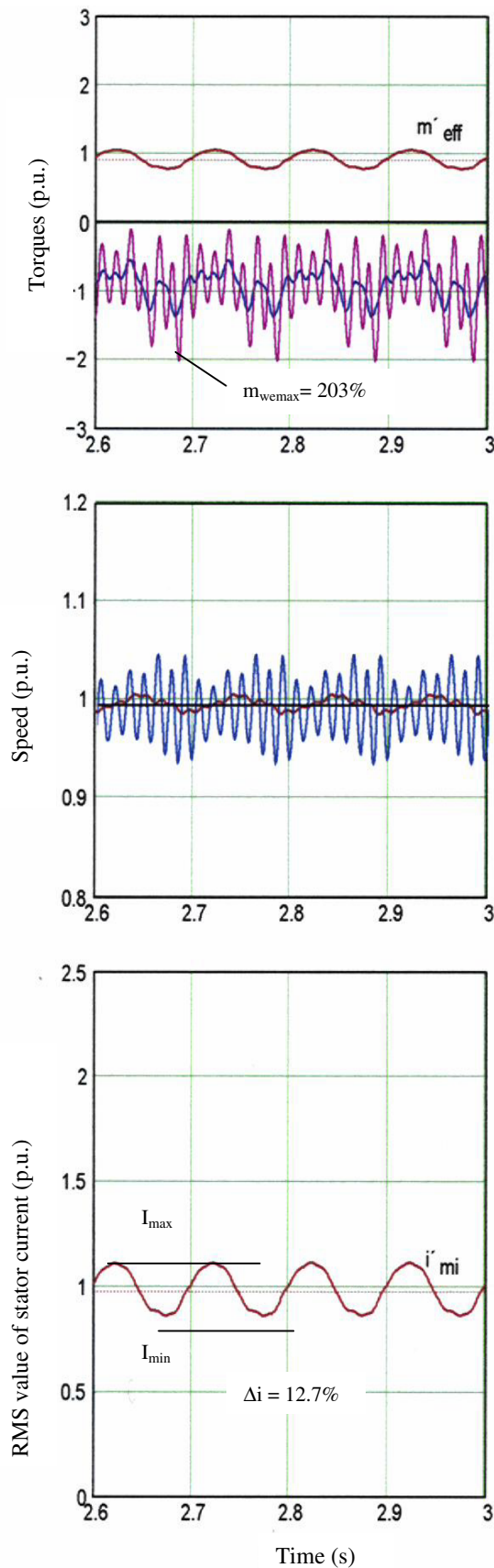
Basic specifications:  $P_n = 1800 \text{ kW}$ ;  
 $I_n = 1940 \text{ A}$ ;  
 $M_n = 17254 \text{ Nm}$ ;  
 $n_{0n} = 1000 \text{ min}^{-1}$ ;  
 $J_M = 120 \text{ m}^2\text{kg}$ ;  
 $P_{w\max} = 1645 \text{ kW}$

#### 3.3.1 Design 1

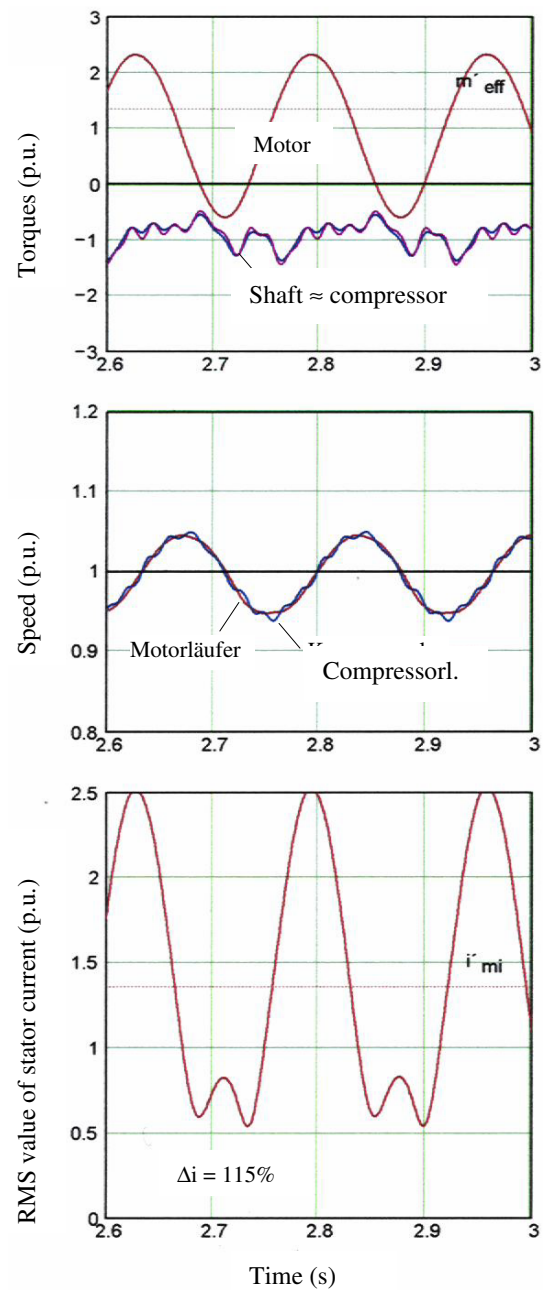
$J_A = 5 \text{ m}^2\text{kg}$  (without flywheel);  
 $c_w = 1,000,000 \text{ Nm/rad}$   
 (rigid coupling);  
 $f_{e10} = f_{ecl} = 5.9 \text{ Hz}$ ;  $f_{e20} = f_{em} = 72 \text{ Hz}$



Picture 11a: Oscillations at 1000  $\text{min}^{-1}$



Picture. 11b: Oscillations at  $600 \text{ min}^{-1}$



Picture 11c: Resonance with  $f_{eel}$  at  $n = 365 \text{ min}^{-1}$

The 1<sup>st</sup> design did not include an additional flywheel, whilst a rigid coupling was part of the design. Such a configuration is favorable from a design point of view and hence in terms of costs. With a view to operating parameters, however, this solution was not optimal:

The oscillating current in percent is calculated using the  $I_{max}$  and  $I_{min}$  parameters stated in Fig. 11:

$$\Delta i = \frac{I_{max} - I_{min}}{2 \cdot I_n} \cdot 100 \quad (9)$$

(where  $I_n$  – nominal current of the motor). At nominal speed, the oscillating component of the

current totals 3.5% and is thus still small enough (Fig. 11a). At the lower end of the speed setting range, however, this value already totals 12.7% (Fig. 11b) – too high a value for weak grids. Earlier literature [9; 12; 17] mentions a value of 30% as a standard value for the permissible oscillating current. Today, the mains voltage fluctuations ( $\rightarrow$  voltage flicker – refer to section 3.5.3) caused by the oscillating currents are the decisive criterion for the permissible oscillating current. This means that a very low limit value applies to weak grids. Since the motor in question is operated at an inverter, the *oscillation damping* of the inverter can be set. Fig. 12 shows that the oscillating current can be reduced to around 3% in this case.

The crucial factor for the change in design was the relatively high torques of the shaft which obviously cannot be influenced by oscillation damping. Fig. 10 shows that the higher-order ( $v = 4, 5, 7$ ) oscillating torques cause resonance sharpness at  $f_{e20}$ . Fitting an additional flywheel with  $J_A = 100 \text{ m}^2\text{kg}$  on the one hand reduces the shaft torque in the speed setting range, but also causes more resonance sharpness just outside the speed setting range on the other (Fig. 12). Furthermore, one also clearly sees the reciprocal influences of current oscillations and shaft torque. At  $f_{p1} = 21 \text{ Hz}$ , mechanical resonance would be present (refer to appendix A1) which also strongly increases the oscillating current via the movement of the motor rotor. In contrast to this, the shaft torque is increased near the electromechanical resonance.

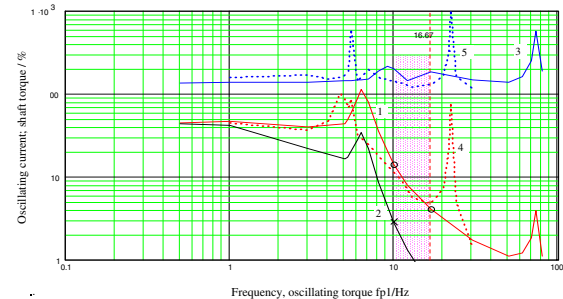
This small example shows that increasing the mechanical inertia often fails to improve the mechanical and electrical oscillation behavior if the position of the natural frequencies is not sufficiently taken into consideration. It is hence important to check – on the basis of the *amplitude response* (Fig. 12, for example), if possible – which measures (rigidity) of the coupling, flywheel, oscillation damping) ensure the optimum design.

### 3.3.2 Design 2

$$\begin{aligned} J_A &= 400 \text{ m}^2\text{kg} \text{ (with flywheel);} \\ c_w &= 180,000 \text{ Nm/rad (elastic} \\ &\quad \text{coupling);} \\ f_{e10} &= 2.3 \text{ Hz; } f_{e20} = 9 \text{ Hz} \end{aligned}$$

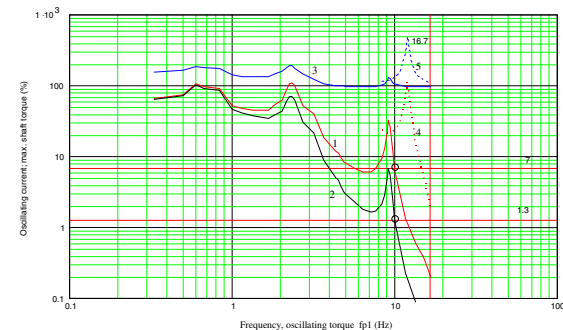
The increase in the moment of inertia and the reduction of torsional rigidity lead to correspondingly low natural frequencies. Fig. 10 shows that the intersection points of all the oscillating-torque frequencies are below the lowest operating speed, i.e. below  $600 \text{ min}^{-1}$ , with these natural frequencies. However, in the case of continuous operation at  $525 \text{ min}^{-1}$ , the frequency of the fundamental-component oscillating torque

would trigger the mechanical resonance. The amplitude curve in Fig. 14 also shows the corresponding increase in oscillating current.



Picture 12: Amplitude curves for oscillating current and maximum shaft torque

- 1 -  $\Delta i$  at  $J_A = 5 \text{ m}^2\text{kg}$
- 2 -  $\Delta i$  with oscillation damping
- 3 - Shaft torque at  $J_A = 5 \text{ m}^2\text{kg}$
- 4 -  $\Delta i$  at  $J_A = 100 \text{ m}^2\text{kg}$
- 5 -  $m_w$  at  $J_A = 100 \text{ m}^2\text{kg}$



Picture 14: Amplitude curves for oscillating current and maximum shaft torque

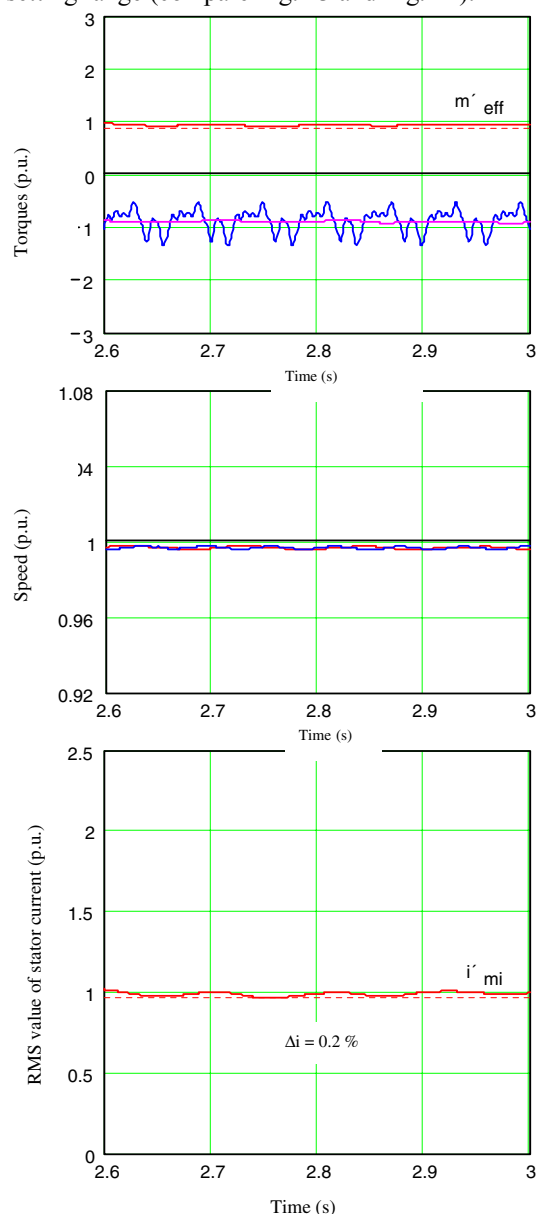
- 1 -  $\Delta i$  at  $J_A = 400 \text{ m}^2\text{kg}$
- 2 -  $\Delta i$  with oscillation damping
- 3 - Shaft torque at  $J_A = 400 \text{ m}^2\text{kg}$
- 4 -  $\Delta i$  at  $J_A = 50 \text{ m}^2\text{kg}$
- 5 -  $m_w$  at  $J_A = 50 \text{ m}^2\text{kg}$

Figs. 13a and 13b show the time characteristics of the torques, speeds and currents for the 2<sup>nd</sup> design (refer to 11a and 11b). Due to the additional flywheel with almost 4 times the moment of inertia of the motor, there is practically no more oscillation for shaft and motor torque at  $1000 \text{ min}^{-1}$ . The oscillation of the motor current is correspondingly low. However, at  $600 \text{ min}^{-1}$ , the current oscillation still totals 6.8% because the mechanical natural frequency occurs at around  $530 \text{ min}^{-1}$ , i.e. shortly below the smallest continuous operating speed. In the case of a squirrel-cage induction motor *without* inverter supply, the values for the moment of inertia and for the torsional

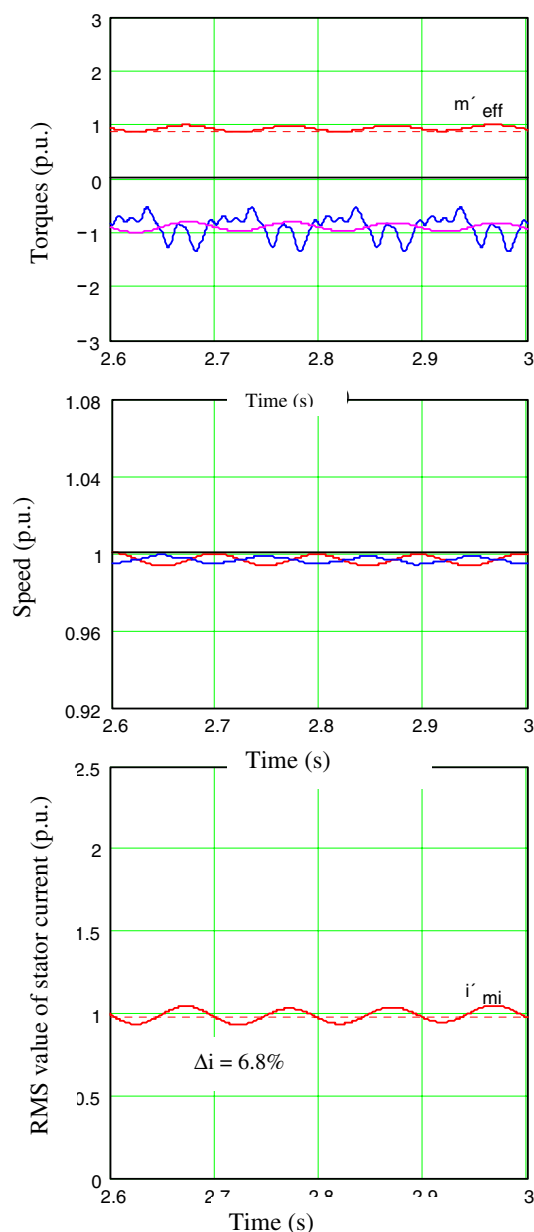
<sup>1</sup> The oscillation speeds in Pict. 11 and 13 are related to the respective synchronous speeds ( $\rightarrow$  deviation from the value of 1).

rigidity would have to be precisely adhered to. *With* inverter supply, additional oscillation damping can be achieved by electronic means. Characteristic 2 in Fig. 14 shows this damping effect – the current oscillation being down to around 1.3% at the lower end of the speed setting range.

Characteristics 4 and 5 in Fig. 15 were calculated for a smaller flywheel ( $J_A = 50 \text{ m}^2\text{kg}$ ). In this case, the mechanical natural frequency totals 12 Hz, so that the resonance occurs at around  $720 \text{ min}^{-1}$ , i.e. in the middle of the speed setting range. The current and torque values in the resonance point show that such a design is not acceptable, even with oscillation damping. Due to the high moment of inertia of the flywheel, the torque of the shaft has the value of the mean load torque within the speed setting range (compare Fig. 13 and Fig. 11).



Picture 13a: Oscillations at  $1000 \text{ min}^{-1}$



Picture 13b: Oscillations at  $600 \text{ min}^{-1}$

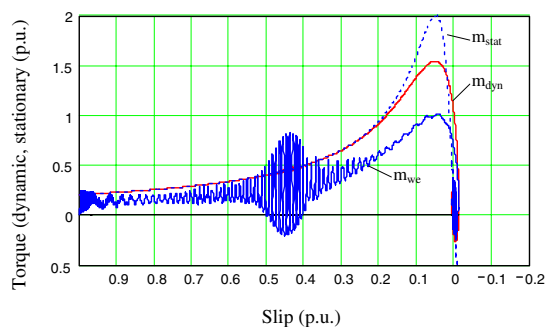
Another interesting question is which oscillating-torque components cause *resonance excitation*. Fig. 14 shows 5 points of resonance – 3 of which are quite distinct (marked in the table). In the table, the points of resonance are represented by their respective  $f_{p1}$  values (with the pertinent speed values in column 2 being determined therefrom using (8)).

Speed		Natural-frequency excitation with		Excitation by oscillating torque of the ordinal number					
$f_{pl}/\text{Hz}$	$n/\text{min}^{-1}$	$f_{eel} = 2.3\text{Hz}$	$f_{em} = 9\text{Hz}$	1	3	4	5	7	8
9.2	525		x	x					
3.1	186		x		x				
2.3	137	x		x					
0.8	50	x			x				
0.6	36	x				x	(x)		

The oscillation torques and their ordinal numbers, respectively, in the table which are responsible for resonance excitation are shown in Fig. 10. It can be seen that in this case the oscillation torques with the ordinal numbers  $v=7$  and 8 (and certainly also the higher ones) do not trigger any noticeable resonance. Notwithstanding this, the oscillation torques until  $v=10$  should be taken into consideration in the calculation.

*Transient resonance excitation* always occurs during starting. Fig. 15 shows the asynchronous starting of the compressor drive (motor without inverter). During the short-time identity of oscillating-torque frequency and mechanical natural frequency, oscillation excitation occurs. However, since the frequencies are identical for a short time only, the full resonance sharpness which is due to damping does not occur. This means that the shorter the time needed for passing through the resonance range, the lower the oscillation amplitudes.

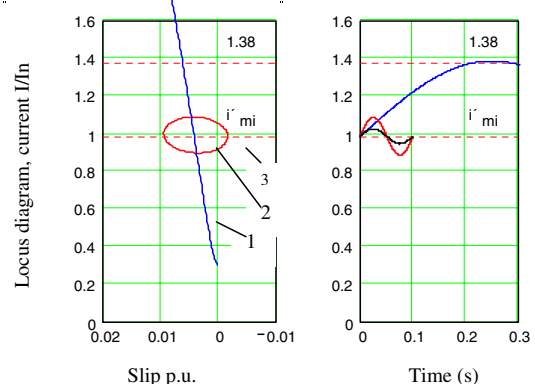
During starting, the motor with inverter develops at least the nominal torque. This leads to a higher acceleration rate below the breakdown torque and hence to a shorter time of frequency match and hence also a lower resonance excitation. Furthermore, the inverter offers the possibility to block a critical speed range, so that even unintended setting of the  $n$ -setpoint at such a speed will lead to a speed slightly above or below such setpoint.



Picture 15: Transient resonance during starting

### 3.3.3 Oscillation damping

The strong influence of the mechanical inertia and of the torsional rigidity of the shaft assembly on the oscillation behavior was discussed in detail. In conjunction with the description of the amplitude curves in Figs. 12 and 14, the oscillation damping was mentioned as a 3rd parameter. This method of reducing torsional oscillations can be implemented with inverter-fed drives only and concerns the limitation of the air gap oscillating torque and the oscillating current. The inverter permits the adjustment of the rotating-field speed of the motor by a suitable design of the internal inverter control system. The amplitude curves show that the oscillation damping becomes increasingly effective in the case of sudden speed changes, i.e. in the range of higher oscillation frequencies, i.e. in the speed setting range. When the load, for example, causes a quick reduction of the *rotor* speed, the *rotating-field* speed is also reduced, so that the increase in slip and thus ultimately also the oscillating current are limited. **However, this limitation of air gap torque and oscillating current also means increased oscillation of the rotor speed** (the slip oscillation is limited, but the speed oscillation is increased!). The ultimate design aim is the limitation of torque and current oscillations – with the magnitude of the speed oscillation playing only a secondary role. **This also means a limited importance of the cyclic irregularity which reflects the quality of the oscillation behavior on the basis of the speed oscillation [10].**



Picture 16: Oscillation damping

1 – stationary (1 Hz); 2 – dynamic (10 Hz); 3 – with oscillation damping

## 3.4 Electrical design

Following optimization of the oscillation behavior, the motor, inverter and transformer must be



dimensioned and the pre-selection of the motor must be checked.

The **motor speed** is determined by the compressor speed. If the operating speed is between two synchronous speeds, a gearbox must be used for the squirrel-cage induction motor without inverter – with a motor with the lower synchronous speed being typically chosen for the squirrel-cage induction motor with inverter supply (-> operation in the field weakening range).

The **rated power** of the motor is subject to the condition  $P_n > P_{RMS}$ , where  $P_{RMS}$  is not the effective power of the compressor, but the effective air-gap power. As a result of the mechanical inertia, the dynamic value of the oscillating current and of the oscillation damping, the calculated curves of the air-gap torque in Fig. 13 show a far-reaching smoothing, so that the mean value of the compressor power can be used as a measure for the selection of  $P_n$  (refer to section 3.1) by way of approximation. This means that the motor design does not pose any problem with regard to its electrical values – the decisive factor being the mechanical stress, i.e. the curve of the shaft torque, however, on condition of a low-inertia design of the shaft assembly (refer to Fig. 11).

The **inverter** is designed on the basis of the operating current. Whilst the motor is designed on the basis of the RMS value of the pulsating current or torque, the inverter must be designed on the basis of the maximum operating current  $I_{max}$  (refer to Fig. 11b) because of the minimum thermal capacity of its valves. There are 2 reasons for the maximum smoothing of the current of a compressor drive: compliance with the limit for flicker voltages at the point of mains connection and use of the smallest inverter possible (the latter factor being a matter of cost). A safety margin of 5% to 10% is common, in particular, in view of the possibility of mains undervoltage conditions. The most commonly used inverter type today is the pulse-controlled inverter with voltage link and non-controlled input bridge.

Drives with  $P_n \geq 1$  MW should be generally connected to the grid via an own transformer. In the case of inverter drives, there is an additional requirement for minimizing the grid's exposure to harmonic currents, i.e. for a transformer design with two secondary windings with a 30° offset of the voltages of these windings (for more details, please refer to the section on "System perturbation"). Since the above-mentioned pulse-controlled inverter draws only a minimum reactive-power component from the grid, the transformer is designed on the basis of the active power of the drive. The rated apparent power of the transformer is subject to the

following relationship, taking the motor and inverter losses as well as a safety margin into consideration:  $S_m \geq 1.15 \cdot P_n$ . In the case of a weak mains supply, even a higher power value can be selected with a view to the voltage dips.

### 3.5 System perturbation

Compressor drives are often fed via weak grid feeders, so that it is mandatory to keep system perturbation under control. A particularly important requirement is to control system perturbation at the medium-voltage busbar because further loads are often connected to it. It is not only important to ensure the undisturbed operation of the various loads, but also to adhere to the limit values specified by the utility companies.

#### 3.5.1 Voltage reduction during starting and during continuous operation

A simple and quick rough calculation can be performed for the starting of the squirrel-cage induction motor without inverter. The starting current is described by the following formula (standardization of all the variables to the corresponding nominal parameters of the motor; assumption: active power of the mains supply is negligible in relation to the reactance):

$$i'_A \approx \frac{1}{\frac{S_n}{S_k''} + u_k \cdot \frac{S_n}{S_{Tn}} + \frac{1}{i_A}} \quad (10)$$

( $S_k'' = 68$  MVA – short-circuit power of the medium-voltage busbar;  $S_{Tn} = 2$  MVA – nominal power of the transformer;  $u_k = 0.08$  – short-circuit voltage of the transformer;  $S_n = 2.12$  MVA – nominal apparent power of the motor;  $i_A = 6$  – starting current of the motor at the rigid mains).

With these values, the starting current becomes  $i'_A \approx 3.67$ . The voltage drop at the medium-voltage busbar thus becomes:

$$\Delta u_{SM} = i'_A \cdot \frac{S_n}{S_k''} = 0.113 \quad (11)$$

This value is not acceptable for a medium-voltage busbar (limit value according to VDEW: 3%).

Continuous operation of the squirrel-cage induction motor without inverter at nominal power and with

the approximation as aforesaid is subject to the following relationship:

$$\Delta u_{SM} = u_N \cdot \left[ 1 - \sqrt{1 - \left( \frac{i_N \cdot x'_N}{u_N} \cdot \cos \phi \right)^2} + \frac{i_N \cdot x'_N}{u_N} \cdot \sin \phi \right] \quad (12)$$

With  $u_N = 1$ ,  $\cos \phi = 0.85$ ;  $i_N = 1$  and  $x'_N \approx S_n/S''_k = 0.031$ ,

$$\Delta u_{SM} = 0.016$$

This value is smaller than 3% and hence acceptable.

Equation (12) is also applicable to starting and continuous operation of the squirrel-cage induction motor with inverter. As starting also takes place with approximately the nominal current, the following relationship applies to both operating conditions with  $\cos \phi_U \approx 0.96$ :

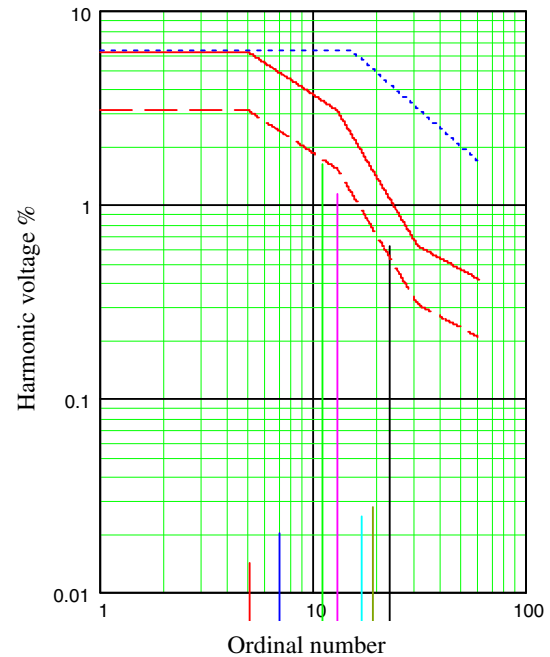
$$\Delta u_{SM} = 0.009$$

With an inverter, the voltage dip at the medium-voltage busbar is very small both in starting mode and during continuous operation.

### 3.5.2 Harmonic voltages

The major disadvantage of an inverter drive is the fact that it injects harmonic currents into the grid. However, feeding the inverter via a 3-winding transformer leads to an approximately sine-shaped mains current. This current only contains harmonic currents with the ordinal numbers  $v = 12 \cdot k + 1$  ( $k = 1, 2, 3, \dots$ ) – the distortion of the busbar voltage is this strongly reduced. The harmonic currents caused voltage drops via the mains impedance, i.e. the harmonic voltages. Fig. 17 shows that the actual values still remain safely below the limit values according to characteristic 2. This is proof of the fact that the voltage distortion limit values are adhered to with the 12-pulse input circuit of a pulse-controlled inverter even in the case of a grid with a relatively weak short-circuit power (68 MVA).

Limit characteristics: 1- VDE 160 2- VDEW,  $k_N=1$  3 – VDEW,  $k_N=0.5$



Picture 17: Harmonic voltages at the medium-voltage busbar

### 3.5.3 Flicker

The term "flicker" refers to the luminance fluctuations of lamps which are caused by voltage fluctuations. The amount of the luminance fluctuations perceived as disturbing depends on the frequency of these fluctuations. Different flicker limit characteristics were determined that can be used in order to determine the permissible voltage fluctuations for each frequency and hence the permissible oscillating current. The maximum eye sensitivity, i.e. the minimum value for the permissible voltage fluctuations, is in the order of around 8 Hz for sine-shaped fluctuations. The frequencies of the oscillating torques of piston compressors are also in this frequency range, so that a check of flicker conditions is not absolutely necessary. Fig. 18 shows the permissible oscillating currents vs. frequency with the power coefficients  $k_s$  (in percent) as parameters. This coefficient reflects the ration between the nominal apparent power of the motor and the short-circuit power of the medium-voltage busbar in question. The characteristics were calculated for the limit interference factor of the individual installation  $Alt = 0.05$ . On the basis of the general data in [15], the following relationship was determined for the maximum permissible oscillating current:

$$\Delta i_{zul}(f_{p1}) \approx \frac{1}{F(f_{p1})} \cdot \frac{S_k''}{S_n} \cdot \sqrt[3]{\frac{A_{lt}}{4.6 \cdot f_{p1}}} \quad (13)$$

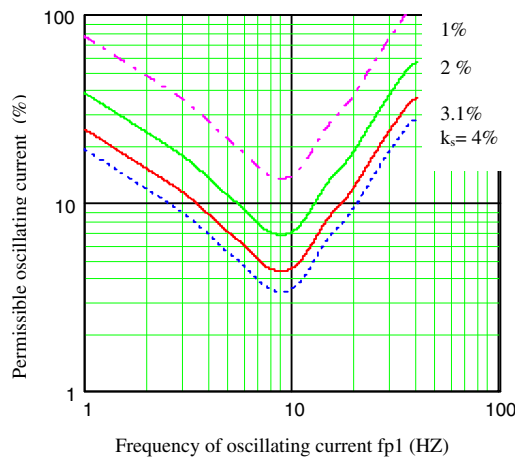
with the electrical form factor  $F$ . In the case of the example of the compressor drive in the Reitbrook underground gas storage, the coefficient  $k_s$  is calculated as follows:

$$k_s = \frac{P_n \cdot 100}{\cos \phi_n \cdot S_k''} = \frac{1.8 \cdot 100}{0.85 \cdot 68} = \underline{3.1\%}$$

For the lower operating speed ( $\rightarrow f_{p1} = 10$  Hz), the relevant characteristic shows for the maximum permissible oscillating current:

$$\Delta i_{zul} = \underline{4.3\%}$$

Fig. 14 shows an oscillating current of 7% for the fixed-speed squirrel-cage induction motor. With oscillation damping, however, a value of 1.3% is achieved, so that the important requirement concerning adherence to the flicker limit is also safely met.



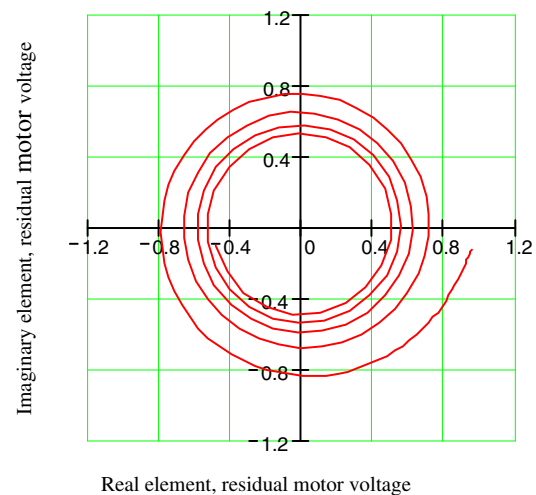
Picture 18: Limit values of the oscillating currents for an individual installation ( $\rightarrow A_{lt} = 0.05$ )

### 3.6 Interference from the main

Operation of the fixed-speed squirrel-cage induction motor with undervoltage leads to a reduction in motor torque according to the square of the voltage and an increase in current in inverse proportion to the voltage. The inverter-fed squirrel-cage induction motor is substantially less susceptible to undervoltage conditions. When the mains voltage drops, for example, by 10%, the internal inverter controller maintains the full voltage and hence the full breakdown torque up to a speed of approx. 85%, so that the current in this range is not higher than under

undisturbed conditions. The breakdown torque does not drop and the current does not rise until a range of  $> 85\%$  is reached because the output voltage of the inverter cannot exceed the input voltage.

The different behavior of fixed-speed and variable-speed squirrel-cage induction motors is more important in the case of the extremely unpleasant short-time mains interruptions. These interruptions occur when switching occurs in the grid of when a short circuit must be cleared. As a result of such an interruption, the motor is no longer capable of developing a motor torque, so that the load torque slowly decelerates the rotor. Even worse, the rotating field does not immediately disappear for energetic reasons – the rotating field is supported by currents circulating in the rotor cage and decays with the rotor time constant. The field is thus "attached" to the rotor and induces the so-called *residual voltage* with speed frequency in the stator winding. When the mains voltage is automatically restored, the difference between mains frequency and rotor frequency means that the residual voltage has a differential angle in relation to the mains voltage that cannot be determined in advance (refer to Fig. 19). If this angle is in the range of  $180^\circ$  (opposition), very high short-circuit currents occur (12 to 20 times the nominal current!) which cause correspondingly high forces in the winding and torsion torques in the shaft assembly – with damage to the insulation or to the shaft assembly being a frequent consequence. If the angle is sufficiently outside the opposition range, there is no risk of damage, but the asynchronous torque is often smaller than the load torque in the case of compressor drives, so that re-starting is not possible.



Picture 19: Residual voltage during short-time mains interruption  
 $U_N$  – mains voltage  
 $U_R$  – residual voltage, opposition range

The process described in the foregoing applies to the squirrel-cage induction motor without inverter. With inverter supply, the speed also drops. However, the link isolates the mains circuit from the machine circuit, so that the above-mentioned hazardous short-circuit conditions cannot occur. Furthermore, quality inverters include the special "*kinetic support*" circuit variant that ensures stability up to around 5% of the nominal speed on the one hand and additionally ensures that safe re-starting without surge current and without surge torque is possible on mains voltage recovery.

#### 4 Summary

The oscillating torques of the compressor require a careful design of the drive because there is always a risk of excitation of unacceptably high torque and current oscillations. Certain reservations exist with regard to the introduction of the inverter drive for piston compressors because several ranges of interference frequencies rather than a few interference frequencies now occur as a result of the variable speed, so that the risk of resonance excitation is increased. This means that detailed modal analyses are necessary during the engineering and configuration phase in order to ensure the safe design of the drive. A PC program was found to be a useful tool to this effect which simulates, in particular, the electrical part of the drive system, i.e. motor and inverter, including system perturbations, with the required precision. As a vital component of the analysis, it is also necessary to determine the electromechanical natural frequency with sufficient precision in addition to the mechanical natural frequency of the system consisting of motor, shaft, coupling, flywheel, compressor. It is shown, amongst other things, that increasing the mechanical inertia not always leads to a reduction of oscillations and that the criterion of the cyclic irregularity  $\delta$  which is still commonly used today provides only a rough estimate of the shaft stress and may even provide misleading statements with regard to the oscillating current. Although the use of the inverter requires a higher engineering and configuration input (which can, however, be reduced to a reasonable extent thanks to the above-described program or a similar program), it also provides several major benefits during operation, such as better control capability and adaptation of technological parameters, significantly lower oscillating currents (reduced risk of flicker), safe and stress-free starting (nominal torque already at nominal current!), high stability in the case of short-time mains interruption and complete avoidance of

dangerous short-circuit conditions on voltage recovery.

#### 5 References

- [1] Beckert, U.; Neuber, W.: Feder- und Dämpfungsziffer der Asynchronmaschine. *Elektrie*, Berlin 42 (1988) 10, pp. 381-383
- [2] Bendler, H.: *Technisches Handbuch Verdichter*, VEB Verlag Technik, Berlin (1986)
- [3] Cierniak, S.: High Pressure Reciprocating Compressors – modern ways of solving problems, 8<sup>th</sup> Int. Recipr. Mach. Conf., Denver (1993)
- [4] Cierniak, S.: Nischenprodukt „Kolbenkompressor“, *Deutsche Pumpen und Kompressoren* (1996)
- [5] Cierniak, S.: Reciprocating compressors in natural gas underground storages in Germany, „Energy News“, Helsinki/Finland, (June 2000), pp. 24-26
- [6] Cierniak, S., Lampe G.: Aplikacia Piestovych Kompresorov V Podzemnych, Slovgas, Bratislava/Slowakia (Jan. 2000), pp. 2-5
- [7] Cierniak, S.: German packager expands with full range of Ariel's compressor line, „Compressor Tech Two“, Waukesha/USA (March-April 2002), pp. 70
- [8] Jordan, H.; Lorenzen, W.; Taegen, E.: Erzwungene Pendelungen von Asynchronmaschinen. *Elektrotechnische Z*, Edition A 84 (1963), pp. 645-648
- [9] Käppner, A.: Über die Projektierung großer Drehstromantriebe für Verdichter und die Netzurückwirkungen bei Anlauf und Betrieb. *Siemens-Z.* 40 (1966), supplement "Motoren für industrielle Antriebe", pp. 37-47
- [10] Knop, G.: Drehschwingungsgerechte Auslegung von Antriebssträngen mit Kolbenverdichtern. *Industriepumpen + Kompressoren* (2002) 3, pp. 142-146
- [11] Leonhardt, A.: Periodisch schwankende Belastung von Asynchronmaschinen. *Elektrotechn. und Maschinenbau* 81 (1964), pp. 581-586
- [12] Scheck, H.: Synchronmotoren für große Kolbenverdichter. Company magazine of VEM Sachsenwerk (1959)
- [13] Schuiskey, W.: Leistungsspendlungen von Induktionsmotoren bei pulsierender Belastung. *Siemens-Z.* 40 (1966), supplement "Motoren für industrielle Antriebe", pp. 84-86

- [14] Stiebler, M.: Frequenzverhalten von Drehstromantrieben bei aufgedrückten Drehmomentpendelungen. Builetin of SEV No. 25 (1969), pp. 1182-1189
- [15] VDEW: Grundsätze für die Beurteilung von Netzurückwirkungen. Verlags- und Wirtschaftsgesellschaft der Elektrizitätswerke m.b.H., Frankfurt a.M. (1992)
- [16] Vetter, G.: Handbuch Verdichter, Vulkan Verlag, Essen (1990)
- [17] Zettler, B.: Elektromotorische Antriebe von Kolbenkompressoren. AEG-Mitteilungen 54 (1964) 11/12, pp. 713-719



# **Economizing the engineering costs of packaging reciprocating compressors to diverse customer specifications: some methods and strategies**

by:

**Dr.-Ing. Siegmund Cierniak**  
**Compression Systems**  
**HGC Hamburg Gas Consult**  
**GmbH**  
**Hamburg**  
**Germany**

**Harinder S. Gujral, M. Sc.**  
**President**  
**PCA Process Compressors**  
**of America, Inc.**  
**Houston / Texas**  
**USA**

**Reliability and economics of compression systems –  
recent trends in the market of  
reciprocating compressors  
March 27<sup>th</sup> / 28<sup>th</sup>, 2003 Vienna**

## 1. Introduction

Over the past two decades or so the engineering specifications that accompany a purchase requisition for process reciprocating compressors, especially for applications in the petrochemical and chemical industries have become exceedingly complex, diverse and above all rather bulky. Engineering and Equipment specifications, written in single space on A4 or similar size papers-on both sides of the paper in some cases-, and approximately 25-30 mm thick are rather the norm than exception these days. In fact, 60 mm thick purchase requisitions are hardly a rare event.

The main reasons for these elaborate changes have been explained in considerable depth in a paper that was presented at the 2<sup>nd</sup> EFRC Conference<sup>1</sup> in The Hague in May 2001, by John W. Middleton. Further understanding and appreciation of these developments can be obtained from a second paper<sup>2</sup> that was presented at the same EFRC Conference by Jerry Jones.

Driven essentially by market economic forces, that resulted in substantially reduced maintenance budgets, a highly mobile maintenance work force that lacked job continuity, extremely low manning levels, and the absence of spare or standby machine availability the Petrochemical Industry went through a long period of what has been described by Jones as the Dark Age of Reciprocating Compressors. Consequently the Petrochemical, or more specifically the Refinery Industry was forced to initiate and develop practices that could be expected to increase the reliability of rotating equipment (such as reciprocating compressors), which in turn should result in increased plant availability<sup>1</sup>.

A very significant implication in Middleton's paper is that the 3 year uninterrupted target stipulated in API 618-4<sup>th</sup> Edition<sup>3</sup> is a very ambitious target that cannot be fulfilled even by machines that may be in conformity with these API Specifications. We all know of course that there is presently no machine on the market that can claim strict conformity with API 618.

The 30 to 60 mm specifications that accompany many purchase requisitions for Reciprocating Compressors and other critical items of Rotating Equipment are therefore a direct outcome of these developments, and their aim is to correct the difficulties and problems faced by the industry during the 'dark ages' without resorting to higher maintenance budgets, and manpower availability or spare compression capacity.

The changes that have been put into effect by more detailed and in most cases more complex specifications however come, as is often the case with any

change, with a price- to the compressor supplier, and in the long run also to the compressor user.

This paper attempts to a) define the nature of these changes as well as their impact on the compressor industry, and b) recommend certain mechanisms that can be developed and practiced to better cope with the problems that the compressor industry, especially the small to medium size companies, faces as a direct consequence of these changes.

The extended specifications have been written with the intention of addressing 3 key elements of compressor design namely

**Reliability/Availability, Condition Monitoring /Safety and Energy / Environmental requirements.<sup>2</sup>**

Understandably so, the greatest emphasis however is on **Reliability/Availability** issues followed by **Condition Monitoring/Safety** and **Energy/Environmental** demands in that receding order.

## 2. The Compressor Vendor

The typical compressor proposal or design engineer is by training neither a critical prose reader nor a professional with meticulous book keeping and clerical capabilities. The purchase requisitions and the engineering specifications that need to be followed in the execution of such an order however place a high premium on these very traits.

It is not surprising therefore that a proposal engineers performance in many compressor vendor companies is not judged so much by his success rate in obtaining new business-which is the real rationale behind his employment in the first instance- but by his ability to correctly document, calculate and address all salient aspects of the customer specification.

The proposal engineer's and the order execution engineer's jobs have over the past two decades become increasingly strenuous and difficult since the prevailing business conditions have forced the Compressor manufacturing and packaging companies to consistently reduce the number of engineers that they employ for such assignments, when in reality the ever increasing complexity of the specifications requires them to do just the opposite. The Compressor Industry is a branch of business in which long- term survival in most parts has been very difficult over the past two decades or so. Combined with the usual cyclical variations as far as demand patterns for new equipment are concerned, this Industry has generally always suffered from a chronic overcapacity in manufacturing-but

not in engineering- although in reality the emphasis for this business is far greater in it's underlying engineering capability than in manufacturing. Little wonder therefore that a large number of leaders in this field of business have over the past two decades vanished from the scene. There is hardly any manufacturer of API 618 type compressors today in the USA, (and USA is undoubtedly is the biggest user nation of process equipment) which is still in business and is not looking for a merger or acquisition.

The obvious expectation in such a situation, from the Compressor Vendor's perspective is the standardization of equipment and engineering specifications in order to lower the engineering and order execution expense amongst other things- some thing that is not in conformity with the issues addressed in Middleton's paper. These are however very valid issues from the compressor customer's point of view, and ultimately like in any other business the Supplier or Vendor must deliver what the customer requires.

### 3. Enunciating the Problem

The solution obviously lies in developing systems and methodologies that would enable the typical Compressor Vendor-especially the small and medium size companies-to cater to very specifically tailored needs of each customer, with the cost effectiveness that can normally only be achieved with standardized procedures.

A major issue is the relative irrelevance to which codes such as API 618 have been increasingly relegated over the years, in a sense by the very user companies for whose benefit these codes were initiated at some point in time, and who continue to be leading members of the American Petroleum Institute. There is hardly any refinery or major petrochemical plant that does not specify some version of API as the basis for it's

Compressor specification. The problem lies in the fact that most, if not all, major users of API 618 reciprocating compressors (the same of course also applies to users of API 617 centrifugal compressors) in the world have introduced their own wide range of amendments, elaborations and restrictions to the API 618 stipulations- and the amendments or elaborations introduced by the different companies are not always common or uniform. Nor are they consistent or constant, since technology and knowledge is consistently changing.

The ability to adhere, imbibe or at the least comment or request a waiver to those stipulations of a customer's inquiry that cannot be satisfied by a

vendor, are crucial to the creation of a meaningful proposal that addresses the customer's needs and simultaneously safeguards the Compressor Vendor's interests. Because of the manpower and resource constraints under which the compressor vendors work, the reality often is very different.

A large number of the companies either cannot submit detailed meaningful proposals in a timely fashion thereby restricting their own chances for more business, or submit proposals that require extensive written and in-person clarifications after the submission of the proposal at considerable cost to both sides. Quite apart from the higher cost that is associated with bid conditioning after submission, such approaches are in some parts of the world proving to be extremely risky, since increasing number of companies summarily reject bids that do not sign binding compliance statements. Based on the writer's personal experience, an even greater risk lies in the fact that pre award or bid conditioning agreements are often not fully or correctly understood by both sides during such meetings, and the record notes or minutes recorded at these meetings are at times vague or unclear that can lead to considerable problems at a later stage in the order execution. Such experience is more common when dealings are conducted in a foreign language (typically in English while both parties are not native English speakers) and record notes are taken in telegraphic or incomplete sentences.

### 4. "The" Solution

There is no simple solution to this problem that can enable a Compressor Vendor to quote and execute orders to a very large variety of customers, in conformity with a huge plethora of differing specifications in a timely and cost effective manner.

PCA has however thought out a system, and initiated working on it, that we believe will address the differing engineering and equipment requirements for a large variety of specifications in order to enable any compressor vendor to respond to the requirements of the customer requisition at considerable savings in time and costs. The system in our view will also translate the proposal details into a set of unambiguous and technically clear order specifications in the event of an order, within a relatively short period of time, while substantially reducing the need for long written commands or verbiage for in-house instructions.

### 5. Application of "the" Solution

The solution as foreseen divides the engineering work related to the execution of any order for a non standard or specially engineered compression sys-

tem or unit (referred hereafter as a 'spec-compressor' for writing convenience) into 3 distinct phases.

- Phase I: for pre-order work
- Phase II: during the order execution period
- Phase III: for the order documentation that has to be usually submitted after or at the time of delivery of the equipment

The proposed solution is proposed to be commercially marketed as a software program that can be integrated into the machinery selection and cost estimation programs that are commonly employed by many Compressor Vendors during the Phase I activities. In the event of an order i.e. in Phase II, the program will be able to incorporate and monitor the compliance requirements that have been stipulated and/or agreed for the spec-compressor during Phase I. Data and information compiled during Phase I and II will be available for incorporation and compliance in the final documentation (Phase III) that has to be submitted at the time of delivery of the equipment.

In developing the proposed solution, it is undertaking a detailed and comprehensive review of a large number of compressor specifications from leading companies that are major users of API 618 based process compressors.

Since no two specifications are alike, it is not possible to develop solutions or a program that permits universal application-but the program will cross reference a similar or identical requirement wherever that happens to be the case, when reviewing different specifications.

## 6. The Program – A Brief Synopsis

The main objective of the proposed programs is to provide the Compressor Vendor with a handy tool to review the detailed specification requirements of the user-company or customer, without having to study and review extensive, time consuming documentation. The program is intended to guide the Compressor Vendor in arriving at a series of Quote or Decline decisions at an early stage of the offer preparation. Since compliance ability with certain technical requirements, (e.g. availability of reference machines, or specific design features) can be a crucial factor in determining the outcome of receiving or losing an order, such indications can be useful in assisting the company's sales management in deciding whether to proceed with the offer preparation work or pursue alternate opportunities.

In cases where the initial decision based on the above- referred indications is to proceed with the Phase I of the project, the program will guide the

Compressor Vendor in identifying all requirements that require:

- ◆ Corrective cost calculation factor
- ◆ Corrective delivery period factor
- ◆ A waiver/exception or commentary relating to a specific requirement, either with or without a corresponding price and delivery impact.

Such a program can in some cases also furnish the necessary format for computing the cost adders resulting from specific stipulations of the user specification that are normally not available in the standard design offering of the Vendor -e.g. when a change of materials of construction is mandated. In other cases the program will draw the program operators attention to the nature of action that needs to be taken for compliance with specifications.

It has to be possible to carry out the vast majority of the operations with this software program, the program user need not necessarily possess special expertise in the field of compression equipment, after a short initial training period in the use of the software and a minimum guidance from an experienced compressor professional.

The program is being designed to deliver at the end of an operation a summary report for the company's sales management that would be critical in determining the total cost and delivery impact in relation to the company's standard API 618 machine, and also furnish a written text for all waivers and exceptions that should to be incorporated into the text of the offering.

## 7. Limitations and Restrictions

The program or solution should not intended for the thermodynamic calculations and/or machinery selection which of course is a function that would have to be carried out by the Compressor Vendor, from their existing product line and existing selection programs if any. The program or solution presented here is by way of additional support that is expected to enable the Compressor Vendor to review his selection or offering in the light of the additional stipulations or requirements that have been stated in the User Companies specifications, as stated above.

It has to cover most of the specific mechanical features and limitations that are stipulated by the user companies for the spec-machine, including but not limited for example to:

- Rod loading and rod reversal stipulations,
- Piston velocity and RPM limitations,
- Cylinder Appurtenances,

- Design stipulations for Valve Internals, cages and seats,
- Crankshaft Bearings –Type and materials of construction,
- Selection criteria for type of distance pieces,
- Installation of packing case assemblies,
- Cooling arrangements for packing assemblies.

Wherever possible or feasible, the program is expected to warn the Compressor Vendor to review respectively modify the proposed selection-if for example the lower permissible piston speed stipulated for the Spec-Compressor has been exceeded in the standard selection made by the Vendor.

The program has not to be designed to review or cover compressor controls, or instrumentation arrangements, since these are usually inquiry specific requirements.

## 8. Concluding Remarks

An indication of the proposed approach and depth of coverage that the program will offer can be had from the enclosed Attachments 1,2 and 3 to this paper that include samples of the underlying logic and procedures around which the programs are being written or designed for Phase I.

The examples enclosed here are based on an actual set of specifications issued by a major Compressor User Company.

It is to be hoped that the proposed project will live up to it's expectations that have been outlined earlier in this paper and we look forward to receiving constructive guidance from the End User, Compressor Vendor and Engineering Contracting Companies.

## 9. References

1. Reciprocating Compressors: Reliability in Design A Practical Approach  
John W. Middleton, Conoco Limited, U.K.  
from 2<sup>nd</sup> EFRC-Conference
2. Operation and Maintenance of Reciprocating Compressors in the New Millennium- Jerry Jones BP Grangemouth Scotland, from 2<sup>nd</sup> EFRC-Conference
3. API Standard 618 "Reciprocating Compressors for the Petroleum, Chemical and Gas Industry Services"–1995, American Petroleum Institute, Washington D.C.



### DECISION CRITERIA – A COMPONENT CATEGORY – COMPRESSOR BLOCK

1	2	3	4	5	6
S. No.	STIPULATION	CUSTOMERS OBJECTIVE	COMPRESSOR VENDOR'S CAPABILITY OR ACTION	RESULT	DECISION to Revise Selection/ Quote / Decline
1	Permit change out of cylinders	To accommodate later day changes in pressure & flow with minimum disturbance.	Availability of adequate family of cylinder sizes	Yes/ No	Quote / Decline
2	Lower or higher limitations of R.P.M. & average piston speed. (API 618 – 2.2)	User company's operating philosophy based on experience.	Availability of adequate design.	Yes/ No	Quote / Decline
3	Limitations concerning maximum allowable rod loading (API 618 – 2.4)	Achieve higher degree of compressor reliability and longevity.	Computation of maximum rod load taking part load operation for each stage, relief valve set pressure, and min. suction pressure.	Yes/ No	Quote / Decline
4	Horizontal cylinders only shall be provided. (API 618 – 2.6.1)	Owner company's philosophy and cylinder drainage requirements.	Availability of horizontal design.	Yes/ No	Quote / Decline
5	Vertical cylinders allowed-if with complete drainage. (API 618 – 2.6.1)	Cylinder drainage requirements.	Availability of adequate design.	Yes/ No	Quote / Decline
6	Fabricated C.W. Jackets not permitted. (API 618 – 2.6.3.4)	Maintenance / operational problems with salty or brackish cooling water.	Availability of cast or forged cylinder jackets for C.W.	Yes/ No	Quote / Decline

### DECISION CRITERIA – A (continued)

#### COMPONENT CATEGORY – COMPRESSOR BLOCK

1	2	3	4	5	6
S. No.	STIPULATION	CUSTOMERS OBJECTIVE	COMPRESSOR VENDOR'S CAPABILITY OR ACTION	RESULT	DECISION to Revise Selection/ Quote / Decline
7	Designed for continuous operation over full range specified conditions.	Customer comfort level & machine availability.	Demonstratable reference. (min. 2 units over 2 years). For comparable conditions.	Yes/ No	Quote / Decline
8	Designed for continuous operation on full recycle.	Minimize shut-down	Availability of adequate design.	Yes/ No	Quote / Decline

## DECISION CRITERIA – B

### COMPONENT CATEGORY – COMPRESSOR BLOCK

1	2	3	4	5	6
S. No.	STIPULATION	CUSTOMERS OBJECTIVE	COMPRESSOR VENDOR'S CAPABILITY OR ACTION	RESULT	DECISION
1	Duration of rod load reversal and magnitude. (API 618 – 2.4.4)	Durability and compressor availability.	Computation of a) duration of reversal in minimum crankshaft degrees and b) magnitude of combined loads in both directions	CONFORM  NON-CONFORM	DECLINE /QUOTE with Comments on Operational Restrictions
2	Cylinder Appurtenances Piston rod run-out shall be measured directly adjacent to the cylinder-packing flange. (API 618 – 2.6.2.1)	Reliability of piston rod run-out measurements.	Review existing design and cost effect of modifications.	CONFORM  NON-CONFORM	Quote with Comments (with / without price impact)
3	Cylinder Appurtenances adequate clearance to permit use of torque wrenches. (API 618 – 2.6.2.11.4)	Maintenance Convenience.	Review existing design and cost effect of modifications.	CONFORM  NON-CONFORM	Quote with Comments (with / without price impact)
4	Valve design stipulations- * No valve lifters. * Non-metallic valve plates or * Fully milled metal valve discs and plates. (API 618- 2.7)	User Company Philosophy on Maintenance & Operational Convenience.	Review existing design with valve supplier, including cost effect.	CONFORM  NON-CONFORM	Decline/ Quote with Comments and price impact

**DECISION CRITERIA – B (Contd.)**  
**COMPONENT CATEGORY – COMPRESSOR BLOCK**

1	2	3	4	5	6
S. No.	STIPULATION	CUSTOMERS OBJECTIVE	COMPRESSOR VENDOR'S CAPABILITY OR ACTION	RESULT	DECISION
5	Arrangement to retain complete valve assembly in position while cover plate is removed/installed (API 618 – 2.7.5)	Maintenance Convenience.	Check presence of design feature.	CONFORM  NON-CONFORM	Decline/ Quote with Comments
6	Capacity Control Method – Customer Stipulations. (API 618 – 2.7.12)	Customer Operational Philosophy. Convenience.	Not covered by this program. Requires separate review.		
7	Cylinder Appurtenances adequate clearance to permit use of torque wrenches. (API 618 – 2.6.2.11.4)	Installation, maintenance and operational consideration.	Design Check	CONFORM  NON-CONFORM	Decline/ Quote with Comments
8	Stipulations concerning crankshaft, connecting rod and crosshead materials. (API 618 – 2.9)	Customer or Owner Philosophy – Design integrity.	Check design integrity and design feasibility of modifications.	CONFORM  NON-CONFORM	Decline/ Quote with Comments
9	Stipulations relating to design of crankshaft bearings, and materials of construction. (API 618 – 2.9.2)	Owner's Philosophy concerning bearing life span.	Check existing design and feasibility of design modification including change of frame size.	CONFORM  NON-CONFORM	Decline/ Quote with Comments & price impact

**DECISION CRITERIA – B (Contd.)**  
**COMPONENT CATEGORY – COMPRESSOR BLOCK**

1	2	3	4	5	6
S. No.	STIPULATION	CUSTOMERS OBJECTIVE	COMPRESSOR VENDOR'S CAPABILITY OR ACTION	RESULT	DECISION
10	Selection criterion for type of distance piece. (API 618 – 2.10.1)	Owner's Philosophy & Operational Convenience.	Review of existing design and feasibility and cost impact of modifications.	CONFORM  NON-CONFORM	Quote/  Quote with comments and cost impact
11	Requirements relating to installation of packing case assemblies. (API 618 – 2.11.2)	Assembly and Maintenance Convenience.	Review existing design and feasibility of design modifications.	CONFORM  NON-CONFORM	Quote/  Quote with Comments
12	Vent & drain pipe filterings – Materials of construction and connections. (API 618 – 2.11.3)	Maintenance convenience and machine availability.	Review of existing design and feasibility and cost impact of modifications.	CONFORM  NON-CONFORM	Quote/  Quote with Comments & cost impact



**DECISION CRITERIA – B (Contd.)**  
**COMPONENT CATEGORY – COMPRESSOR BLOCK**

1	2	3	4	5	6
S. No.	STIPULATION	CUSTOMERS OBJECTIVE	COMPRESSOR VENDOR'S CAPABILITY OR ACTION	RESULT	DECISION
13	Design requirements for cooling passages and sealing arrangements. (API 618 – 2.11.4.2)	Owner's Philosophy concerning bearing life span.	Review of customer requirements.	CONFORM  NON-CONFORM	QUOTE  Quote with comments / waiver.
14	Non-Acceptance of direct cooled packing assemblies by water. (API 618 – 2.11.5)	Owner's Philosophy	Review possibility of oil cooling if indirect cooling not possible.	YES / NO	QUOTE  Quote with comments and possible price impact
15	Additional requirements relating to buffer gas and venting arrangement. (API 618 – 2.11.8)	Owner's Philosophy Maintenance & Operational Convenience.	Review compatibility of vendor's existing design with customer stipulations,	CONFORM  NON-CONFORM	QUOTE  Quote with comments / waiver

### DECISION CRITERIA – C COMPONENT CATEGORY – DRIVE SYSTEMS AND CRITICAL SPEEDS

1	2	3	4	5
S. No.	STIPULATION	CUSTOMER'S OBJECTIVE	COMPRESSOR VENDOR'S CAPABILITY OR ACTION	RESULT
1	Torsional Analysis of the complete compressor/gear/driver System for VSDS or geared motor drives. (API 618-2.5.2)	Equipment Reliability	In-house or hired capacity for performing Torsional Analysis	Evaluate Price and Delivery impact on proposal
2	Response Analysis of the rotating system during all possible resonance conditions, which may occur during run up and over complete speed range for variable speed drivers. (API 618- 2.5.2)	Equipment Reliability.	In-house or hired capacity for performing Torsional Analysis	Evaluate Price and Delivery impact on proposal
3	Modal Damping not to exceed 1% when calculating the resulting stress in relevant components, in every response analysis. (API 618- 2.5.2)	Equipment Reliability.	In-house or hired capacity for performing Torsional Analysis.	Evaluate Price and Delivery impact on proposal

# **Influence of piston-ring design on the capacity of a dry-running hydrogen compressor**

**by:**

**Dr. N. Feistel, Burckhardt Compression AG,  
Winterthur, Switzerland**

**Reliability and economics of compression systems -  
recent trends in the market of  
reciprocating compressors  
March 27<sup>th</sup> / 28<sup>th</sup>, 2003 Vienna**

**Session 6**

## **Abstract:**

In order to achieve the highest possible volumetric efficiency during oil-free compression of hydrogen, it is necessary to maximize the performance of the dry-running sealing systems. The compression of small and medium flow rates to high pressures, as required for filling gas bottles and for process-gas compression in the chemical industry, can be viewed as especially critical aspects here. Due to the very small piston diameters typically involved in the final stages, the covering of the sealing-element joints plays a significant role here. The results of tests conducted with a variety of piston-ring designs in a dry-running crosshead compressor are used to elucidate the most important differences and the related consequences for the hydrogen capacity.

## 1 Introduction

Due to the extraordinarily high costs associated with potential production losses, high demands are placed on the reliability of crosshead compressors, which are today used mainly by the chemical industry for the purpose of compressing process gas. The notable rise in the performance of dry-running sealing systems over the last few years has been accompanied by demands for ever longer maintenance intervals.

However, not all such demands can be fulfilled with a sufficiently low specific energy consumption. Particularly as concerns the oil-free compression of hydrogen, the capability of simple sealing systems to manage high pressure differences is attended by a low volumetric efficiency. Although such sealing systems have a low price, they can lead to a design of unnecessarily large machines and penalize the operator with higher operating costs and often with a rapidly decreasing flow rate.

Gas leakages from piston-rod sealing systems are usually under critical observation, their rates being closely monitored, whereas gradual drops in flow rate often remain unregistered, or are tolerated until their consequences assume significant proportions. In the case of large crosshead compressors with a drive power of several hundred kW, an average loss of 10 % in capacity over a period of 8000 hours generates expenses which by far outweigh the costs saved by the sealing elements. In other words, one often saves at the wrong end here.

Different concepts are used for sealing compression chambers of crosshead compressors, in accordance with the type of operation involved (single or double acting compression). These concepts range from relatively leaky designs such as piston rings with a butt or scarf joint, to gastight constructions costing up to twice as much. The results of tests conducted with a variety of piston-ring designs in a dry-running crosshead compressor are used to elucidate the most important differences and the related consequences for the hydrogen capacity.

## 2 Various styles and applications of piston rings

Piston rings for double-acting cylinders with large diameters usually are one-piece rings with a butt or scarf joint (Fig. 1 a, b). In the case of these designs, the joint is not sealed either axially or radially, thus minimizing the risk of failure by fracture even for brittle materials. However, progression in wear is accompanied by a proportional increase in the flow

area of the ring joint and a resultant increase in the quantity of leakage gas.

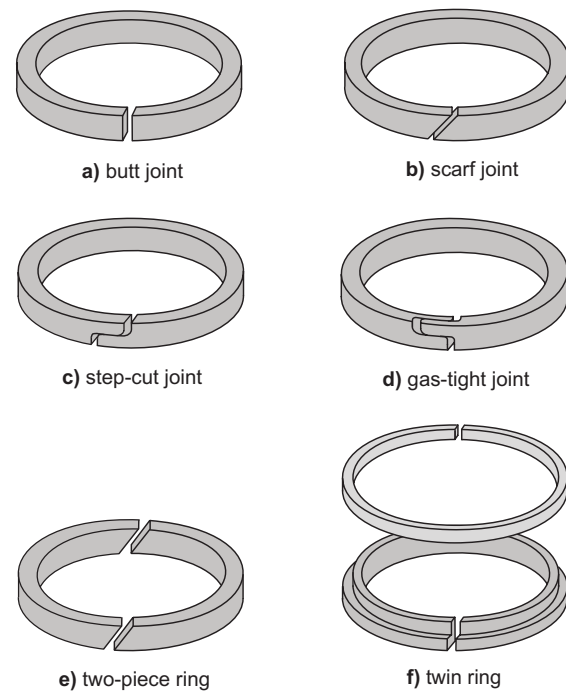


Fig. 1: Various styles of piston rings

The covering of the sealing ring joint plays a major role, particularly in the case of single-acting compression stages with small cylinder diameters. Experiments with a single-acting air compressor<sup>2</sup> have shown that already at a ratio of 10 % between the flow area of the joint and the total flow area of a piston ring (sum of joint, axial and radial flow areas), 77 % of the total leakage gas flows through the ring joint. Under these conditions, the joint gap - as opposed to<sup>1</sup> - can be regarded as the dominating flow area for the leakage mass flow. All the more astounding is the occasional use of two-piece designs (Fig. 1 e) with scarf joints even for the compression of gases possessing a low molecular weight to high pressures.

In accordance with the sealing function required, piston-ring joints can be shaped to any degree of complexity within the bounds determined by the material properties and ring dimensions. Particularly when it comes to handling high pressure differences, however, dry-running materials with a strong tendency toward cold flow can cause a failure of the ring joint, while brittle materials are susceptible to fracture. A logically advisable increase in the axial dimensions of the piston ring is limited by the simultaneous increase in frictional heat which impairs tribological conditions. The use of high-temperature polymers can also create problems

during the sealing of very light gases, because as the degree of wear increases, the high modulus of elasticity prevents full compensation of the gaps created between the sealing element and cylinder wall as a result of uneven material wear. In addition, modern polymer blends not only improve the sealing efficiency, but often also enable longer operating periods, especially in the case of very dry gases. Consequently, a great challenge is posed by the gastight sealing of ring joints for dry-running compression of hydrogen to high pressures, as required during the filling of gas bottles, for example.

The simplest design of a joint seal - termed step-cut joint (Fig. 1 c) - only involves covering in the axial direction, radial flow around the sealing element being possible. The abrupt reduction in the ring's cross-section on the transition to the joint overlap results in fracture in the case of brittle materials (Fig. 2). Although rounding the transition off carefully with a large radius lowers the risk of failure by fracture (Fig. 3), a dynamic pressure difference  $p_{\text{dyn}}$  of more than approximately 3 MPa is not permissible for the polymer blend used here.



Fig. 2: Step-cut piston rings made of a brittle polymer blend and exhibiting fracture of the overlapping joints

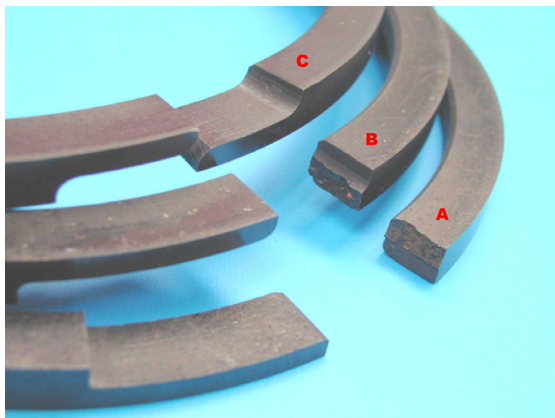


Fig. 3: Avoidance of failure by fracture through a large radius at the transition to the step-cut joint ( $A = 1 \text{ mm}$ ,  $B = 2 \text{ mm}$ ,  $C = 4 \text{ mm}$ )

In the case of piston rings with a gastight joint (Fig. 1 d), the joint is also sealed radially. However, this type of joint sealing is very susceptible to fracture, due to the additional reduction in the cross-section of the overlap.

In the case of the twin ring - another gastight piston-ring design - the butt joint of the rectangular sealing ring is sealed by a surrounding, L-shaped cover ring (Fig. 1 f). If both parts of the twin ring are made of the same material, the problems mentioned above might occur again either as failure by fracture or creep in the region of the joint, or as a result of insufficient wear compensation. With this style, however, it is possible to design the cover ring with small dimensions out of a high-temperature polymer, leaving the remaining space for the sealing ring consisting of a polymer blend, for instance. In addition, the distribution of the pressure difference along the frictional sealing surface<sup>2</sup> in the case of the twin ring results in unequal wear of the two ring parts. Especially if high loads are exerted on the twin ring, this effect can increase the wear of the sealing ring compared with the wear of the cover ring by a factor of up to 3 (Fig. 4).



Fig. 4: Unequal wear of cover ring and sealing ring made of high-temperature polymer (bottom), compared with a new twin ring (top)



### 3 Experimental set-up and methodology

#### 3.1 Experimental set-up

The influence of piston-ring design on the hydrogen capacity was investigated using a dry-running, two-stage, horizontal crosshead compressor (Fig. 5) with a stroke of 160 mm, maximum speed of 850 min<sup>-1</sup> and maximum drive power of 400 kW. The compressor was designed for a maximum final pressure of 20 MPa and a maximum average piston velocity of 4.0 m/s.

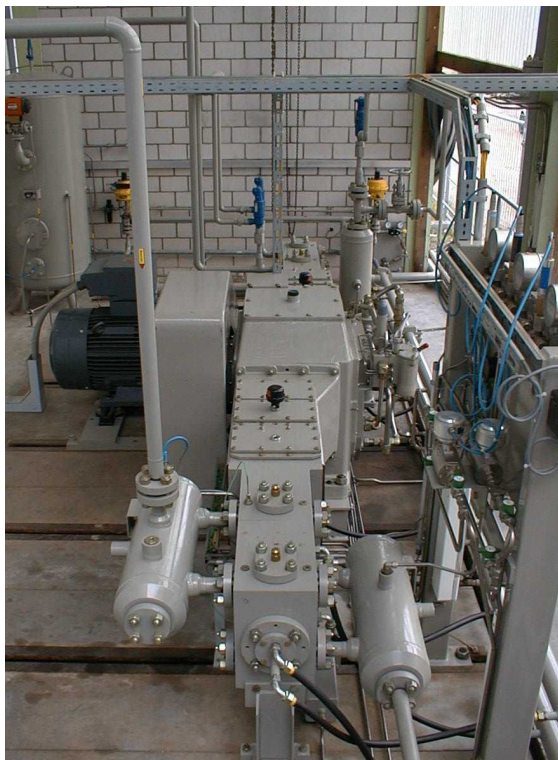


Fig. 5: Two-stage, crosshead hydrogen compressor for investigating the operational behaviour of dry-running sealing systems

With a piston diameter of 75 mm, the first, double-acting stage compresses the hydrogen using a total of eight piston rings (four on each side of the centrally positioned guide rings). The second stage, also with a piston diameter of 75 mm and equipped with nine piston rings, increases the pressure single-acting at the rod side of the piston. The piston rod diameter in both stages is 50 mm. To cover a large range of pressure differences while minimizing gas losses, operation took place in a closed cycle at a suction pressure higher than atmospheric pressure. The gas cycle was fed with hydrogen having a dew point  $\leq -65$  °C.

The hydrogen flow rate was measured with a thermal mass flowmeter for potentially explosive atmospheres (Fig. 6). With the bypass concept, a fraction of the gas flow to be measured is routed via a small sensor tube, where it causes a temperature difference between two electric windings (acting as both heaters and resistance-temperature detectors) which is proportional to the mass flow rate<sup>5</sup>. Whereas the differential pressure flow meters still enjoying widespread industrial use also entail a determination of density, the thermal mass flowmeter directly supplies the sought quantity. Compared with simple and robust throttle elements such as orifices and nozzles, which can withstand adverse operating conditions, a disadvantage of the thermal mass flowmeter is that it needs to be carefully protected from gas pollution by means of a filter with a pore diameter of less than 5 micrometers. The device used allows the measuring of hydrogen flow rates up to 400 standard cubic meters per hour (scm/h) with an accuracy of  $\pm 0.2$  % of full scale.



Fig. 6: Measurement of hydrogen flow rate by means of a thermal mass flowmeter for potentially explosive atmospheres

#### 3.2 Methodology

The various piston ring designs also influence the pressure distribution inside the sealing system. Whereas in the case of new piston rings of a gas-tight design, the entire pressure difference is typically sealed by just one or two sealing elements at the ends of the sealing system<sup>3, 4</sup>, the pressure difference in designs where joint sealing is either absent or only present in the axial direction is distributed simultaneously to different extents among all the sealing elements<sup>2</sup>. For the latter, the first objec-

tive was to investigate the dependence of the capacity on the number of piston rings. Measurements involving different numbers of piston rings possessing a step-cut joint, single-acting compression from 2.4 to 6 MPa and a speed of  $725 \text{ min}^{-1}$  showed that the flow rate of new piston rings stops increasing once the number of sealing elements has reached four (Fig. 7). On dismantling of the piston, it turned out that all joints were aligned in a straight line in the presence of up to four piston rings, and in blocks of two or three sealing elements each in the presence of more rings.

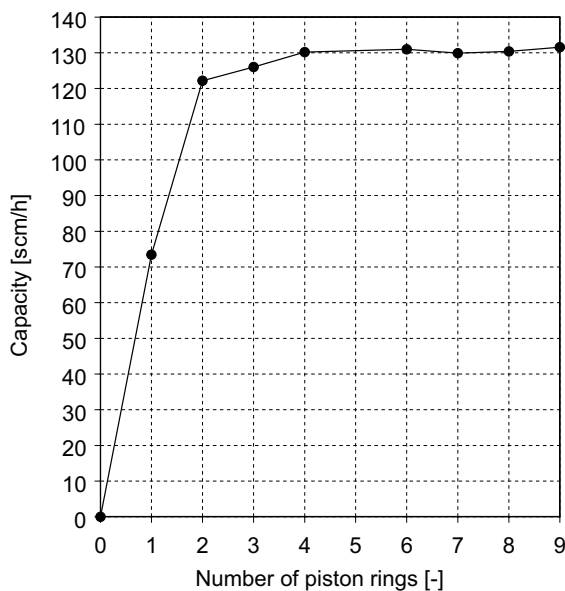


Fig. 7: Dependence of capacity on the number of piston rings with a step-cut joint, given single-acting compression ( $p_s = 2.4 \text{ MPa}$ ,  $p_d = 6.0 \text{ MPa}$ ,  $n = 725 \text{ min}^{-1}$ )

In all tests, the true sealing rings were made of carbon/graphite-filled PTFE with an average coefficient of linear thermal expansion in the circumferential direction of  $87 \cdot 10^{-6} \text{ K}^{-1}$  over a temperature range of 20 to  $150^\circ\text{C}$ . In all designs, the piston rings had an axial dimension of 5 mm and a radial dimension of 6 mm (including an annular spring width of 1 mm in the case of the two-piece piston rings). The scarf joints of the one-piece piston rings cut at an angle of  $30^\circ$  turned out to have an average clearance of 2.66 mm at room temperature. Given a radial piston clearance of 0.75 mm, this results in an area of  $1.98 \text{ mm}^2$  left unsealed by the piston ring. The two-piece rings, whose scarf joints were also cut at an angle of  $30^\circ$ , turned out to have an average total clearance of 2.75 mm, resulting in a similar gap area of  $2.04 \text{ mm}^2$  distributed among two joints. The average overlap of the two joint halves of the step-cut piston ring was  $11.3^\circ$ ; the joint clearance of 1.93 mm results in an uncovered gap area of  $1.43 \text{ mm}^2$  at room temperature.

#### 4 Tests with double-acting compression

In the case of double-acting compression, the piston sealing elements are only subjected to the dynamic pressure difference  $p_{\text{dyn}}$  varying between the suction and discharge pressure, the static pressure component  $p_{\text{stat}}$  being omitted due to the identical suction pressure at both ends of the piston (refer to the notation for definitions). Double-acting pistons are designed with diameters ranging far beyond 1000 mm, the 75-mm variant used in these tests accordingly representing the low end of the diameter spectrum. However, of particular interest here was the effect of the high dynamic pressure differences, in whose case smaller piston diameters are usually employed.

The tests were intended to first demonstrate the differences between the behaviour of new gastight twin rings and that of piston rings with a scarf or step-cut joint used frequently for double-acting pistons. Of each of these three variants, eight piston rings were investigated at a speed of  $494 \text{ min}^{-1}$ , the suction pressure being raised at a constant compression ratio of 3.5 in steps of 0.4 MPa from 0.4 to 1.6 MPa. For these tests, the second compression stage was eliminated by removing the valves. At every load step, the compressor was operated for approximately one hour in order to achieve thermally stable conditions, and then for a subsequent hour during which the capacity was measured at 30-second intervals in order to form an average value. The average flow rates are plotted as a function of the suction pressure in Fig. 8.

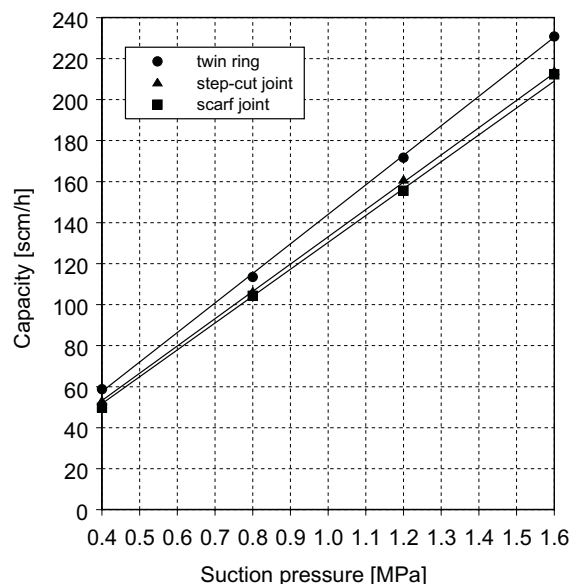


Fig. 8: Dependence of capacity on piston-ring design in the case of double-acting compression

Apparently, there are only small differences between the flow rates of piston rings with step-cut and scarf joints with slightly higher values for the step-cut joint. Only the twin rings were able to achieve a somewhat higher capacity, amounting to 7.5 % compared with the piston rings with step-cut joints. However, it seems more likely that this better flow rate is attributable not to a lower gas leakage between the two compression chambers, but to an improved sealing efficiency of the first twin ring located right next to the compression chamber, which results in a lower clearance volume.

As the degree of wear increases, all piston ring designs without complete joint sealing experience a continuous increase in the flow area of the joint until the leakage becomes unacceptably high. Although piston rings with a step-cut joint prevent a direct flow through the growing cross-section of the gap, a flow around the joint overlap is nevertheless possible. If one half of the joint overlap is removed in order to simulate a fracture of step-cut joints occurring frequently in practice, this results in an average joint clearance of 12.72 mm for the eight piston rings. Fig. 9 shows the effects of the uncovered gap area - now grown to an average of 9.45 mm<sup>2</sup> - on the flow rate. A drastic reduction to roughly 40 % in the case of the twin-ring design was accompanied by a continuous rise in the outlet temperature to a peak value of 187 °C during the last load step. If a single, intact piston ring is used in the central section of the piston though, the capacity rises again and the temperature assumes the value of approximately 135 °C common during standard operation.

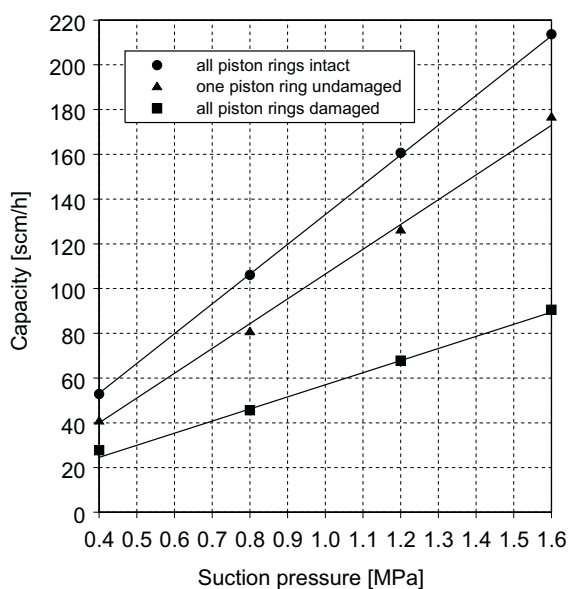


Fig. 9: Dependence of the capacity on the state of the step-cut joints of eight piston rings in the case of double-acting compression

This highlights the advantage of maintaining the best possible joint sealing also during double-acting compressions of hydrogen, even if the resultant benefits are hardly apparent in the new state of the piston rings. The twin ring proves advantageous here, since its sealing element is designed to wear completely in theory without permitting a direct flow through the joint.

## 5 Tests with single-acting compression

If the pressure after the last sealing element of a single-acting piston is lower than the suction pressure of the compression stage under consideration, the dynamic pressure component  $p_{dyn}$  is supplemented by a static pressure difference  $p_{stat}$ . In contrast to the dynamic pressure difference, the static pressure component remains effective at a constant level during the entire rotation of the crankshaft, and a backflow into the compression chamber can be ruled out; consequently, the static pressure difference constitutes the primary load parameter influencing the leakage rate, therefore placing the highest possible demands on sealing technology. Table 1 shows the individual load steps and related pressure components for the tests involving the single-acting piston.

suction pressure $p_s$ [MPa]	1.2	2.4	3.6	4.8
discharge pressure $p_d$ [MPa]	3.0	6.0	9.0	12.0
constant pressure after the last sealing element $p_z$ [MPa]	0.4	0.8	1.2	1.6
dynamic pressure difference $p_{dyn}$ [MPa]	1.8	3.6	5.4	7.2
static pressure difference $p_{stat}$ [MPa]	0.8	1.6	2.4	3.2

Table 1: Pressure exerted on the piston rings during single-acting compression

With nine piston rings in each case designed as twin rings, one-piece rings with a scarf joint, one-piece rings with a step-cut joint and two-piece rings with scarf joints, the flow rates were measured at various load steps and at a speed of 494 min<sup>-1</sup> over a period of 1 hour. The average values are plotted as a function of the suction pressure in Fig. 10. As with double-acting compression, there is a small difference between the designs comprising scarf joints and step-cut joints, the values for the scarf joints being lower by 4.9 % on average. The higher capacity in



the case of piston rings with a step-cut joint is attributable to a slightly lower joint clearance (see chapter 3.2) and maybe to a somewhat better sealing efficiency due to the overlap, but compared with the gas-tight twin-rings the flow rate is 16 % lower.

Of note are the poor values obtained for the two-piece design, although the total gap area of its two scarf joints is only slightly larger than that of the one-piece variant's scarf joint, and although the two ring segments were pressed additionally against the cylinder wall by an annular spring. Consequently, the fact that the flow rate of the two-piece rings is 30.5 % lower than that of the twin rings must be due to other disadvantages of this design, such as unstable and uneven contact between the segments and the cylinder wall, for instance. Removing the annular springs causes the flow rate to fluctuate strongly and drop as far as 52.3 % of the twin-ring level.

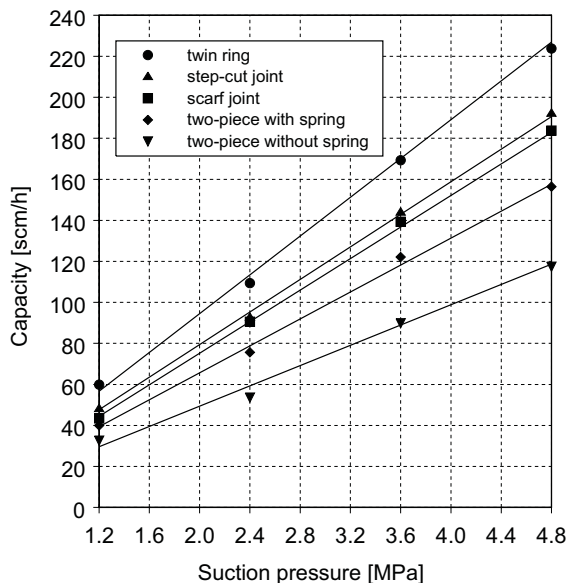


Fig. 10: Dependence of capacity on piston-ring design during single-acting compression

## 6 Tests with progressive wear

As notable variations in capacity were established already on new piston rings of various designs during single-acting compression of hydrogen, the next step was intended to investigate the influence of progressive wear on flow rates with and without elaborate joint sealing. In the case of designs without joint sealing, of particular interest here was the state of wear in which gas transport is no longer possible. To attain this state of wear within a reasonable period of time, only four piston rings were subjected to a suction pressure of 2.4 MPa and a

final pressure of 6.0 MPa at a speed of 725 min<sup>-1</sup>. As numerous preliminary experiments had revealed that the selected carbon/graphite-filled PTFE exhibits unfavourable wear characteristics in dry hydrogen, the subsequent test phases were also expected to be correspondingly short.

Fig. 11 shows the relative flow rates of piston rings with a scarf joint as a function of time, with respect to an initial value of 136 scm/h. After dropping sharply at the beginning of the experiment, the flow rates leveled off somewhat; after just 480 hours, however, a state was reached in which the specified final pressure could still be maintained, but without any significant flow rate. As mentioned earlier, all the sealing elements of piston rings without fully sealed joints participate in sealing pressure, but to different extents. Table 2 shows the average values for the radial wear of four sealing elements, each obtained by five measurements along the circumference of the sealing rings. The wear values rise from the first sealing element (positioned right next to the compression chamber) to attain a maximum value of 1.12 mm at the last sealing element. At room temperature, this results in an increase in the gap area of the joint from 1.98 to 7.04 mm<sup>2</sup>. Although thermal expansion reduces this value slightly during operation, the indefinite temperature after the last sealing element is not likely to be higher than 40 to 60 °C. On the other hand, the uneven removal of material along the circumference of the sealing element and deformations in the region of the joint suggest the existence of additional flow areas during operation.

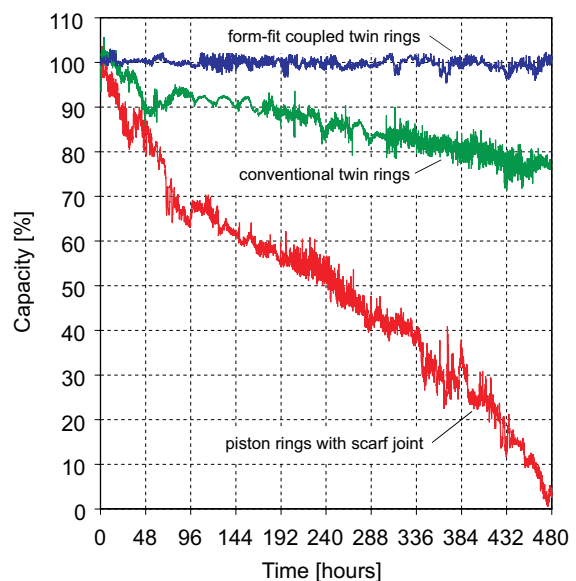


Fig. 11: Relative capacity vs. time of four piston rings with a scarf joint, conventional twin rings and form-fit coupled twin rings (measurement interval: 300 seconds)

During single-acting operation, the flow rates of new twin rings were considerably higher than those of piston rings with a scarf joint. However, a test of four twin rings under the above-mentioned conditions reveals a gradual drop in the capacity to only about  $\frac{3}{4}$  of the initial value after 480 hours. A comparison between the wear rates of the two piston ring designs is only possible to a restricted extent, due to the unknown influence of the cover ring made of a high-temperature polymer. In the case of the twin rings, the highest wear of 1.15 mm was also established for the last sealing element (Table 2), although the related cover ring only exhibited an average wear of 0.49 mm. Already described earlier on, this unequal wear of the sealing ring and cover ring gives rise during operation to a gap which contributes significantly to the drop in the flow rate (Fig. 12).

If gap formation is prevented through form-fit coupling between the sealing ring and cover ring (Fig. 12, 13), the capacity can be maintained at a value of 164 scm/h - corresponding to the flow rate of new twin rings - for the entire duration of the test (Fig. 11). The large differences in the wear rates of the coupled twin rings are typical of gastight sealing elements which, in their new state, seal the entire pressure difference with just one or two sealing elements<sup>3, 4</sup>. The concentration of the dynamic and static pressure components at the two ends of the sealing system results here in a maximum value of as much as 1.76 mm at the last sealing element, a stable, high capacity being ensured by the outstanding wear compensation properties. A distribution of the pressure difference among several sealing elements, fundamentally beneficial to the life of a sealing system and exhibited by piston rings with a scarf joint, does not prove to be of any practical use for single-acting compression of hydrogen, in view of the disastrous consequences for the capacity.

Design	Ring no. 1	Ring no. 2	Ring no. 3	Ring no. 4
piston rings with a scarf joint [mm]	0.76	0.79	0.82	1.12
conventional twin rings [mm]	0.69	0.51	0.61	1.15
form-fit coupled twin rings [mm]	0.73	0.32	0.30	1.76

Table 2: Average wear of individual piston rings after 480 hours of operation ( $p_s = 0.24$  MPa,  $p_d = 6.0$  MPa,  $n = 725$  min<sup>-1</sup>, piston ring no. 1 being located right next to the compression chamber in each case)

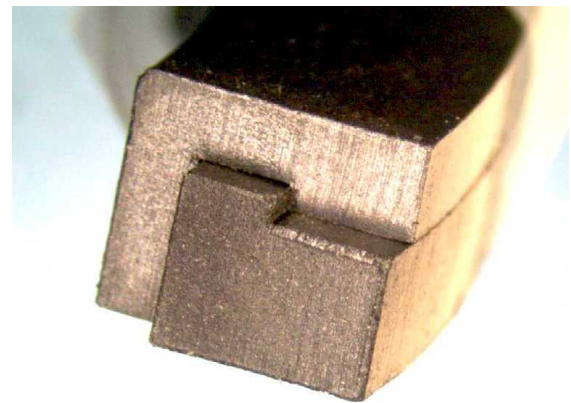


Fig. 13: Form-fit coupled twin piston ring (patent pending)

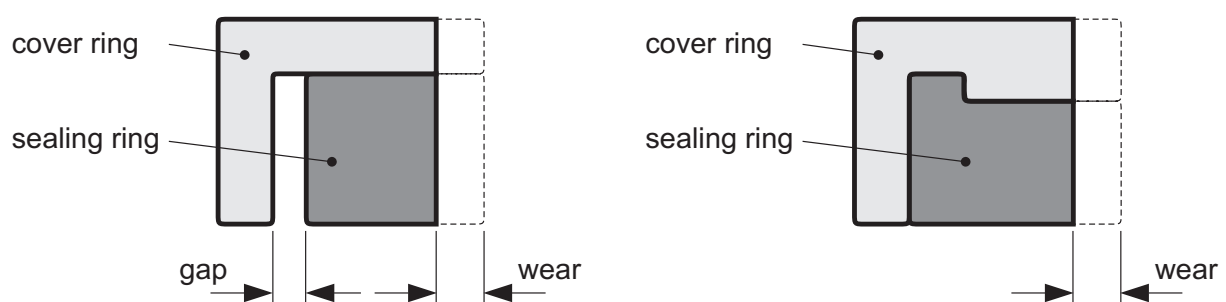


Fig. 12: In contrast to the form-fit coupled design (right), unequal wear of the sealing ring and cover ring making up a conventional twin ring results in the formation of a gap (left), thus impairing the sealing efficiency



## 7 Summary

Tests involving a dry-running compression of hydrogen using piston rings of various designs have shown that thorough joint sealing proves useful in maintaining a high volumetric efficiency for long operating periods, even in the case of double-acting pistons subjected to high loads. Although hardly any differences are evident in the new state, wear of designs without joint sealing leads to a drop in the capacity, accompanied by a rise in temperature, making it necessary to replace piston rings exhibiting a relatively low degree of radial wear, while designs with joint sealing allow a much longer utilization of the available ring thickness. The twin ring proves advantageous here, in that its sealing element is designed to wear down completely in theory without permitting a direct flow through the joint.

As observed on piston-rod sealing systems, the static pressure difference in the case of single-acting pistons constitutes the load parameter which mainly influences the leakage rate; this pressure difference needs to be sealed carefully to ensure a high volumetric efficiency despite progressive wear. Notable deviations become evident here between the various designs already in their new state. The two-piece design, in particular, exhibits very unfavourable characteristics comprising a low, extremely fluctuating flow rate, despite the fact that its total joint clearance is comparable with that of the one-piece design.

Especially in the case of single-acting pistons, wear compensation is extremely important for minimizing the flow area of the joint with progressive wear. Here, the sealing efficiency of the conventional twin ring deteriorates gradually because the distribution of the pressure difference along the frictional sealing surface results in unequal wear of the sealing ring and cover ring, thus creating a gap between the two ring parts. Form-fit coupling between the sealing ring and cover ring makes it possible to maintain the capacity at the high level provided by gas-tight designs, thus optimizing utilization of the radial ring thickness. Advantages offered by piston-ring designs without joint sealing during compression of gases with a high molecular mass, such as resistance to creep and fracture, and a distribution of the pressure difference among several sealing elements, are cancelled in the case of hydrogen due to the sharp drop in the capacity to unacceptably low levels.

## Notation

$p_s$	suction pressure [MPa]
$p_d$	discharge pressure [MPa]
$p_z$	constant pressure after the last sealing element [MPa]
$p_{dyn}$	dynamic pressure difference: $p_{dyn} = p_d - p_s$ [MPa]
$p_{stat}$	static pressure difference: $p_{stat} = p_s - p_z$ [MPa]
$c_m$	average piston velocity [m/s]
$n$	speed [ $\text{min}^{-1}$ ]
PTFE	polytetrafluoroethylene

## References

- <sup>1</sup> Bartmann, L.:  
Beitrag zur Bestimmung der Leckverluste im Arbeitszylinder eines Kolbenkompressors Dissertation TH Karlsruhe, 1968
- <sup>2</sup> Beckmann, W.:  
Ermittlung von Einflußfaktoren auf das Betriebsverhalten trockenlaufender Kolbenringdichtungen Dissertation TU Dresden, 1985
- <sup>3</sup> Vetter, G.; Feistel, N.:  
Betriebsverhalten trocken laufender Kolbenstangen-Dichtsysteme von Kreuzkopfkompressoren Industriepumpen + Kompressoren 4, 2002
- <sup>4</sup> Feistel, N.:  
Beitrag zum Betriebsverhalten trocken laufender Dichtsysteme zur Abdichtung der Arbeitsräume von Kreuzkopfkompressoren Dissertation Universität Erlangen-Nürnberg, 2002
- <sup>5</sup> Doebelin, Ernest O.:  
Measurement systems: application and design – 4th ed.  
McGraw-Hill, New York, 1990
- <sup>6</sup> Woollatt, D.:  
Factors affecting reciprocating compressor performance  
Hydrocarbon Processing, June 1993, pp. 57 - 64
- <sup>7</sup> Liu, Y.; Yu, Y.:  
Prediction for the sealing characteristics of piston rings of a reciprocating compressor  
Proceedings of the 1986 International compressor engineering conference – at Purdue West Lafayette, Indiana, 1986, Volume III



# **Reliable high-pressure-CO<sub>2</sub>-compression by means of well-aimed compressor design**

**by:**

**Johannes Greven and**

**Klaus Hoff**

**Central Division of Technology**

**Neuman & Esser GmbH & Co. KG**

**Übach-Palenberg**

**Germany**

**Session 6**

## **Reliability and economics of compression systems – recent trends in the market of reciprocating compressors March 27<sup>th</sup> / 28<sup>th</sup>, 2003 Vienna**

### **Abstract:**

With the high-pressure-CO<sub>2</sub>-compression above abt. 70 bar, considerable damages in the high-pressure stages can come about if design rules are not taken into account. By means of a special example – a CO<sub>2</sub>-compressor restored by Neuman & Esser – the compressor's correct design is shown. First photos show damages that are caused when the design is wrong. Then the report contains rules that must absolutely be adhered to when doing the thermodynamic design of the compressor. Moreover the constructional details, in particular of the high-pressure stages, are explained. Material data are given for accomplishing possible corrosion problems.

## 1 Introduction

High-pressure carbon dioxide is used for the production of urea as fertilizer and as additive for forage. The production of urea is made in two partial reactions. For the first reaction ammonia and carbon dioxide with a pressure of abt. 200 bar are needed. This first partial reaction leads to the production of ammonia carbonate which, in the second partial reaction, becomes urea by separating water.

The basis of this report are findings which Neuman & Esser could accumulate when eliminating problems at a Demag driving mechanism of such a fertilizer production plant. The problems described in the following chapter came about after having modified an existing driving mechanism to this CO<sub>2</sub>-process. In this context please note that the problems showed only appeared so severely after a running time of one year. Similar problems could be found at compressors of the same process.

## 2 Starting situation

### 2.1 Process description

The compressor is a four-crank Demag – driving mechanism (27B4). The compressor compresses saturated CO<sub>2</sub>. The theoretic process data were determined with the design programme of Neuman & Esser and can be taken from the following table:

Stage	Suct. press. [bar]	Disch. press. [bar]	Suct. temp. [°C]	Disch. temp. [°C]
1	1.37	4.31	38.0	136.0
2	4.16	13.38	45.0	146.9
3	13.04	40.78	45.0	145.7
4	40.0	112.91	45.0	143.9
5	111.22	214.84	60.0	127.2

Table 1: Calculated process data

The process is made in a way that the first three stages are arranged on one crank of the driving mechanism and the gas is compressed by means of double-acting cylinders. The fourth and fifth stage

are arranged together on one crank, with the gas being compressed crank-side in the fourth stage and cover-side in the fifth stage. Further to the plant, each stage is equipped with one suction and one discharge pulsation vessel. Between the different stages there is always one gas cooler operated with cooling water and one liquid separator. The balance chamber between the cylinders of the fourth and fifth stage is connected with the suction pulsation vessel of the fourth stage by means of a pendulum line.

The original plant is shown in figure 1.

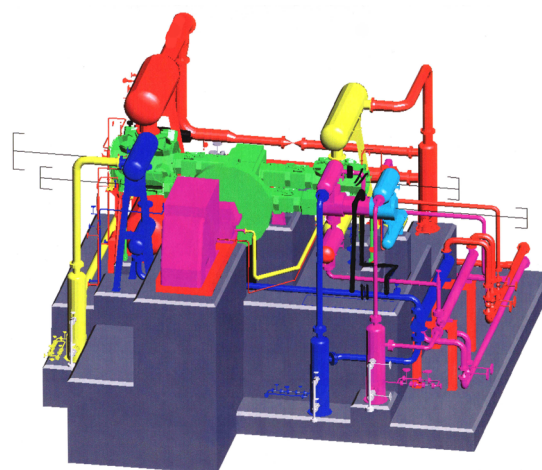


Fig. 1: Process gas system of the CO<sub>2</sub>-plant

### 2.2 Description of damage

The damages which the plant sustained were restricted to the cylinders of the fourth and fifth stage.

#### 2.2.1 Description of damage fourth stage

In the fourth stage there were strong erosion appearances in the suction-side flow channels. These were not only limited to the area between suction nozzle and suction valve, but could also be found at the outlet of the balance chamber.

**In figure 2 the cylinder of the fourth stage is shown.** Distributed at its circumference this cylinder has two suction and two discharge valves and is equipped with a connection for the pendulum line from the balance chamber. In order to not lead the lube oil supply through the cooling water jacket, the lubrication connections were located at the height of the balance channel. Through an axial groove in the cylinder liner (not shown) between liner and cylinder wall, the oil is led to the actual lubrication point. The cylinder is made of **forged steel**.

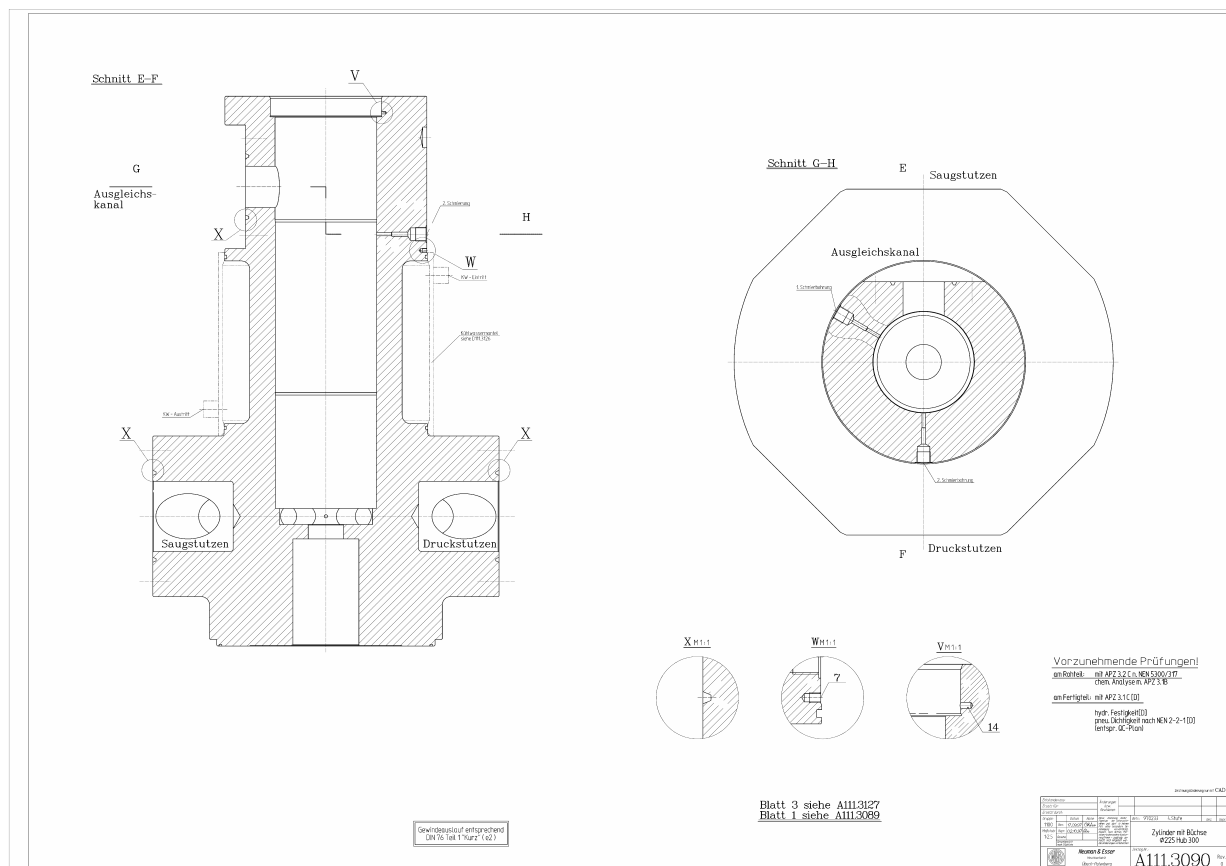


Fig. 2: Cylinder fourth stage

Figure 3 shows exemplarily the erosion appearances at the suction-side entry of the gas in the cylinder of the fourth stage behind the suction nozzle.



Fig. 3: Erosion damage behind the suction nozzle of the fourth stage

Similar appearances, even if not as serious as those mentioned above, could be found at the outlet of the cylinder gas passage to the valve pocket (see figure 4).

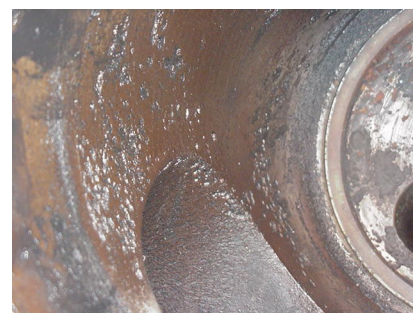


Fig. 4: Erosion damage at the outlet of the gas passage to valve pocket

At the suction valve seat, too, there are considerable erosions (figure 5).



Fig. 5: Erosion damage at suction valve seat

The damage at the outlet flange of the balance chamber to the pendulum line is shown in figure 6.

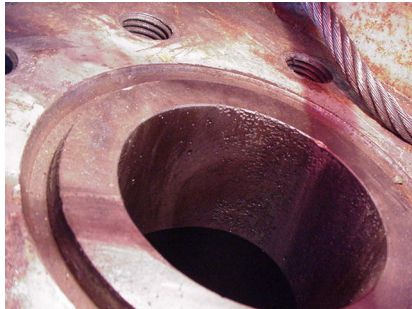


Fig. 6: Damage at the outlet flange of the balance chamber

The discharge-side flow channels of the fourth stage did not show any damage at all.

## 2.2.2 Description of damage fifth stage

In the fifth stage there were heavy damages at the piston in the area of the piston ring grooves, at the cylinder liner and at the cylinder in the area of the lube oil supply.

Figure 7 shows the cylinder construction of the fifth stage. Here, too, forged steel construction with a cooling water jacket was realized. The lube oil distribution to the actual lubrication point in the cylinder liner was ensured by means of an axial groove in the cylinder liner between liner and cylinder wall. The lube oil connection was located at the circumference of the connection flange for the fixation at the cylinder of the fourth stage

Figure 8 shows the cylinder's internal wall after having removed the liner. Erosion damages when the oil enters the channel between liner and the cylinder's internal wall (in fig. 8 on the right) and when the oil passes through the liner to the lubrication point (fig. 8 on the left side) can clearly be seen. At this point a crater has formed. This crater is the origin of an erosion channel that was not provided for by the design.

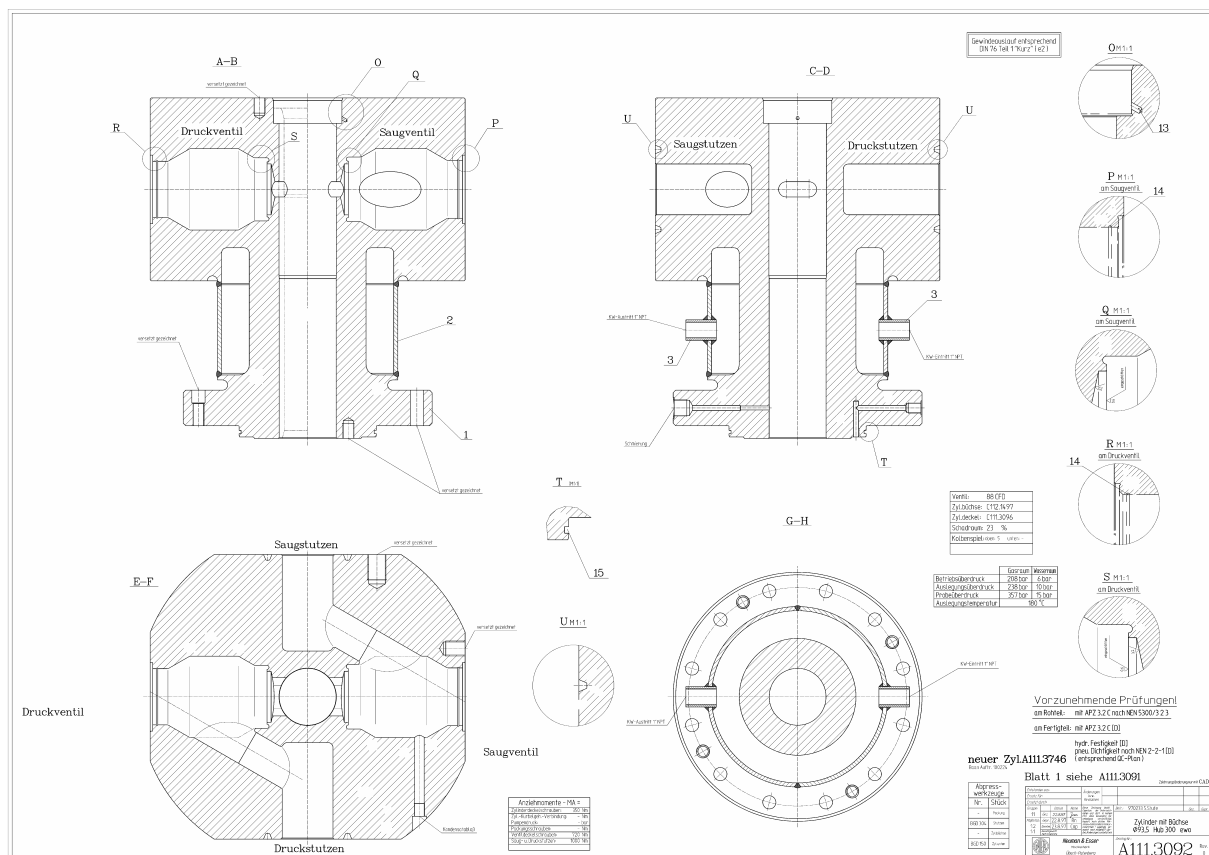


Fig. 7: Cylinder fifth stage



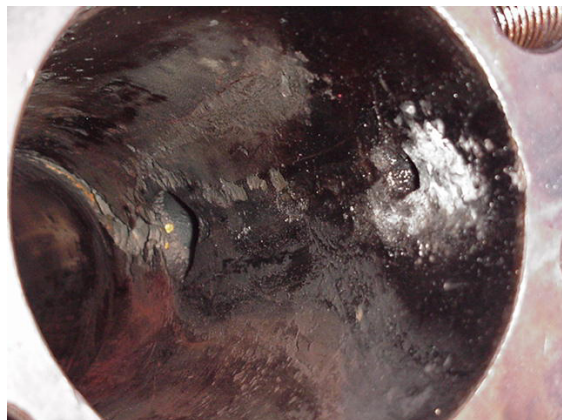


Fig. 8: Erosion damage at the internal wall of the cylinder fifth stage after having removed the liner

Figure 9 shows the damage at the piston of the fifth stage. The erosions appear in particular at the groove ground diameter.

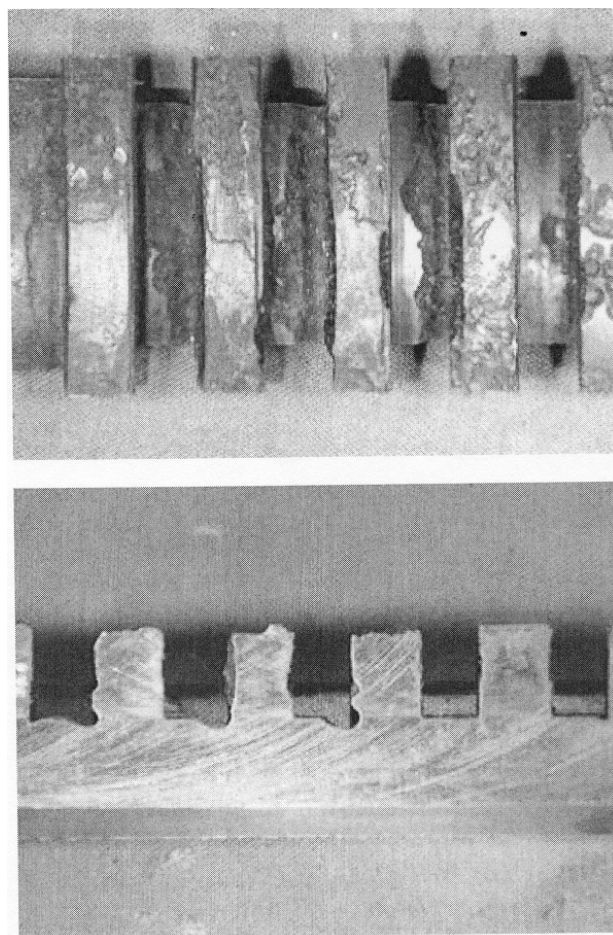


Fig. 9: Erosion damage at piston fifth stage

### 3 Reason for the damages

#### 3.1 Damages at the fifth stage

Since the damages suggest rather an erosion than a corrosion, it was likely to come to the conclusion to examine possible reasons for an erosion more in detail. Comparable erosion damages appear in particular with pumps due to cavitation. Cavitation is marked by the fact that if the vapour pressure of a liquid falls below a certain point, vapour bubbles are formed in the liquid that break down all of a sudden when the pressure rises again. Due to the great difference of the specific volumes locally high pressure peaks are generated when the vapour bubbles break down. If this process takes place in the proximity of a wall, such pressure peaks fatigue the surface and lead to material erosion.

Thus it is highly probable that the reason is to be looked for in the parallel appearance of liquid and gaseous phase of the carbon dioxide. The compression of carbon dioxide is shown in the pressure-enthalpy-diagramme (**black line in figure 10**).

From the diagramme it can be taken that the total compression process takes place beyond the saturation line. As it seems a phase transformation of the carbon dioxide does not take place, since the process is not led into the wet steam area.

However, a pressure release into the wet steam area is anyway possible when taking the leakages into consideration. It can be supposed that the pressure release of the gas across the piston ring area of the fifth stage is approximately isenthalpic - when assuming a low flow velocity of the leakage flow - since the energy exchange with the cylinder wall is small. If there is a pressure release from the suction stage of the fifth stage to the suction pressure level of the fourth stage (the balance chamber is connected with the suction pulsation vessel of the fourth stage), so the state of the leakage is to be found at the end of the pressure release into the wet steam area of the carbon dioxide (see figure 10, vertical line of suction state of the fifth stage). The assumption that the pressure release of the leakage gas current into the wet steam area is responsible for the damages, complies with the erosion appearances at the piston ring grooves. When re-transforming the liquid CO<sub>2</sub> into gaseous CO<sub>2</sub>, pressure peaks come about - similar to those with cavitation - that result in a fatigue of the material. The re-transformation takes place since with rising compression of the fifth stage the isenthalpic

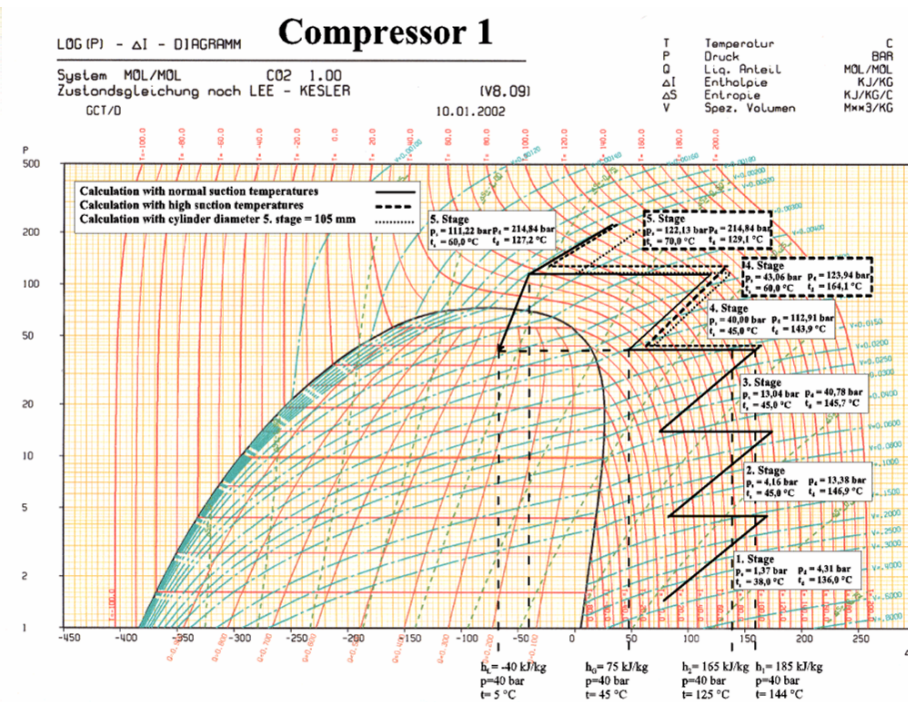


Fig. 10: Presenting the process in the pressure-enthalpy-diagramme of CO<sub>2</sub>

pressure release takes place into the direction of the saturated CO<sub>2</sub>-steam. From a certain compression onwards, the situation is even such that the gas releases entirely into the area of the overheated CO<sub>2</sub>-steam. During that time the explosion-like transformation of the liquid carbon dioxide that was captured in the grooves, takes place. The same process generates the fatigue appearances of the cylinder material in the lubrication groove at the liner's outside surface. Here, too, the captured liquid CO<sub>2</sub> in the lubrication oil is suddenly transformed into the gaseous state when the compression in the fifth stage rises.

The observation that the damages only appear heavily after a longer running period, can also be explained by means of the pressure-enthalpy-diagramme. With new piston rings the leakage flow is still very small. That's the reason why on the one hand only a small volume of CO<sub>2</sub> can transform into the liquid state and can thus cause damages. On the other hand the small leakage flow is stronger heated by the wall resulting in a shifting of the state towards larger enthalpy values and thus towards the saturation line (more on the right side in the p-h-diagramme). With increasing wear the leakages rise, too, and thus the damage mechanisms described above become stronger.

### 3.2 Damages at the fourth stage

It still has to be clarified why the suction side of the fourth stage, too, was damaged by strong erosion. Since the leakage gets into the balance chamber across the ring area of the fifth stage, liquid CO<sub>2</sub> can accumulate there. Via the pendulum line and the suction pulsation vessel the balance chamber is connected with the suction-side cylinder gas passages of the

fourth stage. As soon as suction valves of the fourth stage open, an unimportant compression of the carbon dioxide in the balance chamber takes place. Via the pendulum line this, partly liquid, CO<sub>2</sub> is transported directly into the suction area of the cylinder of the fourth stage. Since there it mixes up with the much warmer gas of the volume stream, here the described sudden transformation of the liquid CO<sub>2</sub> takes place, too. This explains the strong damages at the suction-side cylinder chambers. The transformation partly takes already place in the balance chamber and in the pendulum line, so that these damages can also be explained.

## 4 Measures for avoiding the problems

### 4.1 Thermodynamic process management

As described in the preceding paragraph, the damages are caused by the liquid CO<sub>2</sub> arising during the pressure release across the ring area of the 5th stage. Thus measures are to be taken that avoid a pressure release into the wet steam area in unfavourable cases, too.

The easiest method is to increase the stage suction temperatures. This measure was first realized at the existing compressor by adjusting the cooling water volume. Since an increase of the stage suction temperatures goes along with an increase of the stage pressures, this measure could not be put into



action until reaching the required temperature. With the existing plant the safety valve set pressure of the discharge-side installation parts of the 4<sup>th</sup> stage was reached before an isenthalpic pressure release into the wet steam area could be avoided (see dashed line in figure 10).

This is aggravated by the fact that the isotherms in the p-h-diagramme above the critical point (73.77 bar, 30.95 °C) run rather horizontally, so that part of the possible shifting of the stage suction state of the 5th stage into the favourable, right side of the diagramme is absorbed again. Nevertheless, a clear improvement of the problems could be stated after having implemented these measures as first step.

Since this measure did not suffice in accordance with the p-h-diagramme, an enlargement of the cylinder diameter of the 5th stage was introduced as further improvement. This did not mean any additional expenditure since due to the erosion the cylinder of the 5th stage was damaged in a way that it had to be replaced in any case.

However, due to the now changed gas forces it became necessary to first check the driving mechanism with regard to its limiting values with the Neuman & Esser recalculation programme. It showed that there was no inadmissible load of the driving mechanism parts.

After having modified the cylinder of the 5th stage and having risen the temperature of the last two stages accordingly, the dotted compression in the p-h-diagramme, shown in figure 10, is obtained. It can be seen that with isenthalpic pressure release from the suction stage of the 5th stage to the suction pressure level of the 4th stage, the wet steam area is not reached.

In order to have in any case a sufficient safety distance to the wet steam area, the minimum stage suction temperatures acc. to **figure 11** in dependence on the stage suction pressure are to be chosen. The temperatures were determined in a way that even in case of pressure drop of a leakage flow with sound velocity no liquid CO<sub>2</sub> can occur.

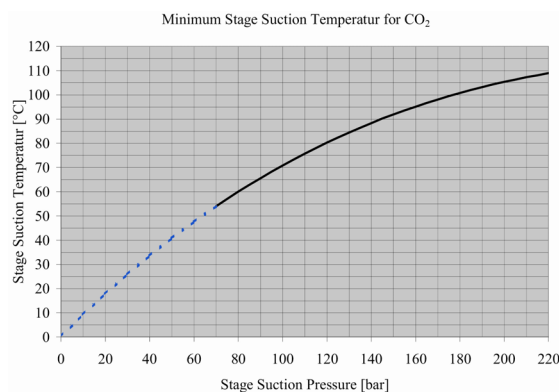


Fig. 11: Minimum stage suction temperature as function of the stage suction pressure

## 4.2 Constructional changes

In addition to the measures described in paragraph 4.1, a constructional change at the balance chamber was carried out. As can be seen in figure 1, the pendulum line between suction pulsation vessel and balance chamber was removed. The connection at the suction pulsation vessel was blind-flanged.

The balance chamber itself was equipped with a further connection at the bottom side so that it became possible to pass through this chamber. For this process hot gas of the discharge line of the 3<sup>rd</sup> stage is taken and, after having passed through the balance chamber, it is led back to this line. The adjustment of this bypass flow is ensured by means of an orifice located between the two connections into the main line. The balance chamber is passed through vertically from the top to the bottom.

On the one hand this measure makes sure that no accumulation of lube oil can get into the balance chambers. On the other hand the well-aimed feeding of hot gas ensures a heating-up of the 4th and 5th stage. With the pressure release of the leakage gas flow across the piston ring area of the 5th stage this leads to a heat input with the consequence that this pressure release is connected with an enthalpy growth. The gas' final state in the balance chamber is thus even further away from the saturation line in the p-h-diagramme.

Since a cooling of the balance chamber of the cylinder of the 5th stage would be counterproductive, it was refrained from entirely by removing the cooling water jackets. Due to the now very high temperatures in the area of the 4th and 5th stage (abt. 160 °C) it was necessary to equip the pistons that were originally equipped with PTFE-rings, now with PEEK-rings in order to avoid an increased wear by material flow. However, this

measure will result in an increased wear of the cylinder liners.

By removing the cooling water jackets it was possible to refrain from the costly and damaging lube oil supply via the connection flange of the cylinder of the 5th stage and the axial groove on the outside surface of the liner. The long lubrication oil channel between the lubrication point and the check valve in combination with the unfavourable process management, was responsible for the considerable erosions in this area.

Due to the new cylinder construction of the 5th stage (see **figure 12**) the lubrication oil is now fed directly in the area of the lubrication point. The length of the lubrication oil channel between lubrication point in the cylinder and check valve is thus minimized.

## 5 Corrosion precaution measures

### 5.1 General

As far as corrosion is concerned, pure, dry CO<sub>2</sub> is absolutely safe for all materials used for the manufacture of compressors. In particular in the low pressure stages and there mainly in the cold installation parts, CO<sub>2</sub> oversaturated with water can lead to corrosions. This corrosion is due to the fact that carbonic acid is formed (H<sub>2</sub>CO<sub>3</sub>) when CO<sub>2</sub> dissolves in water. However, the rate of the pure carbonic acid is very small. Abt. 0.1 % carbonic acid (H<sub>2</sub>CO<sub>3</sub>) is formed. 99.9 % is still there as dissolved CO<sub>2</sub>. So the solution of CO<sub>2</sub> and water forms a medium-strong acid. Thus the saturated solution can, depending on pressure and temperature, decrease with rising pressures to a pH-

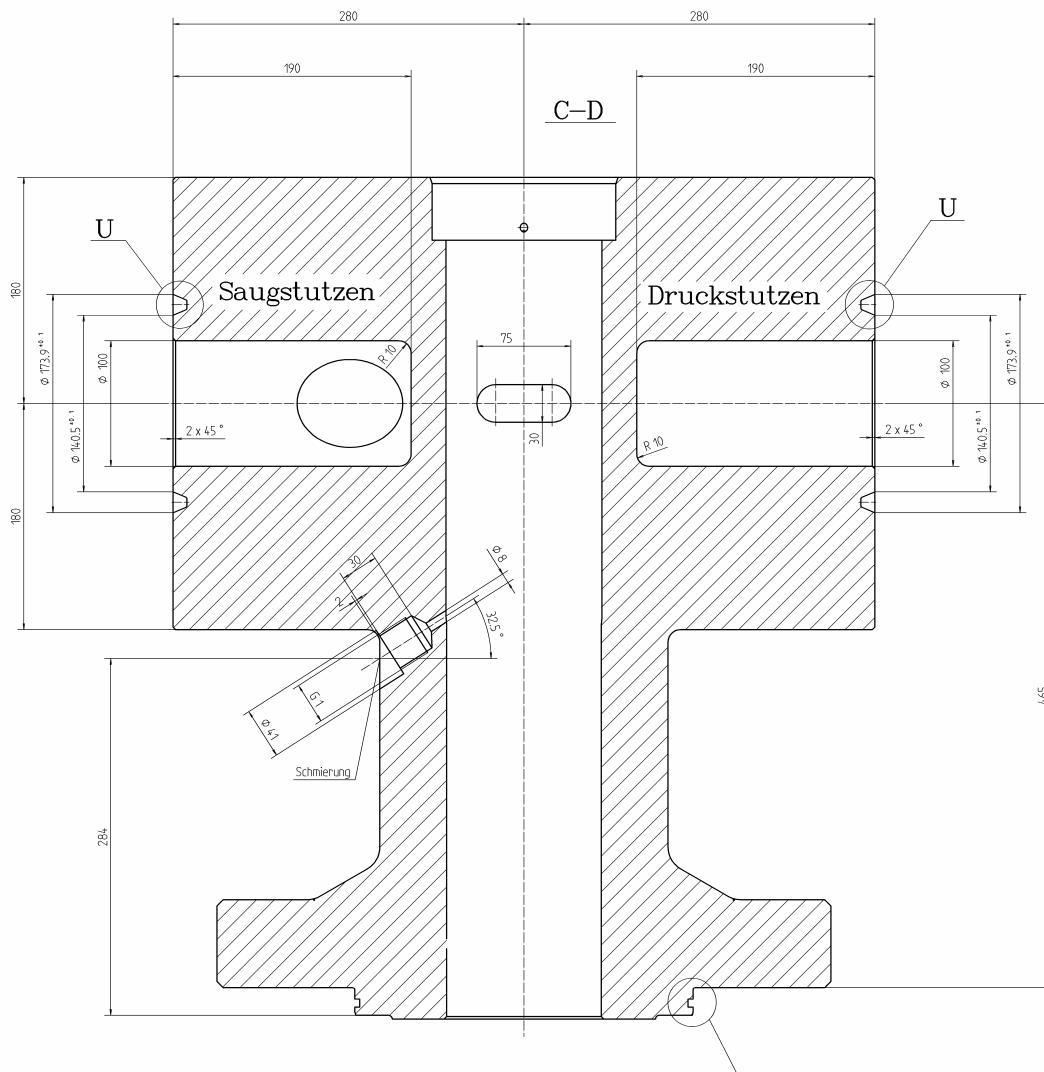


Fig. 12: New cylinder construction of the 5th stage

value of 3.3. Consequently the compression of CO<sub>2</sub> can become problematic at all parts of the installation where, due to the process, water precipitates from the gas. The free water then forms a saturated solution containing carbonic acid.

When selecting the material, a differentiation is to be made between humid and dry CO<sub>2</sub>. Another differentiation is to be made between lubricated and unlubricated compression.

## 5.2 Dry CO<sub>2</sub>

Up to 500° C all types of steel and cast iron are very well resistant against dry CO<sub>2</sub>. So, with the lubricated as well as with the unlubricated compression, no CO<sub>2</sub>-specific details must be taken into account when selecting the material.

## 5.3 Humid CO<sub>2</sub>

In presence of water carbon dioxide attacks unalloyed iron under hydrogen development, as far as the pH-value lies below 4. With humid CO<sub>2</sub>, the pH-value falls below this critical limit.

### 5.3.1 Lubricated design

Experience has shown that despite the known attack, no special corrosion appearances occur at unalloyed steels and types of cast iron. The lubrication oil contained in the gas ensures sufficient corrosion protection. Consequently you are free when selecting the compressor and plant materials.

Deviating from this, you have to choose the same materials as for unlubricated construction if there is hydrogen sulfide.

### 5.3.2 Unlubricated construction

With this type of CO<sub>2</sub>-compression certain corrosion precaution measures are necessary. With a pH-value below 4, the corrosion attack of unalloyed iron material takes place. Because of the presence of atmospheric oxygen, an attack takes place with pH-values above 4 due to depolarization (oxydation of the hydrogen formed). The corrosion speed then rises with increasing rate of oxygen. The aggressiveness of humid CO<sub>2</sub> is considerably increased in presence of hydrogen sulfide. So the combination water/carbon dioxide/ hydrogen sulfide is much more aggressive than any mixture of

2 of these components. Grey iron is heavily attacked by humid CO<sub>2</sub> with the iron being separated and the graphite lamella still being held together by corrosion products so that the workpiece appears to be unattacked. This corrosion being typical for grey iron is designated as graphitic corrosion.

However, Neuman & Esser does not avail of any experience of their own according to which a component made of grey iron had failed with this application due to graphitic corrosion. Consequently it is likely to suppose that the corrosion attack only gets on slowly and thus does not lead to failure during a component's lifetime because of the given cast allowances.

At the compressor itself the same materials are to be chosen for slightly corrosive gases. For example, the material X20Cr13 is recommended for valves. Pistons should be made of aluminium alloys and stainless steel resp. in accordance with EN 10088-1. At plant-side all pipes and vessels should be made of stainless steels (EN 10088-1, DIN EN ISO 1127). In order to avoid caustic corrosion (embrittlement) the components are to be annealed after welding.

## 6 Summary

In the paper at hand it is shown by means of a special example which design rules are to be taken into account for the high-pressure compression of carbon dioxide. First the damages in the area of the high-pressure stages were laid down in detail.

In the following it is shown that when designing the plant the key lies in choosing the correct temperatures for the process. It is decisive that in any case the formation of liquid CO<sub>2</sub> is avoided. In this context special attention has to be paid to the pressure release of leakage flows. Even if the real process lies beyond the saturation line, the pressure release of the leakage flow into the wet steam area can take place and can cause problems.

As support for the correct thermodynamic design, useful constructional information is given.

Finally the selection of material is briefly dealt with.

## Literature

1. Dechema-table of materials



# **DRESSER-RAND**

## **High speed separable compressors – an alternative for slow speed integral-engine compressors for natural gas transmission and gas storage**

by:

**William C. Wirz, Product Manager  
Separable Gas Compressors  
Dresser-Rand Company  
Painted Post, New York  
U.S.A.**

**Reliability and economics of compression systems –  
recent trends in the market of  
reciprocating compressors  
March 27<sup>th</sup> / 28<sup>th</sup>, 2003 Vienna**

### **Abstract:**

Natural Gas Transmission and Gas Storage applications have been typically addressed by the installation and use of slow speed Integral – Engine Compressors. These large machines are located throughout the world and are the backbone of the natural gas industry. They are efficient in terms of fuel consumption, through turndown and capacity control techniques. However, they have a very high installation cost, typically requiring large foundations. Since this machine is also an “engine”, these machines are regulated environmentally for exhaust emissions output. Integral-Engine Manufacturers are no longer producing new machines of this type, so an alternative to this type of machine needed to be developed.

This paper will review the design work that has been accomplished by Dresser-Rand Co. to develop and successfully apply modern High Speed Compressors with absorbed power up to 8MW as an alternative to the slow speed Integral-Engine Compressor. This paper will address development of the compressor, reliability, installation cost, and capacity control techniques.

## 1 Introduction

For well over 70 years, natural gas transmission and storage has been accomplished with slow rotative speed reciprocating compressor equipment. Typically these types of compressors were known as “Integral Engine - Compressors” which had the prime mover integral with the gas compressor.



Picture 1. –Typical “Integral Engine – Compressor”

Many of the thousands of these compressors are still in operation with replacement parts available. In addition, upgrades to these compressors are available to clients in the areas of emission reduction and compressor cylinder reliability improvement. However, Integral Engine – Compressor equipment is no longer being manufactured with the last of these machines being built “as new” in 1997 and 1998. There are three major factors that contributed to the demise of this type of product: High cost to clients, higher installation costs, replacement technologies.

A replacement to this product had to be found. Key to developing a replacement reciprocating compressor technology was to nearly duplicate the load capability, power, capacity or flow control capability, and compression efficiency found typical to these units. Also developing a product with the knowledge and experience gained from prior “Integral Engine – Compressor”, Refinery Compressor, High Speed Compressor, Regulation and Compressor Valve Technology would enhance a total solution to a replacement compressor for Gas Transmission service. In other words, a compressor designed and integrated with the best available technology provides the client with a modern, reliable compressor.

In the following chapters of this paper, the reader will understand how all of the experience, tools for design, testing, manufacturing considerations and a concern for reliability came together in a total

solution for a replacement, higher rotative speed, compressor technology for Natural Gas Transmission and Gas Storage applications.

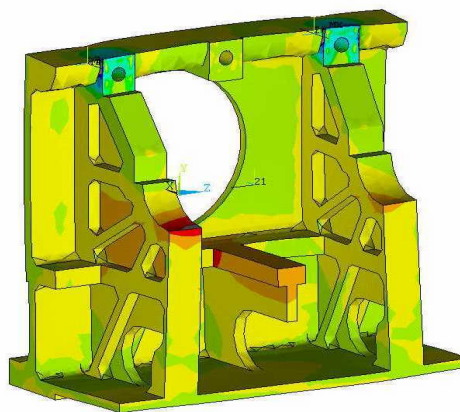
## 2 Compressor Design

### 2.1 The Compressor Frame and Running Gear

The compressor that was designed to fulfil the need for Gas Transmission, Storage, and Gasfield application where a larger (high power – MW) compressor is needed is the **BOS** compressor. **BOS** stands for **B**ig **O**ilfield **S**eparable. By definition, “Separable” means that the compressor is separate from the prime mover. With compressor rotative speeds nominally at 900 and 1000 rpm, this compressor is suitable for direct connection to modern electric motors and natural gas or diesel engines.

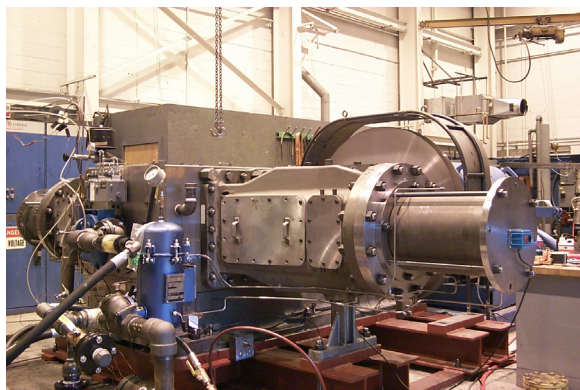
But what type of design tools, analysis and testing are necessary to develop a high rotative speed, high load and power capable compressor? Experience and proven design techniques coupled with Finite Element Analysis and testing are needed to verify the design before the first compressor is placed in service.

Having reliable compression equipment is crucial to the success of gas plants. Modern tools for analysis enables the designer to understand areas of potential weakness in the design and correct them in the design stage rather than in the field.



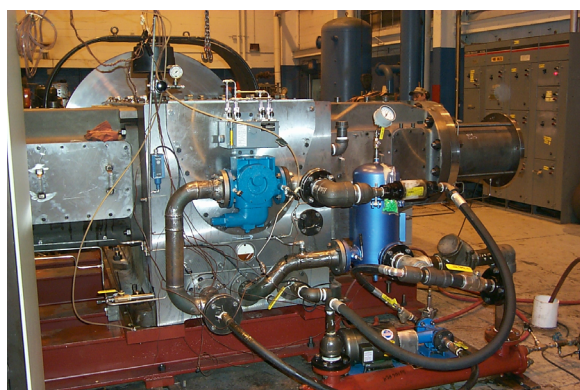
Picture 2. Finite Element Analysis of the BOS Compressor Frame modelled in “Tension”

In addition to Finite Element Analysis Modelling, the results of the design must be verified in laboratory. Full scale testing at full load capacity is the only way to ensure the compressor will operate as the designer intended.



*Picture 3. BOS Compressor Frame and Running Gear on Full Load Test in the D-R Laboratory*

As important as the running gear component design (crankshaft, frame, etc.), are the ancillary systems supporting reliable compressor operation. The lubrication oil system is critical to successful operation of the running gear. This too must be tested to understand the heat loads for oil cooler sizing as well as determining whether the oil pump size is adequate for proper lubrication of the compressor running gear.



*Picture 4. BOS Compressor Frame – Lubrication System Test in the D-R Laboratory*

Disassembly of the compressor after testing is required to determine the success of the test by verifying if there is any distress to the running gear components. If distress is encountered the parts must be re-designed and tested again. It is also recommended to test a running gear in an overload condition to account for possible compressor upsets and potential damage that could occur.

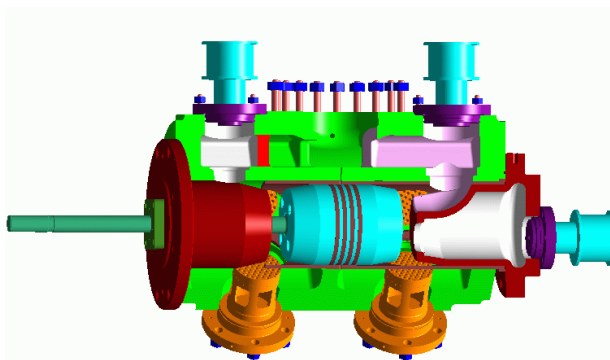
Upon inspection of the BOS compressor after laboratory testing, there was no distress found on any of the compressor running gear components despite a mechanical run test at 15% above the rated load of the compressor running gear.

## 2.2 Compressor Cylinder Design

Two compressor cylinder designs will be discussed. The first will be a cylinder suitably designed for Gas Transmission and Storage application. The second is a compressor cylinder design primarily designed for Gas Gathering application.

### 2.2.1 Gas Transmission and Storage Cylinders

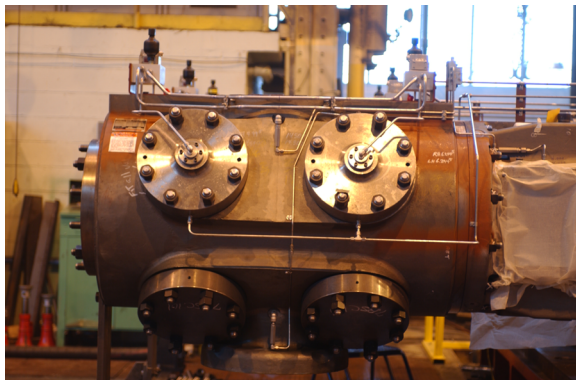
Gas Transmission cylinders are unique in their design. These cylinders are capable of large flows at very low ratios of compression (typically 1.2 – 1.8 ratios). At these low ratios the designer needs to be concerned with unobstructed gas flow passages. Consequently, these flow passages tend to be large. Likewise, compressor valving is selected to maximize the flow with very low compressor valve power losses. These cylinders are usually designed without water jackets for cylinder bore cooling. This is due to the temperature rise of the gas at low ratios not being a factor to be concerned with for overheating. Non-cooled cylinder bores are also a benefit to manufacturing. Single wall castings are easier to manufacture and are less likely to result in casting problems and scrap. The benefit is minimized cylinder spoilage during the manufacturing process. As important as other design considerations is the capability of the cylinder to accommodate capacity control systems. Many of these systems are “built in” to the cylinder design. Other capacity control systems can be added external to the compressor such as “clearance pockets” or delayed suction valve closing mechanisms.



*Picture 5. Cross-section of the BOS Pipeline and Storage Cylinder*



Referring to picture 5., this cylinder is designed with ample gas passages to minimize gas passage loss. Since power loss is critical to low ratio compression where large flow rates are encountered, the designer bevelled both ends of the piston to facilitate compressed gas exiting the cylinder thus minimizing power consumption. The cylinder is also designed with “built in” capacity control pockets found on both the outer and frame ends of the cylinder. The size of these pockets can be customized to trim the flow control steps to the client’s particular process. Also the cylinder can be easily modified to bypass gas back to suction, completely unloading the outer end for a 50% step in gas flow control. The cylinder as shown is equipped with a clearance pocket, which when activated via a clearance valve, adds clearance to the outer end of the compressor cylinder, changing the volumetric efficiency allowing for a flow capacity step.



Picture 6. Actual BOS Compressor Pipeline Cylinder as shown in picture 5.

## 2.2.2 Gas Gathering Compressor Cylinder Design

Gas Gathering requires high ratios of compression for each stage. Typical ratios are between 2.2 and 4.1 ratios. Unlike gas transmission cylinders, minimal cylinder clearance is an important factor in cylinder design for optimum performance and efficiency. The designer must also be concerned with the effects of gas pre-heating, gas velocities in the gas passages and optimum valve sizing to allow for minimal valve power losses. Efficiency in cylinder design also has to be considered from the standpoint of manufacturing. Cylinders that are easy to cast and machine will translate into improved first pass yield, lower manufacturing costs, which ultimately results in the client receiving higher overall value in the product. The design of these cylinders for the BOS also posed an added

complexity in that the cylinders had to accommodate two different compressor strokes.

Designing cylinders for high rotative speeds generally results in shorter stroke cylinders. For this cylinder design both 7.25” and 8.5” compressor strokes had to be considered. Higher rotative speeds has the designer concerned about total reciprocating weight. The governing equations for inertia load for a slider-crank mechanism are shown below:

$$F = m r \omega^2 \cos \omega \tau + m (r/l) r \omega^2 \cos 2\omega \tau$$

Becomes a maximum when  $\tau = 0$

$$F = m r \omega^2 (1 + r/l)$$

Where:

$\tau$  = time (secs.)

$F$  = Inertia Load (lbs)

$m$  = mass (Total reciprocating mass)

$r$  = crankshaft radius (inches)

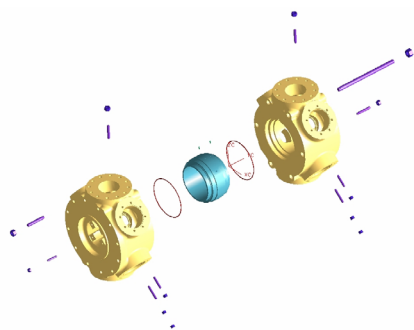
$\omega$  = angular velocity (rad/sec)

$l$  = connecting rod length (inches)

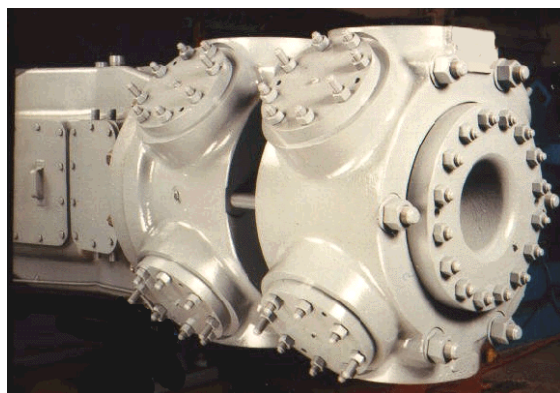
This equation points out the inertia load considerations. As the rotative speed increases, the inertia load goes up by the square of the speed. Reciprocating mass (primarily the mass of the crosshead, piston and rod weight) and crank radius increase the inertia load linearly. Therefore for short stroke, high speed compressors units, it is desirable to have piston and rod weights which are light as possible so as not to inertia overload the unit when gas is not being compressed. But how can the piston and rod assemblies be of reduced weight when typically accommodating various strokes with the same cylinder involve lengthening the piston and therefore increasing the reciprocating weight?

Dresser-Rand has solved the problems of gas pre-heat losses, heavier than necessary reciprocating weights, and complex casting and machining processes with the **DART** cylinder design (**D**resser-Rand **A**dvanced **R**eciprocating **T**echnology). As shown in picture 7., this cylinder design utilizes a common single wall casting for both the frame end and outer end valve chests. Gas pre-heat losses are minimized with external gas manifolding. A center tube which makes up the cylinder bore can be lengthened or shortened to accommodate various strokes. This simple iron “tube” eliminates the need for expensive cylinder liners. The tube is inexpensive and easy to manufacture facilitating ease of replacement (should this be necessary) and minimal downtime. The DART design facilitates commonality in pistons, wear parts, and castings regardless of a change in stroke. The design also allows for absolute minimum piston and rod weight

since the piston need only be designed to resist the gas loads not changes in compressor stroke. The cylinder also maximizes the use of current compressor valve technologies for compressor valves and cylinder regulation.



Picture 7. Isometric View of the D-R “DART” Cylinder Design



Picture 8. “DART” cylinder fully assembled

### 2.2.3 Compressor Cylinder Testing

Cylinder testing is essential to understand the cylinder performance (flow, power) as a result of the design. Mechanical integrity of the design also needs to be understood to avoid reliability issues of the compression equipment in the field. As part of the rigor of D-R design development process is to include a “Demonstration” phase in which all newly developed product is tested under operating conditions controlled by D-R. This means not only laboratory testing and measurement but also field-testing. As shown in picture 9., a D-R DART compressor cylinder is mounted on the “Closed Loop” Test Facility at the D-R Painted Post plant for performance testing under full load conditions and also to develop a complete performance map.



Picture 9. D-R DART Cylinder on the “Closed Loop” Test Facility

The results of the testing of both the Gas Transmission Cylinder and DART cylinder indicate that the cylinder designs have met expected performance. For some operating conditions, better than predicted performance has been observed. Mechanical integrity of wearing parts, bolted joint assemblies, and gaskets showed no indication of premature problems. The cylinders operated for many weeks, accumulating well over 20MM cycles of operation without incident.

## 3 Compressor Capacity Regulation

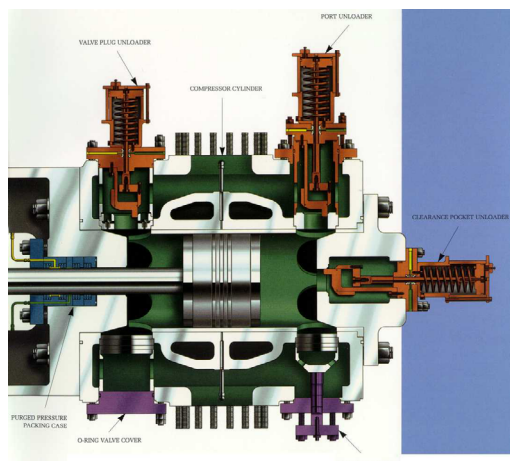
Compressor capacity control is key particularly to gas transmission and gas storage applications of compression equipment. It is less of a factor in routine gas gathering applications, but occasionally a load step is required involving a pneumatically operated clearance pocket or manually adjusted variable volume overhead. For the purposes of discussion in this chapter, automatic systems for capacity control will be discussed. These systems require a control system, but do not require the intervention of a compressor station operator due to the logic built into these types of control systems.

### 3.1 Compressor Capacity Control by Adding Clearance

For many years, capacity control has been accomplished by adding fixed clearance (volume pockets) to ends of compressor cylinders as well as valve port and plug unloaders. Opening and closing volume pockets and valve ports with pneumatically operated clearance valves allows the load steps to change incrementally and automatically. The effect of opening the volume pockets reduces the volumetric efficiency and flow of the gas through the compressor cylinder. These volume pockets port unloaders are as applicable today on high-

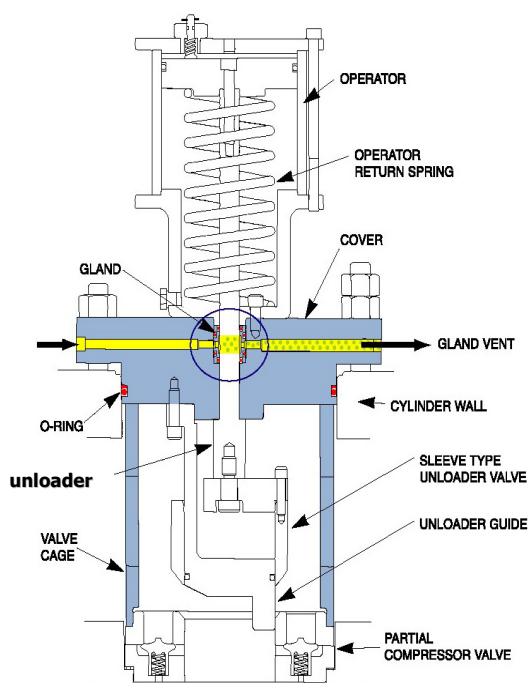


speed compressors. They are reliable systems and proven in design and application.



Picture 10. Compressor Cylinder Equipped an Outer End Volume Pocket and Pneumatic Clearance Valves

The success of these volume pockets depends on the repeated actuation of the pneumatic clearance valves and their ability to open, and upon closing, seal the gas from entering the volume pocket.



Picture 11. Cross-Section of a Pneumatic Clearance Valve

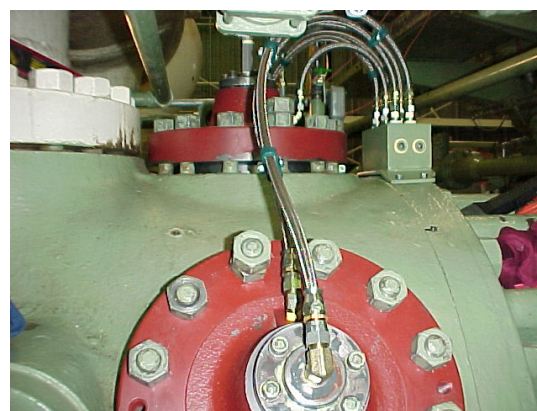
Picture 11 shows a typical pneumatic clearance valve used on D-R compressor cylinders. A gas pressure is applied to the top of the operator which forces the unloader sleeve downwards to seal. Sealing occurs when the unloader sleeve bevel

comes in contact with a sealing bevel ( Note: bevels are at different angles) effecting a line contact seal. This seal is extremely effective and leak free. When the pneumatic clearance valve is actuated via an applied gas pressure, compressor loading occurs. Conversely, when the gas pressure is removed cylinder unloading occurs.

This type of pneumatic clearance valve is used on clearance volume pockets as well as valve plug and port unloaders. These valves have been reliably applied to high-speed compression equipment for over 40 years.

### 3.2 Compressor Capacity Control by Delayed Suction Valve Closing or Infinite Step Control

Developed in the 1950s by Ingersoll – Rand for use on Integral Engine – Compressors for capacity control, this system utilized a mechanical means to distribute a hydraulic pressure to activate a compressor valve unloading mechanism which delayed the closing of the suction valve as gas was compressed. This bypasses a portion of the gas back to suction. The amount of gas bypassed is adjustable and hence flow capacity can be adjusted. Ingersoll-Rand named this Infinite Step Control. In 2001, D-R expanded on this technology and developed modern controls for this capacity control system improving reliability and capability and named it D-R ISC ( Infinite Step Control ). This updated system was field tested on an Integral Engine – Compressor and in D-R's laboratory on high-speed compressors for gas transmission service at speeds up to 900 rpm.



Picture 12. D-R ISC applied to an Integral Engine - Compressor

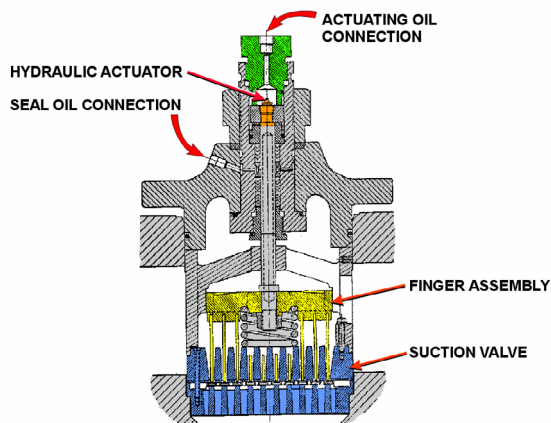
This field testing along with D-R laboratory testing allowed for the application of the D-R ISC to be placed on five (5) BOS high-speed gas transmission

compressors. All of the inlet valves on each cylinder are equipped with the D-R ISC system.



Picture 13. – BOS Compressor Cylinder with D-R ISC Mounted (Note: Only One Solenoid is Required per End for Compressor Valves)

As with any system of this type, the reliability is a function of the moving parts. D-R has utilized the compressor valve actuator (picture 14.) component of this system since the 1950s.



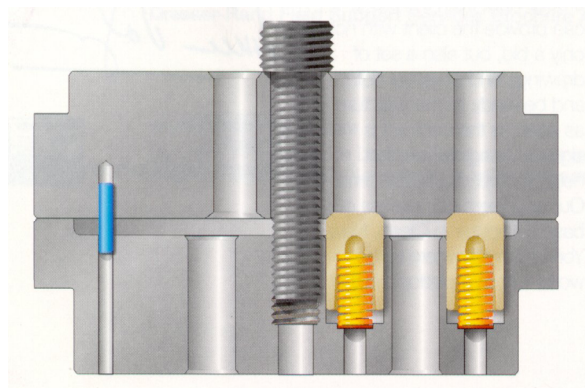
Picture 14. – Compressor Valve Actuator for D-R ISC

## 4 Compressor Valves

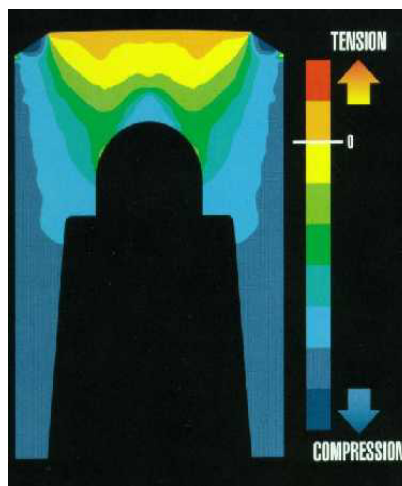
Reliable compressor valves are essential to successful operation of any compressor. Much effort is done by compressor and valve manufacturers to select the correct valve and springing using Dynamic Valve Aalysis (DVA).

Despite using the DVA tool there are occasional upsets or start up conditions that will damage compressor valves. An example of an upset would include dirt or water into the gas system.

A robust valve to tolerate some upset conditions and a valve that is easily serviced is what is required. D-R has utilized the MAGNUM compressor valve as the valve of choice for pipeline and gas storage cylinders. Why?



Picture 15. D-R MAGNUM Valve



Picture 16. Finite Element Analysis of a MAGNUM Element

The D-R MAGNUM compressor valve utilizes a common valve sealing element regardless of valve diameter. This means that a client need only have in inventory one sealing element and all valves can be maintained! This is far different from maintaining an inventory of plates for each diameter compressor valve used in a typical multi-stage compressor.

In terms of design characteristics, the element is made from D-R Hi-Temp material. The element geometry allows for the critical load carrying portions of the element to be largely in compression as shown in picture 16., when analyzed using Finite Element Analysis. The parts of the element that are in tension are only 1/25 the tensile limit of the element material.



The MAGNUM valve is field proven for high speed operation and use with capacity control systems.

## 5 A Completely Designed High Speed Compressor

All of the design work is completed for the frame and running gear including a full complement of compressor cylinders with field compressor valves and capacity control systems. What is the capability of the BOS compressor?

### Frame and Running Gear:

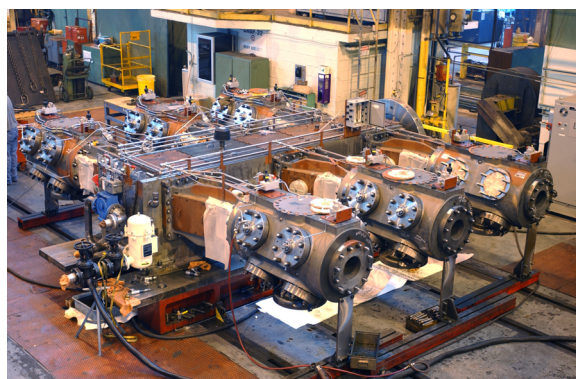
Configurations Available - 2/4/6 throws  
Maximum Rod Load - 400 kN MACCRL  
Maximum Gas Load - 400 kN MACGL  
Standard Stroke - 184 mm and 216 mm  
Rated Speed - 1000 rpm and 850 rpm respectively  
Nominal Power/throw at Rated Speed - 1.40 MW and 1.36 MW respectively  
Minimum Operating Speed - 500 rpm  
Piston Speed at Rated Speed - 6.1 m/sec.

### Gas Transmission Cylinders:

Bore..... : 13.00 - 17.00 inches  
Stroke..... : 7.25 - 8.5 inches  
MACCRL..... : 400 kN (90,000 lbs.)  
MACGL..... : 400 kN (90,000 lbs.)  
Piston Rod..... : 3.25 inches  
Valves..... : Magnum

### Gas Gathering Cylinders:

Bore..... : 6.00 - 32.00 inches  
Stroke..... : 7.25 - 8.5 inches  
MACCRL..... : 400 kN (90,000 lbs.)  
MACGL..... : 400 kN (90,000 lbs.)  
Piston Rod..... : 3.25 inches  
Valves..... : Magnum



Picture 17. – BOS Compressor on D-R Test Stand – D-R ISC Mounted - Ready for Shipment!

## 6 Compressor Maintenance

D-R has sold many high-speed compressors for Gas Transmission, Gas Storage and Gas Gathering applications. They have proven to be trouble free provided normal maintenance is done on the equipment. Clients like the fact for a given size compressor (power and load capability) to have compressor components that are smaller, lighter, and easier to handle. Routine maintenance or overhaul typically done on slower speed compressors consumes much time in dismantling, while on high speed compressors, because the components are smaller and lighter, dismantling, servicing and re-assembly is accomplished in a fraction of the time.

Detrimental to Reciprocating compressors is dirt / debris and liquids in the gas stream or dirt in the oil system.



Picture 18. Debris removed from Compressor Gas Piping

Dirt and liquids cause lubrication system break down resulting in rapid wear of cylinder bores and compressor piston grooves. Care must be taken to ensure cleanliness in the compressor gas system and lubrication systems to establish a predictable maintenance schedule versus unscheduled compressor shutdowns.

Compressor Manufacturers do an excellent job in describing the routine maintenance required for the compressors they furnish. If proper maintenance as described in the Operators Manual is followed, the reliability of the compressor units will be greatly improved.

## 7 The Economics

High Speed compressors are generally less expensive than their slower speed compressor

counterparts. The higher rotative speed allows for a higher horsepower for a given torque according to the formula:

$$\text{BHP} = \text{TN} / 63000$$

Where:

BHP = Compressor Power (Brake Horsepower)

T = Torque (inch-lbs.)

N = Rotative Speed (rpm)

From the formula above, a 6000 HP, 300 rpm compressor will have a higher torque than a 6000 HP, 1000 rpm compressor. The higher torque means a larger crankshaft diameter, larger bearings, etc., which translates in a higher cost of the equipment to the client.

Since the flow capacity of a compressor is a function of the compressor rotative speed, stroke and cylinder size, the physical size of slow speed cylinders are generally longer for a given flow. This also means a higher cost to the client.

Installation is another consideration. The high speed compressors are generally set on a “skid” and are sold as compression packages. Typically the prime mover, piping, controls are also part of the package design. Depending on the scope of supply this type of system is likely less expensive than the conventional “block mounted” compressors typical to Integral Engine – Compressor units.



*Picture 19. BOS Compressor Mounted on a Compressor Skid complete with Electric Motor*

## 8 Conclusions

This paper has presented information that supports that experienced designers, coupled with modern engineering design tools can design, build, laboratory test and field test a viable high speed

compressor as a replacement to slower speed Integral Engine – Compressor units for Gas Transmission and Gas Storage applications. These high speed compressors also tend to have a lower total installed cost and a quicker return on investment.

The attractiveness of the high speed compressor units is enhanced for Gas Transmission and Storage application when complemented with a full line of capacity control systems. This makes high speed compressors equal to Integral Engine – Compressors for capacity / flow control.

Separating the compressor unit from the prime mover provides the client with the opportunity to couple this compressor with the latest technologies in Electric Motors and Gas Engines.

Properly designed and tested high speed compressors are a viable alternative to slow speed compression equipment due to their operating efficiency, installation cost and ease of maintenance.

## 9 Acknowledgements

The author would like to acknowledge the Design / Development Team and Development Engineering Laboratory who put many hours of work into the design and testing of all of the compression equipment presented in this paper. The author would also like to thank our clients who gave us much input and suggestions to enable D-R to design a complete high speed compressor product to meet their needs.



## Innovation and Technology

---

M. Hastings / Brüel & Kjær; J. Schrijver / Thomassen

- **Improved monitoring strategy developed in close cooperation between the machine manufacturer, instrument supplier and end-user gives positive results**

L. van Loon / Alloy Carbide

- **Carbide coatings: use on reciprocating compressor piston rods and hyper compressor plungers**

B. Spiegl, D. Artner, P. Steinrück / HOERBIGER Ventilwerke GmbH

- **System for direct wear monitoring of rider rings in reciprocating compressors**





**Brüel & Kjær Vibro**

THOMASSEN  
COMPRESSION  
SYSTEMS



## **Improved monitoring strategy developed in close cooperation between the machine manufacturer, instrument supplier and end-user gives positive results**

by:

Mike Hastings, Brüel & Kjær Vibro, Denmark

Jos Schrijver, Thomassen Compressor Systems, The Netherlands

### **Reliability and economics of compression systems - recent trends in the market of reciprocating compressors**

**March 27<sup>th</sup> / 28<sup>th</sup>, 2003 Vienna**

#### **Abstract:**

Reciprocating compressors play a critical role in the petrochemical industry, but are some of the least monitored machines in the plant despite being some of the most maintenance demanding machines. An instrument supplier, Brüel & Kjær Vibro (BKV) and a machine manufacturer, Thomassen Compression Systems (TCS), teamed up to provide a more effective solution to overcome this problem. This cooperation resulted in re-evaluating existing measurement techniques, improving them where possible, and combining these together with a more effective service strategy in order to improve the reliability and accuracy of monitoring reciprocating compressors. The focus was on automatically monitored on-line measurement techniques that do not require a lot of diagnostic resources, such as the rod drop monitoring technique.

## Introduction

Reciprocating compressors are widely used in the petrochemical industry, and will continue to be used because of the many processes that require their high pressure and variable loading characteristics. These machines, however, are much more maintenance demanding than their centrifugal and axial compressor counterparts. This issue becomes even more important as petrochemical process technology improves and consequently the time between plant shutdowns is increased. This makes the reciprocating compressor increasingly the bottleneck when optimising plant maintenance and operation strategies.

## Many reciprocating compressor monitoring techniques available

Experience shows that the cylinder components such as the valves, piston rings, wear bands (wear bands), packing case, piston, piston rods, and crosshead pin, have been identified as the major cause of both planned and unplanned shutdowns. There are a number of performance, vibration, acoustic emission and other measurement techniques that can be used for both the on-line and off-line monitoring of these components. A few of the techniques are used for safety monitoring, some for automatic condition monitoring (also called predictive monitoring, which includes early fault detection, fault trending and performance monitoring), and others are just for diagnosis.

Some of the measurement techniques used specifically for the cylinder portion of the reciprocating compressor are listed below. These particular measurement techniques have proven to be accurate, repeatable and reliable for detecting and diagnosing reciprocating compressor faults when properly set up and used. Fig. 1 shows the typical sensor configuration for these measurements.

- **Rod drop** – A fixed proximity probe automatically measures the distance from the probe tip to the rod, which is proportional to the wear of the wear bands (also called rider bands, rider rings).
- **Impact vibrations** – An accelerometer can be used for safety monitoring of machine components that are loose (e.g. worn pins), damaged (valves, bearings, rings, rods, crossheads, crankshaft, etc.), unbalanced or for

detecting the presence of liquids in the gas stream.

- **Valve cap temperatures** – This is one of the most effective safety and condition monitoring methods for detecting incorrect valve condition or operation.
- **Stuffing box seal temperature** – Automatic condition monitoring for seal leaks.

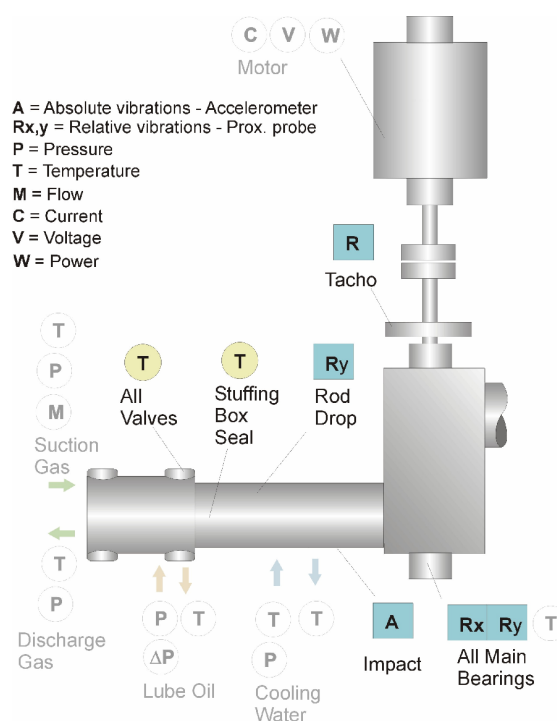


Fig 1 Typical measurement sensors for a reciprocating compressor. The minimum recommended installation according to the findings from the TCS/BKV cooperation is shown with the coloured symbols (boxes for vibration measurements, circles for process).

There are also a number of automatically monitored calculated performance monitoring parameters for monitoring reciprocating compressors that require minimal diagnosis, such as flow, rod load, discharge temperature, volumetric efficiency and power.

## More monitoring has to be done

Despite that much maintenance is needed for reciprocating compressors, and the fact that there are a wide range of measurement techniques available for monitoring these machines, condition monitoring is not done as widely as is done for other critical machines. In fact, reciprocating compressors are some of the least monitored critical machines in

many plants. What is most disturbing is that most of the previously mentioned measurement techniques, contrary to popular belief, can give effective results if properly set up and used.

## Industrial cooperation to find a solution

BKV and TCS formed a long-term cooperation in order to come up with a solution for overcoming the lack of confidence and limitations of the various measurement techniques so that end-users can reduce maintenance costs and downtime. The solution that came out of this cooperation was based on evaluating the customer's needs, evaluating and modifying the existing monitoring techniques, integrating these into the monitoring system, and providing low-cost yet effective services that ensure proper installation, set-up, fine-tuning and long-term operation.

After evaluating the customer requirements, the emphasis was to focus on those measurement techniques that are automatically monitored and do not require extensive resources for diagnosis from the end-user's side, yet still can give accurate reliable results (Fig. 2 shows some of these recommended measurement techniques). Other measurement diagnosis techniques such as PV-diagram analysis, which can still be offered as a solution to customers that require it, were not part of the initial focus since these still require a lot of diagnostic resources that many end-users can't provide, and it is difficult to automatically monitor these to alarm limits.

The TCS/BKV reciprocating compressor monitoring solution provides the following benefits to the end-user:

- The BKV COMPASS safety and condition monitoring system was selected as the standard platform, which can also be used for other machines in a plant-wide application (see Fig. 3)
- Since the machine manufacturer and instrument supplier work together, instrumentation

on the machine is matched to the monitoring system and fine-tuned as a fast and efficient service

- The machine manufacturer has compressor test facilities for researching new monitoring techniques and analysing or refining existing ones
- Sales and support network for the monitoring solution is essentially "doubled"
- The machine manufacturer can provide machine dependent variables for calculated performance monitoring parameters such as power, volumetric efficiency, rod load, flow and discharge temperature
- The cooperation is not a merger, so both companies are unaligned – the solutions can be used with all makes of compressors
- It is possible for both the machine manufacturer and the instrument supplier to have remote access to the monitoring database, so site visits can be minimized.

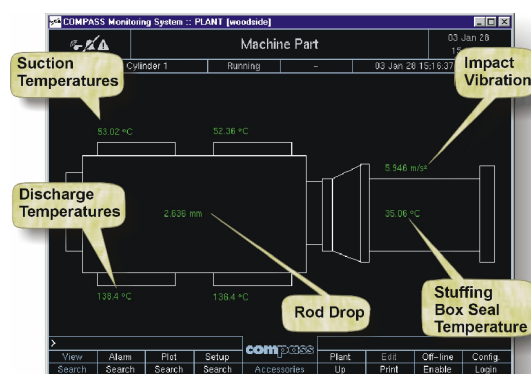
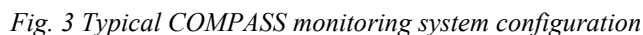


Fig. 2 COMPASS screen view showing recommended measurements for each cylinder.



The rod drop measurement was one of the measurement techniques that were ideal to focus on. This is because the end-user's confidence for the rod-drop measurement was low, despite there was considerable downtime associated with changing the wear bands too early or too late. Some instrument suppliers even recommend to their customers not to use the rod drop monitoring technique at all, or suggest to get advice from the OEM machine supplier.

In summary:

- are generated on deviations, not on the absolute levels. As seen in Fig. 4, the suction valve temperatures for two cylinders vary over time more than 20 °C due to changing process conditions (from 44 to 65 °C). The temperature deviation from one suction valve to another, however, varies only 1.5 °C, which means the temperature deviation or spread measurement is much more sensitive in identifying a valve problem.

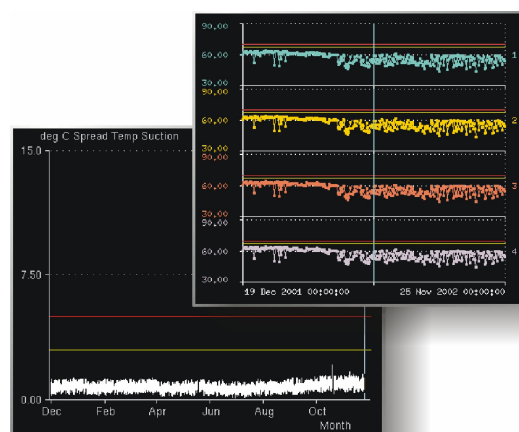


*Fig. 4 Upper plot: Actual temperature for each suction valve (20 °C deviation over time). Lower plot: Temperature deviation between the four valves (1.5 °C deviation).*

The reliability and accuracy of other reciprocating compressor measurement techniques were also

addressed by the TCS/BKV cooperation but are not included in this paper. This includes for example the calculated performance parameters (power, volumetric efficiency, rod load, flow, discharge temperature), which can also be automatically monitored to alarms limits. The implementation of these particular measurement techniques are described in another paper [1].

## Case Studies

The examples presented below are a direct result of the TCS/BKV cooperation. Most of these case studies are focused on rod drop measurements for reciprocating compressors processing natural gas, but other monitoring techniques are also described.

### Improved rod drop measurements

Rod drop monitoring can give effective results if properly set up and used. In Table 1 below, statistical deviations for the rod drop wear and actual dimensions are given for six different machines for different applications at different locations. The monitored rod drop measurement just prior to wear band replacement is compared to the actual physical dimensions of the bands measured during disassembly. In all situations, an optimized rod drop measurement technique was implemented within the TCS/BKV cooperation. As seen in the table, the average difference between the rod-drop wear measurement and the physically measured bands is less than 0.15 mm.

Wear Band Measurement Deviations	Difference (mm)	Difference (%)
Mean deviation	0.15	5.607966
Average deviation	0.143125	7.73997
Minimum deviation	0	0
Maximum deviation	0.4	29.62963
Standard. deviation	0.107438	7.570485

*Table 1 Statistical comparison of wear band wear for a number of different machines as determined by monitoring rod drop just before replacement, and the physical dimensions as measured during replacement.*

Another method of using rod drop measurements to the maximum effectiveness is the use of several averaged rod drop measurements. This makes it a little easier to identify a trend so maintenance can be planned ahead of time, as shown in Fig. 5.



*Fig. 5 Different averaging routines are done simultaneously on the same rod drop measurement. The 4-day average can establish a good long-term trend. The non-averaged measurement is important for catching short-term faults such as the lubrication fault shown in Fig. 6 or the sand-in-the-cylinder problem shown in Fig 7.*

### Lubrication problem

The wear bands normally wear at a slow, constant rate for most applications, so a trend can be used for planning maintenance well ahead of shutting down the machine, as shown on the left-hand side of the plots in Fig. 5. Unfortunately the wear-band wear can be accelerated due to other factors, such as loss of lubrication. This was the case for a natural gas compressor, which had a partially blocked lubrication flow. This can be seen in Fig. 6 by the rapid rate of wear and the high peak-to-peak noise associated with this rod drop measurement. A non-averaged rod drop measurement is ideal for identifying this very rapid wear-band wear. For this type of measurement, it is best to set up an annunciation alarm that is triggered by a rapid wear rate rather than by absolute level limits, as for example 0.05 mm/hr, trended over say one day. In this particular example, the wear rate was so high, that even if the lubricator fault is identified within one day, there is still only one-day warning before the wear bands are completely worn down.



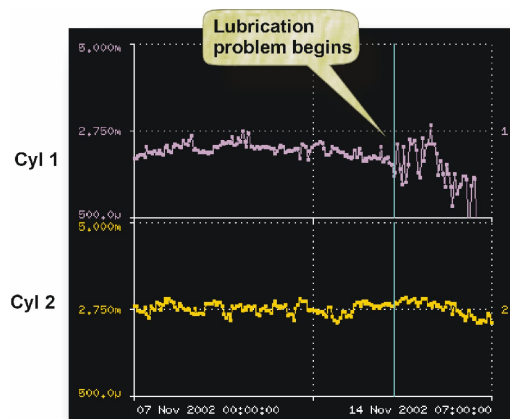


Fig. 6 Rod drop measurement for cylinder 1 indicating rapid wear due to a lubrication problem.

### Sand in the compressor

A reciprocating compressor at a natural gas compression station experienced a sharp increase in wear band wear similar to the that in the previously mentioned case study. In this case the rapid wear band wear is due to a faulty sand filter that allowed sand to enter the cylinder, resulting in accelerated wear. Similar to the previously mentioned lubrication problem case story, an additional rod drop measurement can be set up to monitor only to rate-of-wear alarm limits, in addition to those rod drop measurements that are set up to monitor to only absolute level limits (i.e. those rod drop measurements with different averages).

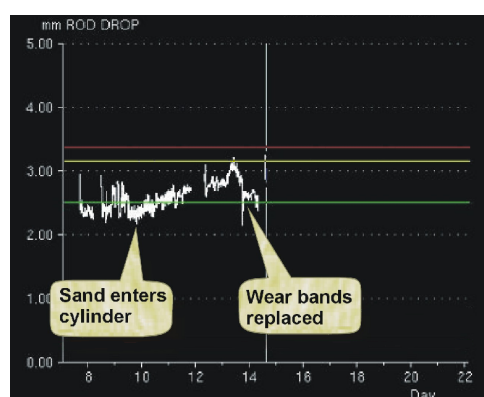


Fig. 7 Rod drop measurement indicating rapid wear due to sand in the cylinder (this is an inverted rod drop measurement).

### Defective valve in a free-floating piston compressor

In a free-floating piston compressor, there is no contact between the piston and the cylinder liner during normal operation. A rod drop measurement is useful here - not for trending wear-band wear to plan for replacement - but for indicating if the piston is properly centered in the cylinder liner. The rod drop measurement for a free-floating piston is normally flat with no downward trend. In Fig. 8, a faulty suction valve resulted in a change in pressure distribution within the cylinder, and consequently a change in the position of the piston.

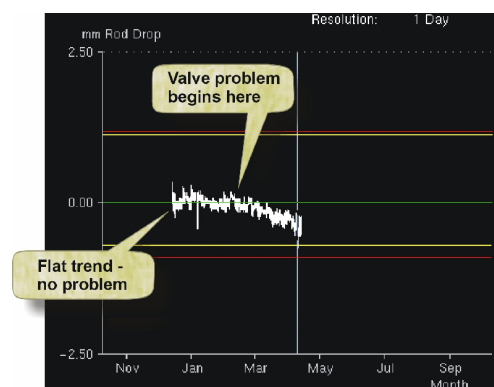


Fig. 8 Free-floating piston compressor with a damaged suction valve.

### Broken piston ring detected by impact monitoring

Impact safety monitoring protects the compressor from rapid destructive faults such as broken components or liquid ingestion. The measurement can also be trended as a condition monitoring measurement to keep track of increasing clearances such as for worn sliders, rod bearings, etc. Fig. 9 shows a compressor with a broken piston ring.

The constant percentage bandwidth (CPB) spectrum measurement in the lower plot of Fig. 9 indicates a 1k Hz signal amplitude increase. In this case the 1k Hz increase is not necessarily due to the impact signals themselves, but is most likely the result of structural resonances being excited by the impacting pieces of the broken piston ring.

The CPB measurement is a composite spectrum consisting of a series of individually filtered measurement components that each have a bandwidth that is a constant proportion of the centre frequency (6% in this example). It is much more sensitive to non-sinusoidal impacts than an FFT, and has much higher resolution at lower frequencies.

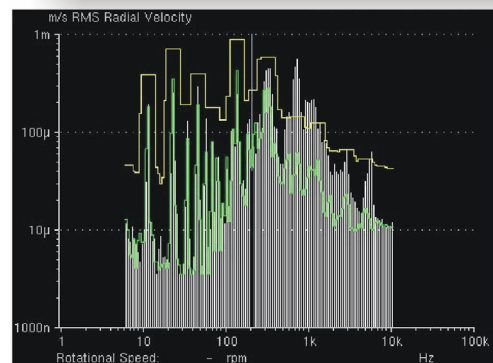
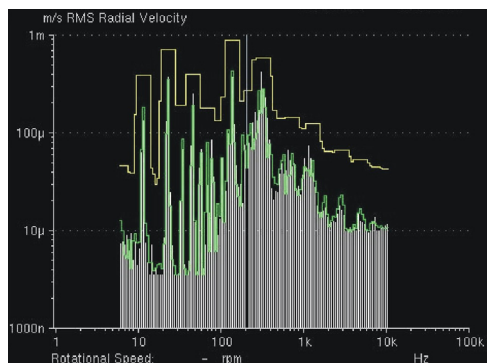


Fig. 9 Lower plot: Impact monitoring of a broken piston ring using a constant percentage bandwidth measurement (CPB) showing an increased 1k Hz signal. Lower plot: Normal operation.

### Leaking suction valve

The overlay plot in Fig. 10 shows the suction valve temperature for two different cylinders of the same machine in an unmanned gas compression station. As seen in the plot, on Oct 20, one of the cylinders suddenly increases 3 °C warmer than the other. This temperature spread is observed for 10 days up until repair, which was done Oct 30. The suction temperature spread returns to normal after the valve repair.

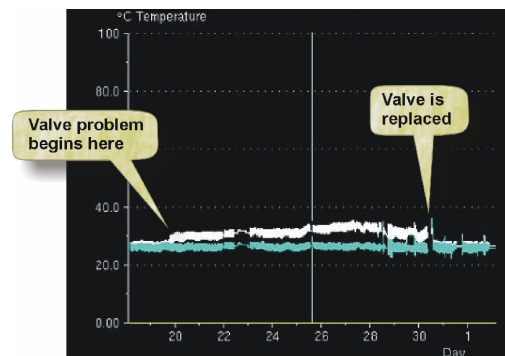


Fig. 10 A suction valve temperature increase due to a faulty valve.

### Conclusion

The TCS/BKV cooperation was aimed at helping reciprocating compressor end-users to reduce maintenance costs and downtime. There are several accurate measurement techniques that can be used for monitoring most of the reciprocating compressor potential failure modes, but these are not always being. This is partially due to the difficulty in setting up these measurements and a lack of knowledge and confidence in the monitoring solutions.

After evaluating customer needs, it was determined that using reliable automatic monitoring techniques that require minimal diagnosis expertise from the end-user, will give faster, more effective results. Educating end-users in using diagnostic and analysis tools such as PV-diagram analysis will not give immediate results, and thus is not the focus of this cooperation. Automatic monitoring techniques were evaluated and refined from both a technical and service point of view to improve their effectiveness. This approach is proving itself successful as demonstrated by the case studies. There is, however, a “learning curve” in promoting and refining this solution, so the TCS/BKV cooperation is intended as a long-term project.

### References

- [1] Lau G. M. Koop, “Performance monitoring on reciprocating compressors - A rational extension of condition monitoring”, paper presented at the 2<sup>nd</sup> EFRC symposium, Amsterdam, May 18, 2001



# **Carbide coatings: use on reciprocating compressor piston rods and hyper compressor plungers**

**by:**

**ir. Luc van Loon,  
Alloy Carbide Europe  
Antwerp  
Belgium**

**Reliability and economics of compression systems -  
recent trends in the market of  
reciprocating compressors  
March 27<sup>th</sup> / 28<sup>th</sup>, 2003 Vienna**

## **Abstract:**

The use of coatings on piston rods and plungers in reciprocating compressors has become common practice not only in order to increase the life time of the piston rod itself, but even more in order to avoid unscheduled shut downs by increasing the life time of the pressure packing rings. Except for its wear and corrosion resistance the coating also has to be adapted to the packing ring material, process gas and lubrication. This can be obtained by applying the correct surface roughness and profile. Another important issue when using coatings on piston rods is the lack of specifications and non-destructive tests. This creates an uncertainty for maintenance and production engineers who therefore sometimes prefer not to use coatings. Different types of coatings that are actually available on the market are discussed with their pros and cons. Properties and surface finishing techniques of RAM<sup>®</sup> carbide coatings used on piston rods and hyper compressor plungers are treated more in detail including practical tests and minimum property requirements to guarantee a reliable coating.

## 1 Introduction

In reciprocating compressors several problems can occur in the packing and oil wiper ring area of the piston rods. The most important problems are the following: (1) Gas leakage, caused by axial wear grooves on the packing area of the piston rod. This leakage is mostly not allowed because of security and environmental reasons. Besides of this, the leakage also causes production loss. (2) Wear of packing rings: damaged piston rod surfaces will damage the packing rings causing expensive packing ring replacements. (3) Wear of the piston rod: when wear grooves are too deep or the piston rod diameter is too small to be repaired, the piston rod has to be replaced.

In order to avoid these problems it is cost effective to improve the wear resistance of the piston rod packing and oil wiper ring area. Many different surface treatments are available which makes the choice of the best surface treatment for the application quite difficult.

The properties of the surface treatment and the interaction with the packing material, the process gas, the amount and type of lubrication and the production parameters will be decisive to make a correct choice. Therefore it is not only important to know the features of the different surface treatments, they also have to be specified in detail. It will be shown that specifying the type of treatment and the chemical composition of it, does not guarantee a good coating.

An overview of different surface treatments is given in this paper and the proprietary RAM<sup>®</sup>-coating is discussed more in detail.

The most important properties with regard to reciprocating compressors and how they should be introduced in coating specifications are explained in order to help engineers to make the best coating choice.

Since the surface roughness and profile are as important as the coating type itself, different profiles and finishing techniques are discussed.

An extreme application where RAM<sup>®</sup> carbide coatings have proven their use are hyper LDPE-compressor plungers that operate at +/- 1500 bar with bronze metall packing rings. RAM<sup>®</sup> carbide coatings have proven to be a good alternative to solid tungsten carbide plungers for 1<sup>st</sup> stages avoiding catastrophic plunger failures.

## 2 Wear resistant surface treatments

### 2.1 Need for surface improvement

In order to improve the surface properties of a piston rod, the wear and corrosion resistance have to be improved. A further improvement can be obtained by improving the surface roughness and profile, adapting it to the packing ring material and the lubrication.

In Table 1 a comparison is made between the surface treatments that can be used on piston rods. For piston rods the most important properties are the bond strength, the hardness, the porosity and the base material temperature during the treatment.

Surface treatment	Hardness HRc/HV	Thickness depth	Bond strength	Porosity	Application temperature
Inductions- or flamehardening	45-60 HRc	< 2mm	/	0	> 500°C
Cementation	< 65 HRc	< 2 mm	/	0	> 500°C
Nitriding	< 65 HRc	< 2 mm	/	0	> 500°C
Hardchrome	< 60 HRc	< 0.5 mm	good	low	> 100°C
Thermo-chemical oxides	2000 HV	< 0.1 mm	good	low	> 500°C
Flamespraying	< 45 HRc	< 5 mm	low	10%	< 100°C
Plasmaspraying	< 60 HRc	< 0.5 mm	low	5%	< 100°C
Spray&fuse	< 60 HRc	< 2 mm	good	2%	> 1000°C
Detonation coating	< 1400 HV	< 0.3 mm	good	< 1%	< 100°C
RAM coating	< 1400 HV	< 0.3 mm	good	< 1%	< 100°C

Picture 1: Surface treatments used for compressor piston rods

### 2.2 Surface treatments

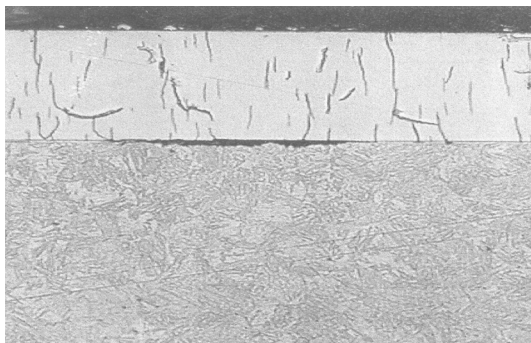
#### 2.2.1 Hardening

The oldest surface treatment that is often used as a standard by compressor manufacturers, are techniques where the surface of the piston rod is hardened without applying a coating. Aside from induction and flame hardening also diffusion treatments are used where atoms like nitrogen (nitriding) or carbon (cementation) diffuse into the base material in order to harden the surface layer. These techniques don't have delamination problems, are low cost and have good impact resistance. Limitations are: the limited hardness and

therefore the lower wear resistance; deformations caused by thermal stresses; micro-crack forming during hardening.

### 2.2.2 Electrolytic chrome plating

A frequently used technique was the electrolytic hardchrome plating. Although this is a low cost technique that provides a good bond strength and a good impact resistance, the use is limited because of crack formation through the coating and because of the limited hardness. Hardchrome platings are normally not indicated for use with PTFE packing rings in non-lubricated applications.



Picture 2: Crack formation in hardchrome plating

### 2.2.3 Thermo-chemical oxides

A special surface treatment is the thermo-chemical oxide coating. With this technique a liquid product is applied to the surface and then transformed to an oxide in an oven at high temperature. The advantages are the high hardness and the good general corrosion resistance. Disadvantages are: the low coating thickness (0,05 mm); thermal deformation caused by the high application temperature (+/- 550°C); brittleness; susceptible to sub-surface corrosion.



Picture 3: Underlayer corrosion on oxide coated NH<sub>3</sub> piston rod

## **2.3. Thermal spray coatings**

Thermal spraying is a group of techniques where coating material (in powder or wire form) is heated by a heat source (flame, plasma, electric arc) and projected on a surface. The advantage of these techniques is the low base material temperature during coating (no structural changes, no deformations), disadvantages are the limited bond strength, the low hardness and the high porosity (2-10%) for some of the techniques.

### 2.3.1 Flame spraying (cold spraying)

Flame spraying is the oldest thermal spray technique where a oxy-acetylene flame is used to heat powder or wire that is projected on the surface by compressed air.

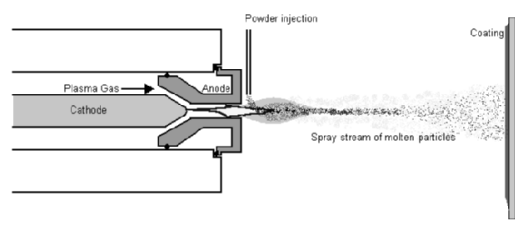
The equipment used, is low cost and easy to operate. The coating quality is very limited with a low bond strength, high porosity, low hardness and limited corrosion resistance. This technique should not be used on piston rods.

### 2.3.2 Spray and fuse (hot spraying)

With this technique special low melting powders are sprayed on the part by flame spraying after which it is fused by an oxy-acetylene burner or in an oven. The coating formed has low porosity, good bond strength, hardness to 60 HRc and good impact and corrosion resistance. Wear resistance can be approved by adding up to 50% carbide particles. The major limitation of this treatment is the fuse temperature that is about 1100°C causing deformations and structural changes in the piston rod. This is the reason why these coatings are not used anymore on piston rods.

### 2.3.3 Plasma spraying

The plasma spraying technique uses a plasma heat source to heat up powders.



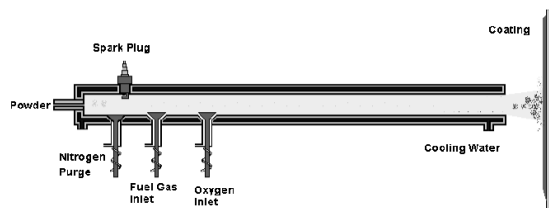
Picture 4: Plasma coating gun



Because of the very high heat input this technique is mostly used to spray high melting materials like oxides. Bond strength remains limited and porosity is still quite high.

### 2.3.4 Detonation coating

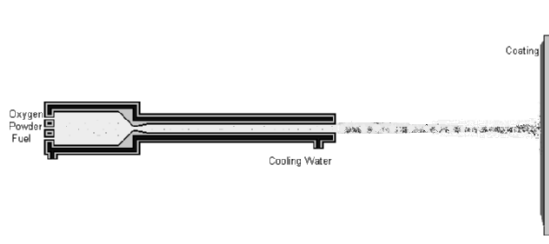
In this technique detonation shock waves are used to accelerate packages of powder material to supersonic speed. Upon impact on the surface the kinetic energy is transformed to heat creating a very high bond strength.



Picture 5: Detonation gun

The obtained coatings have a very low porosity. This coating technique is very appropriate to spray high carbide containing coatings with superior wear resistance.

### 2.3.5 HVOF spraying



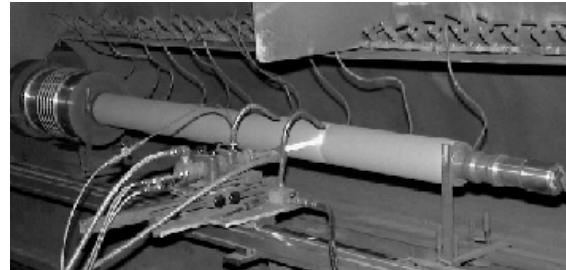
Picture 6: HVOF gun

HVOF (High Velocity Oxygen Fuel) coatings are developed based on the principle that renders the detonation coatings there superior quality. With this technique the supersonic particle speed is not obtained by a shock wave, but by burning gas under high pressure. This creates a continuous supersonic powder flow resulting in homogeneous porous- and defect-free coatings.

## 2.4 RAM<sup>®</sup> carbide coatings

The RAM<sup>®</sup> coating technology is a High-Velocity-Oxygen-Fuel (HVOF) thermal spraying technique developed by Alloy Carbide Company in Houston. With this technique a powder material is injected in

a hydrogen-oxygen flame and accelerated through a converging-diverging nozzle, attaining a velocity of about 1000 m/s. In order to obtain the optimal velocity and temperature for each individual particle, it is necessary to use powder with a very narrow grain size distribution.



Picture 7: RAM<sup>®</sup> coating system

The HVOF technique has been developed as an alternative for detonation spraying. While the detonation spraying is a discontinuous technique where packages of powder are accelerated by a gas explosion, the RAM<sup>®</sup> coating is a continuous process. For piston rods and hyper compressor plungers carbide based powders are used.

## 3 Coating properties

Coatings on compressor piston rods and plungers are primarily used in order to increase the surface wear resistance. Wear is the accumulated loss of material and dimensional changes of a component caused by mechanical stresses. The resistance of a coating against these stresses depends on (a) the structural integrity of the coating (porosity, lamellar structure) and (b) on the basic material properties of the coating.

These material properties are (1) resistance to plastic deformation of which hardness ( $H$ ) is a measure, (2) resistance to elastic deformation which is usually referred to as the Young's modulus ( $E$ ) and susceptibility to crack propagation or brittleness ( $K$ ). These properties are in turn determined by the phases present, their relative proportions, intergrain adhesion (determined by powder manufacturing route), porosity, grain size, hard particle shape and distribution.

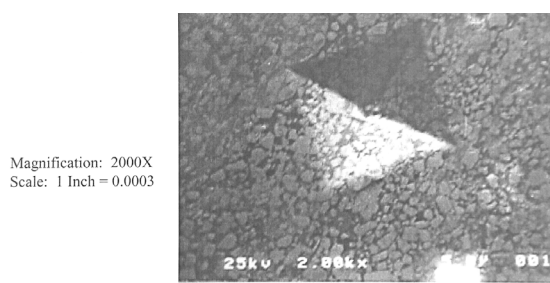
Since we are in fact not interested in the wear resistance of the coating, but more in the life time of the coated part and sometimes the counterpart, a coating can only be successful when it remains on the part. This is determined by the bond strength of the coating and also by the residual stresses in the coating. For piston rods and plungers this is most of the time the main concern. A short lifetime is sometimes preferable above a long but

unpredictable lifetime. Therefore the bond strength has to be high enough so that the lifetime of the coated part depends on the coating material properties and not on the bond strength. The residual stress in RAM<sup>®</sup>-carbide coatings is always compressive inhibiting crack growth caused by thermal fatigue (e.g. during direct contact between coating and metallic seal rings because of lubrication failure).

Finally the corrosion resistance plays an important role in order to guarantee the lifetime of piston rods especially where corrosive gases or humidity are involved.

### 3.1 Wear resistance of RAM<sup>®</sup> carbide coatings

As discussed above, the wear resistance of a RAM<sup>®</sup> carbide coating is determined by its materials properties like resistance to plastic and elastic deformation and its brittleness. These properties are in turn determined by: the phases present (very hard WC, CrC in tough metal binder), their relative proportions (> 75% carbide), intergrain adhesion (good wettability of WC by Co and Ni, diffusion reaction between WC and Co during powder manufacturing by sintering), porosity (< 1vol. % micro porosity (< 5µm)), carbide grain size (< 5 µm), carbide distribution and contiguity (evenly distributed with a very short free path) coating structure (homogeneous non-lamellar structure because of the continuous powder feed). Picture 8 shows a Vickers hardness indent SEM micrograph at 2000 x magnification.



VICKERS DIAMOND HARDNESS  
INDENTATION IN RAM<sup>®</sup> 10

Picture 8: Vickers hardness indent in RAM<sup>®</sup> 10

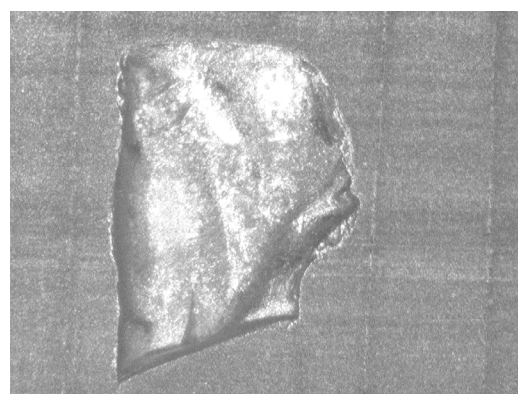
The unusual combination of very hard carbide particles in a ductile metallic matrix provides the exceptional wear resistance of RAM<sup>®</sup> carbide coatings. The most important feature of the RAM<sup>®</sup> coating is the low porosity that is obtained by the very high particle speed obtained by the hydrogen flame, but even more by the powder that is

specifically developed for and adapted to the RAM<sup>®</sup> coating system.

In piston rod applications primarily two types of wear can occur. (1) Abrasive wear can be induced by solid particles in the gas or by hard particles in the packing material (glas fiber reinforced PTFE, graphite, PEEK, bronze, babbitt or cast iron). In this case the good wear resistance of RAM<sup>®</sup> carbide coatings is obtained by the very high carbide content and the high carbide contiguity (the degree of contact between carbide grains). (2) The other type of wear is called adhesive wear which is caused by contact with metallic packing rings, back-up rings or packing cups. This contact can originate from a lack of lubrication, misalignment (especially in the case of carbide plungers), wear of piston rings, piston rod deformation etc... .

An important property needed for a good adhesive wear resistance is a high heat conductivity (for RAM 1: 65 W/mK) so that the heat generated on the surface is quickly dissipated into the base material. Another advantage of carbide is that it has a very low tendency to cold weld to other metals.

For 1<sup>st</sup> stage hyper compressor plungers wear can also be caused by dynamic friction between metallic parts due to misalignment or through lack of lubrication. This causes thermal fatigue cracking that results in material break-out and finally in plunger failure by breaking or fragmentation.



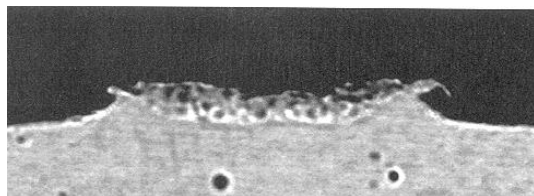
Picture 9: Thermal fretting fatigue cracks and broken-out material on solid tungsten carbide plunger

RAM<sup>®</sup> carbide coatings are here a good alternative to solid carbide plungers because thermal fatigue will only result in coating failure avoiding a catastrophic plunger failure. An extra advantage of carbide coatings sprayed with the RAM<sup>®</sup> system is their residual compressive stress that improves their fatigue resistance. This is only true when subsequent grinding is performed properly as explained here below.

### 3.2 Bond strength of RAM<sup>®</sup> carbide coatings

As already stated above, one of the most important properties for a coating on piston rods and hyper compressor plungers is the bond strength. Coating delamination will not only cause damage on packing-, rider- and piston rings, but also on the valves.

Even more, it creates an uncertainty for production and maintenance engineers because it cannot be detected during production nor can it be predicted. The bonding mechanism of RAM<sup>®</sup> coatings can be compared with a metallurgical cold-weld bond. Because of the very short dwell time of the powder particles in the hypersonic flame, the particles are in a solid-plastic or solid-liquid state in which the carbide particles are in a solid state whereas the metal-based binder phase is liquid or plastic. The kinetic energy of the powder particles ( $v_p = 800\text{--}1000\text{ m/s}$ ) is transformed to heat upon impact on the base material, creating a metallurgical cold-weld bond as shown in picture 10.



Picture 10: Cold-weld bond

Very important to obtain this bond is the clean and roughened surface that is obtained by grit blasting with white aluminum oxide.

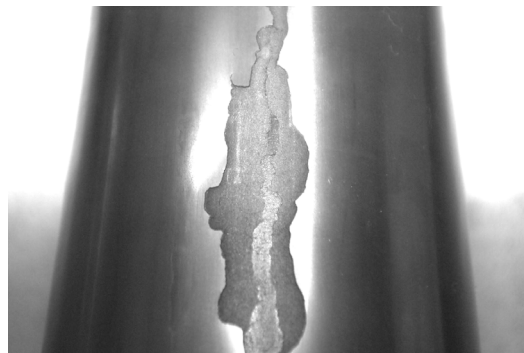
### 3.3 Corrosion resistance of RAM<sup>®</sup> carbide coatings

In many compressor applications corrosive gases or gases that are diluted with corrosive products are used. In these cases the coating has to be very corrosion resistant.

Since tungsten carbide has a very good corrosion resistance against most acids, the corrosion resistance of RAM<sup>®</sup>-coatings is determined by the metallic matrix. Therefore Alloy Carbide developed different types of powders with a very high corrosion resistance.

Successful applications are Chlorine, HCl, H<sub>2</sub>S, Ammonia and CO<sub>2</sub>-Gases.

Aside from surface corrosion, underlayer corrosion can also be a problem. Underlayer corrosion occurs when the corrosive products reach and attack the base material after penetration of the coating through porosities or micro-cracks. The thus formed corrosion products push the coating away causing it to delaminate (picture 11).



Picture 11: Underlayer corrosion

Also corrosion resistant base materials (like stainless steel, nickel alloys, titanium) are prone to underlayer corrosion because their protective oxide layer is removed by grit blasting (Aluminum oxide) prior to coating.

The very low, non-through porosity in RAM<sup>®</sup> carbide coatings and the absence of microcracks makes it almost insensible to underlayer corrosion.

## 4 Coating tests

In order to define and verify the above mentioned properties, many coating tests are developed. The major problem is that most of these tests are of destructive nature making them useless on the coated parts itself. This can be solved by spraying coating samples on which the destructive tests can be performed. The problem is that these tests are very time consuming and costly. Therefore tests have been developed that can be performed just after coating. They can easily be used in the coating specifications aside of the results of general destructive coating tests that are performed for each new powder lot.

### 4.1 Wear tests

Since wear resistance is the main goal of using a coating, it is obvious that testing the wear resistance is important. On the other hand testing wear resistance can be avoided by testing the properties that are responsible for obtaining the wear resistance. Therefore wear resistance tests are only performed during development and after changes on

the coating system or coating materials. They are normally not done for each application.

Typical wear tests are pin-on-disc with (abrasive wear) or without (adhesive wear) abrasive product, Miller test (ASTM-G 75-95) (slurry abrasion response of material), emery paper test, etc. An interesting and easy to perform test is the block-on-ring test (ASTM G-77-97) where a coated ring is pressed against a material (e.g. packing ring material). This test can also be carried out with lubrication in order to test the influence on the wear resistance of the coating and packing ring material.

## 4.2 Hardness test

An easy to perform and not expensive test is the hardness measurement. For HVOF sprayed carbide coatings this is always performed by a Vickers or Knoop hardness method in which a pyramid diamond is pressed into the material. The hardness is the resistance of the material against plastic deformation. Although the impression is very small it should not be performed on the sprayed part itself since it creates a stress concentration. The hardness measurement should be performed on a sample that is sprayed together with the part. Although hardness values are very often used as a measure of wear resistance, the hardness value is not always a good indication of wear resistance. This is only the case when the dominant wear mechanism is the same as the dominant deformation mechanism during indentation. This is generally the case when the coatings are subjected to abrasion or sliding wear against harder materials. With softer counter-bodies the wear mechanism is not plastic deformation. Another limitation of hardness is that it does not reckon with corrosion and thermal cycling during use of the coating.

## 4.3 Porosity tests

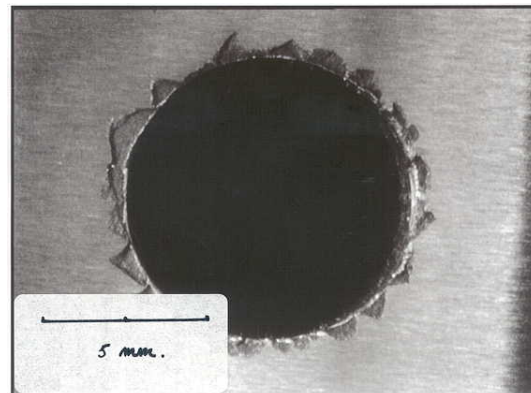
Porosity measurements are normally only possible on a transverse cut of the coating, making it a destructive test that has to be performed on a separate sample. There are three alternatives that give a good indication of the porosity level in the coating. The first one is the hardness value. This will be lower when the measurement is done in a zone containing a porosity. The indentation will also have a non-symmetrical shape.

The second method is the dye penetrant which can be performed on the coated part itself and is non-destructive. The amount of development of the dye product gives a good indication of the porosity level for experienced eyes.

Finally porosity can be checked by microscopic inspection of the surface.

## 4.4 Bond strength tests

The bond strength is probably the most critical property of the coating-base material system. It is also the most difficult to measure. A well known standard measuring method is defined by ASTM C633-79 where the end face of a cylindrical sample is sprayed and glued to a counter sample. A tensile test gives the bond strength. This is a very complicated and time consuming test and limited to the tensile strength of the glue which is lower than the bond strength of the coating. Therefore most of the thermal spray companies develop their proper bond strength tests. Two good alternatives are the bending test where a steel strip is sprayed together with the part and after coating bent around a 12.5mm diameter rod. When the coating does not spall off the bond strength is good.



Picture 12: Result of Morisset test showing good bond strength

A second bond strength test is based on the Morisset test where the coating is pushed away from the base material using a punch (picture 12).

The coating should not spall off to more than 1 mm from the punched hole. The advantage of this test is that one can use the same base material and dimensions as the piston rod or plunger. In both tests the samples can be further destructively analysed for hardness, porosity and structure.

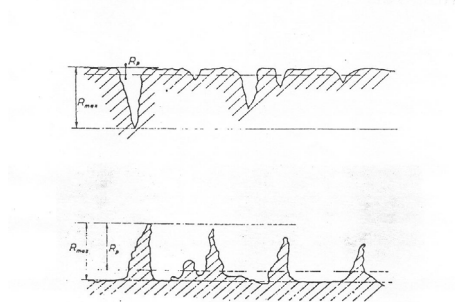
## 5 Piston rod and plunger coating surface finishing

For piston rods and hyper plungers not only the wear resistance and hence the life time of the rod or plunger has to be considered, but also the life time of the packing rings. A wear resistant surface



(without grooves, cracks and corrosion) is the best guaranty against packing ring wear.

A further improvement can nevertheless be obtained when the surface profile and roughness is adapted to the packing material and the lubrication. Many users only specify roughness  $R_a$  and  $R_z$  parameters and not the profile while this is often more important.



Picture 13: Two profiles with same  $R_a$  and  $R_z$

In picture 13 one can see 2 different profiles with the same  $R_a$  and  $R_z$  value. The roughness and profile is determined by the finishing techniques.

## 5.1 Surface finishing techniques

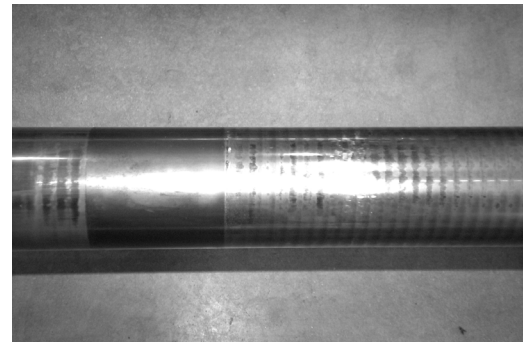
In order to obtain these very specific surface finishes, special finishing techniques have been developed by Alloy Carbide.

### 5.1.1 Grinding

The first stage in finishing RAM<sup>®</sup> carbide coatings is always diamond wheel grinding. A lot of attention has to be given to the correct choice of the diamond wheel (type of diamond used, diamond coating, binder material, concentration, etc...). The aim is to create as little heat as possible during grinding because this can deteriorate the surface properties and induce subsurface micro-cracks. During grinding the wheel has to be kept sharp because a dull wheel tends to plow and rub creating more heat. A badly dressed or untrue wheel will also create scattering on the surface that is very difficult to remove afterwards. Besides of the wheel choice also the grinding parameters have to be chosen correctly. Fast operation is in this case detrimental to the coating and unfortunately not detectable.

### 5.1.2 Honing

After grinding it is advisable to perform an external honing operation. This is done to obtain a perfect geometry and to remove the grinding spirals that are always present. These grinding spirals can not be removed by superfinishing and create an unwanted action on the packing rings.



Picture 14: Grinding spirals appearing after use

This is not measured by roughness parameters like  $R_a$  or  $R_t$  because the profile can only be measured over much longer measuring lengths (5-10 mm). This shows the importance of profile measurements. Picture 14 shows grinding spirals on a piston rod after several years of service.

### 5.1.3 Superfinishing

In order to obtain the correct surface roughness and surface profile, it is necessary to finish the coating by a superfinishing technique. This is a low temperature process that removes the surface layer created by grinding and honing. It can either be done by using diamond cloth, diamond paste or diamond film. Depending on the diamond grain size and the sequence of finishing steps used, the desired roughness and profile can be obtained.

## 5.2 Piston rod surface profiles

For piston rods one has to distinguish between lubricated and non-lubricated applications.

For lubricated rods, the roughness has to be low with a high BAC.

When PTFE packing rings are used in non-lubricated applications, a low roughness would induce too much friction heat, creating temperatures of more than 200°C. Therefore the roughness has to be higher for non-lube applications with a toothed profile. Using this profile the PTFE will be transferred from the packing rings to the piston rod



during start up (1-2 days) after which PTFE will run against PTFE.

Important is that the initially applied profile remains unchanged as long as possible. This is achieved by the unusual combination of ductility and hardness of the RAM<sup>®</sup> -carbide coatings. Fragile oxide coatings, hard chrome plating and soft metallic coatings are therefore not indicated.

Since LDPE hyper compressor plungers always run on lubricated bronze packing rings, the profile (Wt) and the roughness (Ra, Rz) have to be as low as possible. At this moment Ra values as low as 0.003 µm are obtained on solid carbide plungers. On RAM<sup>®</sup> carbide coated 1<sup>st</sup> stage plungers Ra values of 0.01 µm are obtained. For these extremely low roughnesses the profile and bearing area ratio are of lesser importance.

## 6 Piston rod and plunger coating specifications

Since the difference in coating quality sometimes depends on small details it is important to specify the coating in such a way that a bad quality is excluded. This can make things very difficult and expensive especially when the buyer wants to verify the specifications in house. A minimum of coating properties and dimensional requirements however should be specified in order to obtain a good functional part.

### 6.1 Coating type specification

Following data should be specified in order to define the type of coating: (1) full chemical composition (e.g. WC-6Co-4Cr), (2) coating technique (HVOF), (3) coating gun. Using brand names for the powder and gun can be limiting, but can on the other hand guarantee that you get the exact same coating as before.

### 6.2 Coating properties specification

#### 6.2.1 Hardness

Although hardness is not always a good measure of wear resistance, it gives at least a good idea of the coating quality and it can easily be verified on a sample sprayed together with the part.

All hardness measurements should fall within the specified range (f.e. 1050-1250 HV<sub>300</sub>).

#### 6.2.2 Bond strength

Bond strength should be a general specification. A bend test or other representative tests could be specified.

#### 6.2.3 Porosity

Since porosity has a considerable influence on the wear resistance and also on the corrosion resistance of the coating it should be specified. Verifying the specified value can only be done destructively on a sample. When experience is available in the company a visual dye penetrant inspection can give a good indication of the porosity.

#### 6.2.4. Corrosion resistance

When the process gases are corrosive or contain corrosive additives or humidity, this should be mentioned in the specification if the coating choice is left to the coating company. Otherwise the corrosion resistance should be covered by the coating type specification.

## 6.3 Dimensional requirements

### 6.3.1 Surface roughness and profile

Not only Ra values that give an idea of the average roughness, but also Rz (indication of porosity and roughness profile), W (indication of periodic profiles generated by grinding pitch) and bearing area ratio (BAC) (indication of wear resistance and lubrication film promotion) should be specified. If the choice of these parameters is left to the supplier, the type of packing ring material and lubrication have to be mentioned.

### 6.3.2 Dimensional specifications

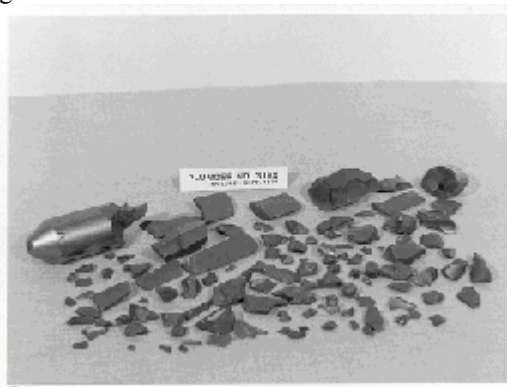
All dimensional requirements should be on the drawing. If a drawing is not available, the minimum requirements are diameter, diameter tolerance and piston rod run-out.

## 7 RAM<sup>®</sup> carbide coatings on hyper LDPE compressor plungers

For the production of LDPE (Low Density PolyEthylene) the ethylene gas has to be compressed to very high pressures (up to 350 MPa). Today for this application hyper compressors with

solid tungsten carbide plungers with stationary bronze packing rings are used.

Since solid carbide is a brittle material there is always the danger of plunger fracture caused by thermal fatigue or fretting fatigue cracking. This not only causes very costly failures and production losses, but even more creates very dangerous situations because of the explosivity of the ethylene gas.



Picture 15: Fragmented solid WC plunger

As supplier of solid tungsten carbide plungers since more than 40 years, Alloy Carbide has been asked to develop a cost effective and less critical alternative for these solid plungers.

Since their development, the RAM<sup>®</sup>-carbide coatings are being used very successfully for more than 15 years now. This is only on 1<sup>st</sup> stage plungers that operate at 150 MPa and more. For second stage plungers solid carbide plungers are preferred.

## 8 Conclusion

Although carbide coatings are very well known and accepted in the compressor world for applications on piston rods and plungers, it is clear that it is still very difficult to distinguish between a good and a lesser coating. Since the technical aspects of coating materials and coating systems are very complex the knowledge of them is most of the time not present in the end user companies. It is therefore very difficult to draw up a specification that guarantees the right coating for the application. Most of the time the end user has to rely on the coating company to make up their specification. Even so, the kitchen secrets that sometimes make the big difference can not always be embedded in a technical specification.

As important as the coating itself is the manufacturing and preparation of the basematerial and even more the finishing of the coated part. One should never forget that the coating is only a part of

a component that has to operate in a tribological system. Also this knowledge has to be present in the coating company in order to supply a part that fulfills all requirements. A good reference is sometimes the best choice.

## References

- <sup>1</sup> M. Factor, I. Roman: "Microhardness as a Simple Means of Estimating Relative Wear Resistance of Carbide Thermal Spray Coatings" *J. Thermal Spray Techn.*, 2002, 11, pp.468-495.
- <sup>2</sup> Chang-Jiu Li, Yu-Yue Wang: "Effect of Particle State on the Adhesive Strength of HVOF Sprayed Metallic Coating" *J. Thermal Spray Techn.*, 2002, 11, pp.523-529.
- <sup>3</sup> L.-M. Berger et al. "Hardmetal-like coatings-a comparison of properties and potentials of the different systems" *DVS Berichte Band 175*, 1996, pp. 61-65.
- <sup>4</sup> H. Kreye et al. "Influence of the Fuel Gas on Microstructure and Properties of HVOF-coatings" *DVS Berichte Band 175*, 1996, pp. 95-98.
- <sup>5</sup> J.D. Nuse, J.A. Falkowski "Surface Finishing of Tungsten Carbide Cobalt Coatings Applied by HVOF for Chrome Replacement Applications." *Aerospace/Airline Plating and Metal Finishing Forum Cincinnati*, March 27, 2000.
- <sup>6</sup> J. Badger, A. Torrance "Understanding the Causes of Grinding Burn Helps Alleviate the Problem" *Cutting Tool Engineering*, 2000, 52, no. 12.
- <sup>7</sup> G.S. Upadhyaya "Cemented Tungsten Carbides" Noyes Publications, NJ, 1998.
- <sup>8</sup> M. Jakobuss "The Dynamics of Diamond Retention in Grinding Wheel Systems" *Intertech 2000*, Vancouver Canada, July 17-21, 2000.
- <sup>9</sup> S.W. Webb "Thin Metal Coatings and Diamond Tool Performance" *Intertech 2000*, Vancouver Canada, July 17-21, 2000.



## **System for direct wear monitoring of rider rings in reciprocating compressors**

**B. Spiegl, D. Artner, P. Steinrück**

**Research & Development**

**HOERBIGER Ventilwerke GmbH**

**Vienna, Austria**

## **Reliability and economics of compression systems - recent trends in the market of reciprocating compressors**

**March 27<sup>th</sup> / 28<sup>th</sup>, 2003 Vienna**

### **Abstract:**

Increasing demands for higher compressor reliability supported by the trend towards a condition orientated and forward planning maintenance strategy in the industry require comprehensive compressor condition monitoring.

Large compressors with preferably horizontal opposed cylinder configuration use so called rider rings for supporting the weight of the piston and the rod. Especially in non-lube and mini-lube compressors the wear of rider rings is the main reason for planned and unplanned shutdowns, whereby the monitoring of the wear situation becomes of essential importance in order to safeguard the compressor availability, in particular where no backup machines are installed.

Currently used systems are based on rod-drop measurement in the intermediate piece giving results with limited accuracy due to sensor location and other influences [1,3]. The measured values do not allow a reliable assessment of the actual wear situation and wear rate.

In the presentation a new approach is outlined which allows a determination of the present distance between piston and liner with highest accuracy; independent of temperature, speed and contaminations. Furthermore, for the new system no on site calibration is necessary.

## 1 Introduction

Especially in process gas applications the majority of all larger reciprocating compressors show a horizontal opposed cylinder configuration. In order to support the usually high weight of both, piston and rod against the cylinder liner, rider rings are used for transferring the gravity forces to the cylinder liner and guiding the piston itself, piston rings are applied for sealing.

Rider rings differ in design and width from the piston rings (Fig.1 and 2). They usually consist of a ring, a split ring or several ring segments which show single slots at their surface, in order to avoid pressure buildup in the direction of motion. Filled and reinforced plastic materials based on PTFE or other high temperature plastics like PEEK have proven successful as materials for rider rings in non-lube or mini-lube compressors.

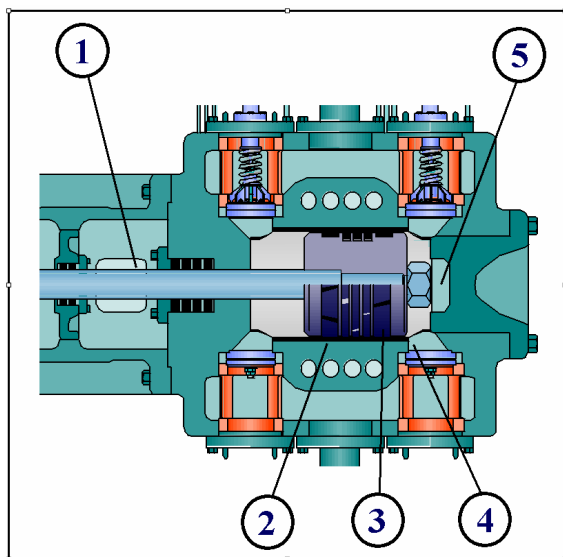


Fig.1: Cross section of a typical compressor cylinder. Location of a rod-drop sensor (1). Possible positions for direct wear monitoring sensors: in the cylinder wall (2), rider ring or piston (3), compressor valve (4) and in cylinder cover(5).

Depending on design features, on the operating and lubrication conditions these rider rings are subjected to wear, thus reducing the distance between piston and cylinder liner. If the wear situation of the rider rings is not monitored or not paid consideration a possible contact of the piston with the cylinder liner will lead to severe damages on the cylinder liner which are difficult to repair, cost and time intensive and can cause complete plant shutdowns.

Depending on the design of piston and rider rings, the rider rings may rotate during operation or they

are intentionally prevented from rotating. Basically an even rotation of rider rings would increase their service life; it bears, however, the risk that this rotation which can hardly be controlled comes to an abrupt stop and that apart from a possible lateral shifting of the piston also increased wear may occur immediately.

Enhanced by the trend to dry running or mini-lube compressors the monitoring of the wear condition of rider rings in horizontal compressors gains essential importance, as very often in modern plants no backup machines are installed for cost reasons. This means an even higher importance of secured compressor availability.

Most of the available rider ring wear monitoring systems only permit indirect measuring of actual wear. This meets the demand of the compressor user for reliable information on the actual wear situation and estimation of the remaining service life only partially.

## 2 Requirements for rider ring wear monitoring systems

### 2.1 General market trends

The expectations concerning a monitoring system for rider ring wear are defined among others by general frame conditions, such as the importance of the compressor in the plant, the targeted maintenance strategy, the availability and the costs of service personnel, the existence of a backup machine etc.

As mentioned above the demands to such systems are quite different for dry running or high speed machines without backup compressor than for lubricated slow running machines where a standby compressor is available. The trend that can be observed in modern industry tends to a condition based maintenance strategy with at the same time reduction of maintenance personnel and it requires apart from precise information on the wear situation also a reliable trending of wear rates depending on operating conditions, in order to optimally plan service intervals and to avoid unforeseen compressor downtime.

### 2.2 Limitations of non direct measuring methods

With most of the non direct methods the rod drop in the intermediate piece (Fig.1) is measured. Thereby the wear of the rider rings and/or the remaining gap between cylinder and liner is determined from the outside of the cylinder. This can be done by the

help of inexpensive limit switches or with continuous measuring systems preferably based on eddy current sensors, with or without connection to top dead center sensors.

The location of the sensor position between piston and crosshead and consequently the extrapolation of the measured signal has a limiting effect on the accuracy of the actual distance value. Additional influences like piston rod flexure, cross head movements, load and temperature changes can hardly be taken into account [1,3]. Due to the dependence on the piston rod geometry and material such systems have to be calibrated on site. Sophisticated analysis methods may unveil additional information like for instance the wear status of piston rings. [4].

### 2.3 Requirements to an ideal system

A system which fulfils the actual and the future requirements should be able to meet the many needs from the most different fields.

The measuring signal should be attributed directly to a wear value, to the gap between piston and liner, independent of the operating condition, the service life, temperature and also without any subsequent

correction or extrapolation. The requirement for reliable trending even raises the need to repetitive accuracy lower than 0.03 mm unaffected by temperature or operating condition.

The life time of the systems should exceed multiple service intervals, there must not be any drifting of signals.

An ideal system should not require cost intensive calibration on site and should permit processing of the signal in different process control systems.

### 2.4 System related problems of direct wear monitoring

Demands on accuracy and reliability of the information given by the measuring signals, require more direct measuring methods, if possible inside the compression chamber in order to predict the actual distance between piston and liner.

Obvious ideas like sensors in the rider ring (Fig.1) which give signals to the outside, or distance sensors that are positioned in the cylinder wall [3] or in compressor valves [2] fail due to the actual state of the art, due to the critical ambient conditions in the

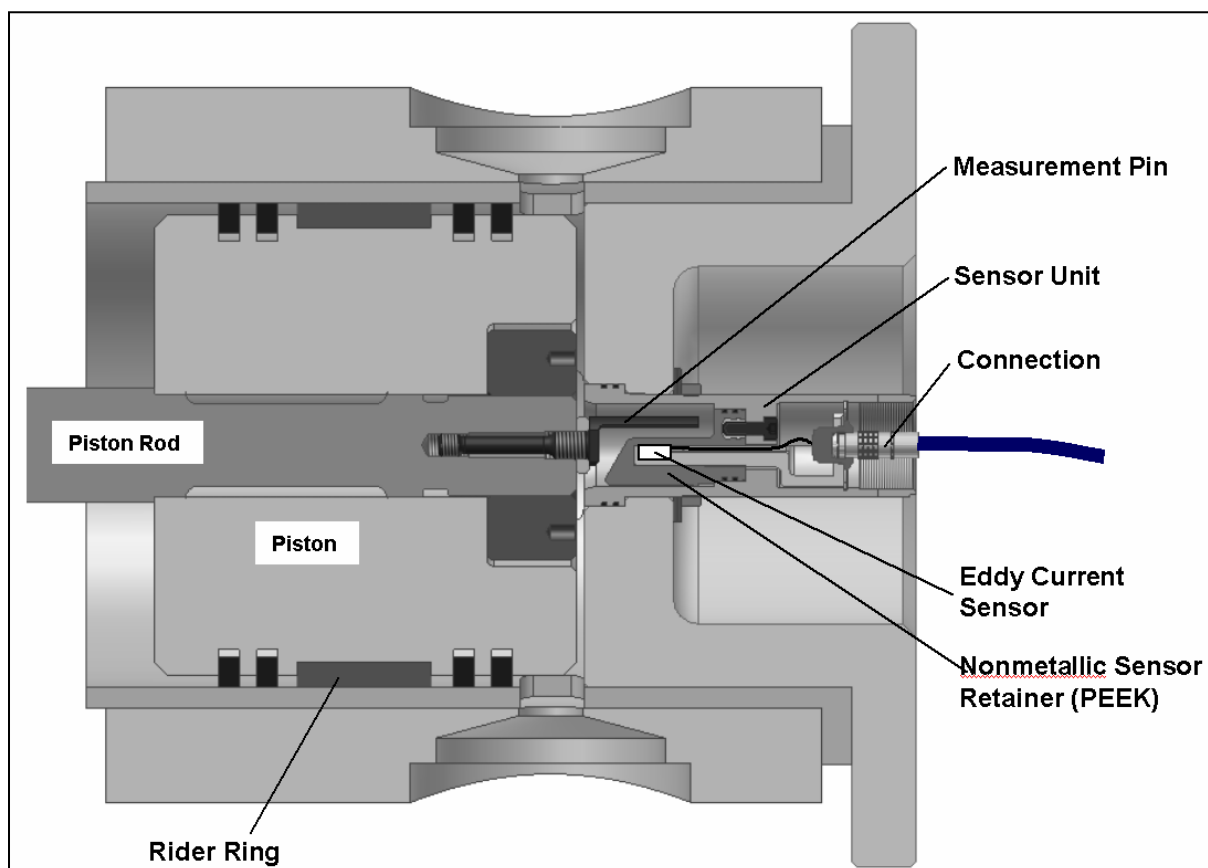


Fig.2: New concept for direct wear monitoring. Sensor unit located in the cylinder cover and measuring pin mounted on the piston rod.



compression chamber like pressure or temperature or due do assembly problems like cable connections, like non applicability for Ex- certification, lack of corrosion or temperature resistance and many more. In [3] possible measuring principles for direct wear measuring are compared and a system is presented for the installation in the cylinder liner on basis of a capacitive sensor. With capacitive systems pollution has a serious impact on the signal. Besides merely technical problems also problems of acceptance which would e.g. surely be connected to cables in the compression chamber even make the challenge more difficult.

Also for very promising most modern technologies based on SAW-sensors (Surface Acoustic Wave) [2] the basic applicability is undermined by factors like limited resistance against pulsating gas pressure, corrosion attack and difficulties with cable connections.

### 3 New concept for direct wear monitoring of rider rings

The difficult challenge of a gas tight, temperature resistant, corrosion resistant and pressure fluctuation enduring measuring sensor and the respective cable connection can be solved by decoupling the tasks and/or positioning of the measuring sensor outside the gas flooded chamber.

#### 3.1 Design

A system which is designed this way is favorably located in the cylinder cover due to the given construction of existing compressors. Fig. 2 and Fig.3 showing the design and installation in the cylinder cover. A measuring pin which is shaped to the needs of the measuring method is screwed into the piston rod and correctly aligned. The sensor unit is installed in the cylinder cover. It detects the vertical position of the measuring pin when it plunges into the sensor unit.

The sensor unit is installed in the cylinder cover and seals with two O-rings and a soft iron sealing to the outside. It is fixed with a nut and a package of disc springs. Inside the sensor unit made of chromium steel there is the sensor retainer made of reinforced PEEK. Due to the sealing between sensor retainer and the metal sensor unit, the sensor is not in the gas flooded area and accessible from outside.

#### 3.2 Components

The sensor used is based on an eddy current sensor with increased measuring accuracy and extended

measuring range. The construction of the sensor has been developed in accordance to the application with emphasis on sufficient pressure resistance. That has been achieved by choosing a sensor design which enables the transfer of high compressive stresses and thereby acting as a structural support to the nonmetallic sensor retainer, especially for the wall separating the compression chamber and sensor. Due to the design optimized by finite element analysis (FEA) the stress level in the sensor retainer is reduced to uncritical levels with attention on the prevention of tensile stresses.

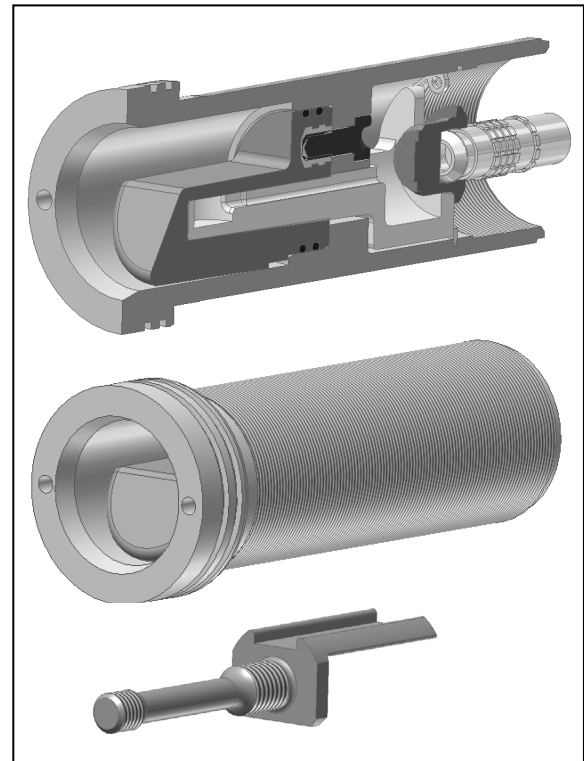


Fig.3: Different views of the sensor unit and one possible design of the measuring pin.

The measuring pin has an angular shape with flat underside in its front. The rear design depends on the type of fixation. Depending on the piston rod geometry there are different systems (based on an extension bolt, clamping ring,...) for utmost dynamic safety. The shape of the measuring pin is defined by the requirement for high measuring accuracy with lowest possible outer diameter of the entire sensor unit.

#### 3.3 Function

The system monitors the vertical shift of the piston position relative to its starting position. Due to the geometric situation this shift of position is directly

correlated to the change of the gap between piston and liner.

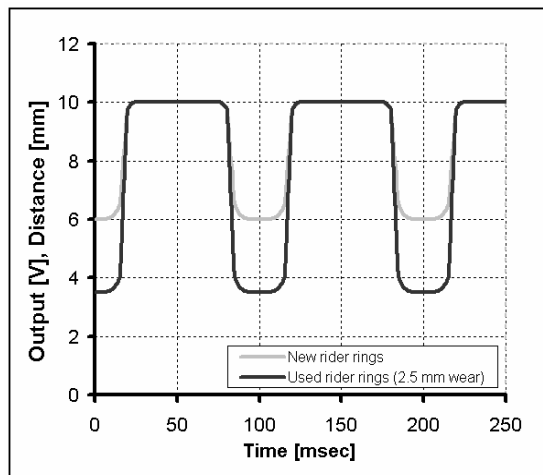


Fig.4: Typical output signal for a new and used rider ring.

The positioning measurement takes place in the upper dead center area. As soon as the pin moves into the sensor unit, there is a rapid change of signal (see Fig.4). With increasing depth the signal approaches a threshold level and remains constant when the pin overtravels the sensor. After reversal of the movement in the dead center the measuring pin is moved out of the sensor unit and the signal decreases.

### 3.4 Performance of the system

Due to the measuring position the change of the remaining gap between piston and liner is monitored directly. The shape of the measuring pin together with a customized eddy current sensor gives a measuring accuracy lower than 0.03 mm thus permitting a reliable estimate of wear situation and wear rate.

The installation in the compression chamber exposes to higher temperature changes which are caused among others by changes in operating conditions or by compressor control. Temperature influences are automatically detected by the sensor unit and are compensated without external interference. Thus reliable measuring results can already be obtained at first assembly independent of temperature.

As the sensor unit communicates with a measuring pin of standardized geometry, the system supplies first informative results immediately after assembly. Calibration on site is not necessary (Plug and Play).

The pressure resistant execution permits an application for pressures up to 200 bar and

temperatures up to 200°C. The selection of corrosion resistant and anti-ageing materials like chromium steel and PEEK allows an application in chemically aggressive environment.

### 3.5 Assembly situation

Direct wear monitoring within the compression chamber requires interference with single components of the compressor or even their reconstruction in order to simplify installation in new units. The problem of fixation and securing of the measuring pin can be solved by selection of the adequate fixation type depending on the piston rod geometry. The assembly of the pin takes place after the installation of the piston and its final connection to piston rod and cross head. Also the adjusting of the clearance between piston and cylinder cover has to be finished as there must not be any turning of the piston after assembly and adjustment of the measuring pin.

The measuring pin is screwed into the prepared thread (see Fig.2 and 3), depending on the type of fixation selected, it is adjusted in its position and then fixed by the safety nut. Apart from this type of assembly other mounting possibilities with utmost dynamic safety are available as well. A centric recessed bore is machined into the cylinder cover for installing the sensor unit. Due to the special design of the measuring pin and the sensor unit, the outer diameter is only 45 to 50 mm. A pin with circular cross section or a cylindrical extension of the piston rod would result in a total outer diameter of more than 75 mm for the same signal quality.

The entire sensor unit is inserted into the cylinder cover, correctly aligned and fixed. After the assembly of the cylinder cover at the compressor, the system is immediately ready to operate after plug in.

In case of cylinder cover cooling there are several API- confirm installation variants available, apart from the general question whether such a cooling is necessary [5]. For new compressors the preparatory installation of a pipe, welded or casted, would be favorable and cost efficient.

### 3.6 Integration into process control systems

For the analysis of the measured signal in a distributed control system (DCS) two types of signals are available: a real-time signal as shown in fig.4 as well as an already calculated single distance value which can directly be attributed to a wear value.

Basically four different types of installation on a compressor are possible:

- Integration into HOERBIGER HydroCOM CCM with condition monitoring platform via the field bus line with alternative use of the real-time signal or the measured distance value.
- Integration into existing process control systems by using the measured distance value (0 to -10V)
- Stand alone unit with or without continuous display
- Offline unit where only pin and sensor unit are installed and data acquisition is done by portable electronic units.

The processing of signals in a process control system permits the utilization of the full functionality. This allows the estimation of the wear situation, trending and calculation of the remaining service life. Also the installation of an offline version without process control system may be a good alternative, especially for remote compressors where wiring would cause enormous expense. By monitoring the wear condition via a portable system the full performance of the system can be used.

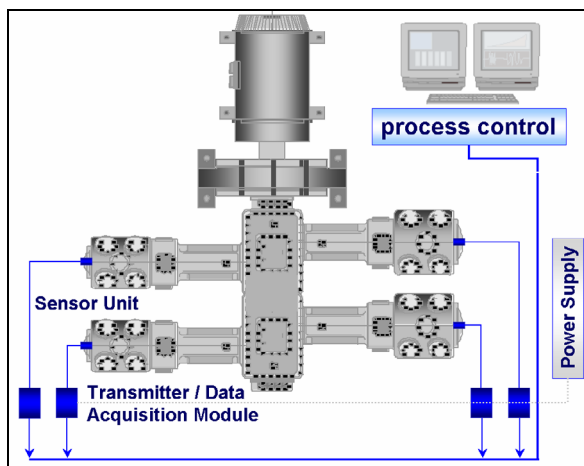


Fig.5: Installation scheme for a direct wear monitoring concept located in the cylinder cover and integration into process control system.

## 5 Conclusions

Reciprocating compressors are critical components in the process, gas and oil industry. Safeguarding the compressor availability is of essential

importance, especially where no backup machines are installed.

In process gas machines with usually horizontal opposed cylinder configuration rider rings are used to support the weight of the piston and rod. The wear situation strongly depends on the operating condition and material composition. By the trend to non-lube operation the service life is reduced substantially so that the rider ring wear is often the main reason for compressor shutdowns. The modern industry tends toward a forward planning condition oriented maintenance strategy and requires - apart from precise information on the wear situation - reliable trending of wear rates depending on operating conditions in order to optimally plan service intervals and to avoid unforeseen compressor shutdowns.

The customer demands in regard to accuracy and reliability can only partly be fulfilled by non direct wear monitoring systems like rod drop measurements in the intermediate piece. Direct wear monitoring inside the compression chamber requires highest resistance of the sensor system, electronics and cabling against temperature, gas corrosion and pressure.

The presented monitoring concept allows the direct detection of vertical position changes of the piston in the upper dead center position. Due to the direct correlation between the piston drop and the gap between cylinder and liner a reliable estimation of the real wear situation is possible. By locating the sensor unit in the cylinder cover and mounting a measuring pin on the piston rod the gas flooded area in the compression chamber can be separated from the electronics and the sensor. This can be achieved by using a customized sensor retainer design. Thereby the problems of corrosion, contacting and cabling are solved. The high pressure resistant execution of the sensor retainer and the tailor made eddy current sensor permit the usage in high differential pressure and temperature applications.

Due to the sensor position and the used sensor system, signals with highest accuracy are provided which gain clear insight into the actual wear situation and allow trending and the calculation of the remaining service life. Temperature influences caused by the sensor position are detected and compensated automatically within the electronic data acquisition system. This also applies to temperature changes initiated by process variations.

The interaction between the sensor unit and a measuring pin with standardized geometry

supported by high electronic accuracy makes any kind of on site calibration obsolete.

A straightforward integration of the signals into a process control system allows the utilization of the entire functionality of the system. Beside a standalone configuration a installation option without cabling is possible. For this purpose a portable data acquisition is used to check the actual wear situation.

## 5 Literature

[1] Machu G., Radcliff C.; Rod dynamics of reciprocating compressors; Internal development report, not published, 2003

[2] EP 09 77 017

[3] Koop L.G.M.; A new approach for reciprocating compressor wearband thickness detection; IMECHE 1999, C556/010/99

[4] Wolf K.; Leistungsfähigkeit von mobilen Online – Diagnosesystemen – eine Studie; 6. Workshop Kolbenverdichter KÖTTER; 2002

[5] Kaeyser C.C.H.; Kühlung der Verdichterzylinder – Wahrheiten und Unwahrheiten; 6. Workshop Kolbenverdichter KÖTTER; 2002



## Operation and Maintenance

---

J. Lenz, A. Brümmer / KÖTTER Consulting Engineers

- **Trouble-Shooting in a natural gas compressor plant**

H. Stehr, M. Pavlevski, N. Divadkar / Hoerbiger KT Asia Services

- **Process know-how and the effects on product design and engineering**

M.I.Comyn et al. / ExxonMobil International Limited

F. Boer / Thomassen Compression Systems bv

- **Reliability experienced with offshore reinjection compressors**

A. Rumpold / HOERBIGER Ventilwerke GmbH

- **New technologies pave the way for on-line CCM systems becoming standard for reciprocating compressors**

E. Drewes / PROGNOST Systems GmbH

- **Improved high speed safety protection for critical compressors**





# **Trouble-Shooting in a natural gas compressor plant**

by:

**Dr. Johann Lenz**

**Dr. Andreas Brümmer**

**KÖTTER Consulting Engineers**

**Rheine, Germany**

**Reliability and economics of compression systems -  
recent trends in the market of  
reciprocating compressors  
March 27<sup>th</sup> / 28<sup>th</sup>, 2003 Vienna**

## **Abstract:**

Inadmissibly high vibrations had occurred in the main pipelines between the discharge-side pulsation dampers of a newly installed natural gas compressor. A duly conducted measurement analysis of the reason for these vibrations indicated that they were caused by strong pressure pulsations in the cylinder rooms and in the downstream connection pieces to the pulsation damper vessels. A direct link between these pressure pulsations and the mechanical vibrations was found in the region of the double-acting cylinders. The mechanical natural frequency of the connected pipe bends also added quite considerably to the amplitude of the vibrations. Two recommendations were adopted in parallel in order to reduce the vibrations. First pulsation damper plates were installed directly on the gas-outlet flange of the cylinders to reduce the pressure pulsations. The influence of the pulsation damper plates on the compression process in the cylinder room and the unsteady flow were modelled theoretically. Then the mechanical natural frequency of the pipeline was displaced upwards out of the critical frequency range. Proposed designs for a reinforcing system were examined and checked using the Finite Element method. Finally, the manufacturer carried out a measurement investigation confirming the effectiveness of the measures adopted and the safety of the plant in operation.

## 1 Introduction and problem definition

Germany operates over forty underground natural gas storages to cover demand peaks in the consumption of natural gas. Reciprocating compressors are often used to charge the gas into these storage sites, because they are highly efficient and can cater for the variety of different operating conditions encountered.

Despite having conducted acoustical and mechanical pulsation studies of the compressor and the connected pipelines, greatly increased vibrations occurred in the connection lines between the discharge-side pulsation damper vessels, when a two-stage natural gas reciprocating compressor having a total power output of 7 MW was put into operation. The cause of these vibrations could not be subsequently explained by the studies.

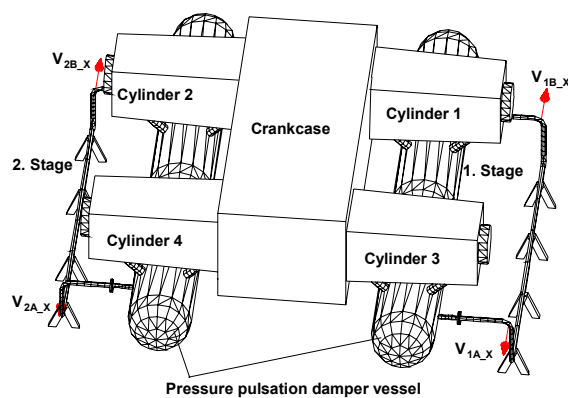


Fig. 1: Schematic diagram of reciprocating compressor, discharge pressure pulsation damper vessels, connection lines and the four points, at which vibrations were measured.

## 2 Measurement investigation

The first measurement of vibration rates made at the pipe bends in the modified version of the system shown in Fig. 1 exceeded the manufacturer's admissible standard levels several times over.

Therefore at the same time pressure pulsations and vibration rates at cylinder no. 4, at the pressure-pulsation damper vessel connected to it and in the pipe bends were recorded selectively for further analysis (Fig. 2).

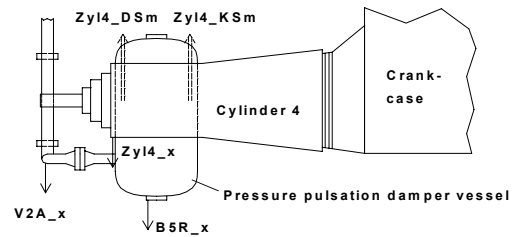


Fig. 2: Position of measurement points for detailed analysis of vibrations at cylinder 4.

Fig. 3 shows portions of the signals measured at cylinder 4 when running up and when operating the compressor plant. The cylinder room (Zyl4\_KS m) at the crankshaft end was shut off by controlled valve-suppression, when this measurement was taken.

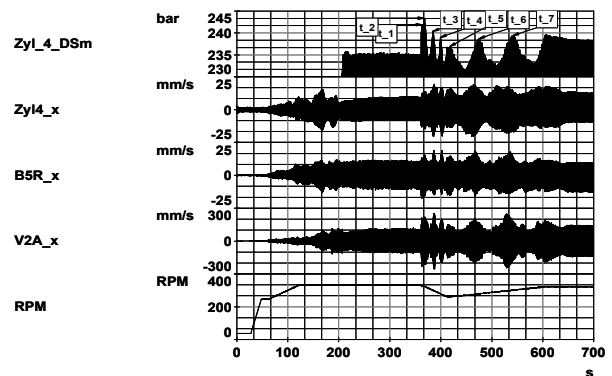


Fig. 3: Simultaneously recorded vibrations and pressure developments at cylinder 4.

The chart shows the development of cylinder room pressure on the cylinder end, vibration rates at different measurement points and rotational speed extending over a period of about 11 minutes from plant start-up. Especially at pipe bend  $V_{2A\_X}$ , there is no recognisable increase in vibration at the measurement points, when the plant is running up ( $t = 40 - 60$  s), so the likelihood of vibration being excited solely by the inertia force of the compressor can be ruled out. Once pressure has built up in the cylinder room ( $t > 200$  s), however, continuously increased vibrations of about  $V_{2A\_X} = 100$  mm/s become evident at the pipe bend measurement point. The compressor is run at its rotational speed in the period  $t > 360$  s (other operating conditions remaining constant), this being accompanied by a marked instance of short-time increases ( $t_1$  to  $t_7$ ) in cylinder-space pressure and in vibration rate at the measurement points shown.

Colour charts of the amplitude spectra of the vibrations were produced to allow more precise examination of the relationship between the increased pressure pulsations and the vibrations. To do this, the recorded time-signal was divided into small, overlapping time sections ( $\Delta t = 1.6$  s), the amplitude spectrum (FFT) for each section then being duly calculated and represented as colour chart (amplitude level identified by colour) along the time-axis. The colour chart in Fig. 4 clearly shows that, at cylinder 4, two separate amplitude increases (58 Hz; 63 Hz) occur at different times along the x-axis. Comparing the times of the maximum increases in cylinder room pressure in the function envelopes in Fig. 3, the 63 Hz amplitude increase is the only one occurring at the same time in each case (Fig. 4). While the order of magnitude of the vibration rates measured at the cylinder is not a cause for concern, those at the pipe bend (measurement point  $V_{2A\_x}$ ) are inadmissibly high, especially the 63 Hz recording (Fig. 5).

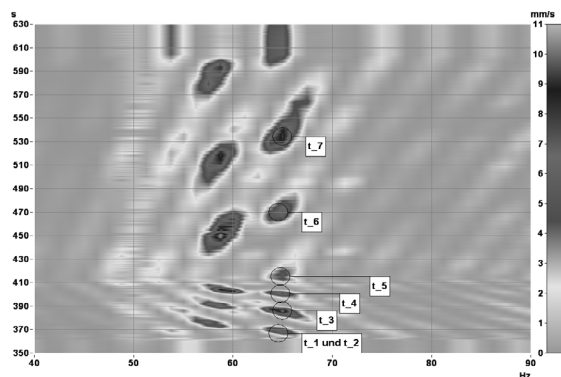


Fig. 4: Colour chart of amplitude spectra for measurement point  $Zyl4\_x$  at the cylinder within the time range  $t = 350$  to  $630$  s (time signal from Fig. 3).

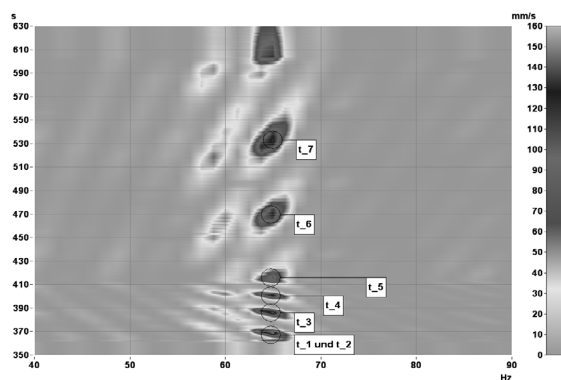


Fig. 5: Colour chart of amplitude spectra for measurement point  $V_{2A\_x}$  at the pipe bend within the time range  $t = 350$  –  $630$  s (time signal from Fig. 3).

There is a striking increase in vibration between cylinder and pipe bend (compare scale of Fig. 4 and Fig. 5).

To arrive at an explanation of this increase in amplitude, the natural frequency of the pipe bend was analysed with the compressor plant at a standstill (Fig. 6).

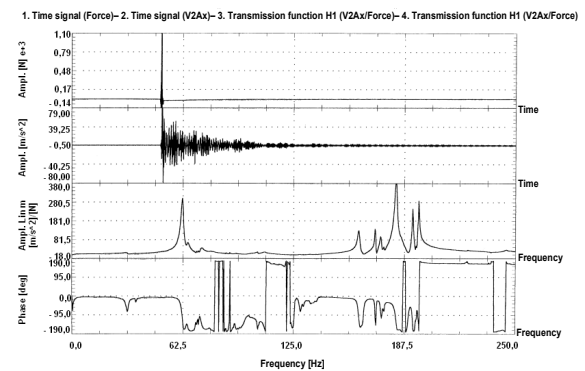


Fig. 6: Transfer function of acceleration signals of a force impulse excitation.

Excitation was produced by means of an impulse hammer at measurement point  $V_{2A\_x}$ , at which the acceleration response was also recorded along the x-axis in each case. An amplitude increase occurs at about 62 Hz, accompanied by a  $180^\circ$  phase-shift between excitation and response signal. Accordingly, the increase in operational vibration between cylinder and pipe bend is caused by a mechanical natural frequency, thus disclosing the transmission path of vibrations emanating from the cylinder. To ascertain the cause of the cylinder vibrations, the measured development in cylinder room pressure from Fig. 3 at the maximum point ( $t_2 = 368.2$  s) and at the succeeding minimum ( $t_2^* = 375.6$  s) are plotted over time in Fig. 7.

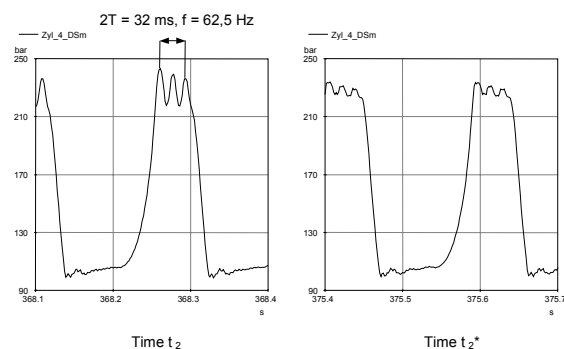


Fig. 7: Measured pressure pulsations at 330 rpm ( $t_2$ ) and 300 rpm ( $t_2^*$ ).

Pressure pulsations of up to 25 bar peak-to-peak (depending on rotational speed) occur at a frequency of  $f = 62.5$  Hz in the process of exhausting the natural gas (Fig. 7). These pulsations are the actual cause of the increased vibrations, which are transmitted mechanically from the cylinder, through the pulsation damper vessel, to the pipeline. The pulsation is excited by an acoustic natural frequency in the intermediate pipe (the connection between cylinder and pressure pulsation damper vessel), when it coincides with higher-harmonic frequencies of the rotational speed. The same effect was also found to exist in the other cylinders of the compressor.

The acoustic natural frequency in the intermediate pipe can be subjected to a simplified theoretical examination in isolation. The acoustic marginal conditions (open - closed) produce an natural (resonant) frequency at  $\frac{1}{4}$  the wavelength. When the temperature of the natural gas and the real gas factor are taken into account, the result is a calculated frequency of about 68 Hz, which correlates with the effects ascertained through measurement.

### 3 Recommendations

Reduction measures were necessary for two reasons. In the first instance, the measured pipeline vibrations of over 100 mm/s eff. caused additional dynamic stress capable of resulting in damage to the pipeline. Secondly, the pressure pulsation in the cylinder room resulted in not inconsiderable dynamic strain on the drive unit. These additional loads correspond to a weight of about 10 tonnes, applied to the piston rods at a frequency of 63 Hz.

Accordingly, a combined approach to an effective reduction of the vibrations was proposed and implemented to make sure the plant would operate safely and reliably. Pulsation damper plates were to be installed with the intention of dampening the exciting pressure pulsations, and at the same time, the natural frequency of the pipeline was to be moved out of the excitation range by providing a dynamically stable support. Operational requirements made it essential to rectify the critical situation in the course of a once-off modification.

#### 3.1 Installation of patented KÖTTER pulsation damper plates

The crucial need was to introduce a means of reducing the pulsations inside the cylinders and in the connection pipes to the discharge-side pulsation dampers that, while producing the desired acoustic

effect, would result in hardly any loss of pressure. The plant compression levels guaranteed by the manufacturer would otherwise cease to be maintainable.

The decision was therefore taken to replace the existing orifice plates fitted on the discharge-side cylinder flanges with patented “pulsation damper plates based on the KÖTTER principle”. The unsteady, compressible, viscous compression and gas flow in the compression room and in the connection pipes was simulated numerically with a view to ensuring that the modifications would duly achieve their purpose. The simulation was based on the one-dimensional Navier-Stokes equation, the equation of continuity, the energy equation and the equation of state.

This system of partial non-linear differential equations can be converted by a transformation of coordinates to lines of indeterminate cross-derivation - so-called characteristics - to produce conventional differential equations.

The flow field is then numerically integrated along the characteristics by means of a space-time discretisation. Marginal conditions used in the simulation were the known speed of the piston and a constant pressure in the discharge-side pulsation damper vessel, in which (as substantiated by the measurements) only faint traces of interfering pulsations at a frequency of 63 Hz were still to be found. Allowance was also made for the opening and closing of pressure valves as a function of flow ratios.

To begin with, the original system including its orifice plates was modelled for the purpose of validation. Fig. 8 illustrates the measured indicator diagram together with the calculated, time depending pressure at the discharge-side cylinder flange.

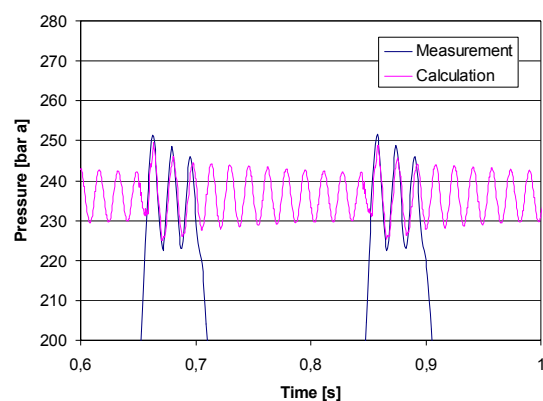


Fig. 8: Measured indicator diagram and calculated pressure inside the connecting pipe in original state.

It can clearly be seen that each time the pressure valve is opened (accompanied by the associated, abruptly beginning mass flow), a feebly dampened acoustic natural frequency is excited in the cylinder room and in the connection pipe. This acoustic resonance is responsible both for the increased strain on the drive unit and for the inadmissibly high pipe vibrations. The amplitude of the gas vibration is very decisively determined here by favourable or unfavourable coincidence between the opening of the valve and the phase angle of the acoustic resonance (see Fig. 7).

The pulsation damper plate (Fig. 9) was then incorporated into the design model as the second stage of the simulation.



Fig. 9: Gas inlet side of patented “pulsation damper plate based on the KÖTTER principle” fitted to cylinder output flange of second stage.

While only one parameter can be varied in an orifice plate (namely the diameter of the plate), the pulsation damper plate offers many adjustment options. Apart from providing a choice of number of bore holes, hole pattern and bore-hole diameters, the venturi-like openings of this plate can be formed “at will”, so the pulsation damper plate permits optimisation of acoustic or flow-conducting characteristics without additional loss of pressure.

Fig. 10 illustrates the outcome of this design process with the calculated time depending pressure at the discharge-side cylinder flange with pulsation damper plates installed. The measured indicator diagram after implementation of the modification is included in the figure for comparison purposes.

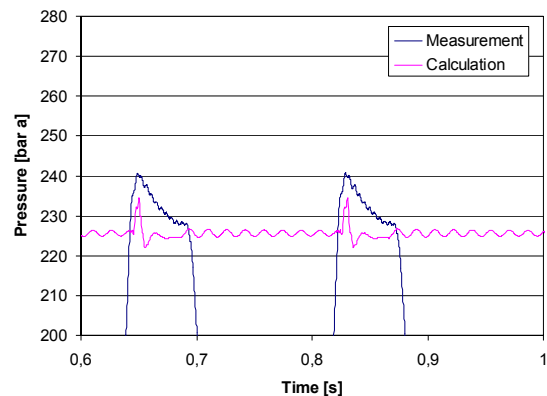


Fig. 10: Measured indicator diagram and calculated pressure inside the connecting pipe with pulsation damper plate installed.

The theoretically ascertained satisfactory effect of the pulsation damper plates is confirmed by subsequent measurement. There are no more significant gas vibrations to be found in the indicator diagram either. The above-mentioned additional strain placed on the drive unit by alternating pressure loads on the piston has been eliminated by this means, and the alternating pressure amplitudes in the connection pieces have also been distinctly reduced. However, it can still be seen that the measures adopted have only slightly increased the degree of acoustic damping provided, when the pressure valve is closed. The reason for this is the predetermined installation position of the pulsation damper plate.

The only usable flange was located directly at the cylinder, which means that the pulsation damper plate is sited at the acoustically closed end, when the pressure valve is closed.

### 3.2 Additional stiffness and damping in the region of the pipe bend

Furthermore, to make sure that the critical vibrations would no longer be excited by the pulsations still present in the connection pieces, the natural bending frequency of the pipe bends and pipe sections was displaced to a higher frequency ( $> 70$  Hz) by means of an additional ‘A’ support, and broadband damping was incorporated. Because of the high temperature of the gas and the pipeline, a special means of connecting the support (Fig. 11) was chosen for the region of the pipe bend (at the positions of the measurement points in Fig. 1).



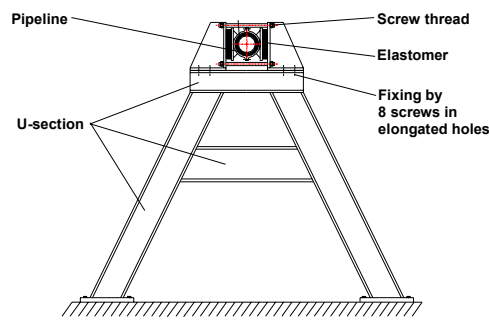


Fig. 11: Additional 'A' support as modification of pipeline section.

The elastomer coating shown in Fig. 11 is arranged without direct structure-borne noise bridges in such a way that the actual surface pressure of the elastomer (a decisive dynamic parameter) can be adjusted and optimised in situ by altering the tightening torque of the four bolts. Compared with conventional elastomer inserts, which are inserted directly between pipe and pipe clamp, the heat convection inherent in this design tolerates higher temperatures at the outside of the pipe.

Since the elastomer coating employed can only be used up to about 90°C, the design in question was essential in the present case to provide for additional dissipation of heat.

A Finite Element calculation was performed in advance to optimise the dynamic characteristics of the intended pipe connection. The Finite Element model (FE) of the original pipeline section was adjusted with reference to the measured characteristic shape, thus making it possible to allow for the influence of the actual marginal conditions of the pipeline in a simplified FE model (bar model).

Fig. 12 shows the calculated mode of the first bend in the pipeline with the optimised 'A' support and the elastomer connection. Then the natural frequency is displaced upwards by 30% as a result of this modification. The critical factor determining the position of the first natural bending frequency is the dynamic stiffness or rigidity of the elastomer.

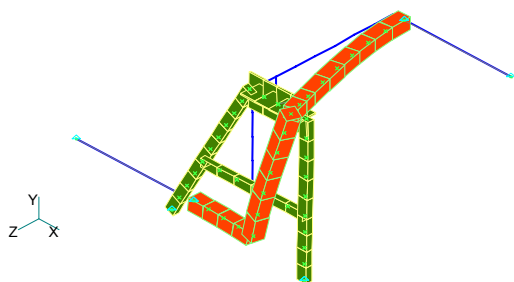


Fig. 12: FE model with 'A' support and elastomer, first natural bending frequency 79.4 Hz.

## 4 Checking the modifications

In conclusion, the work of modification was followed by an examination of the measures implemented. To do this, the manufacturer arranged a detailed measurement of vibrations within the whole system at different operating points of the compressor plant, so as to rule out the possibility of any localised displacement of the pipeline vibration problem to other points. At an effective value of 15.5 mm/s, the maximum vibration rate measured in the process was well below the admissible standard value of 28 mm/s eff. The measurements also failed to disclose any relocation of the vibration problem.

Renewed measurement of the natural frequency of the first characteristic bending form or shape indicated a frequency of 83 Hz in the pipeline with 'A' support. In the light of the simplified FE model and the normal deviation of elastomer characteristics from manufacturer's specifications, this indicates good compatibility and confirms the validity of the procedure described above. The results of an additionally conducted measurement of operating vibrations at measurement point  $V_{2Ax}$  in the modified system are shown in Fig. 13 for the purpose of comparison with the measured vibrations of the original system.

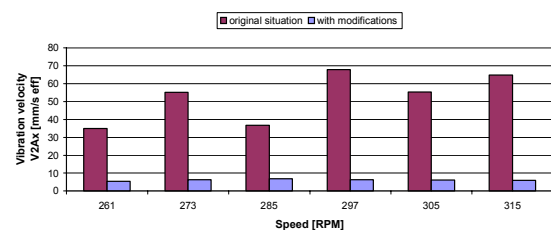


Fig. 13: Measured pipe bend vibrations in original situation and following modification.

The comparison of the vibration situation before and after modifications impressively confirms the effectiveness of the measures adopted. A final examination of power loss attributable to the pulsation damper plates also demonstrated the precision employed in designing for pressure loss at the compressor output.



## **Process know-how and the effects on product design and engineering**

by:

**Harald Stehr, Michael Pavlevski and Nitin Divadkar**  
**Hoerbiger KT Asia Services**  
**Singapore**

**Reliability and economics of compression systems -  
recent trends in the market of  
reciprocating compressors  
March 27<sup>th</sup> / 28<sup>th</sup>, 2003 Vienna**

### **Abstract:**

In the past, the main focus with the design, engineering of compressor components and the key wear parts was sitting within rather narrow and set boundaries around the actual machine, neglecting the peripheral process environment, acting upon the compressor. However, the plant environment as a whole yields the most critical effects like catalyst debris, chemical reactions or liquids influencing the compressors reliability and plant availability. Based on the shared inputs of process experts in refineries, chemical industries etc, together with in house applications know-how. A direct link between the overall process information, the product specifications and the compressor operation has been generated and included in daily engineering standards. As an outcome of this holistic approach different projects, not only carried out to optimize the compressor and plant availability, but also to increase overall process efficiency are described. The projects were related to the re-design and optimization of compressor cylinders and wear parts for HDPE and LDPE processes, and to optimize a RDS process using a special control scheme and hardware.

## 1 Introduction

Product development, design and engineering of reciprocating compressors and equipment has in most cases been addressed using given operating parameters like

- compressor design information (RPM, bore, stroke, clearance, ...)
- gas data (pressures, temperatures, ...)
- gas composition

However, the compressor is integrated in a process environment and is therefore strongly influenced by process conditions and influences the stability and flexibility of the process likewise. Due to unforeseen influences depending on upstream piping, reactors or catalysts the actual operation may strongly deviate from the design condition giving unexpected operating conditions. An example may be: Dirt in the gas may lead to fouling of components (cf. Figure 1) and consequently to a reduction of performance and lifetime.



**Figure 1: Fouling of a compressor valve.**

Often different processes by various licensors, even operating different gases show similar effects. Examples for process related effects are:

- Presence of condensate  
In recycle stages the gas usually is in saturated condition. Due to light molecular weight and low drag forces, the gas cannot entrain the liquid and consequently the liquid accumulates within the piping of the compressor. Reaching a critical level liquid slugs pass through the compressor and cause high load on the compressor valves or sealing rings. The transfer film of cylinder and packing rings required for low friction and wear is washed away leading to increased wear rates.
- Oil and debris  
In order to avoid wear of cylinder and packing rings compressors are often

operated at high lubrication rates causing increased loads acting on compressor valves mainly from sticktion effects. In case of flow regulation of compressors the amount of oil within an idling cylinder accumulates even more. Recycle cylinders often receive debris from the catalysts and other process components thus increasing wear and reducing the mean time between failures.

Since in many refineries the reciprocating compressor is often treated as a “black box” the compressor may be operated far from its design conditions, additionally causing load on reciprocating compressor equipment.

Thus analyzing the common processes with respect to understand the periphery of the compressor gives additional information to ensure that the reliability of compressors is optimized. Furthermore, using new equipment (e.g. HydroCOM) to control the operation of the compressor also the flexibility of operating the whole process within a plant can be enhanced.

## 2 The approach to process know how

A roadmap has been drawn from general industrial areas to pure technical parameters like gas properties and operating ranges. Within this analysis the main focus has been set on describing the process environment and identifying process parameters that do influence the operability of reciprocating compressors and their components.

The main areas of applications have been identified as

- Air (e.g. PET bottle blowing)
- Gas (e.g. Recovery of Carbon Monoxide – HYCO)
- Industrial Gas (e.g. Oxygen)
- Natural Gas (e.g. Natural Gas refueling stations, CNG)
- Oil Refining (e.g. Continuous Catalytic Reforming – CCR)
- Petrochemical and Chemical (e.g. Polypropylene)
- Refrigeration (e.g. Industrial Cooling)

In all the examples given above the operation of reciprocating compressors is strongly influenced by process parameters. As examples may be given:

Process	Examples for critical process parameter
PET bottle blowing	unloading/regulation cycles
Carbon Monoxide - HYCO	carbon particles
Oxygen	temperature, explosiveness
CNG	High pressures, condensate during de-pressurization
RDS	high amount of liquids and dirt, flow control
Polypropylene	chemical reactions
Industrial Cooling	Condensate

**Table 1: Critical process parameters.**

## 2.1 Detailed process analysis

Within the description of the different processes key indicators for a successful operation of reciprocating compressor components are defined. Especially of interests are

- compressor lubrication
- gas conditions (condensate)
- process line (make up or recycle lines)
- chemical reactions
- compressor capacity control to optimize the process

## 3 Process Know How and Failure analysis

Compressor components often have typical failure modes that are also strongly related to the process the compressor is working in. Putting together the results of failure analysis investigations with the information about process environment, the product design as well as the engineering parameters can be adjusted in order to ensure an increase of the safety margin of operation.

### 3.1 Wear parts failure modes

Classical failure modes of sealing elements are breakage, pitting or delamination of valve sealing elements due to excessive opening or closing impacts caused by sticktion effects. In addition highly localized loads, e.g. due to liquids passing through the valves, result in breakages of inner webs and forced rupture of rings. Examples for failures are given in the Figures below.



**Figure 2: Impact failure of a valve plate caused by sticktion.**

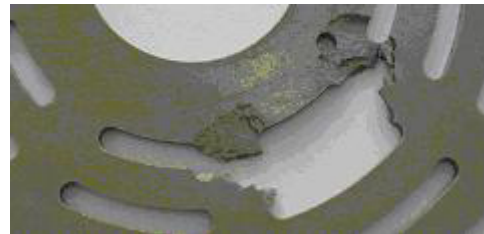


**Figure 3: Failures of a sealing element due to liquids.**

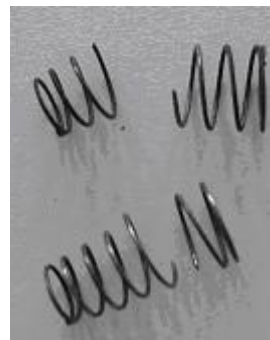


**Figure 4: Spring failure due to abrasive wear**

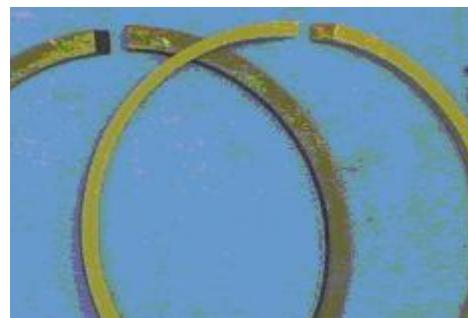


**Figure 5: Wear on cylinder rings**

Evaluating failures matching these conditions on a statistical basis accounting for the operating processes a clear relation can be found. Examples for process related component failures are:

### 3.1.1 Liquids

CCR, HDS, ...: In recycle stages if most processes in refining and chemical applications gas in a saturated condition is compressed. Therefore liquids may drop out of the gas stream and accumulate within the piping. After reaching a critical level the liquids are carried over the compressor valves into the compression chamber. Besides causing additional load on the compressor valves the liquids also wash away the so-called transfer film on piston rods and cylinder liners needed for low wear of gliding surfaces and consequently reducing the life time of cylinder and packing rings.

Liquid problems can also be related to lubricants. Especially for the compression of light gases oil is used to increase the sealing of piston rings. In many case high lubrication rates, especially in regulated compressors cause large amounts of oil passing through the compressor valves as well.

CNG: Natural gas is compressed to high pressures for fueling vehicles. Since the process is intermittent the compressor is de-pressurized in idle times causing the gas to cool strongly and liquids to fall out which may cause problems at restart.

Natural Gas: In case the natural gas application contain heavy hydrocarbins a knock out of liquids occurs. The liquids act as a hydrocarbon solvent disrupting the bonding of the transfer film and consequently leading to increased wear rates.

### 3.1.2 Chemical reactions in processes leading to sticktion problems

BTX Aromatics: During the production of benzene, toluene and xylenes via the aromatization of propane and butanes, usually carried out in lubed units sticky substances like tar cover the compressor valves and cause sticktion effects.

Polypropylene (LDPE): In primary compressors polymer-grade ethylene is boosted to 300 bar. The gas, together with recycle gas stream, is compressed to the reactor pressure in a secondary compressor. Above 100°C polymerization effects take place and cause sticktion together with usually high lubrication rates in the high-pressure stages of the primary compressor. Aluminum oxide particles

from the catalyst cause wear on cylinder and packing rings.

### 3.1.3 Chemical reactions in processes leading to wear problems

HYCO: Recovery and purifying CO for the use as a chemical feedstock. A dry adsorption process recovers Purified CO. The compressed gas usually has a low dew point (bone-dry) and contains abrasive carbon particles. Additional carbon particles drop out at 150°C. This caused abrasive wear on contact surfaces of sealing elements, valve springs, cylinder and packing rings. Due to the dry gas even wear on metallic surfaces gets critical as soon as the oxide layer is worn through and may not recover. Valve springs may fail or cause heavy wear in the guard.

## 3.2 Chemical reactions on wear parts

### 3.2.1 Corrosion

In case corrosive gas components (e.g. Sour gas, Chlorine) are part of the process standard materials start to deteriorate causing weakened strength and potentially shortened lifetime. Especially if the gas feed changes critical components may not be known and thus leading to unexpected failures.

### 3.2.2 Special chemical reactions

In case of so-called "Wet PET" application – where the compressed air contains humidity- deterioration of standard cylinder ring material (PTFE with multi fillers including Co and Mo) takes place. Figure 5 shows a ring covered with a green powder causing increased wear rates.

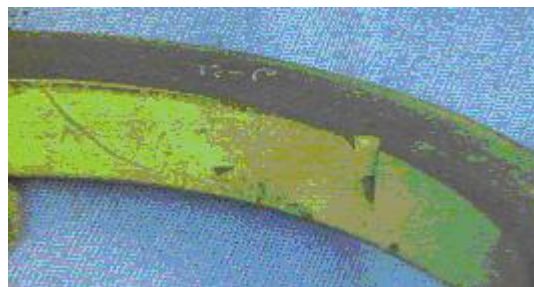


**Figure 6: Abrasive, green deposit (high copper content) on cylinder ring.**

Initial results of the chemical analysis show the material is subject to heavy oxidation, MoS<sub>2</sub> dissociates, Mo is burnt off and copper oxidises leading to the reaction  $2\text{Cu} + \text{O}_2 \rightarrow 2\text{CuO}$



In this special application the standard use of MoS<sub>2</sub> as filler to reduce wear of cylinder rings actually gives the opposite results. Special additional anti-oxidizing fillers have to be used to avoid the chemical reaction.

## 4 Process Optimisation

In many application the processes are controlled using complex schemes of feed gas lines, compressor setups, side stream lines, flare lines and delivering lines to the consuming process unit. Feed gas lines and side streams may also connect to other process segments – all together leading to many constraints of compressor operation in order to satisfy all requirements for pressure and flow constraints.

### 4.1 Standard process schema

The common approach is to utilize standard control schemes for the compressor consisting of on off cylinder regulation and bypass lines to achieve the control logics.

The Figure 6 shows a schema of a Hydrotreating unit that takes hydrogen fresh gas from a PSA (pressure swing absorber) unit. The operation of the PSA is affected in quality and stability within a pressure range within 0.2-0.4 bar.

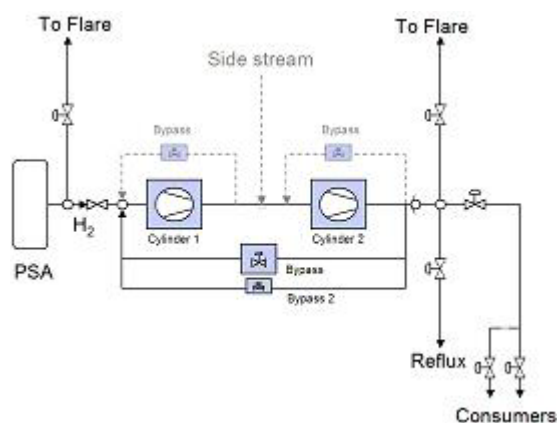


**Figure 7: Schema of a Hydrotreating compressor unit with pressure swing absorber Hydrogen supply.**

In order to keep the suction pressure within this narrow limit two bypass valves are used. Bypass 1 controls the main volume flow through the compressor. Bypass 2 is a faster reacting device used to quickly adapt to pressure fluctuations within the suction duct.

In case a side stream is used to feed gas at a certain pressure into the system the interstage pressure has to be kept constant utilizing e.g. bypass valves via every cylinder. In case of a process trip the gas is

flared first from the discharge line of the compressor, thus wasting energy until further actions to reduce the gas flow are in place.

All together the system is complex and costly, especially accounting for the compression losses utilizing bypass controls.

### 4.2 Optimised process utilizing the HydroCOM control system.

The HydroCOM system enables a full control over the operation of the cuation valves, thus a continuous regulation of the compressor capacity from idle to full load. Since the HydroCOM is capable of regulating different compressor cylinders independently from each bypass loops are not necessary. For fail safe reasons one overall bypass is being kept within the schema. The new layout is shown in Figure 7.

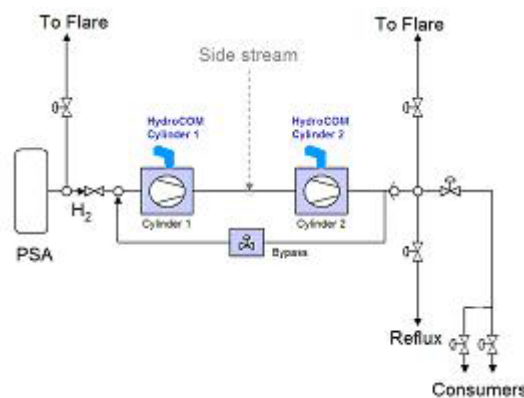


**Figure 8: Schema of a Hydrotreating compressor unit utilizing a HydroCOM system to optimise the process.**

The main points of optimisation can be found within:

- The pressure range required for the PSA system can easily be adjusted.
- The interstage pressure between the compressor sylinders can be adapted to be in line with side stream pressures.
- In case the consumer does not require any gas the gas can be flared at the suction side right from the begin.
- The process equipment can be minimized, thus leading to less incvestment or maintenance costs without sacrificing the control flexibility.
- The consumed energy for compressing the gas can be minized.

## 5 Conclusion

Since the compressor is part of and embedded within a process its operation is affected by the process in the same way the compressor can be utilized to optimise the process conditions.

Ensuring the reliable performance of compressors operating in refineries or chemical processes implies the involvement and understanding of the overall process technology.

Process related operating conditions like catalyst debris, condensation effects or chemical reactions within the gas strongly affect the performance of compressors and compressor parts.

In addition utilizing modern compressor components as the HydroCOM control systems enables a more flexible and reliable operation of the process itself.

All tasks are focused to continuously improve the reliability and the performance as well as to minimize installation, operation and maintenance costs.



# **Reliability experienced with offshore reinjection compressors**

by:

**M.I.Comyn, ExxonMobil International Limited**

**F.Boer, Thomassen Compression Systems bv**

**R.Garza, ExxonMobil Production Company**

**J.S.Hansen, Esso Norge AS**

**I.Bjorkevol, Esso Norge AS**

**G.Wilken, ExxonMobil International Limited**

**Reliability and economics of compression systems -  
recent trends in the market of  
reciprocating compressors  
March 27<sup>th</sup> / 28<sup>th</sup>, 2003 Vienna**

## **Abstract:**

The service history of a pair of medium speed, three stage, reciprocating compressors in offshore re-injection service is described, and the reliability data is presented. The failures which detracted from the reliability, and the corrective measures taken are described. Failed components included pistons, piston rods, piston rings, packings, bearings, valves, o-rings, bolts, instruments, liquid separator vanes and a main drive motor. As production must be deferred whenever the injection compressors are inoperative, to control the flare rate, compressor downtime is uneconomic. Improvements that we would make in the specification of new equipment for similar service are set out.

## Introduction

Esso Norge AS operates the Balder Floating Production Unit (FPU) in the Norwegian North Sea. This turret-moored, ship-shaped vessel produces approximately 60,000 barrels of oil per day (10,000 m<sup>3</sup>/d) and 42 million standard cubic feet per day (1,200,000 sm<sup>3</sup>/d) of associated natural gas. Oil is exported via tanker. Gas is re-injected into the reservoir. The compression equipment, all reciprocating machinery, consists of a single low pressure compressor, two parallel high pressure compressors, and a single fuel gas compressor. This paper concerns only the two high-pressure machines, designated here as HPA and HPB, one of which is shown in Figure 1.



**Figure 1. Balder's C35-4 High Pressure Compressor**

## Production system

Subsea wells are produced via flowlines and risers to the inlet separator, which operates at 8 barg and which separates the crude oil, produced water and natural gas into separate streams for further processing. Gas is fed by a header to the high pressure compressors. Oil is fed to the low pressure separator (operated at 1 barg) where further gas is removed. This low pressure gas is recompressed by the Low Pressure compressor and fed to the high pressure system.

The High Pressure compressors collect gas at 8 barg and compress it to 180 barg. High pressure gas is used for gas-lifting five producing wells. Surplus gas is disposed in an injection well, which provides gas-cap pressure maintenance. There is no sales outlet.

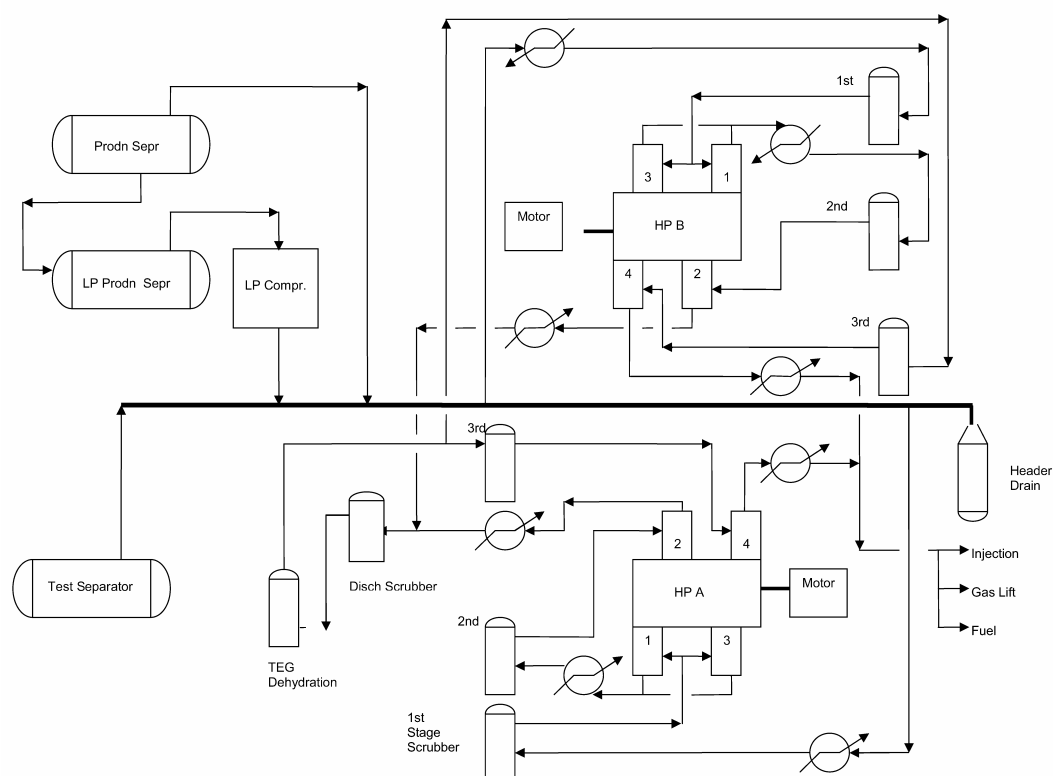
Between the second and third stages of high pressure compression there is a triethylene glycol gas dehydration plant.

Some high pressure gas is further compressed to 330 barg by the Fuel Gas compressor to supply fuel for the four Wartsila Vasa dual-fuel generator sets.

There is a flare system that is designed to accommodate from 0 to 100% of the total gas flow. Any gas not compressed is flared for safety reasons. Pressure is maintained in the gas lines by pressure controllers that relieve excess gas to the flares. Volume of flared gas is kept at a minimum.

A simplified flow diagram is shown in Figure 2.

**Figure 2. BALDER HP COMPRESSION SIMPLIFIED FLOW DIAGRAM**



## HP Compression System

Each compression train takes suction from the common header, which runs overhead, down the FPU centerline. The compressors are fully independent, having all necessary equipment and auxiliaries. The discharge from the second stage of each is married and fed to a scrubber before entering the glycol contactor of the tri-ethylene glycol (TEG) dehydration system. After dehydration, the gas enters the third-stage suction scrubber of each train. It is compressed in the third stage to 180 barg. A portion is routed to the fuel gas compressor, but most is re-injected for gas-lift and reservoir pressure maintenance.

### 1) Machinery Installation

The high-pressure gaslift compressors are identical Thomassen C35-4 motor driven, horizontal, opposed-piston reciprocating compressors, operating four double-acting cylinders in three stages of intercooled and scrubbed compression. These are located on the production deck (above the main deck) of the FPU. Motors are air-cooled, 11 kv, 3300 kw Alstom machines operating at 508 rpm, which drive through a Vulcan flexible membrane coupling.

Each stage is supplied with a suction scrubber, intended to remove condensates (oil and water), a permanent suction strainer, and pulsation dampeners (suction and discharge). The suction of each stage is cooled in a gas-cooler circulated with a liquid cooling medium. There are two first stage cylinders and one each of the second and third stages. Stage data are included in Table 1. The two units have a rated total flowrate of 51250 standard cubic metres per hour at 508 rpm.

### 2) Service History

The principal events are listed in Table 2.

**Table 1. Compressor Stage Data**

HPC (2 units) 926- KB01A/B. 51250 standard cubic metres per hour total flowrate. 508 rpm

Stage	Suction	Discharge	Cylinder configuration
	Press/Temp (Barg / C)	Press/Temp (Barg / C)	
1	8.5 / 60	27 / 145	2 - 410 mm x 290 mm
2	27 / 50	72 / 144	1 - 310 mm x 290 mm
3	72 / 42	184 / 121	1 - 190 mm x 290 mm

## 3) Failures and Correction

### 3.1 Failures - February 2000

From commissioning the units were fraught with frequent trips. Many were associated with high scrubber levels. Demister vane parts were found in the 3<sup>rd</sup> stage suction strainer, after 800 running hours. This was determined to be a fatigue failure. After 1200-1500 running hours, it was found that both compressors had sustained piston damage. HPA 2<sup>nd</sup> stage piston had a spectacular longitudinal crack. The piston rod cracked by low cycle fatigue. HPB 2<sup>nd</sup> stage piston ring lands were broken off; 3<sup>rd</sup> stage piston rings were damaged. Frame bolts and valve cover bolts were found to be stretched. Scrubber demister enclosures and vanes were distorted and cracked.

Corrective action: One-piece 2<sup>nd</sup> stage pistons were replaced with two-piece pistons, similar to the first stage pistons. 3<sup>rd</sup> stage piston rings were replaced with Peek material. Scrubber vanes were replaced with a more rugged design, more suitable for pulsating service. Installed separate suction dampeners for first and second stages. Orifice plates were fitted to reduce pulsation.

### 3.2 Failures - June 2000

Both compressors had repeated vibration trips. After restart attempts noise was heard from within the cylinders. Upon opening it was found that both compressors had extensive damage to pistons: HPA Cylinder 1. Both halves of the piston were separated, crown from hub 3<sup>rd</sup> stage piston was damaged. HPB Stage 2 piston was found loose on rod, with lockwasher tab broken off. Crank end piston washer was fractured into several pieces. Piston rod shoulder was distorted. Cylinder 1 crankshaft counterweight had one bolt fatigued and parted, and the other one bent. Web deflections were out of tolerance.

The owner formed a team to inspect and investigate all aspects of the failure in collaboration with the manufacturers of the compressors and scrubbers.



**Table 2. Service History**

Installation of compressors:	Nov 1996	
Oil production started	30 Sep 1999	
Compressors commissioned	Nov 1999	
Failure No 1	Feb 2000	
Failure No 2	June 2000	
Interim Fix	Aug-Sep 2000	
Periodic inspections started	Oct 2000	500 hours, 1000 hours
Permanent fix	March-April 2001	
Periodic inspections continued		2000, 4000, 8000 hours
Failure No 3	April 2002	
Failure No 4	May 2002	
Inspections continued		10000, 12000 hours

The investigation concluded that liquids had been ingested causing damage to both machines, but short of a total wreck. The scrubbers were found to be marginally under-sized, and unsuitable for pulsating service without an external dampener. The investigation also revealed certain weaknesses in manufacturing and quality control. These had resulted in mis-machined parts, and deviations from drawings. A regime of strict control of new and repaired parts was instituted, utilizing the manufacturer's procedures that were already in place, but which may not have been enforced. It was required that all manufactured parts be fully inspected by the owner's inspector before shipment.

Repairs were made to the machines. All possible checks were made to ensure that the machines were correctly assembled. Scrubbers were enlarged as much as was possible, and level indication and control was improved. A new drain vessel was added to drain condensate from the main suction header. The compressors were put back in service, but were restricted to 50% of normal flowrate, to prevent entrainment. This was accomplished by running single-acting, by unloading the head ends of all cylinders. These measures enabled the plant to get back online, albeit at reduced rate, well before the new scrubbers could be made ready. A considerable amount of work was undertaken: rebuilding the machines, metallurgical investigation, increasing the scrubber heights, improving level instrumentation, and adding a vibration monitoring system to the compressors. Detailed attention was also paid to the operating procedures, checks and monitoring. Improvements were made and the crew was instructed in the details of the changes.

Before re-starting was authorized, a complete hazard and operability study was performed by operators, engineers and supervisors. The principal

results were that operating procedures would be strictly followed, the compressor would be run only with the vibration monitoring system serviceable, the flowrate limitation would be respected, and a program of frequent inspections would be conducted at short intervals. These were set at 500, 1000, 2000, 4000 and 8000 hours on each machine.

After a few weeks, with largely successful operation (few trips, and good inspections), it was decided to increase the flow rate. Studies by the owner and by the manufacturer suggested that flow could be increased to 65% of design without increasing carryover from the scrubbers. This was accomplished by manufacturing and fitting modified cylinder heads to HPB. The machine was then run double-acting on all cylinders. This enabled HPA to be taken out of service for further modification, without losing so much capacity.

The compressor suction systems were redesigned and rebuilt with larger scrubbers, improved level control instrumentation, re-routed suction lines, and larger suction pulsation dampeners. This work was completed on each machine in turn, and was completed during April 2001.

The machines were then run normally, double acting at full flowrate. The special periodic inspections continued.

These inspections did not reveal any cracking of pistons. They did reveal scoring of piston ring lands, severe fretting of first stage piston halves caused by loose steel centering rings, slight deformation of the piston rod shoulder, an unexplained loss of tension in the piston rod at the piston nut, and valve wear and damage. These findings were noted, and tracked. They did not occur all at once, nor in every case. They were not considered sufficiently serious to warrant restriction

in service. There were only minor indications of liquids having been present. There were no large accumulations found.

During the running period several O-rings failed by explosive decompression. The downtime associated with an O-ring failure made such events noteworthy. All O-rings were replaced with a slightly more dense (harder) compound specifically formulated to resist explosive decompression, Parker V1238-95. This corrected the problem, but a few joints have leaked after 4,000-6,000 hours.

### 3.3 Failure - April 2002

During the 8000 hr inspection of HPB, the second stage piston was observed to have unusual wear patterns in the anodizing of the outer surface. Although this posed no immediate problem, it was considered interesting enough to be examined in a laboratory. It was replaced by a spare. After approximately 2000 more running hours, the machine was tripped by frame vibration. It was discovered that the second stage piston crank end had fractured into four large pieces by longitudinal cracking. This was very similar to the original damage found in 2000, and was a major disappointment to all concerned.

A large multi-disciplinary team, including representatives of the manufacturer, was assembled to investigate. Metallurgical examination showed that the piston had failed by fatigue, with a large number of cracks spreading throughout the part, but originating in areas where stresses (calculated by

finite element modelling) were at a level where cracking would not be expected. While the proceedings were still in progress, the failure of May 2002 occurred.

### 3.4 Failures - May 2002

A few days after being restarted, HPB again tripped on vibration. This time it was found that the piston rod had cracked nearly through, and that the bolts attaching the rod flange to the crosshead were not fully tight. The piston rod, near to final fracture, had yielded sufficiently to produce a gap between rod end and coupling flange.

This failure was also fatigue, originating at a small surface defect on the rod boss. The rod was not new. It had been salvaged to make repair, and was known to be slightly bent out of tolerance. It was thought that it would probably survive until a replacement could be found.

It didn't.

Within days, HPB main motor overheated the drive end bearing. Smoke was seen issuing from the shaft seal. The shaft surface was badly damaged, and the rolling element bearings were destroyed. It was decided to lift out the entire motor and install the spare one.

### 3.5 Component failure

The components that failed during service are listed in Table 3.

**Table 3 Component failures in service**

2nd and 3rd stage suction separators	:	Vane failure & vane box cracking.
2nd stage piston, HPA	:	Longitudinal fracture, 2 pieces
2nd stage piston rod, HPA	:	Ring land breakage
2nd stage piston, HPB	:	Fatigue cracks, piston side shoulder
1st stage pistons, HPA & HPB	:	Ring land breakage
	:	Fractures of hub to crown junction [5 halves out of 8]
	:	Erratic piston ring land wear
Crankshaft counterweight bolts	:	Bolt fracture
Big-end Bearings HPA & HPB	:	Micro Fatigue 5 instances
	:	Wiping 8 places
Small end bushes, HPA & HPB	:	Micro Fatigue 5 instances
Big end bearing	:	Partial seizure
2nd stage piston, [redesigned]	:	Longitudinal fracture, 4 pieces
2nd stage piston rods, 2x	:	Fatigue fracture crosshead side
	:	Fatigue cracks, piston side
Compressor Valves	:	Premature plate failures
	:	Unloader actuator failures

**Table 4. Thomassen Compressors with liquid ingestion**

	<u>A</u>	<u>B</u> Balder	<u>C</u>	<u>D</u>
No of machines in service	1	2	3	2
No of machines damaged	1	2	1	1
Counterweight bolt fatigue at free ends (front crank)	yes	yes	yes	yes very low cycle
Piston rod fatigue failure at boss in crosshead flange.	yes	yes	yes, 2x	no, loose
Big end bearing fatigue	yes	yes	unknown	yes
Crosshead flange coupling bolts	–	loose	Fatigue failure	tight
Piston(s) loose	yes	reduced	unknown pretension	yes
Crosshead shoe plastic flow of white metal	yes	no	yes	unknown
Valve Damage	yes	yes	yes	yes
Other	Note 2		Note 2	Note 3
Origin of damage	Note 1	Liquid Ingestion	Liquid ingestion	Liquid ingestion

Notes:

1. Investigation not closed. Liquids have been drained out of system in large quantities, after an emergency shutdown.
2. Suction line routing with pockets, not in accordance with API 618.
3. Suction valve cover blown off machine. Bolts failed by overload, not fatigue. Piston in that cylinder was found full of water.

This overview gives a brief impression of the component failures in the compressor. The majority occurred during the first year of operation. Following are some details of these failures and the anomalous features found.

First stage pistons: 5 halves out of 8 had failed by fatigue. Some halves were found to have a much smaller internal blend radius than designed, appearing at first sight to explain the failures. Fractographic analysis however revealed that the fatigue had in some cases not initiated in the blend radius. This excluded the deviant radius as a basic origin of these failures.

Crankshaft counterweight bolt fatigue. A prominent feature of this failure is that there were two separate failure locations, one of them close to the free end that is screwed into the crankshaft. No plausible explanation for failure could be derived from any of the load mode calculations and the failure could not be explained by the application of primary loads. Fractographic details and fracture mechanics analysis only served to reinforce this conclusion. The nature of this failure is very unusual, yet is shared by the machines compared in Table 4.

Big end bearings showed wiping and some fatigue damage. Some small end bushes showed fatigue damage as well. Both types of bearings operate at

bearing pressure level well below the supplier's rating. In the absence of manufacturing defects, this was perhaps the most convincing indication that the

compressor had been subject to overloading during operation.

Valve plate fracture on all stages has also occurred at various times. Valves show evidence of liquids: crude oil was found on 1st stage valve stems, cloud and vortex patterns were found on the plates. Failures have also occurred on suction valve unloader fingers. These have been hammered so that investigation reveals little of interest. Valve springs have also failed. One batch of springs was found to have unacceptably high hydrogen content, so all were replaced.

The most recent failures have been of a HPB 2nd stage piston of revised design. The piston rod in service with it was found to have cracks in the shoulder. The findings of the piston failure investigation did not match well with what is known of the piston stresses, and the piston rod failure was at a location where problems should not occur, i.e. neither allows simple and straightforward explanation.

It is to the credit of those involved that premature conclusions were avoided, despite the pressure to have the machines back in service at the earliest possible. All the described difficulties led to the familiar controversy of whether problems lie with the compressor or the process system.

Table 4 compares cases of similar compressors that have suffered from liquid ingestion. The significance of this comparison lies in the fact that with the exception of valve damage, each of the encountered problems is in itself an unusual event. A combination is therefore highly unlikely if individual failures are considered as random events. For the C case, that is one of 3 identical machines, all damage has been to one machine, located in a process system where liquids will only affect the damaged machine. The other two have never had failures despite operating at the same process conditions.

The similarity in the nature and scope of damage found is interesting. Repeating damage in any one compressor as a result of inadequate design or manufacturing defects becomes statistically more improbable with each failure that occurs. When this occurs more than twice on any one machine, it is certain that this must be due to operational factors. All the listed machines have exceeded this criterion.

#### 4. Remedial action taken

The failures gave rise to design reviews of the failed components. No really fundamental design shortcomings were revealed. Manufacturing processes, material quality, metrology, and assembly procedures were all re-assessed, and as is usual under such circumstances, the whole QA/QC process was examined. Even in cases where there was no direct evidence of fundamental shortcomings, improvements were incorporated. For example: larger radii at the bottom, and wider spacing of piston ring grooves to prevent the re-occurrence of land fracture, and more attention to instrument and tool calibration.

A proposal to strengthen the piston was not acted upon. Finite element analysis, confirmed by an independent check, showed that strength was adequate for design loads. The decision was made to avoid the risk that the next weakest spot had significantly worse consequences.

Greater attention to a variety of details in the compressor was naturally one aspect, but the owner concurrently made extensive modifications to the suction system. We attempted to track down all possible factors of influence, evaluate them, and undertake indicated improvements. A definite improvement in the reliability and availability of the machinery has resulted. It is illustrated that machine damage cannot be treated as an isolated phenomenon. The operating environment must be an integral part of damage analysis.

#### 5. Piston material

As the pistons are made from aluminium alloy, it is necessary to consider what part the material played in the failures.

The 1st and 2nd stages of the TCS reciprocating compressor are currently equipped with aluminium pistons machined from cast or extruded round bar stock material. Based on the required physical properties the heat treatable alloy EN AW-6082 (AlMgSi1) in the T6 temper was selected. The delivery conditions are specified in accordance with EN 573, EN 755, DIN 1745 and/or DIN 1748, however, the design dimensions of the pistons are outside of the dimensional ranges provided in the referenced standards. The alloy is strengthened by precipitation of coherent or semi-coherent Mg<sub>2</sub>Si-particles. Other alloying elements, such as Fe, Cr, and Mn are added for recrystallization control and grain refining. The T6 temper, solution heat treated and artificially aged, requires a quick cooling

through the critical temperature interval 500 C to 200 C to avoid extensive precipitation of individual Mg<sub>2</sub>Si-particles and phases containing the alloying elements prior to ageing. This quenching sensitivity contributed significantly to the anisotropy of the physical properties in larger diameter extruded and cast material. [1,3]. The change of properties is caused by the temperature gradient in the bar stock during cooling, causing varying microstructural configuration of the precipitates and dispersoids in the aluminium matrix.

From an operational point of view, potential damaging mechanisms for the aluminum pistons are related to corrosion, wear, and fatigue. No known corrosive agents, such as chlorides, are present in the natural gas stream. Wear in rider band and piston ring grooves is minimized by hard anodizing. Fatigue due to cyclic mechanical stress applications and cyclic thermal expansion poses an inherent problem with aluminum alloys. Specifically, extruded material exhibits a susceptibility through textures and preferred orientations of grains and intermetallic phases. Work hardening is the material's response to cyclic loading. The work hardening rate of the alloy is only sufficiently high with coherent or semi-coherent Mg<sub>2</sub>Si precipitates. The rate decreases as more precipitates accumulate individually on grain boundaries or as separate phases in the microstructure during heat treatment and cooling. The loss of plasticity also reduces the toughness. Consequently, the decreased capability for work hardening results in micro cracks at precipitated phases. In addition, areas with stress concentrations, cross section shape changes, and structural surface defects are potential starting points for fatigue requiring precise machining and good surface preparations on the part.

Since fatigue fractures grow at 90 degrees to the main stress direction, defects lying or extending perpendicular to the main stress direction are especially critical. The microstructure of extruded material comprises elongated grains and intermetallic phases making this material more prone to fatigue than cast material, under circumferentially cyclic stress. Fatigue crack growth is an exponential mechanism. The initial fractures are extremely small and grow slowly until they reach a critical size, thereafter causing rapid failure.[2,4]. Microstructural heterogeneity and the anisotropy of physical properties increase the susceptibility to fatigue fracture. The fatigue failures experienced in the pistons of extruded material, were associated with multiple initiation sites at stress risers (shape change, surface breaking defects from intermetallic phases), but not at the

most highly stressed locations, (according to the design analysis). The 2<sup>nd</sup> stage piston that failed during April 2002 fractured longitudinally in a texture related pattern, indicating the presence of circumferential cyclic stresses and elongated microstructural or surface-finish related stress raisers.

In order to mitigate the risk of recurrence of fracture, an integral approach is recommended. This would include evaluation and assessment of the microstructure and the anisotropy of the material prior to machining the piston, as well as strict requirements for surface finish in critical areas of the piston.

## References

1. Aluminum Taschenbuch, Aluminum Verlag Duesseldorf, 1999
2. F.M. Mazzolani: Aluminum Alloys Structures, Pitman Advanced Publication, 1983
3. J.E. Hatch: Aluminum Properties and Physical Metallurgy, ASM, 1984
4. T.S. Srivatsan et al. Influence of Notch Geometry on Dynamic Fracture Behavior of Aluminum Alloys, Alum. Trans. 1, 117-130, 1999.

## 6. Process Factors

While the compressor is the heart of the system, many factors affect what happens in the fluid stream, and all can have an effect on the machine performance.

Process instability was evaluated as a potential contributing factor to compressor failures. The data exhibited several events where the production separator liquid levels appeared to be unstable. The periods of liquid level instability in the process typically were also accompanied by small pressure surges (in order of 1 bar). The pressure surges could be seen on the compressor 1st stage suction pressure. Liquid slugging from the production wells was considered as a potential contributor to scrubber level instability.

Analysis of a spot sample (chromatograph through C10+) of the gas using a process simulator did not indicate any significant changes to fluid properties (i.e. liquid dropout) from the small pressure fluctuations. In addition, there were no concerns identified by the phase curves. However while the HP compressors were shut down, the flared gas streams exhibited occasional dark smoke,



indicating either a liquid slugs or instantaneous changes in gas composition. Sampling of the rich stream was not possible in the few seconds available during these disturbances, which were difficult to duplicate on demand. An online gas analyzer would be useful for troubleshooting. Measures to minimize pressure fluctuations were implemented in an effort to stabilize the gas pressure to the compressor as much as possible.

The pressure fluctuations observed on the compressor suction header appeared to be synchronized with the bottom hole pressure. An automated well production control device has been used successfully elsewhere in the North Sea. Such a device might prove useful. It was noted that the wells that caused the pressure fluctuations did not always do so and if they were shut in for a period of time, they would produce very stable flow for a few days before they began "surging" again.

A compressor suction pressure control valve was added to the suction header. Unfortunately, success in tuning this device has not been good and thus it is not currently in service.

The more significant instability was scrubber liquid level. On several occasions the liquid levels appeared to reach a maximum and remain flat (at transmitter maximum reading). This meant that the actual liquid levels in the scrubber were unknown and liquid may have carried over into the compressor. The high liquid levels did not always result in shutdown since the compressor suction scrubbers had two independent level measurement systems. The primary one was used for liquid level control. The secondary one was used strictly for shutdown. Unfortunately, it was also observed that on multiple occasions the two instruments did not agree with each other nor were they particularly accurate when compared to the sight glass. This being a primary area of concern, much effort went into this problem's evaluation. It was determined that the differential pressure transmitters were not well suited for a floating ship where positive and negative vertical accelerations caused readings to vary considerably. All compressor scrubber level transmitters were upgraded to guided wave radar level transmitters. In addition, to address nuisance trips caused by ship movement during a storm, the distance between the various liquid level settings was increased from 150 mm to 230 mm.

To ensure more positive liquid level control, the liquid level control system was changed to snap acting. The snap acting control permitted use of a larger orifice in the liquid level control valve. The

valve control system was configured to open 25% upon the scrubber level reaching its maximum setting. If the level continued to rise the control system would open the valve to 50% and if necessary to 100% to ensure the liquid level dropped to the normal low setting. This system currently demonstrates positive level control at all times, even during rough weather conditions.

Another process instability also involved the compressor suction scrubber liquid levels. It was noted that occasionally the liquid levels would increase in a very short time. Although increased opening of the throttled liquid level control valve followed this event, it still would occasionally result in high or undeterminable liquid levels in the scrubbers. An analysis of the main compressor suction header indicated that although it was the lowest spot in the gas flow stream, there were no provisions for draining it. As slug flow was theoretically possible a drain accumulation pot with automatic level control was installed. When both compressors are running, liquid drained from the suction header via the pot is typically between 3 and 5 barrels per day.

One consideration after the failures in 2000 was the potential for foam build up in the suction scrubbers. It was thought that foam build up in the 1st stage was possible, but was thought unlikely that the foam would carry through to the 2nd stage suction scrubber. Recent analysis of the liquids indicates that hydrocarbons up to C30+ have been found in the 2nd stage scrubber. The analysis also found silicone, a component in the anti-foam agent. It is therefore possible that there is foam in the 2<sup>nd</sup> stage scrubber. We are evaluating if such foam could cause a higher pressure drop across the mesh pad. The resulting high differential pressure across the scrubber could be siphoning liquid out of the scrubber and into the cylinder. Several trips have been caused by high differential pressure, but it is unclear if these are instrument error or true trips.

Another area of concern is the effect of ship motion. The vertical acceleration might be sufficient to induce siphoning. It is planned to record actual scrubber accelerations.

**Table 5**

**Balder HP Compressors Reliability Data**

**After suction system improvement**

	HPA						HPB					
	Utilization	Machinery	System	Machinery	System	Runhours	Utilization	Machinery	System	Machinery	System	Runhours
	Availability	Availability	Availability	Reliability	Reliability	per start	Availability	Availability	Availability	Reliability	Reliability	per start
<b>2001</b>												
April	91,00	100,00	91,00	100,00	91,00	47,00	87,00	95,00	87,00	96,00	88,00	48,00
May	67,00	70,00	67,00	95,00	92,00	50,00	91,00	100,00	91,00	100,00	91,00	85,00
June	94,00	95,00	94,00	95,00	94,00	85,00	92,00	94,00	93,00	96,00	95,00	95,00
July	71,00	99,00	71,00	99,00	97,00	75,00	63,00	72,00	63,00	97,00	94,00	42,00
Aug	75,53	75,53	76,74	76,38	97,18	97,04	79,50	79,50	95,64	95,14	95,64	95,14
Sep	81,36	100,00	88,38	100,00	88,38	146,45	90,60	99,50	95,00	99,50	95,00	72,48
Oct	98,70	99,95	99,84	99,95	99,84	244,77	97,94	99,31	99,31	99,31	99,31	104,10
Nov	95,13	99,84	98,10	99,84	98,10	85,62	92,90	96,76	96,13	96,76	96,13	74,32
Dec	86,30	90,83	89,60	90,83	89,60	32,10	91,37	99,26	96,75	99,26	96,75	84,97
YTD	84	92	86	95	94	96	87	93	91	98	95	78
<b>2002</b>												
Jan	93,38	98,58	95,32	98,58	95,32	138,95	88,38	94,98	91,31	94,98	91,31	50,58
Feb	64,52	99,43	97,21	99,43	97,21	33,35	48,88	52,08	51,01	98,92	97,85	32,85
March	99,73	100,00	99,84	100,00	99,84	371,01	99,74	100,00	100,00	100,00	100,00	742,10
April	94,31	99,87	99,24	99,87	99,24	116,95	62,62	69,60	68,63	69,60	68,63	93,17
May	41,75	42,80	42,69	52,48	52,37	155,33	55,04	57,32	55,57	57,32	55,57	37,23
June	79,17	91,25	83,03	100,00	91,78	98,17	94,62	99,89	98,88	99,89	98,88	351,99
July	99,83	100,00	100,00	100,00	100,00	742,47	95,95	97,58	96,22	97,58	96,22	178,48
Aug	98,58	99,63	99,08	99,63	99,08	366,72	96,94	98,39	97,69	98,39	97,69	120,21
Sep	84,43	86,63	86,63	86,63	86,63	607,90	96,53	98,74	98,74	98,74	98,74	695,05
Oct	90,92	99,46	98,66	99,46	98,66	56,37	84,93	86,72	85,86	100,00	99,14	126,37
Nov	97,27	97,93	97,48	97,93	97,48	140,07	77,89	78,59	78,29	88,50	88,19	93,47
Dec	99,08	99,93	99,08	99,93	99,08	73,72	68,63	68,78	68,63	68,78	68,63	102,12
YTD	86,91	92,96	91,52	94,50	93,06	241,75	80,85	83,55	82,57	89,39	88,41	218,64

## 7. Reliability Data

Data for 2001 and 2002 are included in Table 5. These data were all collected after the suction system was modified. There is a large improvement in performance compared with the period before modification. Earlier data are not presented because they were not collected with the same rigour.

The intended operation of the machines is continuous ("24 for 365"). If this were achieved Utilization, Availability and Reliability would be 100%. Availability is the best measure of machine performance in these circumstances. We have separated the "machine" from the "system" in order to illustrate the effects of each. The tracking system encodes the reason for any trip and downtime, and can be used to identify the principal causes of unreliability. Of course the operator has internal

targets to be met, and these parameters are used as key performance indicators.

The data show significant variation in time. The high impact of failures and of the mandated inspection program is obvious. The existence of months with availability greater than 99%, even 100%, shows that the machinery is capable of functioning as intended. It remains to eliminate the causes contributing to downtime, especially those which cause damage, and necessarily long repair time.

## 8. Economics of Reliability

The first and most obvious cost of an unreliable machine is the loss of revenue occasioned by the lost production. The most usual calculation of this cost is the product of daily reduction in production

rate times the quoted price of oil. These numbers tend to be very large (eg 1.9 million US dollars per day). They grab the attention, and get people focused on expeditious repair.

In fact this production is not lost, but is deferred. Oil or gas not produced immediately may be produced later, reducing the effective rate of decline. Modern economic models account for this. There is a time dependent cost of lost or deferred production, and it must be considered.

The life cycle cost of ownership should be used as a selection criterion when purchasing capital equipment. As this activity is done well before any actual data is available, it must make assumptions on reliability and the similarity of referenced installations. In many cases reliability is over-estimated, and the cost of break-down maintenance is under-estimated.

When failures occur, repairs must be effected as expeditiously as possible. This inevitably leads to increased costs for normally routine expenditures. The hidden costs of disruption to affected schedules are seldom calculated.

To repair damaged machinery, spares must be readily available. It cannot be expected that parts which by nature have long lead-times can be conjured onto site. Spare parts cost capital dollars, and warehousing them costs operating dollars. There is a constant struggle between the forces to maintain an inventory of spares and those to reduce them. In the case of critical machinery, the ownership cost is reduced if the spares are available when needed. If the machinery is unreliable, larger inventories are needed to control repair time.

In our case spares were needed frequently. Normally held stocks were insufficient. Larger numbers of components were seen to be necessary. Entire sets of spare pistons and rods are now held, as well as the normal valve sets and bearings. So far we have not seen the need to hold a spare crankshaft. It will be a sad day that we discover that this too is a requirement. A spare drive motor was purchased with the original equipment. This has been found necessary; our thanks are due to those who bought it!

Even with adequate spares, downtime is an unwanted cost. Efforts must be maintained to improve the basic reliability to a point where improvement is no longer economic. This optimum point is unfortunately not static.

## 9. Specification of new equipment

We intend that in wet or saturated gas service, that reciprocating compressors be used only where they are specifically required. If reciprocating machinery is selected then we would implement the following:

- a. Comply with corporate or industry standards. At the very least comply with API 618 to the letter.
- b. Never deviate from the agreed specification for reasons of first cost or schedule only. Always consider life cycle cost, which means applying a heavy weighting on operating costs, especially maintenance costs.
- c. Keep the gas dry.
- d. Know the gas composition, and possible variations, and their effects.
- e. Understand the loads imposed and provide adequate resistance. Extra design margin may be valuable if gas composition (and load) varies.
- f. Pay extra attention to piston material and manufacturing quality control.
- g. Consider increased clearance volume if gas composition varies, or liquid dropout is likely.
- h. Fit all the instruments that the compressor frame can bear. Use automatic monitoring and trending, at a high scan rate.
- i. Fit temperature monitors and vibration probes to main motor bearings.
- j. To size scrubber liquid level control valves, consider the instantaneous dump rate, not the average daily condensate accumulation rate.
- k. Use only vane packs and enclosures suitable for pulsating service.
- l. Fit inlet vane devices on all scrubbers.
- m. Perform pulsation studies and mechanical response studies. Always fit the necessary pulsation dampeners or filters.
- n. Do not try to save space by combining suction scrubber and pulsation dampener.
- o. Suction pulsation bottles should include provisions for draining each compartment.
- p. Consider all possible operating conditions, and ranges of parameters when sizing scrubbers.
- q. Use guided radar level transmitters rather than differential pressure gauges on FPU's.
- r. Specify, then monitor construction, to avoid liquid traps and eliminate potential for slugging.
- s. Install a suction header liquid drain pot

- t. Cool the suction gas streams, followed by scrubbing, to reduce liquid dropout further downstream.
- u. Insulate piping to avoid downstream condensation in cold weather.
- v. Install reliable compressor gas flow metering.

## 10. Conclusions

It has not been possible to identify the root cause of failure with absolute certainty. Clues and comparisons abound, leading to the main belief that the problems are related to liquid ingestion. As failures continue, the root cause has not been eliminated.

Since commissioning, it has been recognized that liquid presence has contributed to compressor damage. All subsequent failures can be most easily explained by the presence of liquids and the extra loads they could impose. Efforts have been made to reduce the effects of liquid locally, mainly by scrubber improvements. If liquid is the root cause of unreliability, it may be more beneficial to concentrate remedial work on prevention of carry-over. In short, that means effective separation of the gas and liquid phases.

Process conditions, especially instability are likely to affect reliability of compression, as much or more than the basic machine design details.

While all those participating in the investigations and activities generated by the investigations were at times under pressure, it was the combination of all efforts that proved to be very valuable. That these were performed under co-operative and not under adversarial conditions stimulated open communication and the sharing of information. One question has not been answered and it may be the most important one: Could this all have been prevented, and what factors dictated failures from the outset?

## 11. Postscript. Failure - December 2002

On two separate occasions, on HPB, a stud connecting the cylinder to the crosshead guide fractured. There was evidence of slight relative rotation of the castings.

On 23 Dec 02 HPB second stage piston rod parted. The failure was in the crosshead connection. There was no warning of impending failure. The piston end of the rod also showed distress, distortion of

the shoulder, and stretching of the piston connection. The failure has not yet been analysed. HPA was inspected at 12,000 running hours. The piston rod shoulder was distorted and the piston connection stretch had relaxed.

*Disclaimer: No representation or warranty about the quality, accuracy or completeness of the contents of this paper is given. As circumstances regarding installations differ, a party should not rely on the contents of this paper regarding activities in relation to another installation but instead should make its own independent decisions.*



# **New technologies pave the way for on-line CCM systems becoming standard for reciprocating compressors**

**by:**

**Axel Rumpold**

**Monitoring & Controls**

**HOERBIGER Ventilwerke GmbH**

**Vienna, Austria**

**Reliability and economics of compression systems -  
recent trends in the market of  
reciprocating compressors  
March 27<sup>th</sup> / 28<sup>th</sup>, 2003 Vienna**

## **Abstract:**

On-line Compressor Condition Monitoring Systems (CCM) have proven to be important tools for supporting maintenance of reciprocating compressors. They are well accepted to increase reliability and availability and to reduce operation costs. Early and precise detection of failures enables fast repair work and effective mobilization of limited manpower. Up to now on-line monitoring systems have mainly been applied at machines involved in critical processes. New “slim-line” systems, based on clever conception, focusing on monitoring key-requirements as well as modern techniques for data acquisition, transmission and diagnosis will pave the way for on-line CCM systems as standard equipment for all kinds of reciprocating compressors in the oil, gas and process industry.



## 1 Introduction

Many processes rely on reciprocating compressors, they are indispensable for compression of light gases as hydrogen and dominant in high pressure applications. Reciprocating compressors can also work under variable process conditions with highest efficiency compared to other compressor types. For applications in the process industry, refineries as well as natural gas transport and storage facilities a variety of capacity control systems are available allowing to control the flow of the compressor according to the current demand of the process.

On the other hand reciprocating compressors have been blamed for their poor reliability and high maintenance costs. This fact was changed within the last ten years by introduction of new materials and designs. Subsequently maintenance intervals have been extended starting at 4.000 to 8.000 hrs. to 16.000 hrs, sometimes even up to 24.000 hrs.

At the same time under the economic pressure of the industry on-site personal has been reduced, the amount of spare parts has been cut and standard maintenance work is subcontracted to third parties. The pressure on maintenance in day to day business has increased significantly. The combination of preventive (time-based) and predictive (condition based) maintenance forms the best approach to keep reliability on a high level while extending the service intervals at the same time.

## 2 Tools for predictive maintenance

On-line Compressor Condition Monitoring Systems (CCM) have proven to be important tools for predictive maintenance of reciprocating compressors:

- Early and precise detection of failures reduces the number of unplanned shutdowns and enables fast repair work and effective mobilization of limited manpower.
- CCM systems allow to check the current condition of a compressor. In case of service or repair any work performed can be checked immediately.
- CCM systems provide current data of operation to maintenance. This data serves as the best basis for any design upgrade or problem analysis.

## 3 Parameters to be monitored

Overall wear part failures and process problems have been identified as major causes for unscheduled shutdowns.

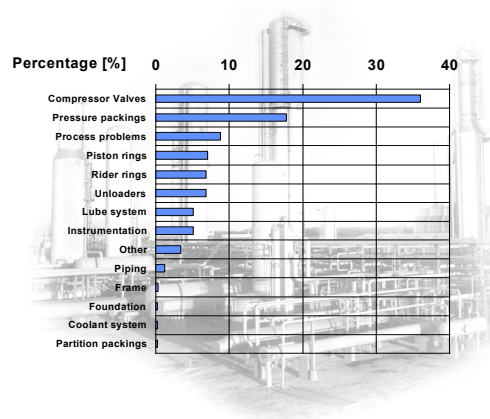


Fig. 1: Typical causes for unscheduled shutdowns

Analysis of the mechanical condition of all major wear parts is the main target of CCM systems. The following monitoring standards for wear parts have developed over the last years.

### 3.1 Compressor valves

Online temperature monitoring is the best approach for analysis of compressor valves. Temperature monitoring requires state-of-the-art temperature transmitters, either directly placed in the valve nest or mounted to the valve cover. Thus the costs are reasonable.

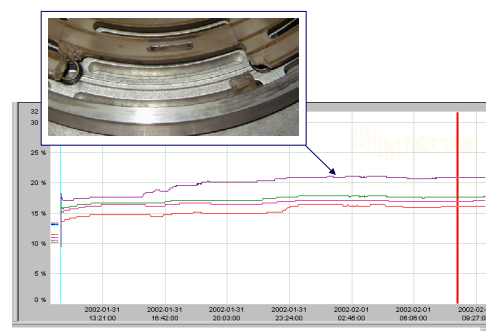


Fig. 2: Typical "bad" valve cover temperature trend

The temperature trend and the actual temperature difference compared to other suction or discharge valves of the same stage (e.g. 5 to 10°C) indicate leakage or clogging of that valve.

The absolute valve cover temperature should never be treated as a shutdown parameter, because then any transmitter failure would cause an immediate shutdown.

Additional monitoring of pV diagrams supports valve monitoring and allows more detailed analysis such as:

- Late closing (oil stiction) effects
- High valve losses
- Pulsation

Additional vibration and ultrasonic monitoring is common for many snapshot monitoring systems and allows detection of loose assemblies and typical valve flutter. The permanent installation of these additional transmitters is quite costly and should be taken into consideration depending on the role of the compressor within the production process.

### 3.2 Rider rings

Depending on the design of the compressor (vertical/horizontal, lube, mini lube/ non lube) rider ring wear is a critical parameter for operation. Rod-Drop monitoring systems have been introduced years ago and are the only solution to measure rider ring wear during operation.

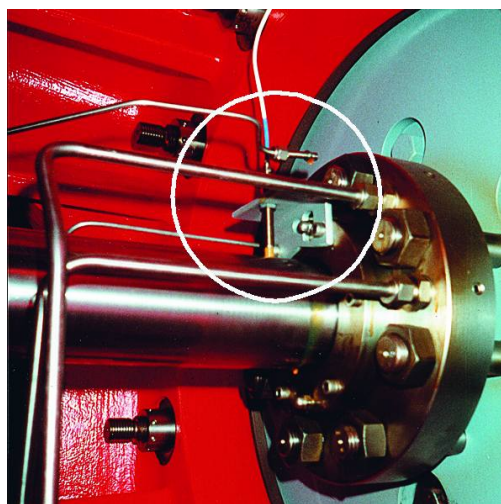


Fig. 3: Rod drop monitoring

### 3.3 Piston rings

Piston ring leakage is indicated by the change of following parameters:

- The gas flow reduces
- The discharge temperature rises
- The pV diagram shows typical rounded “toes” and S-shaped compression lines.

Since the gas flow and the discharge temperature is influenced by many other parameters pV monitoring in combination with discharge temperature monitoring is the easiest way to get clear results.

### 3.4 Packings

A leaking packing results in high vent (flare) gas flows. Temperature monitoring directly on the packing vent line plus additional flowmeters (which are costly and require additional protection against dirt) allow direct and precise detection of any leakage.

### 3.5 Process problems

Abnormal operation of a compressor is safeguarded by typical shutdown parameters as low/high stage pressures, high differential pressure, high discharge temperatures, etc. In case of a shutdown it is a must to track the root cause for the shutdown before starting any repair work. CCM systems trending basic data of operation (acquired from DCS/PLC) allow maintenance to determine the root cause for the shutdown. On the other hand the pV diagram is still the best “fingerprint” of what is happening inside the cylinder.

### 3.6 Capacity control / unloaders

State-of the art capacity control systems like On/off regulation, HydroCOM, clearance pocket control, etc. influence the shape of the pV diagram. Thus the correct working of these systems can be easily determined by monitoring the pV diagram.

HydroCOM additionally offers to check the system via detailed status codes.

## 4 Conception of a CCM System

Until now high sophisticated on-line monitoring and diagnostic systems are installed at critical machines and at compressors with a key role in the production processes (e.g. unspared hypsers in the polyethylene production). Due to their importance referring to safety aspects, vibration monitoring including automatic shutdown function is a central feature.

To cover the market of less critical and smaller compressors, HOERBIGER & PROGNOST Systems - are now introducing a new "slim-line" CCM system based on the following conception.

### 4.1 Focus on key features

As described above wear part failures and process problems are the most (80 percent!) common reasons for unscheduled shutdowns. Thus mechanical condition analysis is the most important feature of a "slim-line" CCM system.

The following figure displays the detailed system conception.

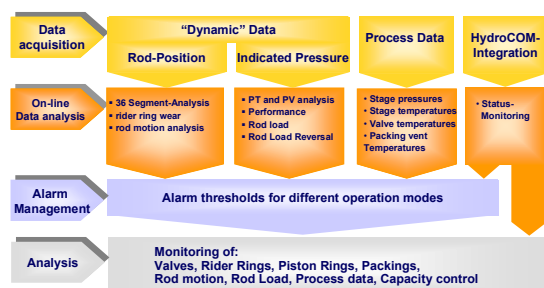


Fig. 4: Necessary system components of a "slim-line" CCM system

### 4.2 Decentralized data acquisition

CCM systems typically need to acquire two different kind of signals:

- "Static" data such as temperatures, stage pressures, flows, etc. which can be measured by state-of-the-art transmitters and sent to the instrumentation room either hardwired or via Ex-certified field bus systems.

- "Dynamic" data such as rod position or cylinder-indicated pressure require special solutions for analogous / digital conversion and data transfer. The existing state-of-the-art bus technologies are not Ex-certified and not tailored for the typical requirements of CCM systems. These signals have to be hardwired from the compressor to the instrumentation room which results in high installation costs.

HOERBIGER always looked for a possibility to acquire all data in the field at the compressor to reduce installation costs and enlarge the economical basis for CCM systems.

Based on the HydroCOM capacity control system which uses Ex-certified field bus technology since 1997 a new device for decentralized data acquisition of "dynamic" data, the so called Fast-TIM (Fast-Transmitter Interface Module), has been developed recently.

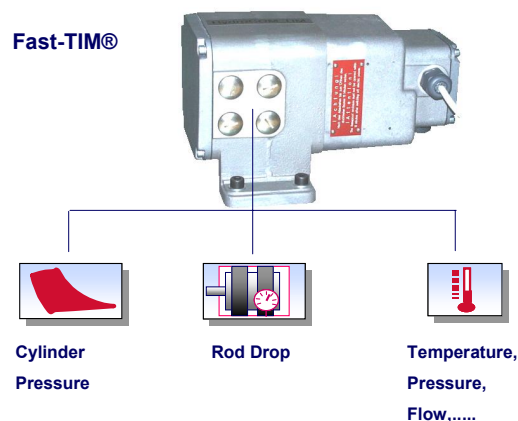


Fig. 5: Fast-TIM

Fast-TIM provides connection for up to 8 intrinsically safe transmitters (indicator pressure, rod drop, temperature, etc.) with following features:

- Ex-certified barrier (ATEX/FM/CSA)
- Triggered and synchronised data acquisition over one crankshaft revolution
- Analog/ digital conversion and data transfer via bus interface to the instrumentation room.

### 4.3 Process data acquisition via OPC or Modbus

In many applications important parameters such as stage pressures, stage and valve temperatures, etc. are already transmitted to the DCS or PLC. For mechanical condition analysis the user of a CCM system requires access to this data, but the variety of DCS and PLC systems does not offer easy data transfer to the CCM.

Following the latest trend in industrial automation (joint effort of several suppliers and Microsoft) OPC (OLE for process control) is defined as the new open interface for data transfer. The CCM system supports OPC and Modbus in order to reduce the costs of data transfer from the PLC/DCS.

## 5 System overview

The new “slim-line” CCM system developed by HOERBIGER & PROGNOST Systems consists of the following components:

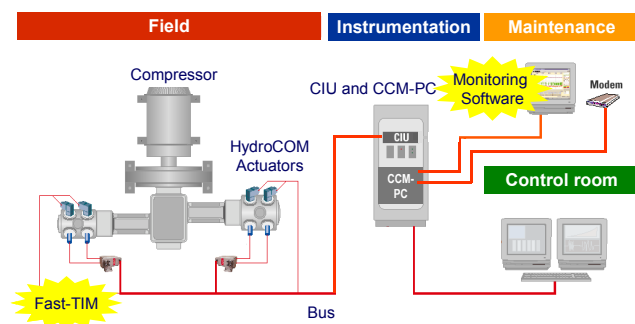


Fig. 6: CCM-System architecture

- Decentralized data acquisition via Fast-TIM. The sensors for cylinder indicated pressure and rod drop are directly connected.
- Via Bus-Interface all measured data is transferred to the CIU installed in the instrumentation room.
- The CCM-PC reads the data from the CIU and the PLC/DCS, data analysis and storage is also provided by the CCM-PC, based on proven PROGNOST software.
- The CCM-PC is internally connected to the company's network (LAN/WAN) and externally via modem. Maintenance on site

can connect using standard PCs, remote access is provided via modem.

The system can be used for reciprocating compressors with and without HydroCOM control.

## 6 Online-data analysis

Data analysis with the CCM PC and the CCM software is accomplished according to the following standard procedures.

### 6.1 Rider ring wear analysis

Many actions inside a reciprocating compressor happen over one crankshaft (360°). The CCM software divides the measured rod drop signal into 36 segments (each 10° crank angle). For each segment an average is calculated and compared to the defined threshold value. This procedure allows to monitor the motion of the rod indicating not only rider ring wear but also loose components (Rod connection). Ring wear is calculated based on the measured rod drop signal and geometry data.

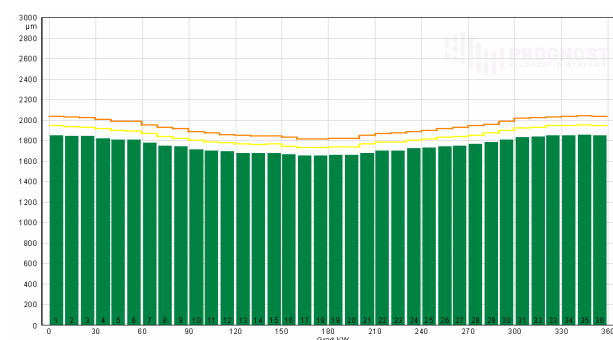


Fig. 7: Segment-Analysis of Rod-Motion

### 6.2 Pressure data analysis

The measured indicated pressure is converted into a pV diagram. The following typical parameters are calculated and analysed:

- Suction and Discharge “toe” pressure
- Suction and Discharge volumetric efficiency

- Polytropic coefficient of compression and re-expansion line
- Indicated power and efficiency
- Suction and Discharge power loss

For detection of typical wear part failures pV diagrams can be overlaid (historic comparison) and compared to the ideal theoretical pV.

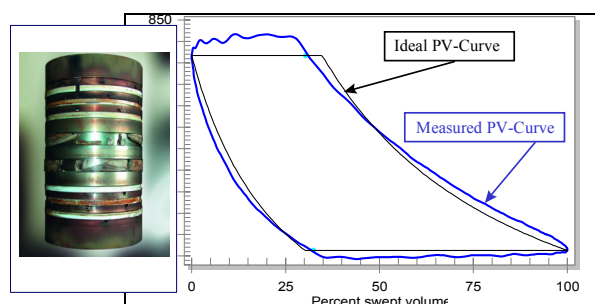


Fig. 8: pV diagram showing piston ring leakage

Based on measured indicated pressure the CCM software calculates the actual rod load on each cylinder. Rod reversals and Maximum rod loads are checked.

### 6.3 Process data analysis

The analysis focuses on suction and discharge pressures, suction and discharge temperatures, valve cover temperatures and packing temperatures.

Additional parameters such as oil temperatures, oil pressures, cooling water temperatures, bearing temperatures, power consumption and flow can be integrated into the analysis.

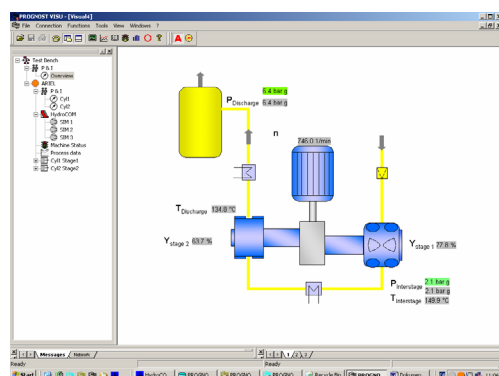


Fig. 9: Process overview

## 6.4 HydroCOM status monitoring

If the compressor is equipped with a HydroCOM capacity control system the current system status including all detailed warning and error messages is displayed by the CCM software.

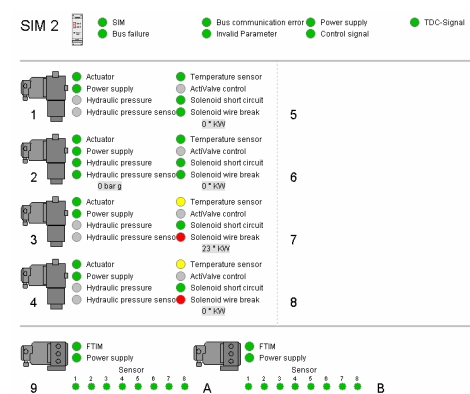


Fig. 10: HydroCOM status

## 7 Data trending and storage

The measured and calculated values are stored for historical trending. In order to provide standard trend data, two different trends are available:

- Short time trend (1 minute average values)
- Long term trend (1 hour average values)

Trends can be edited by the user with text comments.

The dynamic signals are stored in a FIFO storage (first in, first out). This storage contains 360 snapshots of complete revolutions. Linked to a significant event (start, stop, manual release) data is stored separately for a period of 0,25 to 2 hours. This enables the user to compare and analyse any change during this period.

## 8 Alarm management

Alarm management is one of the most important features of the CCM software.

First of all alarms have to be generated. The CCM allows to define thresholds for different operation modes (e.g. different loads or different speeds, etc).



During any mode of operation the current value is always compared with the defined threshold value.

In general any signal or value can be displayed in three different conditions:

- O.K. (green)
- Exceeding 1<sup>st</sup> alarm level (yellow)
- Exceeding 2<sup>nd</sup> alarm level (red)

An overview picture of the compressor shows the current status indicated by traffic lights.

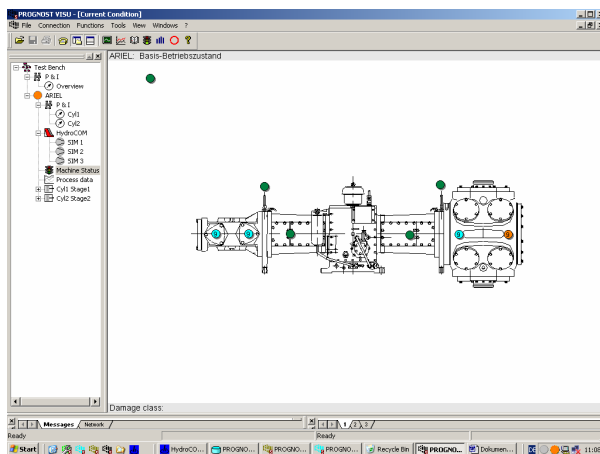


Fig. 11: Compressor status

Since users cannot always look at the CCM screen waiting for alarms or changes the system has to call proactive in case of any abnormal situation. The CCM software can forward alarm messages via LAN, Email, SMS, FAX, Pager, Voice Message or to the DCS.

## 8 Summary

New systems, focusing on essential requirements by using modern techniques for data acquisition, transmission and diagnosis will pave the way for CCM systems as standard for the broad recip compressor market in the oil-, gas- and process-industry.

The described “slim-line” CCM system is a common development of HOERBIGER and PROGNOST Systems. It can be applied at reciprocating compressors with (system = HydroCOM-CCM) or without HydroCOM (= PROGNOST-CCM) control.



# **Improved high speed safety protection for critical compressors**

**by:**

**Eike Drewes**

**PROGNOST Systems GmbH**

**Rheine**

**Germany**

## **Reliability and economics of compression systems - recent trends in the market of reciprocating compressors March 27<sup>th</sup> / 28<sup>th</sup>, 2003 Vienna**

### **Abstract:**

Effective safety shutdown protection systems are extremely important for critical compressors operating in hazardous environments and in un-spared production processes. Due to their particular design, reciprocating compressors require specialized monitoring and analysis techniques for an efficient safety protection system. Naturally, those methods have to provide the highest level of reliability while, assuring that the operational requirement of avoiding false alarms and missed detects is achieved.

The wide array of instrumentation typically installed on reciprocating compressors like vibration and rod-drop measurement, p-V diagram or temperature monitoring offer a broad range of capabilities concerning safety monitoring which are often not fully realized. Existing sensors on a compressor are properly mounted and connected electronically but often the analyses applied to these signals are not using the full potential of "hidden" information to provide the highest degree of safety protection possible. The paper introduces some of the latest advanced techniques of safety monitoring on signals like crosshead vibration, dynamic piston rod vibration and dynamic pressure monitoring and illustrates them with some "real life" case studies.

## 1 Introduction

Within the recent years cost reduction and increase of productivity have been undoubtedly the major challenges for industrial production. For production and maintenance engineers both working on the same goal this sometimes has created a trouble spot.

Production often has to increase their output by utilizing the same machinery as before and apart from process improvements strongly depends on an increase in reliability and availability. Maintenance has to realize this goal while often has to cover the same number of machines with a decreasing number of people. Shrinking budgets frequently lead to a reduction of available spare parts on stock which has been generally advised by finance controllers. As a result reaction to large machinery failures can be time consuming with unexpected shutdowns leading causing heavy damage to the achieved reliability figures.

Naturally this strategy is also applied to reciprocating compressors and therefore more and more machines are considered critical in terms of production, safety and maintenance. Due to this safety protection has become a major point of interest and a higher demand for effective safety protection has become obvious in order to prevent a sudden unplanned shutdown. Only highly effective strategies specially adjusted to this kind of machinery are appropriate to match with the common goals of modern maintenance.

## 2 Critical compressors

### 2.1 Definitions

The population of compressors operated in a certain plant can always be classified in different categories depending on the level of importance. This classification of machinery is often used to determine where maintenance activities, like for example condition monitoring and safety protection, have to be applied first from a cost-benefit aspect.

There are many parameters and methods to determine the importance of machinery from which the following 3 aspects are most commonly used :

1. Importance for production process
2. Criticality of compressed gas
3. Damage history of a machine

There might be additional aspects which are considered depending on the individual compressor.

#### 2.1.1 Relevance for the production process

Analysing the relevance of a compressor for the production process starts with a question:

How is the production affected if the compressor stops ?

Looking at the two opposite extremes illustrates that loss of production is the main aspect to be considered.

If the whole capacity of a compressor is spared by a stand-by compressor which can be immediately started after shutdown of one compressor, the impact on the production is almost zero. Therefore an unexpected shutdown will not be critical, because it does not automatically lead to a loss of production.

If the compressor is unspared and part of a single line process a shutdown will automatically lead to a loss of production. These compressors are usually considered to be critical. Buffer capacity inside the process can help to continue with production for a limited period of time. Therefore fast failure analysis and troubleshooting are required in order to start the compressor before the buffer volume is used up.

#### 2.1.2 Dangerousness of compressed gas

Apart from the relevance of a compressor for the production the type of gas that is processed also influences whether a machine is critical or not. Especially those compressors are considered critical which are working with explosive gases like hydrogen, acetylene etc. or with gases that contain toxics like H<sub>2</sub>S, carbon-monoxide etc. For these machines any gas leakage caused by a major compressor failure might lead to an explosion or fire killing people and damaging other parts of the plant. Therefore any major failures on machines processing explosive or toxic gases can lead to disastrous consequences.

#### 2.1.3. Damage history of a machine

Another important aspect is the maintenance history of a machine. Sometimes certain compressors have been subject to repeated major breakdowns like piston-rod failures etc. Often the exact root cause of such a failure has not been found and a similar failure for the future can not be ruled out completely. Machines with a damage history like this are often characterised critical because they are

considered to cause increased maintenance efforts in terms of work effort and money to be repaired and re-started.

## 2.2 Monitoring requirements

Machinery that has been classified critical naturally has a high demand regarding monitoring and instrumentation. The most common first and fundamental step towards condition monitoring is to install some basic protection. For reciprocating compressors this is usually covered on the machine side by vibration monitoring on the compressor and on the process side by some gas pressure and temperature switches on the process piping. Due to the importance of critical compressors monitoring and protection have to be continuous (online) and should offer capabilities for extended instrumentation and future upgrades in case additional monitoring is required.

## 3 Safety protection

### 3.1 Objectives

The efficiency of a safety protection system can be judged mainly by the

- sensibility regarding machine failures
- time between detection and alarm
- sensitivity to false alarms

As indicated by the name, safety protection is designated to provide safety and to protect machinery. As compared to Condition Monitoring, which focuses on the analysis of the machines' condition, the objective is clearly limited to determination and alarming of critical conditions. As soon as a safety alarm has been registered by the system the machine has to be stopped immediately in order to prevent consequential damage. The prevention of consequential damages is the most important aspect of safety protection.

The consequential damage caused by e.g. a broken connecting rod to the crankcase of a compressor will be more severe and more costly to repair than the broken rod itself. Therefore fast action to shutdown the machine is required. This is usually done automatically through the protection system by releasing a so called trip alarm.

Due to the shutdown requirements of safety protection systems and the involved responsibility

for the machinery the sensitivity to false alarms is an important quality aspect.

## 3.2 Applied strategies

Today the most widespread strategy in safety protection on reciprocating compressors is vibration monitoring. The common setting is using velocity vibration sensors on the compressor crankcase. Fig. 1 shows the typical arrangement for a 4-cylinder reciprocating compressor.

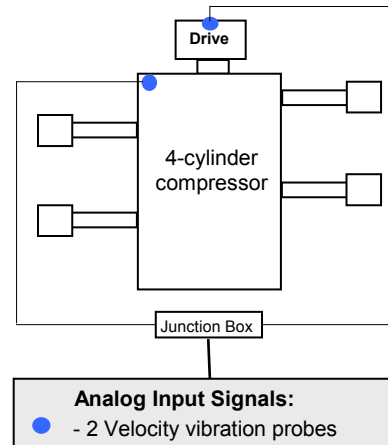


Fig. 1: Frequently used vibration sensor positions on the compressor crankcase and electric motor bearing for safety protection

This so called “seismic switch” was basically designed to protect the machine in case of earthquakes and foundation problems. It uses the low and mid frequencies of the vibration which are analysed by a monitoring rack hardwired to shutdown the compressor in case the vibration exceeds a certain limit. As an advantage it is simple to install and offers a low sensitivity regarding false trips. On the other side the sensibility for failures of machinery parts like piston rod failures is comparably low. This is mainly because those failures are causing high frequency impact vibration in the machine which can not be detected by velocity vibration sensors due to their limited frequency resolution.

Due to this lack of sensibility many operators of reciprocating compressors have experienced severe damages e.g. broken pistons damaged or damaged crossheads without any trip shutdown of their so called “protection system”. This clearly points out a demand for improvements in efficiency regarding sensibility and action time.

### 3.3 Basic characteristics of machine failures

There are two basic types of machine failures :

- long term (wear/fatigue) related failures
- abrupt failures

For both types of failures certain maintenance and monitoring strategies can be applied.

Wear related failures occur after the typical wear potential of a certain wear part has been used up. If the wear part is not replaced in time further operation of the machine can lead to serious failures.

Example: Rider rings on the piston of a recip compressor are totally worn and finally the piston scratches the cylinder liner – a serious damage. This incident is the result of a long term wear process and any damage to the liner could have been avoided by long term condition monitoring of the rider ring wear.

Abrupt failures occur without any significant prior indication. The whole failure usually develops within a few minutes or seconds. The objective is to quickly identify this failure as soon as possible.

Example: A piston rod fails after a liquid slug caused by condensate in the cylinder. The remaining part of the piston rod smashes into the disconnected piston causing severe damage to the liner and cracks in the cylinder. Gas leaks through the cracks and contaminates the plant environment.

Cases like the above described piston rod failure develop very rapidly and often happen without prior indications. This is the type of breakdown which is difficult to detect before it becomes dangerous. Therefore fast and sensitive monitoring equipment is required to provide the necessary safety protection.

## 4 Improved high speed safety protection features

As described in section 3.2 safety protection on reciprocating compressors is often related to vibration monitoring using velocity probes usually based on the compressor crankcase. This setup is focused on 'seismic' activity (earthquake, foundation) and offers only poor protection for most vital machinery components. Using

accelerometers instead of velocity sensors along with placing the probes on the crosshead slides of the cylinders instead of on the crankcase, improves the overall efficiency of vibration based safety protection significantly. Even more improvements can be achieved by application of specialized analysis techniques.

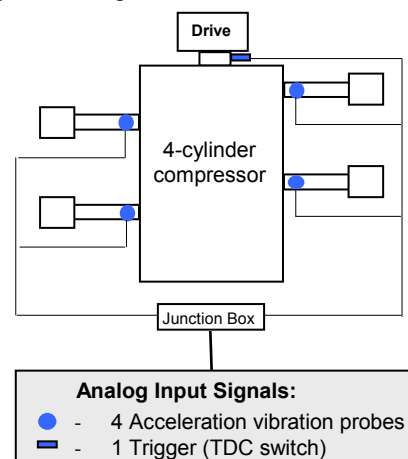


Fig. 2: Recommended sensor positions of accelerometers for safety protection

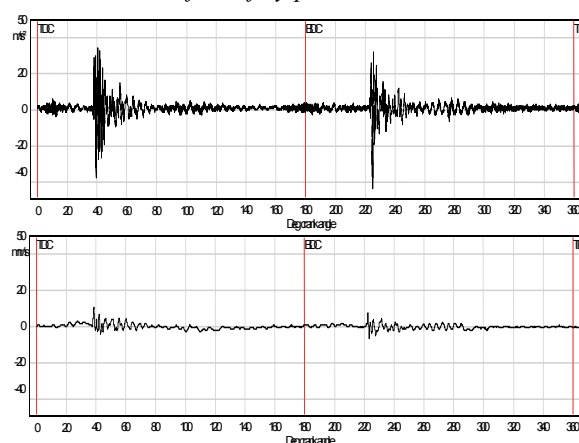


Fig. 3: Comparison of crosshead acceleration and velocity vibration signal showing impacts caused by failed compressor components

### 4.1 Segmented vibration analysis

A proven strategy for vibration analysis has been the so called segmented vibration analysis based on 36 segments per revolution (see Fig 4). This analysis divides the measured vibration signal of a single crankshaft revolution into 36 segments each of 10 degree crank angle. For each segment the RMS vibration value is calculated. The RMS value is preferable as compared to a peak analysis because it offers a lower sensitivity to false alarms caused by incidental events. For every segment there is an individual threshold which can be adjusted independently from each other.



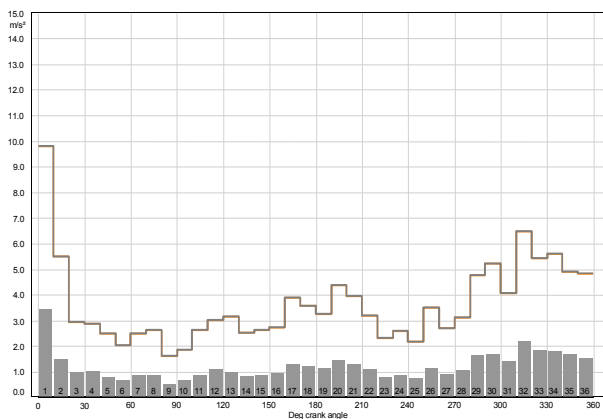


Fig. 4: Segmented crosshead guide vibration analysis including thresholds

Safety alarms are generated in 2 levels:

- Pre-alarm
- Main-alarm (machine trip)

Only the main alarm causes a preconditions for a main alarm are fulfilled. Release of alarms depends on the following conditions:

- 1) Threshold violation in at least 'X' number of specific segments.

If a certain vibration peak occurs always at the same time of the crankshaft revolution it is related to a failure of a certain machine component e.g. crosshead wrist pin. This precondition helps to sort out coincidental events e.g. people working close to the machine.

- 2) Threshold violations in at least 'Y' number of consecutive revolutions.

Repeated violations in consecutive revolutions strongly indicate that the causing event is persistent. This precondition helps to sort out coincidental events e.g. people working close to the machine.

- 3) Threshold violations in 'Z' number of various segments.

Threshold violations can occur in various segments in case of special problems for example broken connecting rods hitting the compressor crankcase.

The above mentioned conditions are evaluated by logical conjunctions (AND/OR) with different X,Y,Z-parameters (see Fig 5).

Certain segments, e.g. those close to the TDC and BDC will be analysed with special concern, because vibration peaks typically caused by liquid slugs will occur close to BDC/TDC.

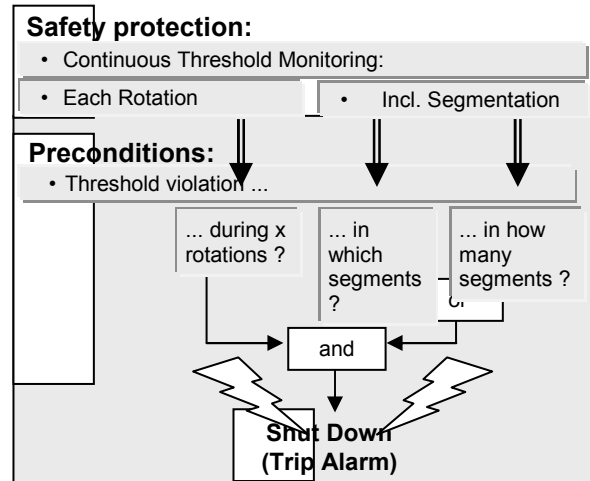


Fig. 5 : Safety alarm release conditions

Example:

A pre-alarm is released on cylinder 1 after threshold violations have been released for segments 1 and 2 being persistent for 5 consecutive revolutions. A main alarm is released if the same conditions continue for additional 10 to 15 revolutions.

## 4.2 Segmented rod vibration analysis

Rod-drop monitoring has been used since many years on reciprocating compressors to analyse piston rider ring wear. Averaging the signal over several revolutions or single point measurements are used to determine the drop of the piston rod caused by rider ring wear. The total benefit from installed proximity probes can be gained by looking at the dynamic signal for every stroke.

The analysis was developed based on the experience that piston rod failures caused by a long-term fatigue or overload process result in significant dynamic piston rod vibration. The key to an efficient analysis was to transfer the reliable segmented approach from the crosshead/cylinder vibration to the rod vibration.

The dynamic rod vibration monitoring utilised for safety protection is based on a 8 segment analysis. Opposite of the safety crosshead vibration it covers the peak-to-peak value of the dynamic rod motion. Due to the physical inertia of the piston rod the number of segments had to be less than 36. Alarming and threshold monitoring preconditions are similar to the crosshead vibration monitoring described in section 4.2. Fig. 6 shows the results of a segmented rod vibration analysis.

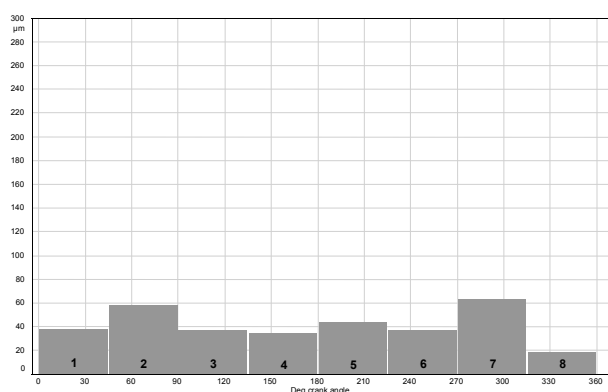


Fig. 6 : Segmented piston rod vibration

### 4.3. Dynamic pressure monitoring

Dynamic pressure measurements obtained through indicator taps are usually transferred to the p-V diagram to analyse the performance and efficiency of the compression cycle. Apart from performance monitoring the dynamic pressure also gives direct information on the actual gas load of the compressor. Overloading caused by increased differential pressure can be monitored and alarmed directly through this reading. Experience showed that large peak-to-peak pressure can build up very quickly within 20-30 seconds caused for example by liquid drops in the gas resulting in large valve losses or finally blocking interstage piping.

For safety monitoring purposes a peak-to-peak analysis can be used which determines the overall pressure difference in the cylinder during one cycle (see Fig. 7). Safety pre- and main alarms are released based on the number of consecutive revolutions an allowed maximum differential pressure has been exceeded. In most cases the allowed differential pressure can be calculated based on the maximum allowed piston rod load given in the compressor design sheet.

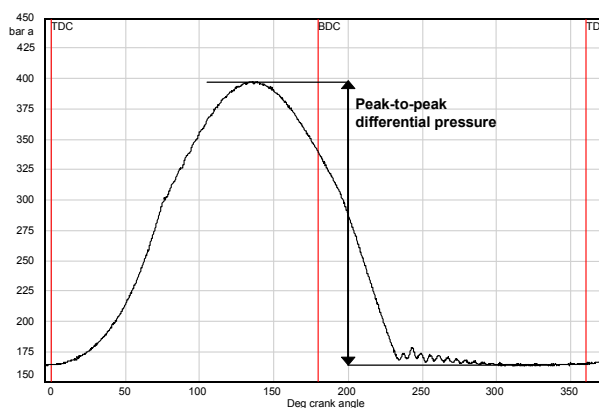


Fig. 7: Peak-to-peak differential pressure

## 5 Case studies

The above described improvements have been developed based on experiences of numerous customers using the Online Condition Monitoring system PROGNOST-NT. The safety protection module offers a built-in online data recorder, the so called ringbuffer, which continuously writes data of every single crankshaft revolution into a revolving memory (see Fig. 8). The ringbuffer is automatically saved in case of a safety pre- or main alarm and allows intensive 'post-mortem' analysis. It also allows a detailed documentation of the failure with all connected online and process data.

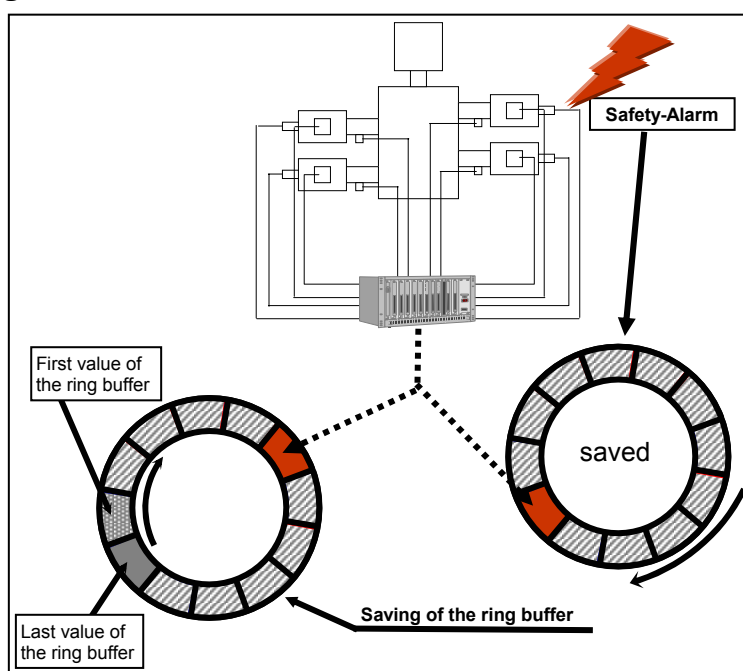


Fig. 8: Online transient ringbuffer for detailed 'post mortem' analysis

The following 3 case studies illustrate the efficiency of the above described safety features.

### 5.1 Piston crack

On a 3-staged 4-cylinder Hydrogen compressor a piston rod failed on the 2<sup>nd</sup> stage cylinder. Without a prior increase the vibration readings suddenly raised 3 to 4 times. The compressor was tripped due to violated RMS vibration readings in more than 3 fixed segments for more than 8 revolutions. Fig. 9 shows the trended RMS vibration of four segments proving the sudden character of the event. The compressor main alarm for trip was released within 11 revolutions after the failure.

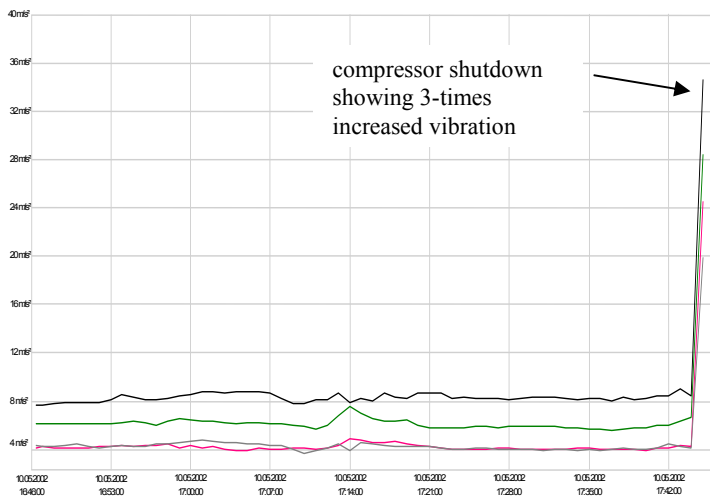


Fig. 9: Crosshead slide RMS vibration of segments 21 to 24 one hour prior to failure

## 5.2 Piston rod failure

On a four-staged 4-cylinder CO<sub>2</sub>-compressor a piston rod failed due to fatigue and continuous overload. During the last days before the failure the compressor was showing remarkably high piston rod vibration of up to 1,2 mm peak-to-peak per cycle. After restart of the compressor with a new piston rod the rod vibration readings went back to a normal level with maximum 0,25 mm of the peak-to-peak rod vibration. Fig. 10 shows the rod-drop reading with the cracked piston rod prior to the failure and after replacement by a new piston rod.

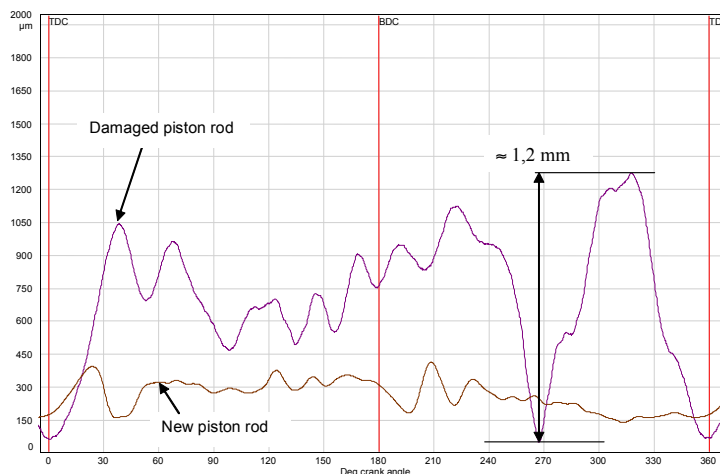


Fig. 10: Dynamic rod drop readings prior to a piston rod failure and for a new piston rod

## 5.3 Gas overload caused by liquids

A 3-staged 2-cylinder compressor for CO-mixed gas designed for an approximate 3<sup>rd</sup>-stage discharge pressure of 300 bar exceeded the final discharge pressure by estimated 250 bar. The dynamic pressure transducer of the 3<sup>rd</sup> stage was calibrated up to 400 bar so the exact reached discharge pressure could not be evaluated. The compressor was stopped and liquids were found in the process piping filling up complete sections of the piping. The increased amount of liquids in the gas were rising the gas mol weight which resulted in an increased pressure drop during the discharge process. The maximum discharge pressure inside the cylinder increased from 300 bar to 395 within 11 seconds (45 revolutions) and reached app. 550 bars within further 12 seconds (50 revolutions). Fig. 11 shows 3 dynamic pressure curves of the 3<sup>rd</sup> stage throughout the incident for the above mentioned situations.

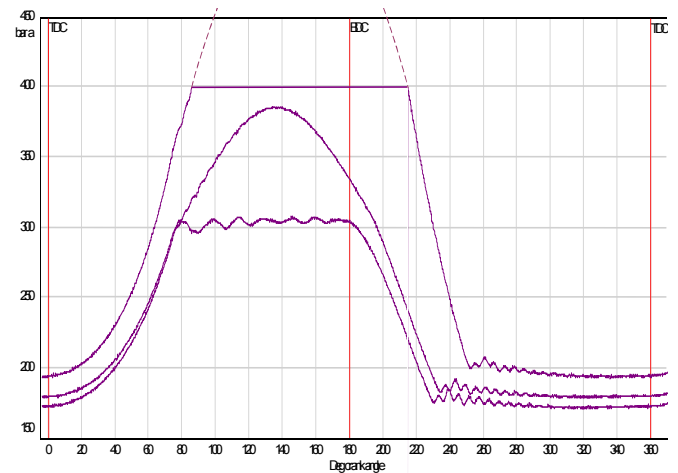


Fig. 11: Dynamic pressure signal showing effects of increasing liquids in the gas

## 6 Conclusions

The efficiency of safety protection on reciprocating compressors can be improved by using specially developed techniques. The discussed advanced methods have proven their capabilities and add substantial benefit to the three relevant subjects of safety protection:

1. High sensibility regarding machine failures
  - a. crosshead acceleration vibration analysed by 36 segments per revolution
  - b. dynamic piston rod vibration analysed by 8 segments per revolution
  - c. dynamic differential pressure analysed per compression cycle
2. Short time between detection and alarm
  - a. main alarms for shutdown can be released after minimum 3 crankshaft revolutions
  - b. direct condition parameters like dynamic pressure indicate changes instantly
  - c. fully continuous online monitoring of every single crankshaft revolution
3. Low sensitivity to false alarms
  - a. alarming only after repeated threshold violations in consecutive revolutions
  - b. threshold violations must repeat in identical segments
  - c. monitoring uses RMS or peak-to-peak values which are less sensitive to sensor defects e.g. offset variations or spiking

The above described techniques offer individual capabilities for various components to be monitored and failures to be detected. They can be applied and individually selected depending on the compressor type and the service the machine is operated in.

In industrial production of the 21<sup>st</sup> century with its high requirements regarding safety, efficiency and environmental protection effective safety monitoring of machinery is a vital subject. Experience has shown that in most cases costs for increased safety protection will be less than 5% of the total value of the equipped machinery while major breakdowns and machine component failures easily reach 10 to 20%. Therefore also economical facts for upgraded safety equipment can be found especially after analysis of self-experienced cases.